

CRANFIELD UNIVERSITY

PETER FRANCIS MAHONEY

DEVELOPMENT OF A SYNTHETIC BONE AND TISSUE MODEL
TO SIMULATE OVERMATCH MILITARY BALLISTIC HEAD
INJURY

DEFENCE ACADEMY
FORENSIC INSTITUTE

PhD THESIS
Academic Year: 2017- 2018

Supervisors: Dr D J CARR 2016-17
 Dr K HARRISON 2017-18
 Dr R CRITCHLEY 2017-18

CRANFIELD UNIVERSITY

DEFENCE ACADEMY
FORENSIC INSTITUTE

PhD THESIS

Academic Year 2017 – 2018

PETER FRANCIS MAHONEY

DEVELOPMENT OF A SYNTHETIC BONE AND TISSUE MODEL
TO SIMULATE OVERMATCH MILITARY BALLISTIC HEAD
INJURY

Supervisors:	Dr DJ CARR	2016-17
	Dr K HARRISON	2017-18
	Dr R CRITCHLEY	2017-18

© Crown Copyright 2018. All rights reserved. No part of this publication may be reproduced without the written permission of the copyright owner.

ABSTRACT

A synthetic bone and tissue head model was built using sequential experiments and tested against impacts with 7.62 x 39 mm MSC ammunition. The key experiment in this series was a forensic reconstruction of two military head injury gunshot wounds. One of the models produced a good representation of the incident. The other was less accurate but did produce a good representation of tangential gunshot wounds. Further work assessed the model against a contact gunshot injury with 5.56 x 45 mm ammunition and looked at the effects of intermediate glass and transparent thermoplastic targets on the wounds produced by 7.62 x 39 mm impacts. Strengths and weaknesses of the model are discussed and further work suggested.

Keywords:

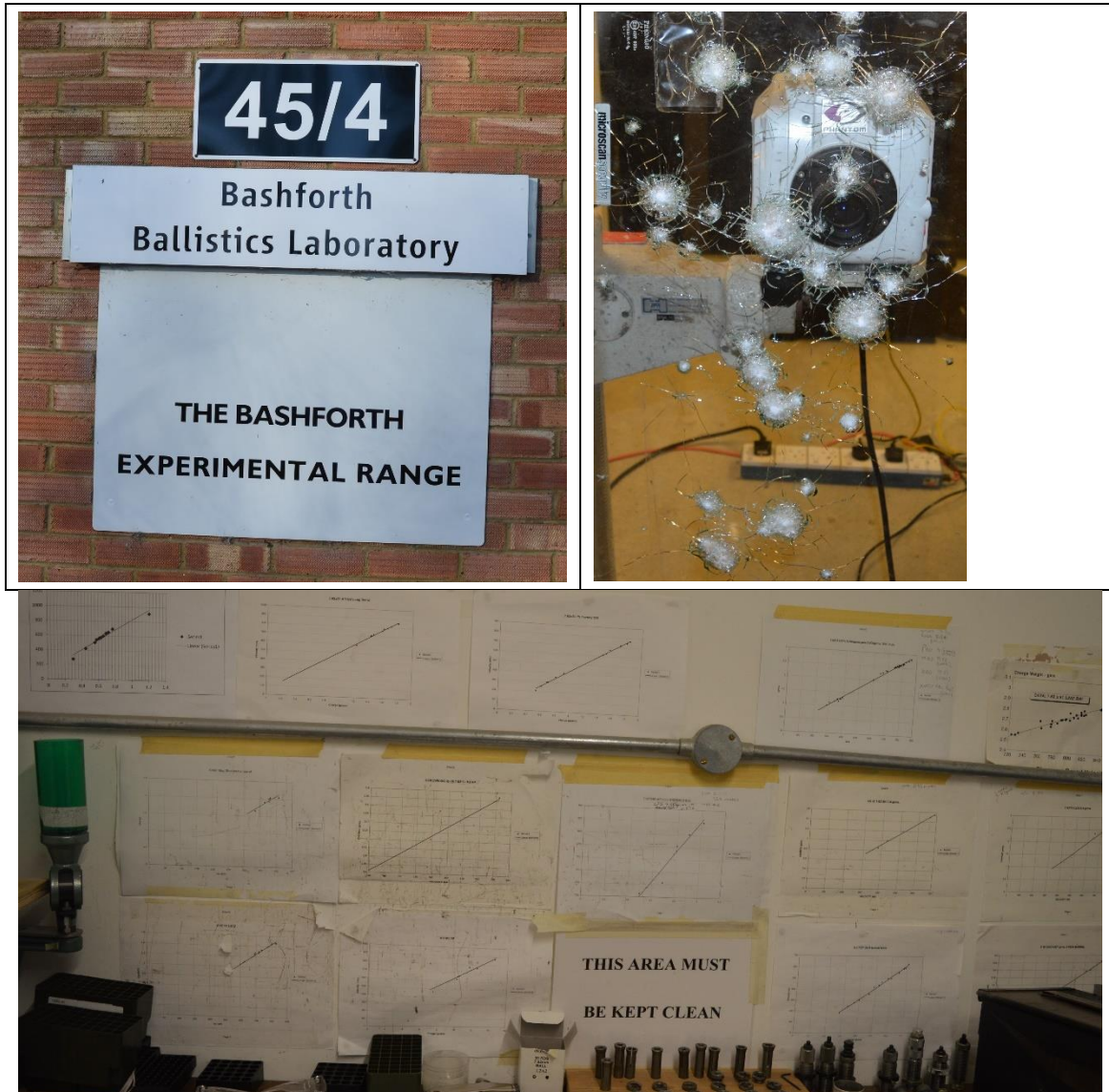
AK-47, 7.62 x 39 mm, Military Helmet, Gunshot, Forensic Reconstruction

ACKNOWLEDGEMENTS

This research would not have been possible without the input from the following individuals:

- Dr Debra Carr, my PhD supervisor, who brought a depth of academic ballistic understanding to my initial proposal and linking to industry contacts to source the materials for the experiments.
- Dr Karl Harrison and Dr Richard Critchley who stepped in as PhD supervisors when the Impact and Armour Group was closed by Cranfield University in the middle of my work.
- Dr Amarjit Samra, Royal Centre for Defence Medicine, for believing in the project and agreeing funding.
- The late Dr Leslie Payne, Ballistic Injury Archive, source of many useful references and resources.
- The Impact and Armour Group at Cranfield University, Defence Academy, sadly no more:
Prof Ian Horsfall
David Miller
Michael Teagle
Claire Lankester
Caroline McKenna
Alan Peare
Richard Critchley
Robert Sheldon
- Lt Col Liz Nelson, Lt Col John Starling (rtd) and WO2 Ian Morton for re-opening the ranges under military jurisdiction for my experiments.
- AET: thanks for your patience and support.

Other individuals are acknowledged after the individual chapters within the thesis.



Figure_Ack 1 Images of the Bashforth range

Top left: external sign

Top right: hazards of ballistic testing; impacts onto a glass screen protecting the V1212 camera

Bottom: ballistic test data in the downloading room.

TABLE OF CONTENTS

ABSTRACT	i
ACKNOWLEDGEMENTS.....	ii
LIST OF FIGURES.....	x
LIST OF TABLES	xiii
LIST OF EQUATIONS.....	xiv
Standard Deviation	xiv
Tear strength	xiv
GLOSSARY.....	xv
LIST OF ABBREVIATIONS	xxvii
1 INTRODUCTION.....	1
1.1 Some views on ballistic head protection	1
1.2 Helmand province, Afghanistan 2014	2
1.3 The nature of military head injury.....	3
1.4 The nature of modern military helmets.....	5
1.5 Could the project have been done with computer simulation?	7
1.5.1 Helmets alone	7
1.5.2 Forensics.....	8
1.5.3 A combined approach	9
1.5.4 Computer modelling conclusions	10
1.6 PhD academic structure.....	10
1.6.1 Gelatine blocks.....	10
1.6.2 Synbone® spheres.....	11
1.6.3 Anatomically correct skull.....	12
1.6.4 Skull with synthetic skin and soft tissue.....	12
1.6.5 Forensic case reconstruction	12
1.6.6 Testing the model against additional conditions.....	13
1.7 PhD chapter structure	13
1.8 Experimental sequencing.....	14
1.9 Declaration.....	15
1.10 References	16
2 AIMS AND OBJECTIVES.....	21
2.1 Aims.....	21
2.2 Objectives	21
3 THE EFFECT OF HELMET MATERIALS AND SIMULATED BONE AND TISSUE LAYERS ON BULLET BEHAVIOUR IN A GELATINE MODEL OF OVERMATCH PENETRATING HEAD INJURY	23
3.1 Abstract.....	23
3.2 Introduction	24
3.2.1 Brain.....	26
3.2.2 Bone.....	28

3.2.3 Skin	29
3.2.4 Head model.....	30
3.2.5 Helmet.....	31
3.3 Materials and Methods.....	31
3.3.1 Gelatine.....	31
3.3.2 Synthetic Bone	32
3.3.3 Horse Scapulae.....	33
3.3.4 Synthetic Skin and Synthetic Bone	33
3.3.5 Helmet Simulant, Synthetic Skin and Synthetic Bone	34
3.4 Measurements	35
3.5 Results.....	41
3.5.1 IBM SPSS v24 analysis.....	42
3.6 Discussion	46
3.7 Conclusions	48
3.8 Limitations of the model	48
3.9 Acknowledgements.....	49
3.10 References	50
4 ASSESSMENT OF POLYURETHANE SPHERES AS SURROGATES FOR MILITARY BALLISTIC HEAD INJURY.....	55
4.1 Abstract.....	55
4.2 Introduction	55
4.3 Method.....	57
4.4 Results.....	58
4.4.1 High Speed Video (HSV).....	58
4.4.2 Pathologists' assessment.....	60
4.5 Discussion	62
4.6 Conclusion	63
4.7 Caveats.....	63
4.8 Acknowledgements.....	63
4.9 References	64
5 DOES PRELIMINARY OPTIMISATION OF AN ANATOMICALLY CORRECT SKULL-BRAIN MODEL USING SIMPLE SIMULANTS PRODUCE CLINICALLY REALISTIC BALLISTIC INJURY FRACTURE PATTERNS?	67
5.1 Abstract.....	67
5.2 Introduction	68
5.3 Method.....	70
5.3.1 Polymer comparison.....	70
5.3.2 Skull fill and conditioning	71
5.3.3 Skull shooting.....	72
5.3.4 Clinician assessment.....	74
5.4 Results.....	75

5.4.1 IBM SPSS v23 analysis.....	76
5.4.2 Summary of Likert-type scores and free text comments	77
5.5 Discussion	80
5.5.1 Limitations of the model	82
5.6 Conclusions	82
5.7 Caveats.....	82
5.8 Acknowledgements.....	83
5.9 References	84
6 BALLISTIC IMPACTS ON AN ANATOMICALLY CORRECT SYNTHETIC SKULL WITH A SURROGATE SKIN/SOFT TISSUE LAYER	87
6.1 Abstract.....	87
6.2 Introduction	87
6.2.1 Gunshot wound characteristics	88
6.2.1.1 Skin and soft tissue gunshot entry wound	89
6.2.1.2 Entrance wound bone damage	90
6.2.1.3 Exit wound bone damage	90
6.2.1.4 Additional fractures	90
6.2.1.5 Skin and soft tissue exit wounds.....	91
6.2.2 Imaging in ballistic investigations	91
6.2.3 This project.....	93
6.3 Method.....	94
6.3.1 Skulls.....	94
6.3.2 Faces	94
6.3.3 Complete model	96
6.3.4 First set of CT scans	96
6.3.5 Ballistic testing	96
6.3.6 Second set of CT scans	98
6.3.7 Pathologists' examination.....	99
6.3.8 Radiologists' examination.....	99
6.3.9 High Speed Video (HSV) examination	100
6.4 Results.....	101
6.4.1 HSV.....	101
6.4.2 Likert-type scores	102
6.4.2.1 Skin/soft tissue appearance and feel	103
6.4.2.2 Entry wounds	104
6.4.2.3 Exit wounds	104
6.4.2.4 Wound tracts.....	104
6.4.2.5 Fracture patterns	105
6.4.2.6 Imaging.....	105
6.5 Discussion	106
6.6 Conclusion	109
6.7 Caveats.....	109

6.8 Acknowledgements.....	110
6.9 References	111
7 FORENSIC RECONSTRUCTION OF TWO MILITARY COMBAT RELATED SHOOTING INCIDENTS USING AN ANATOMICALLY CORRECT SYNTHETIC SKULL WITH A SURROGATE SKIN/SOFT TISSUE LAYER.....	117
7.1 Abstract.....	117
7.2 Introduction	118
7.3 Method.....	121
7.3.1 Ethics and permissions	121
7.3.2 Defence Science and Technology Laboratory.....	121
7.3.3 Model construction	123
7.3.4 Range and flash x-ray	124
7.3.5 CT Scans	125
7.3.6 Pathologist and engineer examination	127
7.4 Results.....	128
7.4.1 Impact event HSV and flash x-ray	128
7.4.2 Summary of bullet trajectories.....	128
7.4.3 Engineering helmet assessment	132
7.4.4 Forensic Pathologist and Military Radiologist assessment.....	133
7.5 Discussion	134
7.6 Conclusions	141
7.7 Caveats.....	141
7.8 Acknowledgements.....	142
7.9 References	143
8 FURTHER ASSESSMENT OF A SURROGATE HEAD MODEL FOR MILITARY BALLISTIC INJURY WITH CASE STUDIES.....	147
8.1 Abstract.....	147
8.2 Introduction	147
8.3 Method-general.....	149
8.3.1 Ranges.....	150
8.3.1.1 Case study 1: Contact wound reconstruction	150
8.3.1.2 Case study 2: The influence of intermediate targets.....	152
8.3.1.2.1 Laminated windscreen	152
8.3.1.2.2 Helicopter window	153
8.3.2 CT scanning and radiology examination	153
8.3.3 Pathology examination.....	154
8.4 Results.....	154
8.4.1 Case study 1: Contact wound reconstruction	154
8.4.1.1 HSV	154
8.4.1.2 Pathologist assessment.....	157
8.4.1.3 Radiologist assessment.....	161

8.4.2 Case study 2: The influence of intermediate targets on wounding patterns in the models	164
8.4.2.1 Laminated windscreen impact	164
8.4.2.1.1 HSV	164
8.4.2.1.2 Pathologist assessment	165
8.4.2.1.3 Radiologist assessment	168
8.4.2.2 Helicopter window impact	171
8.4.2.2.1 HSV	171
8.4.2.2.2 Pathologist assessment	172
8.4.2.2.3 Radiologist assessment	176
8.5 Discussion	178
8.6 Conclusions	181
8.7 Caveats.....	181
8.8 Acknowledgements.....	181
8.9 References	183
9 DISCUSSION	187
9.1 Introduction	187
9.2 The requirement	187
9.3 Review of the academic processes and summary of new knowledge ..	188
9.4 Quality of the experiments	192
9.4.1 Choice of materials and eliminating confounders.....	192
9.4.1.1 Ammunition.....	192
9.4.1.2 Gelatine	193
9.4.1.3 Synthetic Bone versus real bone	193
9.4.2 Use of the Likert-type scale and fracture characteristics	195
9.5 Does the model need to be this complex?	197
9.6 Conclusions	198
9.7 References	199
10 CONCLUSIONS	207
11 FUTURE WORK AND FURTHER DEVELOPMENT OF THE MODEL	209
11.1 Future work.....	209
11.1.1 Benefits and risks of helmets	209
11.1.2 Ballistic mechanisms	209
11.1.3 Anatomical Injury.....	210
11.1.4 Future work-summary	211
11.2 Further development of the model	211
11.2.1 The synthetic PDMS skin/soft tissue	211
11.2.2 Brain simulant	212
11.2.3 The post-mortem cut line in the skull.....	212
11.2.4 Further development summary	213
11.3 References	214
APPENDICES	217

Appendix A Gelatine block preparation.....	219
Appendix B Bullet analysis.....	227
Appendix C Micro CT images from intermediate layers.....	235
Appendix D Synthetic skin analysis	239
Appendix E Synbone® sphere data.....	245
Appendix F Skull data and preparation.....	247
Appendix G Skulls with more than one Likert-type score for fracture pattern of 3 or 4	255
Appendix H Clear Ballistics synthetic gelatine impact sequence and burn .	269
Appendix I Other head models	271

LIST OF FIGURES

Figure_Ack 1 Images of the Bashforth range	iii
Figure 1-1 Preliminary work.....	5
Figure 1-2 PhD academic structure.....	11
Figure 3-1 Gelatine block compared with helmet model.....	25
Figure 3-2 Scapulae experimental set up	34
Figure 3-3 Helmet layers	35
Figure 3-4 Post-impact assessments	36
Figure 3-5 High speed video impact sequence scapula 1, side view	37
Figure 3-6 Measurements within gelatine blocks.....	38
Figure 3-7 Temporary cavity within a skull model.....	39
Figure 3-8 Measurement of temporary cavity	40
Figure 4-1 Synbone® spheres experimental preparation and set up	57
Figure 4-2 Model 3, 5% gelatine fill, V1212 Impact sequence (side view).....	59
Figure 4-3 Model 8, 5% gelatine fill, V12 Impact sequence (from above)	59
Figure 4-4 Model 7, 5% gelatine fill, V1212 Impact sequence (side view).....	60
Figure 5-1 Sectioned 7.62 x 39 mm bullets. Left: Czech; Right Ukrainian.....	73
Figure 5-2 Experimental set up	73
Figure 5-3 Shot skull assessment set up.....	75
Figure 5-4 Frontal impact sequence captured with the V12 camera	76
Figure 5-5 Examples of impacted skulls, reconstructed where possible	79
Figure 5-6 Characteristics of skull gunshot wounds	81
Figure 6-1 Head injury gunshot characteristics	89
Figure 6-2 MU51 Polymer skulls with moulded PDMS faces and scalps	95
Figure 6-3 Details of Ukrainian MSC 7.62 x 39 mm ammunition	97
Figure 6-4 Face 1/Golf at range	98
Figure 6-5 CT scanning at Queen Elizabeth Hospital Birmingham.....	99
Figure 6-6 Pathologists' examination.....	100
Figure 6-7 CT reconstruction images	101
Figure 6-8 Summary of bullet trajectories.....	102
Figure 6-9 Summary of Likert-type score sheets as graphs.	103
Figure 6-10 HSV Impact sequence Face 4	106
Figure 7-1 IMAF and CT Images Incident 1	123
Figure 7-2 Model construction	124
Figure 7-3 Experimental set up at COTEC	126
Figure 7-4 Models awaiting examination after shooting	127
Figure 7-5 Impact events and flash x-ray	129
Figure 7-6 Location of strikes and trajectories models 1 to 3	130
Figure 7-7 Location of strikes and trajectories models 4 to 6	131
Figure 7-8 Engineering helmet assessment	132
Figure 7-9 Simulated injuries and corresponding CT images	136
Figure 7-10 Comparison of skin entry wounds	139
Figure 7-11 Exit wounds, rear of head models	140
Figure 8-1 Experimental set up models 13 and 14	151
Figure 8-2 Experimental set up laminated windscreen impact	152

Figure 8-3 Components of the ‘aviation’ head model	153
Figure 8-4 V1212 Impact sequence model 13.....	155
Figure 8-5 V1212 impact sequence model 14	156
Figure 8-6 Model 13 pathologist examination (1)	158
Figure 8-7 Model 13 pathologist examination (2)	159
Figure 8-8 Model 13 CT 3D reconstruction entry wounds	162
Figure 8-9 Model 13 CT 3D reconstruction lateral view.....	162
Figure 8-10 Model 13 CT 3D reconstruction exit wounds.....	163
Figure 8-11 Transverse cut through model 14.....	163
Figure 8-12 Model 15 V12 HSV front view	164
Figure 8-13 Model 15 V1212 HSV side view.....	165
Figure 8-14 Model 15 pathologist examination.....	167
Figure 8-15 Model 15 CT 3D reconstruction front view	169
Figure 8-16 Model 15 CT 3D reconstruction from above.....	169
Figure 8-17 Model 15 CT 3D reconstruction sagittal cut	170
Figure 8-18 Model 16 V12 HSV, frontal view.....	171
Figure 8-19 Model 16 V1212 HSV, side view	172
Figure 8-20 Pathologist examination helicopter window impact model 16 (1)	173
Figure 8-21 Pathologist examination helicopter window impact model 16 (2)	174
Figure 8-22 Pathologist examination helicopter window impact model 16 (3)	175
Figure 8-23 Model 16 CT 3D reconstruction front views	177
Figure 8-24 Model 16 CT 3D reconstruction side views	177
Figure 8-25 Model 16 CT 3D reconstruction rear views	178
Figure 8-26 Model 16 CT 3D reconstruction viewed from above.....	178
Figure_A 1 Gelatine block preparation	219
Figure_A 2 Assessment of different gelatine % by mass for ‘biofidelity’	220
Figure_A 3 Block validation and dissection	221
Figure_A 4 Graph of DoP against ball bearing impact velocity.....	224
Figure_A 5 Graph of propellant mass against bullet impact velocity	224
Figure_A 6 Mounting bullets within Bakelite (1).....	228
Figure_A 7 Mounting bullets within Bakelite (2) and bullet sectioning	229
Figure_A 8 Microhardness testing.....	230
Figure_A 9 SEM imaging and elemental analysis	231
Figure_A 10 Elemental analysis, selected area 1 (steel jacket)	232
Figure_A 11 Elemental analysis, selected area 1, (copper wash)	232
Figure_A 12 Micro CT samples and set up	235
Figure_A 13 Scapula images	236
Figure_A 14 CT sections through Synbone® specimen.....	236
Figure_A 15 Section through MU51 impact site	237
Figure_A 16 Assessment of synthetic skin samples.....	239
Figure_A 17 Trouser tear test (1)	240
Figure_A 18 Trouser tear test (2)	241
Figure_A 19 Skull preparation	247
Figure_A 20 Preliminary skull CT imaging	248
Figure_A 21 Impact sequence Clear Ballistics 10% Synthetic Gelatine	269
Figure_A 22 Permagel™ burn.....	270
Figure_A 23 Clear Ballistic Gel impact sequence, Clear Ballistic Gel head ...	271

Figure_A 24 MU51 skull with Permagem™ face (side view)	272
Figure_A 25 Impact sequence MU51 Polymer skull with Permagem™ face....	273
Figure_A 26 Impact sequence polystyrene head, 5.56 x 45 mm round.....	274

LIST OF TABLES

Table 3-1 Measurements of the distances shown in Figure 3-6 for each block and material layer combination	42
Table 3-2 Summary statistics for distance 'x'	43
Table 3-3 Summary statistics for distance 'y'	44
Table 3-4 Summary statistics for distance 'z'	44
Table 3-5 Summary statistics for distance 'w'	45
Table 3-6 Summary statistics for 'nL'	45
Table 4-1 Likert-type scores for Synbone® sphere post-impact appearances	61
Table 5-1 Summary of synthetic skull material data	71
Table 5-2 Summary of skull 'fill' (gelatine % by mass or Permangel™)	72
Table 5-3 Likert-type scale for clinician assessments	74
Table 5-4 Descriptive statistics for the effect of polymer type on Likert-type score for fracture pattern	76
Table 5-5 Descriptive statistics for the effect of skull contents and temperature on fracture score.....	77
Table 5-6 Frequency of comments on entry and exit wound appearance plus influence of the post-mortem cut line	78
Table 7-1 Explanation of Likert-type scores	137
Table 7-2 Likert-type scores, Forensic Pathologist (FP) and Military Radiologist (MR).....	138
Table_A 1 Gelatine block raw data.....	222
Table_A 2 Microhardness results	233
Table_A 3 Results of tests on synthetic skin samples	242
Table_A 4 Synbone® sphere data	245
Table_A 5 Raw data for skulls 1 to 19 and 26 to 46, gelatine fills	249
Table_A 6 Raw data for skulls 20 to 25, Permangel™ fill.....	251
Table_A 7 Raw data for skull 47 mineral oil elastomer fill	251
Table_A 8 Raw data for skulls 48- 63 with synthetic faces 1-12.....	252
Table_A 9 Raw data for skulls 60-63, faces 13-16, Permangel™ fill.....	253
Table_A 10 Reviewer comments for skulls	255

LIST OF EQUATIONS

Standard Deviation

$$SD = \sqrt{\frac{\sum(x-\bar{x})^2}{n-1}}$$

\bar{x} = mean value, x =individual values, n =number of observations, \sum = total

Tear strength

$$Ts = \frac{F}{d}$$

From ISO 34-1:2015 (E)

F = median force in Newtons, calculated in accordance with ISO 6133: 2015 (E) using Method A

d = median thickness, in mm, of test piece

GLOSSARY

Anthropometry	The scientific study of the measurements of the human body [1].
Aromatic polyamides	<p><i>Aromatic</i>: compounds related to benzene; ring compounds containing conjugated double bonds.</p> <p><i>Polyamide</i>: natural or synthetic fibres composed of <i>polymers</i> having the same amide group (-CO-NH-) repeated along the chain. Polyamides made with aromatic groups attached to the amide links are called aramid fibres.</p> <p><i>Aramid fibres</i>: fibres made from linear polymers containing the recurring amide group joined directly to two aromatic rings [2].</p>
ARRK	<i>ARRK</i> is an international product development group. It originated in 1948 with Araki Seisakusho in Abeno-ku, Osaku-Shi as a manufacturer of wooden products [3]. ‘ <i>ARRK</i> ’ is believed to be derived from the founder’s name [4].
Axial plane	At right angles to the long axis of the body, i.e. a horizontal plane through a standing person (the usual plane for horizontal CT scan slices) [5]. Also described as ‘ <i>transverse plane</i> ’.
Biofidelity	<p><i>Bio</i>: biological [1].</p> <p><i>Fidelity</i>: exact correspondence to the original [1].</p>
Bloom strength	A measurement of the gelling properties of

	gelatine (according to the method defined by the American scientist, <i>Oscar T. Bloom</i>) described in 'Bloom grams' (the firmness of a 6.66% gel after 17 hours of storage at 10 °C) [6].
Calvarium	The vault of the skull which consists of the frontal, parietal (x2) occipital and temporal (x2) bones [5].
Coronal plane	A section through the body running from head to feet dividing it into dorsal (back) and ventral (front) parts [5].
Cortical bone	Compact outer layer of bone made up of bone tissue arranged in concentric layers [5].
Cranial vault	See ' <i>calvarium</i> ' above.
Delphi study	The <i>Delphi</i> methodology was developed by the RAND (Research AND Development) corporation in the 1950s. The method involves a group of experts replying anonymously to a questionnaire, receiving feedback on the group response, then the process repeating to arrive at expert consensus [7-9].
Doppler radar	<p><i>Doppler effect</i>: an increase (or decrease) in the frequency of waves as the source and observer move towards (or away) from each other [1].</p> <p><i>Radar</i>: a system for determining the direction, range or presence of (moving) objects by sending out pulses of high frequency radio waves and detecting the returning echo [1].</p> <p>Type used in the experiments described in the</p>

	thesis is a <i>Weibel Doppler Radar</i> [10] (see below).
External auditory meatus	The passage in the external ear from the pinna (the projecting part of the ear) to the tympanic membrane (ear drum) [11].
Finite Element	A computational method used for the analysis of solid mechanics problems. The material under consideration is replaced in the model by a 'finite' set of computational points (nodes) or volumes (elements) [12].
Gelatine	<i>Gelatine</i> is a substance made from collagen protein derived from demineralised animal bones and skin (from pigs and cows) [13].
Hybrid III	This is an anthropometric test device (previously known as a 'crash test dummy') originally developed by General Motors and now built by Humanetics Innovative Solutions, MI, USA [14].
Hydrocode	A computational tool for modelling fluid flow [15].
Laminated glass	A form of ' <i>safety glass</i> ' (see below). Glass made of a 'sandwich' of a thin transparent polymer (typically polyurethane) between two glass sheets. The polymer acts to hold glass fragments together in the event of impact and act as a barrier to penetration into the second layer of glass [2].
Likert	<i>Rensis Likert</i> (1903-1981) was an American social scientist who developed scales for measuring attitude [16].

Luger	A 9 x 19 mm bullet designed by <i>Georg Luger</i> (1849-1923) introduced in 1903 [17].
Micro CT	An X-ray computer tomography system with a small sample chamber allowing very fine image resolution [18].
Mild steel core	<i>Mild steel</i> : steel containing a low (up to 0.15 %) by mass of carbon [2]. <i>Mild steel core</i> : a bullet core made out of mild steel.
MU51	A <i>polymer</i> used by ARRK (see above) and [19].
Nasion	The point on the bridge of the nose at the centre of the suture between the frontal and nasal bones [5].
Neck length	The <i>neck</i> or ' <i>narrow channel</i> ' is the first section of the wound channel in tissue or a simulant caused by full metal jacket and solid bullets [20]. <i>Neck length</i> is the distance from bullet entry into the medium to the beginning of the bullet yaw (see below) [21] and Figure 3-6.
Neolithic	A period in early human history associated with the move from hunter-gatherer to farmer. Occurred at different times across the world but in the UK was around 4-5000 BCE [22, 23].
Organosiloxane	<i>Polysiloxanes</i> are silicone rubbers [2]. <i>Organosiloxanes</i> are siloxanes where a silicon atom is substituted by an <i>organyl group</i> [24].

	<i>Organyl groups</i> are organic substituent groups having one free valence at a carbon atom [25].
Para-aramid	Polyamide fibres [see above] with high tensile strength used in ballistic protective materials [26]. ‘Para’ refers to the 1,4 substitution positions on the aromatic ring structure.
Permugel™	<i>Permugel™</i> or <i>Perma-Gel™</i> is a clear synthetic material reported to behave in a similar way to 10% gelatine under ballistic impact. <i>Permugel™</i> can be re-melted and reused [27].
Permanent cavity	<i>Permanent cavity</i> or <i>permanent wound channel</i> is an area of crushed and torn tissue (or tissue simulant), smaller than the temporary cavity, caused by the passage of a bullet or fragment [20]. See Figure_A 3c.
Phantom cameras	The name of a series of high speed cameras made by AMTEC Vision Research [28].
Plasticity	A material property where deformation due to an applied stress is (largely) retained when the stress is removed [2].
Plate glass	A form of glass originally cast on an iron bed and rolled into sheet form [2].
Polymer	<i>Polymer</i> : long chain molecules built up by multiple repetition of groups of atoms known as repeat units [2].

Polyurethane	A group of polymers used to make tough materials with plastic properties [2].
PU8098	A polymer used by ARRK (see above) and [21].
Puppe's rule	Fracture lines from a later bullet hole cannot cross those emanating from an earlier hole [20]. Georg Puppe (1867–1925).
Roma Plastilina Clay	An oil and wax based modelling clay used for ballistic testing [29, 30]. (Reference [30] also links to ballistic test standards).
Safety glass	One of several types of glass designed to contain or minimise fragmentation. Includes ' <i>laminated glass</i> ' (see above), ' <i>toughened glass</i> ' and glass incorporating wire mesh or, ' <i>wired glass</i> ' [2].
Sagittal plane	A section running through the body from top to bottom dividing it into left and right parts [5].
Scapula	Shoulder blade [5].
Shore A Durometer	<i>Durometer</i> : an instrument for testing the hardness of plastics and rubber. There are 12 types of durometer; Type A is the type used for soft rubber [31, 32]. <i>Shore</i> : Albert F Shore (1876-1936) developed the durometer and scale in the 1920s [33].
Silicone rubber	A type of rubber where the main backbone chain is inorganic and the repeater unit is:

	$ \begin{array}{c} R \\ \\ -O-Si- \\ \\ R' \text{ (see } \textit{Organosiloxane} \text{ above)} [2]. \end{array} $
Strain	Distortion of a material by forces acting on it [2]. Expressed as a change in dimension/original dimension or expressed as a percentage.
Strain rate dependency	Material behaviour that depends on how quickly the force (stress) is applied and where the extent of deformation depends on the rate at which loads are applied [34].
Stress	The force per unit area, expressed in Pa N/m ⁻² , acting on a material and tending to change its dimensions, i.e. causing a strain (see above) [2].
Superior nuchal line	A semi-circular line passing outward and forward from the <i>external occipital protuberance</i> . The <i>external occipital protuberance</i> is the central prominence on the outer surface of the flat portion of the occipital bone [11].
Synbone®	Synbone® is a company (formed 1988) based in Switzerland that produces medical models for surgical education and surrogates for ballistic investigation [35].

Temporary cavity	A phenomenon caused by projectile (e.g. a bullet) transferring energy into a suitable material (e.g. gelatine). The energy transferred from the bullet accelerates the material surrounding the bullet away radially creating a hollow space behind the bullet which collapses back down as the material elastically retracts [20]. See <i>permanent cavity</i> above.
Thermoplastic	A material that becomes plastic when heated [2].
Trabecular bone	Thin bars of bony tissue in spongy bone [5].
Transverse plane	See 'Axial plane' above [5].
UP5690	A polymer made by ARRK (see above) and [19].
Vickers hardness test	A method of hardness measurement where a 136 ° diamond pyramid is pushed with a constant force into the surface of the specimen for a specified time. The diagonal lengths of the indentation are measured after the diamond is withdrawn. The Vickers Hardness Number (HV) = the force divided by the contact surface area of the indentation [2].
Weibel doppler radar	Doppler radar (see above) named after founder of Danish electronics company MP Weibel [10].
Yaw	Linear oscillation of a bullet around the axis of the trajectory [36].

References

1. Pearsall J, Trumble B (Eds) (1995) The Oxford English Reference Dictionary. OUP, Oxford, UK
2. Walker PMB (Ed) (1999) Chambers Materials Science and Technology Dictionary. Chambers Harrap Publishers Ltd, Edinburgh, UK
3. <https://www.arrkeurope.com> (accessed 30/01/18)
4. Email Mahoney/ARRK UK 30/01/18
5. Martin EA (Ed) (2015) Oxford Concise Medical Dictionary (9th edn). OUP, Oxford, UK
6. <https://www.gelita.com/en/knowledge/gelatine/properties-of-gelatine/texture/visco-elastic-properties> (accessed 12/03/2018)
7. <https://www.rand.org/topics/delphi-method.html> (accessed 12/03/2018)
8. <https://www.rand.org/about/history/a-brief-history-of-rand.html> (accessed 12/03/2018)
9. Defence Medical Services Support to Civilians on Operations: Report of an Evidence Based Review (2005) ADMEM DMETA Ref 11070
10. <https://www.weibel.dk/about-us/our-story/> (accessed 12/03/2018)
11. Blakiston's Gould Medical Dictionary (1979) (4th edn) McGraw-Hill, London UK

12. Pope DJ, Masouros S (2016) Computational methods in continuum mechanics. In: Bull AMJ, Clasper C, Mahoney PF (Eds) Blast Injury Science and Engineering- a Guide for Clinicians and Researchers. Springer International Publishing Switzerland. pp 199-217
13. <https://www.gelita.com/en/knowledge/gelatine/what-is-gelatine> (accessed 14/03/2018)
14. <http://www.humaneticsatd.com/crash-test-dummies/frontal-impact/hiii-50m> (accessed 14/03/2018)
15. Collins GS (2002) An introduction to hydrocode modelling. <http://citeseerx.ist.psu.edu/viewdoc/download?doi=10.1.1.515.4016&rep=rep1&type=pdf> (accessed 23/3/18)
16. <https://www.britannica.com/biography/Rensis-Likert> (accessed 14/03/2018)
17. Bussard M (2014) Ammo Encyclopedia (5th Edn). Blue Book Publications Inc, Minneapolis, USA. p743
18. <https://www.bruker.com/products/microtomography/micro-ct-for-sample-scanning.html> (accessed 14/03/2018)
19. Mahoney PF, Carr DJ, Delaney R, Hunt N, Harrison S, Breeze J, Gibb I (2017) Does preliminary optimisation of an anatomically correct skull-brain model produce clinically realistic ballistic injury fracture patterns? Int J Legal Med 131: 1043-1053
20. Kneubuehl BP, Coupland RM, Rothschild MA, Thali MJ (2011) Wound ballistics; Basics and Applications. Springer-Verlag Berlin Heidelberg, Germany.

21. Mahoney PF, Carr D, Miller D, Teagle M (2017) The effect of helmet materials and simulated bone and tissue layers on bullet behaviour in a gelatine model of overmatch penetrating head injury. *Int J Legal Med* 131:1765-1776
22. http://www.bbc.co.uk/history/ancient/british_prehistory/overview_british_prehistory_01.shtml (accessed 15/03/2018)
23. <https://www.britannica.com/event/Neolithic-Period> (accessed 15/03/2018)
24. <http://www.ebi.ac.uk/chebi/searchId.do?chebiId=CHEBI:48150> (accessed 15/03/2018)
25. <http://www.ebi.ac.uk/chebi/chebiOntology.do?treeView=true&chebiId=CHEBI:33249> (accessed 15/03/2018)
26. Boussu F, Bruniaux P (2012) Customisation of a light weight bullet-proof vest for the female form. In: Sparks E (Ed) *Advances in military textiles and personal equipment*. Woodhead publishing, Cambridge UK. pp167-195
27. Mabbott A, Carr DJ, Champion S, Malbon C, Tichler C (2013) Comparison of 10% gelatine, 20% gelatine and Perma-Gel™ for ballistic testing. 27th International Symposium on Ballistics, Freiburg, Germany, April 22-26. pp 648-654
28. <https://www.phantomhighspeed.com/> (accessed 15/03/2018)
29. <https://www.sculpturehouse.com/s-99-plastilina.aspx> (accessed 15/03/2018)
30. <https://www.artmolds.com/roma-plastilina-no1-ballistic-clay.html> (accessed 15/03/18) Note: *This reference links to ballistic test standards*
31. http://www.ptc1.com/what_is_durometer.htm (accessed 19/03/2018)

32. ASTM D2240-15e1, Standard Test Method for Rubber Property—Durometer Hardness, ASTM International, West Conshohocken, PA, 2015, www.astm.org (accessed 19/03/2018)
33. <https://archive.is/20150227052925/http://www.ktrcouplings.co.uk/news/the-history-of-shore-durometer-hardness-ktrs-elements-for-rotex-couplings> (accessed 19/03/2018)
34. Özkaya N, Nordin M (1999) Mechanical Properties of Biological Tissues. In: Fundamentals of Biomechanics. Springer, New York, NY. pp 195-218
35. <https://www.synbone.com/company/about-us/> (accessed 21/03/2018)
36. Penn-Barwell JG, Helliker AE (2017) Firearms and bullets. In: Breeze J, Penn-Barwell JG, Keene D, O'Reilly D, Jeyanathan J, Mahoney PF (Eds) Ballistic Trauma -a Practical Guide (4e). Springer Nature, Cham, Switzerland

LIST OF ABBREVIATIONS

“	Inch
©	Copyright
®	Registered
°C	Degrees Celsius
ACP	Automatic Colt Pistol
AK	Avtomat Kalashnikova
ANOVA	Analysis of Variance
BABT/BHBT	Behind Armour Blunt Trauma/Behind Helmet Blunt Trauma
BS	British Standard
CDI	Centre for Defence Imaging
cm	Centimetres
CV	Coefficient of Variation
DMS RSG	Defence Medical Services Research Strategy Group
DoP	Depth of Penetration
DoW	Died of Wounds
DSLR	Digital Single-Lens Reflex
DSTL	Defence Science and Technology Laboratory
DU	Durometer
F	F statistic
FCRL	Flexural Composite Research Laboratory
FE	Finite Element
FMJ	Full Metal Jacket
fps	Frames per Second (for High Speed Videos)
fps	Feet per Second (for ballistic projectiles)
FSP	Fragment Simulating Projectile
g	Gram
gr	Grain
GSW	Gun Shot Wound
HFN	Head Face and Neck
HHS	Human Head Surrogate
HSD	Honest Significant Difference
HSV	High Speed Video
HV	Vickers Hardness
IBM	International Business Machines

in	Inch
ISO	International Organization for Standardization
JTTR	Joint Theatre Trauma Registry
LR	Long Rifle
m/s	Metres per Second
MERT	Medical Emergency Response Team
mm	Millimetres
MRI	Magnetic Resonance Imaging
MSC	Mild Steel Core
N	Newtons
NATO	North Atlantic Treaty Organisation
<i>n</i> L	Neck Length
NS	Not Significant
NTU	Nottingham Trent University
PDMS	Poly(dimethylsiloxane)
PMHS	Post-Mortem Human Subject
PRISMA	Preferred Reporting Items for Systematic Reviews and Meta-Analysis
QEHB	Queen Elizabeth Hospital Birmingham
RCDM	Royal Centre for Defence Medicine
SAER	Small Arms Experimental Range
SD	Standard Deviation
SPSS	Statistical Programme for Social Sciences
TM	Trade Mark
WDMET	Weapons Data and Munitions Effectiveness Team

1 INTRODUCTION

This PhD thesis is presented as a series of papers, either published, submitted for publication or in preparation for publication. Each paper has its own review of the relevant literature. The aim is not to duplicate this in the introduction but to offer a context within which to place the individual papers and the work as a whole.

1.1 Some views on ballistic head protection

'The war has had many surprises in the way of the reintroduction of appliances that were supposed to be entirely out of date, such as hand grenades, but perhaps the most curious is the revival of armour for the person. The French War Office has introduced metal skull caps to their soldiers' uniforms and there is some evidence that they may be of considerable value. Of 55 cases of head wounds, 42 occurred in men who had not worn the armour. Metal skull caps are unfortunately unpopular with the troops-they are too hemispherical to fit the cranium well, they keep in the perspiration, and are apt to cause headaches. Armour for the chest has been suggested too but there is no evidence at present as to its efficacy.'

British Medical Journal (1915) [1]

'So perchance a future generation, with their eyes, necks chests and abdomens protected adequately will view with compassion the men and women of our day who face exploding bombs and shells with, at the most, a metal hat designed to protect their vertex.'

Hamilton Bailey (1942) [2]

'There is a common misconception that such ballistic helmets can protect the wearer from most firearms. However, these helmets whilst offering protection against low velocity projectiles are not designed to resist high energy projectiles from rifles.'

Hamounda et al. (2012) [3]

1.2 Helmand province, Afghanistan 2014

On 24th September 2014 the Medical Emergency Response Team or MERT [4-6] lifted from Camp Bastion, Helmand Province, Afghanistan on what was the last conventional forces combat medevac mission of Operation HERRICK. Two of our four-person medical team were on their first MERT deployment and second ever medical mission. It was my fourth and seventy fourth respectively, amongst multiple other deployments to Iraq, Afghanistan, the Balkans and Africa. On the flight out, we learned that a previous attempt by coalition partner aircraft to reach the casualty had been beaten back by the weight of enemy fire. We were escorted by two helicopter gunships and their concerted attacks on enemy positions allowed us to land. The senior paramedic in the team jumped off with the infantry escort group, located the casualty and he was loaded on.

The injury was depressingly familiar; a neat hole drilled in the unconscious casualty's forehead, just under the helmet line. Removing the helmet revealed the rear of his head as a mess of fractures and a gaping exit wound. We couldn't stop the bleeding despite using all the modern equipment and methods at our disposal. As we lifted from the landing site we were ourselves hit by enemy fire so made for the closer coalition hospital at Kandahar where we could both take care of the casualty and assess the damage to the helicopter.

The reception at the coalition hospital in Kandahar was less practiced than that at Bastion and the receiving team seemed to struggle to understand the underlying injury mechanism, particularly relating the small entry wound with the devastation caused (the injury as expected proved unsurvivable and the casualty died that evening). This poor understanding of ballistic mechanisms is in concordance with the views of Thali et al. [7] when developing their model of ballistic head injury.

This experience and others initiated a project looking at casualties who had 'Died of Wounds', DoW, [8], that is, arrived alive at a deployed medical facility

but died later. One of the conclusions from our work was the need to research further into understanding head protection and military injury [8].

1.3 The nature of military head injury

The UK experience of the importance of head injury in battle casualties in Afghanistan is in line with those of other conflicts and militaries [9]. Champion et al. [10], stated that, while the quality of casualty data captured in different conflicts is very variable, the majority of combat injuries are from penetrating fragments. Quoting from WDMET [11] (Wound Data and Munitions Effectiveness Data Team), an extensive study from 1970 looking in detail at 7,898 patients from the Vietnam War between 1967 and 1969, they state that 37% of fatalities had suffered head injury. In ground combat, 31% of those Killed in Action (that is, dead before reaching a medical facility) had suffered head injury.

Ten years later, Tong and Beirne conducted a systematic review of head, face and neck injury in the recent Iraq and Afghanistan wars plus Israeli experience between 2001-2011 [12].

They also struggled with data quality, finding issues such as the same patient populations being reported by authors in more than one journal, and individual studies having different injury inclusion criteria. Nineteen articles met all their review requirements. The reported percentage of head, face and neck (HFN) injuries ranged from 6.4 to 54%. They concluded that a reported proportional increase in HFN trauma was due to (a) the relative decrease in fatal penetrating torso injury as people are wearing combat body armour and (b) an increase in fragment injury to the relatively unprotected HFN.

Gibson et al. [13] divide the major threats causing head injury in conflict into ballistic, blunt impact and blast mechanisms. They further subdivide ballistic impacts into penetrating injury (producing tissue shearing and crushing) and behind armour (helmet) blunt trauma, BAPT/BHBT. In BHBT the protective

helmet is deformed by a projectile, the skull beneath this is in turn impacted and deformed by the helmet material, and the brain tissue under this area of skull is damaged. In their systematic review of military head injury Carr et al. [9] noted that BHBT is of concern to a number of nations [14-17] but could find no evidence of actual BHBT injuries reported in the open literature.

Rafaels et al. [17] reference Mabry et al. [18] as providing documented examples of BABT but the only text relevant to BHBT head injury in [18] states:

'Another ranger sustained a non-penetrating GSW to the occiput. The round penetrated his Kevlar helmet, causing a scalp laceration, brain contusion, and momentary blindness, but it neither penetrated nor fractured the skull. The patient survived without complication. There are several other anecdotal instances where bullets or fragments impacted helmets but caused little or no injury' [18]

The projects in this PhD thesis are therefore concentrating on a model of overmatch penetrating injury. This is where the projectile (bullet) overmatches the protection provided by the helmet and produces a penetrating head injury. A combination of ammunition and commercially available helmet was selected to create this overmatch (Figure 1-1).

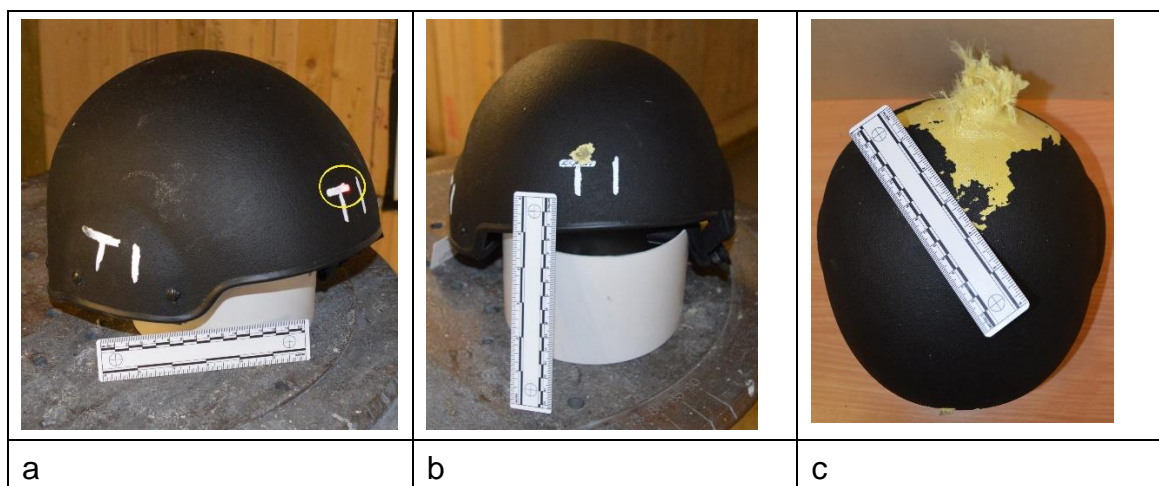


Figure 1-1 Preliminary work

Creating an overmatch event with a protective helmet

(a) On the range prior to impact; aiming laser circled (b) entry site following shooting with 7.62 x 39 mm Mild Steel Core (MSC) bullet impacting at 693 m/s (c) exit site viewed from above.

1.4 The nature of modern military helmets

Military helmets need to absorb and dissipate energy from a range of threats. The key components are an outer shell, a comfort foam liner, a suspension system and a retention system (straps) [3,19]. A variety of materials have been used to achieve this. At the time of the Afghanistan conflict in 2014, many of the helmets had outer composite shells made of para-aramid materials [19] (aromatic polyamides, [20]). This informed the choice of materials for the PhD experiments.

Breeze et al. [21] undertook a systematic review to confirm the cranial structures that should be covered by a helmet and suggested that identifiable external anatomical landmarks (the nasion, external auditory meatus and superior nuchal line) should be used as markers of the margins of the brain and used to rate the cover provided by a helmet. They also described how a greater 'stand-off distance' (the space between the skin and shell of the helmet used to provide protection from blunt impact and BHBT) made soldiers more vulnerable to fragments originating at ground level.

Helmets are tested using a number of mechanisms (summarised in [13, Table 8.3]) which include resistance to penetration by standard projectiles or bullets, and to deformation, although it is difficult to correlate the test standards with expected clinical injury. In a 2014 review of the US Department of Defense test protocols for ballistic helmets the authors state '*For combat helmets, however, the current testing methods and measures have no connection to research on head and brain injury. The lack of connection between injury and current test methods is a significant concern*' [22].

Similar concerns were expressed by Freitas et al. [16] in relation to the lack of defined criteria for injury attenuation from BHBT. They noted that two in service US military helmets (2014) had limits set around transient deformation into Roma Plastilina clay but could not find evidence that these were linked with level of injury in humans. They developed a model (the Human Head Surrogate, HHS) using commercially purchased human crania with synthetic soft tissues (Permugel™ and silicone) supported by a Hybrid III neck assembly. The model, wearing a helmet, was impacted with a series of ammunition types. A ceramic applique was placed at the front of the helmet with the higher energy impacts (7.62 x 39 mm and 7.62 x 51 mm rounds) to ensure that it did not undergo a perforating injury. The bone fractures resulting from BHBT effects were categorised as minor (surface only), moderate (full depth fractures but cranium intact) and critical (cranium fragmented). These, in turn, were mapped across to expected clinical effects including degree of intracranial damage and likely duration of loss of consciousness.

Earlier work by Sarron [15] also looked at BHBT but used a combination of dry human skulls with a synthetic (silicone) fill and fresh cadaveric heads. Both sets of models were instrumented and placed at varying distances behind protective plates of different helmet materials. The plates were impacted with 9 mm bullets and the damage to the underlying skulls and heads accessed. The damage to the skin, scalp, bone, dura and brain of the cadaveric heads was assessed with a four-point scale of 0 to 3 (where 0 = nothing and 3 = severe). Greater stand-

off distances were associated with less BHBT but would make a casualty more vulnerable to fragments originating at ground level as described above [21].

The overmatch model developed for this PhD is a different injury mechanism to BHBT but lessons from the above experiments [14-17] will be considered later in this thesis.

Aims of this PhD are to develop and validate a synthetic model that could be used in future ballistic testing. Discussion around the advantages and disadvantages of synthetic and biological surrogates for investigating ballistic injury occurs in the following chapters. An advantage of a synthetic model is that it can be used in test environments where cadaveric and animal material cannot.

1.5 Could the project have been done with computer simulation?

Tse et al. [23] have recently published a comprehensive review of the current finite element (FE) head and helmet models and how they were developed. They state that the head models have been improved by the use of medical imaging data such as CT and Magnetic Resonance Imaging (MRI). The question is to what extent these models can be used to correctly assess ballistic head injury. Both finite element (FE) and hydrocode simulations have been used for ballistic research. This section will consider a selection of these.

1.5.1 Helmets alone

Tham et al. [24] impacted Kevlar® helmets with steel spheres using a gas gun to determine the response of the helmet to impact. This was then compared to a hydrocode simulation and the authors found good correlation between the two. The hydrocode simulations were used to test the helmet against agreed test standards including penetration and the authors proposed this methodology could be used to assess the ballistic resistance of future prototype helmets. Later work by Tan et al. [25] investigated impacts on an Advanced Combat

Helmet on a Hybrid III head form, again using steel spheres and a gas gun. Accelerations of the model from the impacts were measured using strain gauges, and HSV captured the impact sequences. To build the FE models the helmet/head form assembly was CT scanned and the images imported into medical image processing software which allowed the components to be digitally separated. The actual damage on the impacted helmets was compared with that predicted by the FE simulations and the authors stated good correlation. They also proposed that the methodology could be used to improve helmet design.

1.5.2 Forensics

Raul et al. [26] investigated a case of a young male with three .22 in gunshot wounds (two in the head, one in the chest) to assess if these were the result of suicide or murder. The model used included skull (to assess fracture development) and brain tissue (to assess degree of damage and possible incapacitation from individual gunshots) and calculated likely intracranial effects on the brain tissue from the impacts. The authors proposed that the FE model could be used as an animation to illustrate what happened to a '*doubting audience*' [26].

Earlier work by Mota et al. [27] modelled the impact between a 9 mm steel projectile and human parietal bone. A key aspect of this work was describing how bone shows '*strain rate dependency*'. The authors state that at low strain rates the collagen component of bone dominates but at high strain rates the calcium phosphate (a strong but brittle material) exerts the greatest influence. They propose that such simulations offer a '*sound mechanistic*' understanding of traumatic head injury.

Zhu et al. [28], however, note that characterising the behaviour of bone and soft tissue at the high strain rates experienced in modern combat injury is difficult, and this information is needed to inform the material constants and failure criteria used in FE models. The difficulty in preparing samples of soft tissues

and trabecular bone in particular has meant a wide scatter in the derived data, which in turn will influence the outcome of FE simulations involving biological material.

1.5.3 A combined approach

Aare and Kleiven [29] undertook a combined approach. They were interested in stress on cranial bone, strain on brain tissue, pressure within the brain and acceleration effects from the impact. They echoed Thali's views [7] that head injury from ballistic impacts is not well understood. They were also critical of helmet test procedures stating that different manufacturers use different methods (making comparison difficult) and many only use maximum deflection into a piece of clay applied inside the helmet at the impact site, similar concerns to those of more recent authors [22]. Their concern with previous studies was that these tended to be a simplified head model combined with an accurate helmet or vice-versa.

Their FE helmet model was validated against ballistic tests on a helmet shell and the FE head model validated against cadaveric specimens. The FE model used was a combination of the FE helmet and head. As later confirmed by Freitas [16] they found that the stiffness of the helmet shell influences stresses in the human skull at impact, and that stress in cranial bone increases when contact is made between the helmet shell and the skull at impact. Their measurements of intracranial pressure in the FE model also correlated with those of Sarron et al. [30] who were working with a dry skull model filled with silicone gel. Aare and Kleiven [29] did state that their model had to make assumptions with regards to the properties of materials used which resonates with the concerns of Zhu et al. [28].

An RCDM project used hydrocode models to look at blast load development within the underground trains and London bus during the 7 July 2005 attacks [31] (and to quantify the blast environment the casualties were exposed to). It was essential to correlate the outputs from the hydrocode models with post

mortem reports, scene photographs, and witness statements to confirm congruence between the models and reality.

1.5.4 Computer modelling conclusions

FE and Hydrocode do have a role in in modelling ballistic impact on materials where the properties of the materials are well understood. There have been some useful studies using both FE and hydrocode to understand ballistic impacts on biological materials but at the present time there are still limitations. [28] and models need to be cross checked with actual clinical data [31]. With these caveats in mind the decision was made to base the PhD work around a real-world surrogate rather than a computer simulation.

1.6 PhD academic structure

The thesis is built around a series of experiments summarised in Figure 1-2. The numbers in the figure and the related publication are explained in the following text.

1.6.1 Gelatine blocks

Publication: Mahoney PF, Carr D, Miller D, Teagle M (2017) The effect of helmet materials and simulated bone and tissue layers on bullet behaviour in a gelatine model of overmatch penetrating head injury. Int J Legal Med 131:1765-1776 (Thesis chapter 3).

The aim of this work was to use gelatine blocks which are recognised tissue surrogates for ballistic injury to understand:

- (a) how the layers of material in a head wearing a helmet described above interact with and influence bullet behaviour
- (b) whether any of the synthetic materials have the same interactions as organic material (bone and tissue). The outcome from this project helped shape the choice of materials for the further work strands.

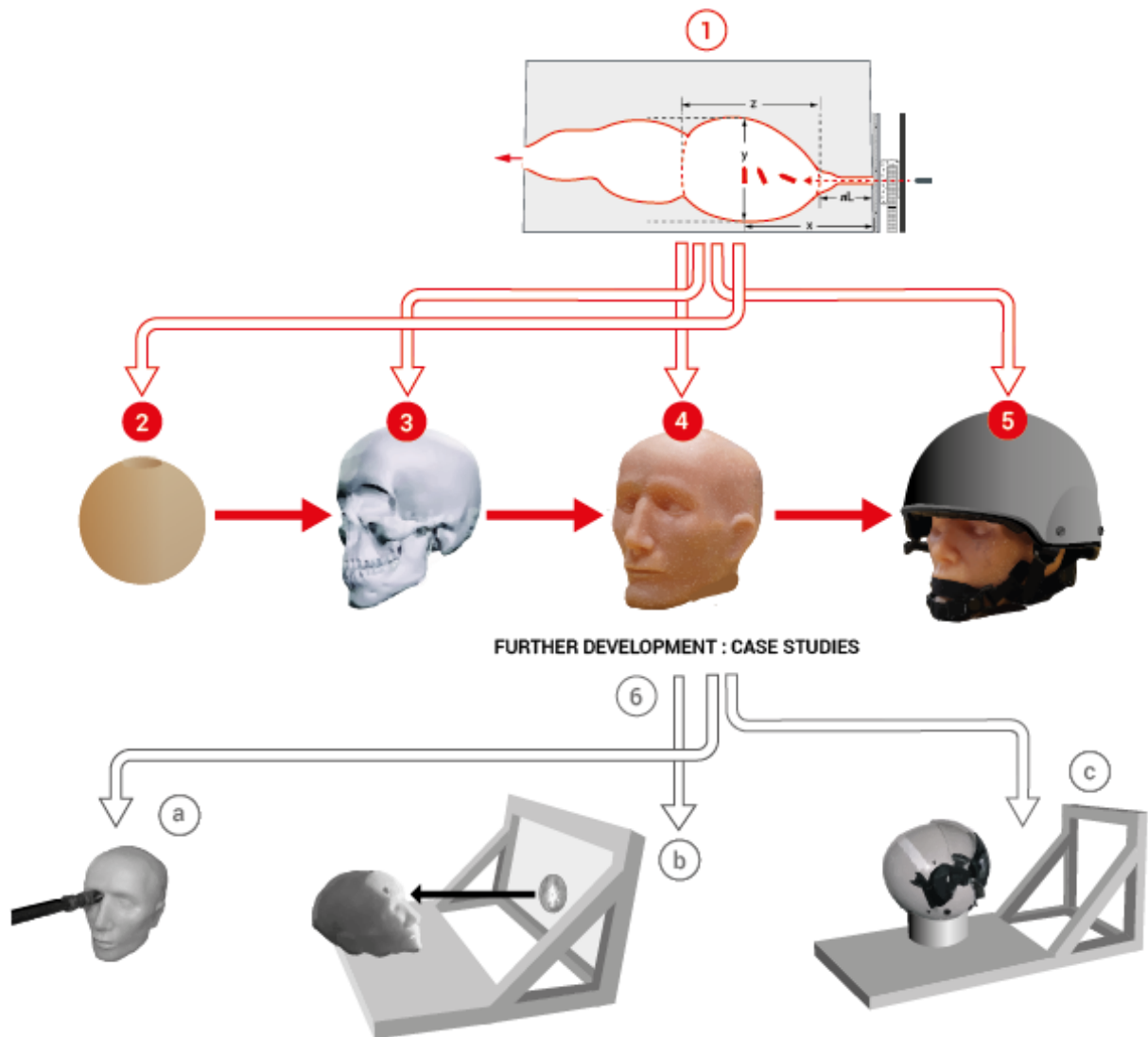


Figure 1-2 PhD academic structure

(1) gelatine blocks [33] (2) Synbone® spheres [34] (3) anatomically correct skull [35] (4) addition of synthetic facial tissues [36] (5) recreation of shooting events [37] (6) case studies.

1.6.2 Synbone® spheres

Publication: Mahoney PF, Carr DJ, Hunt N, Delaney R (2018) Assessment of polyurethane spheres as surrogates for military head injury. Int J Legal Med <https://doi.org/10.1007/s00414-018-1832-6> (Thesis chapter 4).

This short paper investigates the Synbone® sphere model designed by Thali et al. [7] to assess its utility in reproducing military ballistic events at engagement

distances. Synbone® plates (5 mm thickness) were one of the synthetic bones used in the work strand using gelatine blocks described above. Synbone® Spheres have the disadvantage that a helmet cannot be placed upon them.

1.6.3 Anatomically correct skull

Publication: Mahoney PF, Carr DJ, Delaney R, Hunt N, Harrison S, Breeze J, Gibb I (2017) Does preliminary optimisation of an anatomically correct skull-brain model produce clinically realistic ballistic injury fracture patterns? Int J Legal Med 131: 1043-1053 (Thesis chapter 5).

Recognising that Synbone® spheres cannot accommodate a ballistic helmet, this paper builds on earlier work by Carr et al. [32] to assess if an anatomically correct model of a skull produces realistic fracture patterns under ballistic impact. One of the polyurethane polymers used in this work, MU51, was assessed as 250 x 250 x 5 mm sheets in the gelatine block work strand described above.

1.6.4 Skull with synthetic skin and soft tissue

Publication: Mahoney P, Carr D, Arm R, Gibb I, Hunt N, Delaney RJ (2018) Ballistic impacts on an anatomically correct synthetic skull with a surrogate skin/soft tissue layer. Int J Legal Med 132: 519-530 (Thesis chapter 6).

This work takes the skulls evaluated in chapter 5 and adds layers of realistic skin and soft tissue to assess how this influences the development of fractures under ballistic impact. The synthetic skin material used is the same as that assessed in chapter 3.

1.6.5 Forensic case reconstruction

Publication: Mahoney PF, Carr DJ, Harrison K, McGuire R, Hepper A, Flynn D, Delaney R, Gibb I (2018) Forensic reconstruction of two military combat related shooting incidents using an anatomically correct synthetic skull with a surrogate

skin/soft tissue layer. Int J Legal Med <https://doi.org/10.1007/s00414-018-1802-z> (Thesis chapter 7).

The aim of this work was to bring the above research strands together and reproduce the injuries seen in two actual military ballistic incidents. The work was undertaken with the permission of the Wiltshire and Oxford Coroners. The materials used (helmet components, synthetic bone and synthetic skin) are the same as those in chapter 3.

1.6.6 Testing the model against additional conditions

The five papers outlined above have shown areas of the model that need further development. In addition, military ballistic incidents frequently include shootings that occur into vehicles and aircraft. Chapter 8 uses two case studies to test the model further and assesses (a) different ammunition, (b) a development of the synthetic skin, (c) a contact injury (d) the effect of shooting through laminated glass and (e) shooting through a transparent thermoplastic helicopter window.

1.7 PhD chapter structure

The overall structure is therefore:

- Chapter 1: Introduction
- Chapter 2: Aims and Objectives
- Chapter 3: Assessing the effect of gelatine blocks and intermediate layers on bullet behaviour
- Chapter 4: Evaluating the utility of Synbone® spheres for simulating military injury
- Chapter 5: Testing whether an anatomically correct skull produces realistic fracture patterns under ballistic input
- Chapter 6: Assessing the effect of a realistic skin/soft tissue layer on the fracture patterns
- Chapter 7: Using the model to recreate two actual ballistic incidents

- Chapter 8: Further assessment of a surrogate head model for military ballistic injury with case studies
- Chapter 9: Discussion
- Chapter 10: Conclusions
- Chapter 11: Future work and further development
- Appendix A: Gelatine block preparation
- Appendix B: Micro CT images from intermediate layers
- Appendix C: Bullet analysis
- Appendix D: Synthetic skin analysis
- Appendix E: Synbone® sphere data
- Appendix F: Skull data and preparation
- Appendix G: Skulls with more than one Likert-type score for fracture pattern of 3 or 4
- Appendix H: Clear ballistics gel impact sequence and burn
- Appendix I: Other head models

1.8 Experimental sequencing

The academic structure is set out above. Pragmatically, experiments had to be undertaken according to the availability of the consumables, and work strands run in parallel. The MU51 skulls and sheets came from Tai Wan; the Synbone® spheres and sheets from Switzerland. The ammunition was Ukrainian to meet the correct threat profile. The sheets of helmet material and other helmet components were bespoke orders from a UK manufacturer and the ballistic helmet order had to be fitted into a production run. The synthetic skin and faces were built by Nottingham Trent University but timetabled within a series of other projects. The transparent thermoplastic helicopter window was kindly provided by Boeing. CT scanning needed to be arranged around the primary clinical function of the department at Queen Elizabeth Hospital Birmingham. Clinical and engineering colleagues scheduled assessment and review of the shot models around other duties including, in the case of the pathologists, ongoing court cases. In addition, I needed to manage my own clinical and military

duties. The sudden loss and closure of the Impact and Armour Group at the Shrivenham site with the redundancy of the majority of the academic and technical staff (2017) meant that the good will of military colleagues was called upon to open and run the ranges, and civilian academic colleagues stepped in to undertake the required supervision.

1.9 Declaration

I, Peter Mahoney, state that the work presented in this thesis is my own and that co-authors provided guidance on interpreting the research, technical assistance in conducting the experiments and editorial input into the manuscript.

1.10 References

1. British Medical Journal (1915) 2: 143
2. Projectiles and other engines of destruction (1942). In: Hamilton Bailey (Ed) Surgery of Modern Warfare (2nd Edn). E&S Livingstone, Edinburgh. p10
3. Hamouda AMS, Sohaimi RM, Zaidi AM, Abdullah S (2012). Materials and design issues for military helmets. In: Sparks E (Ed) Advances in Military Textiles and Personal Equipment. Woodhead Publishing Series in Textiles Number 122, Cambridge, UK. pp 103-138
4. Shifting sands. In: Nichol J, Rennel T (2009) Medic; Saving Lives from Dunkirk to Afghanistan. Viking, London. pp 347-370
5. Pope CG, Wright C, Lundy JB, Nordmann G, Gower D, Fricks S, Smith LN, Rush S (2015) Military prehospital medicine. In: Buckenmaier C, Mahoney PF (Eds) Combat Anaesthesia: the First 24 Hours. Office of the Surgeon General, Borden Institute, Fort Sam Houston TX. pp 41-55
6. The Medical Emergency Response Team (MERT). In Mayhew E (2017) A Heavy Reckoning; War, Medicine and Survival in Afghanistan and Beyond. Wellcome Collection, London. pp 45-60
7. Thali MJ, Kneubuehl BP, Zollinger U, Dirnhofer R (2002) The 'Skin-skull-brain model': a new instrument for the study of gunshot effects. Forensic Science International 125 (2-3): 178-189
8. Keene DD, Penn-Barwell JG, Wood PR, Hunt N, Delaney R, Clasper J, Russell RJ, Mahoney PF (2016) Died of Wounds: a mortality review. J R Army Med Corps 162: 355-360

9. Carr DJ, Lewis E, Horsfall I (2017) A systematic review of military head injuries. *J R Army Med Corps* 163:13-19
10. Champion HR, Bellamy RF, Roberts P, Leppaniemi A (2003) A profile of combat injury. *J Trauma* 54: S13-S19
11. Champion HR, Lawnick M (2006) Coding of the WDMET Database. Tech Med Inc, Annapolis MD [Accessed online 10/02/2018]
12. Tong D, Beirne R (2013) Combat body armour and injuries to the head face and neck region: a systematic review. *Military Medicine* 178: 421-6
13. Gibson T, Shewchenko N, Whyte T (2017) The skull and brain: test methods behind armour blunt trauma and helmet design. In: Franklyn M, Lee PVS (Eds) *Military injury biomechanics*. CRC Press, Boca Raton, FL. pp 119-158
14. Bass C, Bolduc M, Wacawik S (2002) Development of a non-penetrating, 9 mm, ballistic helmet, trauma test method. *Personal Armour Systems Symposium*, November 18-22, The Hague, The Netherlands. pp61-68
15. Sarron JC, Dannawi M, Faure A, Caillou J-P, Da Cunha J, Robert R (2004) Dynamic effects of a 9 mm missile on cadaveric skull protected by aramid, polyethylene or aluminium plate: an experimental study. *J Trauma* 57: 236-247
16. Freitas CJ, Mathis JT, Scott N, Bigger RP, MacKiewicz J (2014) Dynamic response to a behind helmet blunt trauma measured with a human head surrogate. *Int J Med Sci* 11: 409-425 doi: 10.7150/ijms.8079 (Accessed 23/03/2016)

17. Rafaels KA, Cutcliffe HC, Salzar RS, Davis, M, Boggess B, Bush B, Harris R, Rountree MS, Sanderson E, Campman S, Koch S, Bass CR (2015) Injuries of the head from backface deformation of ballistic protective helmets under ballistic impact. *J Forensic Sci* 60: 219-225
18. Mabry R, Holcomb JB, Baker AM, Cloonan CC, Uborchak JM, Perkins DE, Canfield AJ, Hagmann JH (2000) United States army rangers in Somalia: an analysis of combat casualties on an urban battlefield. *J Trauma* 49: 515-529
19. Breeze J, Lewis E, Carr DJ (2017) Ballistic threats and body armour design In: Franklyn M, Lee PVS (Eds) *Military Injury Biomechanics*. CRC Press, Boca Raton, FL. pp 5-17
20. Boussu F, Bruniaux P (2012) Customisation of a light weight bullet -proof vest for the female form. In: Sparks E (Ed) *Advances in military textiles and personal equipment*. Woodhead Publishing Series in Textiles Number 122, Cambridge, UK. pp167-195
21. Breeze J, Baxter D, Carr D, Midwinter MJ (2015) Defining combat helmet coverage for protection against explosively propelled fragments. *J R Army Med Corps* 161:9-13
22. Combat helmet testing. In: *Review of Department of Defense Test Protocols for Combat Helmets* (2014). Committee on review of test protocols used by DoD to test combat helmets, Board on Army Science and Technology; Division on Engineering and Physical Sciences; National Research Council, National Academies of Science. ISBN 978-0-309-29866-7. pp25-31
23. Tse KM, Tan LB, Lee HP (2017) The skull and brain: computer models for the head and its protection. In: Franklyn M, Lee PVS (Eds) *Military injury biomechanics: the cause and prevention of impact injuries*. CRC Press, Boca Raton. pp175-219

24. Tham CY, Tan VBC, Lee HP (2008) Ballistic impact of a Kevlar® helmet: experiment and simulations. *International Journal of Impact Engineering* 35:304-318
25. Tan LB, Tse KM, Lee HP, Tan VBC, Lim SP (2012) Performance of an advanced combat helmet with different interior cushioning systems in ballistic impact. Experiments and finite element simulations. *International Journal of Impact Engineering* 50: 99-112
26. Raul J-S, Deck C, Meyer F, Geraut A, Willinger R, Ludes B (2007) A finite element model investigation of gunshot injury. *Int J Legal Med* 121: 143-146
27. Mota A, Klug WS, Ortiz M, Pandolfi A (2003) Finite-element simulation of firearm injury to the human cranium. *Computational Mechanics* 31:115-121
28. Zhu F, Saif T, Presley BR, Yang KH (2017) The mechanical behaviour of biological tissue at high strain rates. In: Franklyn M, Lee PVS (Eds) *Military Injury Biomechanics: the Cause and Prevention of Impact Injuries*. CRC Press, Boca Raton. pp103-118
29. Aare M, Kleiven S (2007) Evaluation of head response to ballistic helmet impacts using the finite element method. *International Journal of Impact Engineering* 34: 596-608
30. Sarron JC, Caillou JP, Da Cunha J, Allain JC, Tremecon A (2000) Consequences of non-penetrating projectile impact on a protected head: study of rear effects of protections. *J Trauma* 49: 923-9
31. Hepper AE, Pope DJ, Bishop M, Kirkman E, Sedman A, Russell R, Mahoney PF, Clasper J (2014) Modelling the blast environment and relating this to clinical injury: experience from the 7/7 Inquest. *JR Army Med Corps* 160: 171-174

32. Carr D, Lindstrom A-C, Jareborg A, Champion S, Waddell N, Miller D, Teagle M, Horsfall I, Kieser J (2015) Development of a skull/brain model for military wound ballistics studies. *Int J Legal Med* 129: 505-10
33. Mahoney PF, Carr D, Miller D, Teagle M (2017) The effect of helmet materials and simulated bone and tissue layers on bullet behaviour in a gelatine model of overmatch penetrating head injury. *Int J Legal Med* 131:1765-1776
34. Mahoney PF, Carr DJ, Hunt N, Delaney R (2018) Assessment of polyurethane spheres as surrogates for military head injury. *Int J Legal Med* <https://doi.org/10.1007/s00414-018-1832-6>
35. Mahoney PF, Carr DJ, Delaney R, Hunt N, Harrison S, Breeze J, Gibb I (2017) Does preliminary optimisation of an anatomically correct skull-brain model produce clinically realistic ballistic injury fracture patterns? *Int J Legal Med* 131: 1043-1053
36. Mahoney P, Carr D, Arm R, Gibb I, Hunt N, Delaney RJ (2018) Ballistic impacts on an anatomically correct synthetic skull with a surrogate skin/soft tissue layer. *Int J Legal Med* 132: 519-530
37. Mahoney PF, Carr DJ, Harrison K, McGuire R, Hepper A, Flynn D, Delaney R, Gibb I (2018) Forensic reconstruction of two military combat related shooting incidents using an anatomically correct synthetic skull with a surrogate skin/soft tissue layer. *Int J Legal Med* <https://doi.org/10.1007/s00414-018-1802-z>

2 AIMS AND OBJECTIVES

2.1 Aims

The aims of this study were to:

- A. Develop a synthetic head model suitable for ballistic testing with military ammunition.
- B. Use the model to recreate actual military ballistic incidents.

2.2 Objectives

The objectives of this study were to:

1. Analyse the effects bone, synthetic bone, synthetic skin and helmet materials have on bullet behaviour when impacted as intermediate targets in front of a gelatine block (chapter 3).
2. Critique the utility of the current standard head surrogate (a synthetic bone sphere) for modelling military ballistic head injury (chapter 4).
3. Evaluate the effect of different gelatine fills and structural polymers on the fracture patterns produced in a realistic synthetic skull under ballistic impact (chapter 5).
4. Assess how synthetic skin and soft tissue behaves under ballistic impact and the effect on fracture patterns in a realistic skull model (chapter 6).
5. Evaluate the injuries produced in the models against actual cases and other likely militarily relevant scenarios (chapters 7 and 8).

3 THE EFFECT OF HELMET MATERIALS AND SIMULATED BONE AND TISSUE LAYERS ON BULLET BEHAVIOUR IN A GELATINE MODEL OF OVERMATCH PENETRATING HEAD INJURY

Mahoney PF, Carr DJ, Miller D, Teagle M.

Publication: (2017) Int J Legal Med 131: 1765-1776

3.1 Abstract

The aim of this work was to simulate an overmatch ballistic event against a head wearing a helmet. The experiments were designed to understand how layers of bone (or synthetic bone), synthetic skin and currently used helmet materials influence the behavior of full metal jacket mild steel core (FMJ MSC) 7.62 x 39 mm bullets, impacting on targets with a mean velocity of 650 m/s. Bullet behaviour within 10% (by mass) gelatine blocks was assessed by measurements made of the temporary cavity within the blocks using high speed video and of the permanent cavity by dissecting blocks post-firing. While ANOVA did not find significant difference at the 0.05 level in the mean values of most of the measurements, there was a significant difference in neck length within the gelatine blocks. The addition of material layers did produce greater variability in the temporary cavity measurements under some of the conditions. One of the synthetic bone polymers with a synthetic skin layer produced similar results within the gelatine blocks to the horse scapulae (with residual tissue) and may be suitable for future ballistic experiments.

Key words: Gelatine, Helmet, Ballistic, 7.62 x 39 mm bullet, synthetic bone, synthetic skin

3.2 Introduction

Ballistic head injury remains a significant threat in combat [1]. A recent review of the open access literature [2] concluded that fatal head injuries are mainly from bullets overmatching helmets or fragments penetrating through the face. The authors also stated the need for further research into the causes and severity of head injury to assist designers of military helmets and associated personal protective equipment.

A review of gunshot injury in UK military casualties [3] looked at ballistic features associated with wound severity. The study examined extremity injuries in detail and concluded that factors associated with high energy transfer (bullets that fragmented, bullets that fractured bone and bullets that didn't pass straight through the body) were associated with more complex wounds requiring repeated debridement. Factors influencing outcome from ballistic head injury are even more complicated [4] and include the volume of injured brain, overall casualty physiology (such as the presence of shock and coagulopathy) and whether the impact was from a bullet or fragment.

The aim of the work described here was to simulate an overmatch ballistic event against a simplified model of a head wearing a helmet. The experiments were designed to understand how layers of bone (or synthetic bone), synthetic skin and currently used helmet materials interact sequentially with 7.62 x 39 mm bullets fired under standard conditions and influence the bullet behaviour within 10% (by mass) gelatine blocks. The final model including all layers is summarised in Figure 3.1. Understanding these interactions between the bullet and the material layers should, in turn, offer some understanding of ballistic head injury mechanisms and allow the performance of new protective materials to be assessed and compared.

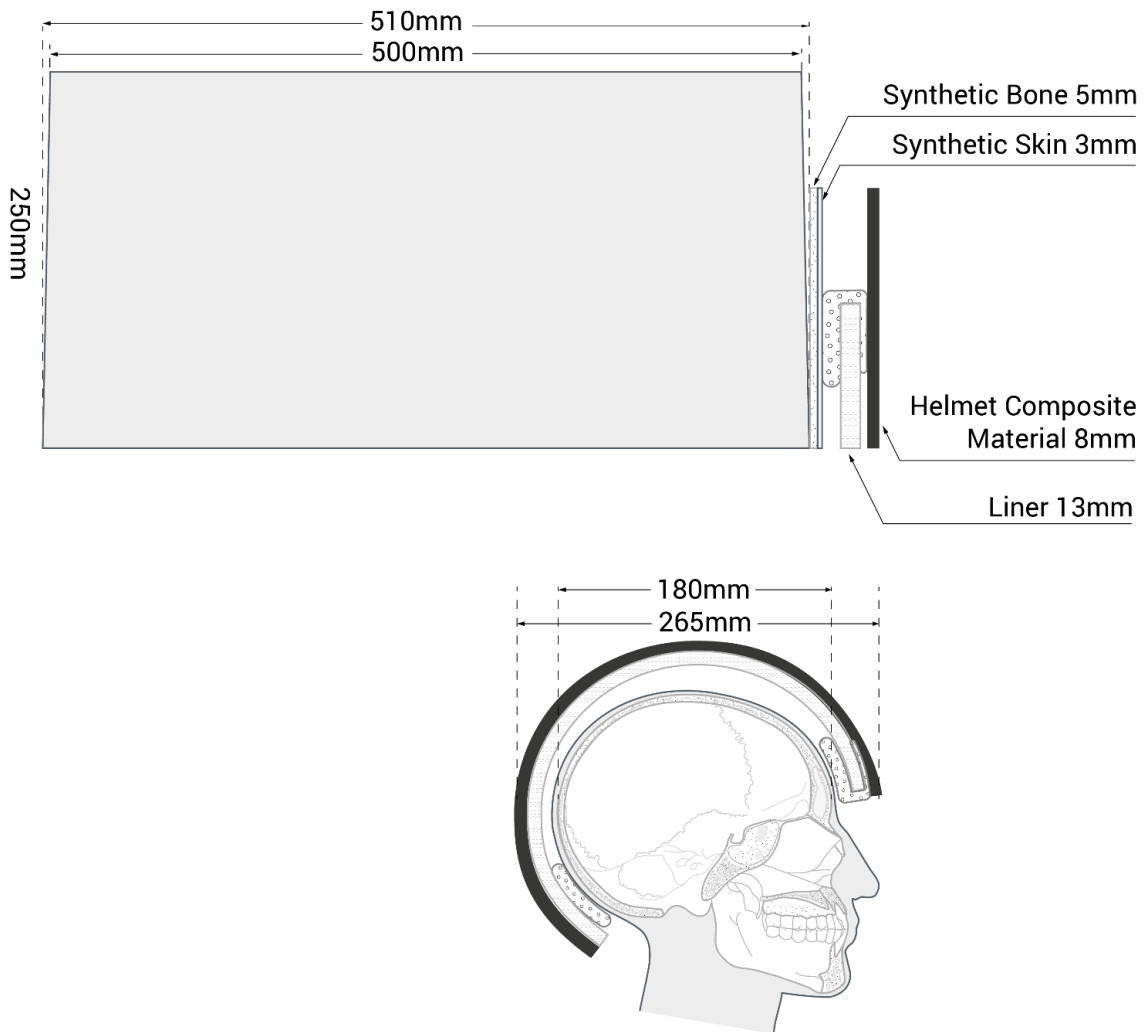


Figure 3-1 Gelatine block compared with helmet model

Upper image: Diagram of 10% (by mass) gelatine block and material layers placed in front of the block. Lower image: Cut away head wearing a combat helmet (on same scale as the block) to illustrate the material layers in situ. The material enclosing the top of the liner in the upper diagram is the comfort pad (seen front and rear in the lower diagram).

A variety of approaches have been used to model ballistic injury including impacts on cadavers, animals and tissue simulants. This has been the subject of a recent review [5]. The authors describe the ethical and practical difficulties in using human materials and in vivo animal specimens for ballistic investigations. Practical issues include the variability in tissue properties among fresh, thawed and embalmed specimens [6]. Tissue simulants such as gelatine

allow ballistic events to be imaged and recorded but lack the complexity of real soft tissue [5]. Our model was constructed around gelatine and synthetic materials (with the exception of horse scapulae in one of the experimental conditions) in order to standardise events as much as possible. Test materials need to be chosen with care and with an understanding of both their benefits and limitations. This will be considered further below.

3.2.1 Brain

Different materials have been used to simulate brain in ballistic impact research. Recent work by Falland-Cheung et al. [7] reviewed the properties of a selection of simulants and investigated mixtures of agar/glycerol and agar/glycerol/water (impacted with a 0.22 in caliber air rifle pellet) compared with deer brain. Agar/glycerol/water specimens conditioned to 22°C behaved in a similar fashion to the deer brain both under impact and in post impact damage patterns. Thali et al. [8] used gelatine 10% at 4°C to represent brain in their development of a 'Skin-skull-brain model'. The model also used a layered polyurethane sphere to represent the skull and silicon for the scalp, and the authors reported that the damage caused to the model by experimental gunshot was comparable to that seen in real injury.

Recent work [9] has reported that synthetic skulls filled with 10% gelatine produced realistic fracture patterns when shot with 7.62 x 39 mm ammunition. No statistical difference was seen when the 10 % gelatine was compared with 3, 5, 7 % gelatine and Permangel™.

Jussila [10] in describing the qualities that tissue simulants should possess, noted that they do not need to be exactly the same biomechanically as living tissue, provided '*the results can be measured and appropriately extrapolated or scaled*'.

While accepting that 10% gelatine is not a completely biofidelic brain simulant [11] its use for the current project allows reference to our earlier work [9] and the bullet behavior to be captured by high speed video.

Different methods have been described for assessing and evaluating the damage caused to gelatine blocks by the bullet impact.

Fackler and Malinowski [12] described four components of missile-tissue interaction (penetration, missile fragmentation, permanent cavity size and temporary cavity size). They assessed these for a series of different bullets impacting on 10% (by weight, sic) gelatine blocks and summarised them as a drawing composite to give a 'wound profile'. They noted that the temporary cavity was largest at the point where the bullet was at maximum (90 degree) yaw. Berlin et al. [13] illustrate a similar observation (Figure 15 of their paper) when looking at cavity size in soap blocks and relating this to bullet 'tumbling' (yaw).

Kneubuehl [14] considers rifle bullet behavior separately for full metal jacket and non-deforming/non-fragmenting bullets, compared with deforming and fragmenting bullets. For the type of bullet used in this current work (full metal jacket, mild steel core, MSC) he describes three distinct sections in the temporary cavity. The first section (the narrow channel or neck) is a straight entry channel. The length of this depends on the form of the bullet tip, the bullet's gyroscopic stability and the angle of incidence at the point of impact with the target [14, p98].

The second section is the widest part of the temporary cavity which begins as the bullet yaws, caused by a combination of decreasing bullet velocity, increased angle of incidence within the gelatine and increased overturning moment acting on the bullet. At 90 degrees yaw, as noted above, the bullet is in contact with the gelatine over its full length, causing rapid deceleration and energy transfer into the gelatine (Figure 3-6). Rotation of the bullet about its centre of gravity forces the base or tip of the bullet into the gelatine at high velocity.

In the third section of the temporary cavity the bullet yaws under the influence of damping forces until it is perpendicular to its direction of travel. It then tends to move forward, rocking backwards and forwards about its centre of gravity, and produces a second temporary cavity.

Fackler and Malinowski [12] estimated the diameter of the temporary cavity by dissecting the gelatin block after shooting and adding together the radial lengths of the two largest radial cracks. Subsequent work by Ragsdale and Josselson [15] using handgun ammunition fired into 20% gelatin found that these simple calculations both over and under estimated the temporary cavity when compared with measurements from high speed films.

Jussila [16] describes how the temporary cavity and its immediate aftermath create damage within the gelatine leaving a permanent channel and fissures. This reflects the kinetic energy dissipated into the gelatine. Jussila described a number of methods to estimate this energy transfer requiring measurement of the fissures within the gelatine. Schyma and Madea [17] moulded foil bags containing acryl paint into the front of gelatine blocks such that the bullet impact spread paint all through the gelatine cracks. This in turn aided crack measurement.

Mabbot et al. [18] dissected gelatine blocks post shooting but also captured the temporary cavity using a high-speed video camera. Once the image file was calibrated using a known length visible in the picture, the pixels could be equated to millimeters. Key measurements were the largest diameter of the temporary cavity and the depth penetration of the bullets into the blocks. Our model uses 10% gelatine blocks, and the bullet impact is assessed through both images captured by high speed video camera and post impact block dissection.

3.2.2 Bone

De Boer et al. [19] measured cranial vault thickness in 1097 autopsy cases. In the adult male subgroup (655 subjects) the mean thickness of frontal bone was 6.15 mm (SD 1.91 mm). The Third Patten Report [20] states that '*a specific*

location on the scapula of a cow has mechanical properties similar to that of the human skull’.

This is reinforced by Smith et al. [21] who investigated the impact of flint tipped arrows on fresh cattle and pig scapulae, used to simulate human cranial bone. Smith et al. described the structural similarities as ‘areas of relatively flat bone consisting of a thin trabecular portion sandwiched between two cortical layers’ [21]. Smith also noted that the scapulae retained up to 5mm of soft tissue and suggested this might be similar to that overlying the human cranium [21].

Bone has been simulated using a number of different polymers. While these lack the intricate structure of real bone [22] they have been shown to produce similar macroscopic fracture patterns to real bone under ballistic impact [8, 9, 23] as described above.

This current work compared impacts on flat sheets of these two types of synthetic bone and routine post mortem specimens of horse scapulae (Royal Veterinary College London). As with Smith’s work [21] the scapulae used in our work retained a layer of soft tissue of around 3 to 5 mm.

3.2.3 Skin

Jussila et al. [24] undertook a review of the ballistic and mechanical properties of human skin and simulants from the published literature. They noted how the structural layers of human skin all have different properties and absorb varying amounts of impact energy, and that this changes with location on the body and a person’s age. They went on to assess a series of synthetic and natural materials against published cadaveric values. Measurements included the threshold velocity required for a given projectile to penetrate the materials and the elongation at break of the materials. The best natural simulant proved to be ‘*semi-finished chrome tanned upholstery ‘crust’ cowhide*’ [24]. One of the natural rubbers tested provided a possible use as a threshold velocity filter for projectile impacts but had much greater maximum elongation than human skin. The authors stated that an easy to use high fidelity synthetic material was needed for wound ballistic research.

Falland-Cheung et al. [25] have also described how factors such as age, sex and health affect the mechanical properties of human skin, and how a reliable synthetic substitute would be useful for impact testing. They compared the mechanical properties of porcine skin with dental silicones. While the properties of the porcine skin and silicones differed, the silicone tear strength was similar to that reported for human skin in the literature.

For this work, synthetic skin was manufactured by Nottingham Trent University Flexural Composites Research Laboratory [NTU FCRL] and is further described below. NTU FCRL are involved in a series of projects with both the Impact and Armour Group and the Royal Centre for Defence Medicine (RCDM) simulating tissue for clinical and ballistic protection projects.

3.2.4 Head model

Watkins et al. [26] illustrate the difficulties in visualizing ballistic events within the skull. They describe a model devised in the mid-1970s consisting of dried human skulls filled with 20% gelatin and covered with two layers of gelatin soaked chamois leather. They further developed this by placing a pressure transducer into the model through the foramen magnum. The models were impacted with either 3mm or 6mm ball bearings in a series of 12 experiments. In the early experiments, they used the pressure traces to understand the mechanisms occurring within the skulls during impact. In the later experiments, a pulsed X-ray source was used to produce a train of 50 images at millisecond intervals during the impact events. A cine camera was used to capture the resulting images. The cine X-ray images were then projected onto a screen and the cavities in the gelatine drawn around frame by frame for analysis. In the last two series, the pressure waves were correlated with the images.

The model used in our current work clearly does not have the morphology of a skull or a head wearing a helmet but does represent an attempt to understand how the material layers in a head model influence bullet behavior.

3.2.5 Helmet

The design of combat helmets has evolved to defeat the ballistic and other threats of warfare [27]. Modern helmets are made of a series of discrete layers. The outer protective layer is usually a reinforced composite shell containing woven fabric. There is then a non-ballistic liner for impact protection and a size adjustment system. Comfort pads are located at the front and rear of the helmet [28]. For the model used in this experiment, para-aramid panels of the same areal density (bulk density x thickness; kg/m²) as an in-service helmet outer layer, the inner non-ballistic liner and a series of comfort pads were sourced from a helmet manufacturer (Morgan Advanced Materials, Coventry) and the model constructed as shown in Figures 3-1, 3-3 and 3-6.

Kieser et al. [29] experimented with 5.56 x 45 mm ammunition fired at deer femur embedded in 20% gelatine. They found that denim fabric draped on the anterior surface of the target caused more rapid bullet yaw, larger and more superficial temporary and permanent cavities and an increased risk of indirect fracture in the femur. A key question in our current work was whether or not the helmet materials would influence bullet behavior and in turn impact on the 'injury' within the gelatine.

3.3 Materials and Methods

The research described in this chapter was carried out in a number of stages.

3.3.1 Gelatine

Gelatine from a single batch (GELITA® AG, UferstraBe 7, D-69412, Eberbach, Germany; Batch: 073358; Bloom strength 263) was used to manufacture 10% (by mass) gelatine blocks. The mould in which the blocks were set and conditioned measured 250mm (w) x 250mm (h) x 500mm (l) producing blocks of 32kg. The sides of the moulds tapered by 1° to facilitate set gelatine removal [30, 31]. After setting, the blocks were conditioned at 4°C for 24 hours. Raw data for the gelatine blocks is presented in Appendix A.

The blocks were placed 10m down range from the end of an Enfield Number 3 Proof Housing at the Small Arms Experimental Range, Cranfield University, Defence Academy of the United Kingdom, Shrivenham.

A 5.5 mm ball bearing was fired at each block and depth of penetration measured and compared with results collected from previously published work to ensure only validated gelatine blocks were used for testing [10,31] The raw data for this is presented in Appendix A.

Each of the six validated blocks was shot once with 7.62 x 39 mm Ukrainian mild steel core ammunition from a single batch (Soviet State Factory, Lugansk, manufactured 1967) ensuring the impact of the bullet did not overlap with the ball bearing tract. The ammunition chosen had been used in our previous work [9] and is representative of an ammunition type NATO troops have faced in recent conflict [3]. Data on bullet assessment is presented in Appendix B.

Impact velocities were recorded using a Weibel W-700 Doppler radar and the impact events recorded using Phantom V1212 and V12 high speed video cameras set up to record the temporary cavity development within the block and the strike face impact respectively (V1212 Sample rate 40,000 frames per second; exposure time 2 microseconds, resolution 384 x 288; V12 Sample rate 28,000 frames per second; exposure time 5 microseconds, resolution 512 x 384).

Subsequent stages added layers in front of validated gelatine blocks into which a single projectile was fired as above.

3.3.2 Synthetic Bone

The experiment was repeated with further blocks of gelatine (n=12) but with sheets of two different types of 250 mm x 250 mm x 5 mm synthetic bone placed against the block strike face:

- a. Synbone®, Synbone AG, Neugutstrasse 4, 7208 Malans, Switzerland, n=6;
- b. ARRK MU51 polymer, ARRK Europe Ltd, Gloucester Technical Centre, Olympus Park, Quedgeley, Gloucester, Gloucestershire GL2 4NF, n=6.

Synbone® flat plates and spheres were used by Smith et al. [22] when evaluating the suitability of polyurethane bone substitutes for trauma simulations. ARRK MU51 polymer skulls were used in our recent assessment of ballistic fracture patterns in synthetic skulls [9]. Example Micro CT scans of the impacts are presented in Appendix C.

3.3.3 Horse Scapulae

Horse scapulae (n=6) were sourced from routine post mortem specimens (Department of Pathology and Pathogen Biology, Royal Veterinary College, London) and each was positioned in front of the strike face of a validated gelatine block. Bone thickness was measured at different sites on each scapula using calipers and a suitable impact site chosen on each (mean thickness 6.5 mm; SD 1 mm) to simulate frontal bone in line with the measurements described by De Boer and Van der Merwe [19]. The horse scapula was secured so as to ensure a flat portion was in contact with the strike face of the gelatine block (Figure 3-2a). As noted above and visible in Figure 3-2 a & b, a layer of soft tissue was present on the scapulae. Example Micro CT scans of the impacts are presented in Appendix C.

3.3.4 Synthetic Skin and Synthetic Bone

Six sheets of synthetic skin were sourced from the NTU FCTL measuring 250 mm x 250 mm x 3 mm. This was constructed in two layers to simulate the epidermis and dermis. Both layers were made using a platinum organosiloxane gel and fibre fillers.

Each sheet was cut into three pieces. One piece of each was secured to the impact face of a sheet of MU51 synthetic bone (n=6) using a two-part silicone adhesive supplied by NTU FCTL to simulate the skin and bone of the forehead.

Each synthetic skin/bone assembly was placed in front of a validated gelatine block and the experiment repeated. A second piece was reserved for the experiments involving helmet layers.

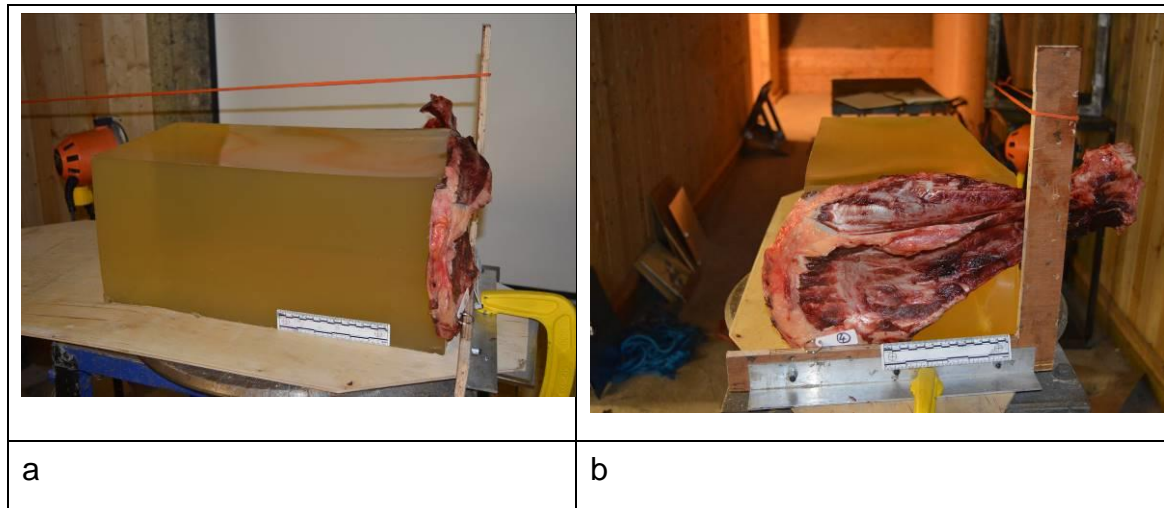


Figure 3-2 Scapulae experimental set up

(a) scapula 6 side view (b) scapula 6 front view.

The third piece of synthetic skin from each sheet was used to confirm material characteristics in accordance with BS ISO 34-1:2015 using a trouser tear test on an Instron 5567 Universal Test Machine (30kN frame limit), computer controlled using Bluehill 2.6 software (2005), and the load cell balanced between each test. Each specimen also underwent hardness testing with a Shore A Durometer. Characteristics of the synthetic skin are summarised in the results section below. Raw data is presented in Appendix D.

3.3.5 Helmet Simulant, Synthetic Skin and Synthetic Bone

Flat sheets of helmet material (250 mm x 250 mm x 8 mm), helmet liner and helmet comfort pads were purchased from a helmet manufacturer (Morgan Advanced Materials, 473 Foleshill Road, Coventry, CV6 5AQ).

The helmet liner was cut to rectangular shapes of 200 mm x 135 mm x 13 mm to allow placement of a comfort pad (Figure 3-3a).

Each layered assembly (n=6) was placed in front of the same MU51 synthetic bone/synthetic skin combination described above and both positioned in front of a validated 10% gelatine block (Figure 3-3b).

The aim was to simulate a bullet perforating a military helmet and the underlying skin and bone layers before entering the brain.

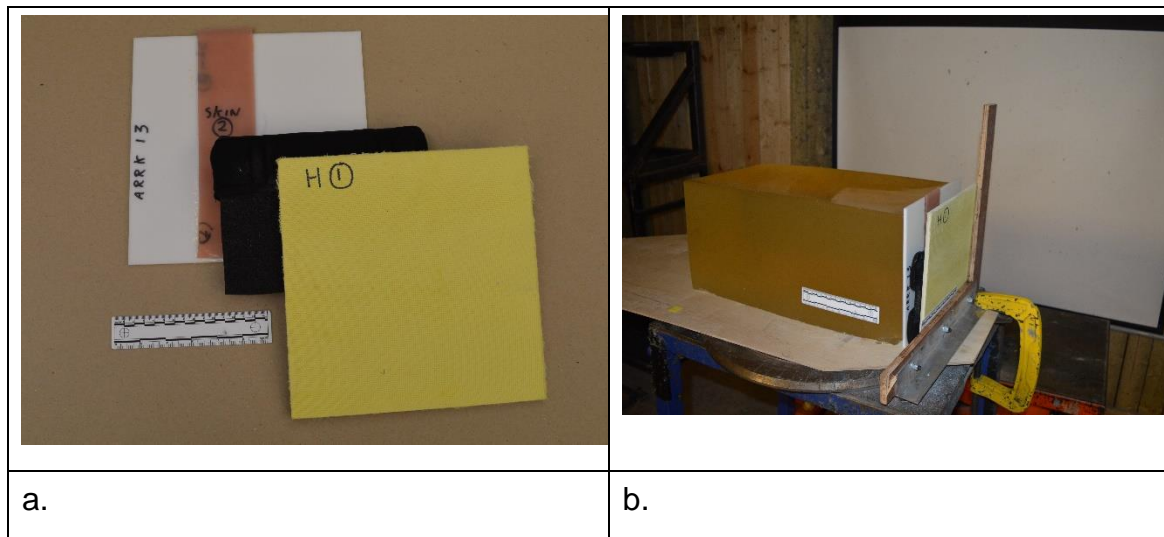


Figure 3-3 Helmet layers

(a) layers front to back: helmet material, liner plus comfort pad, synthetic skin, synthetic bone (b) helmet, liner plus comfort pad and skin/bone layers in situ prior to ballistic impact.

3.4 Measurements

Each gelatine block was dissected post firing by cutting along the permanent cavity and any debris (such as bone and polymer fragments) noted and photographed. Damaged areas within the gelatine permanent cavity were measured and photographed. The condition of the synthetic bones, horse scapulae, synthetic skin and helmet components were also photographed (e.g. Figure 3-4 a & b).

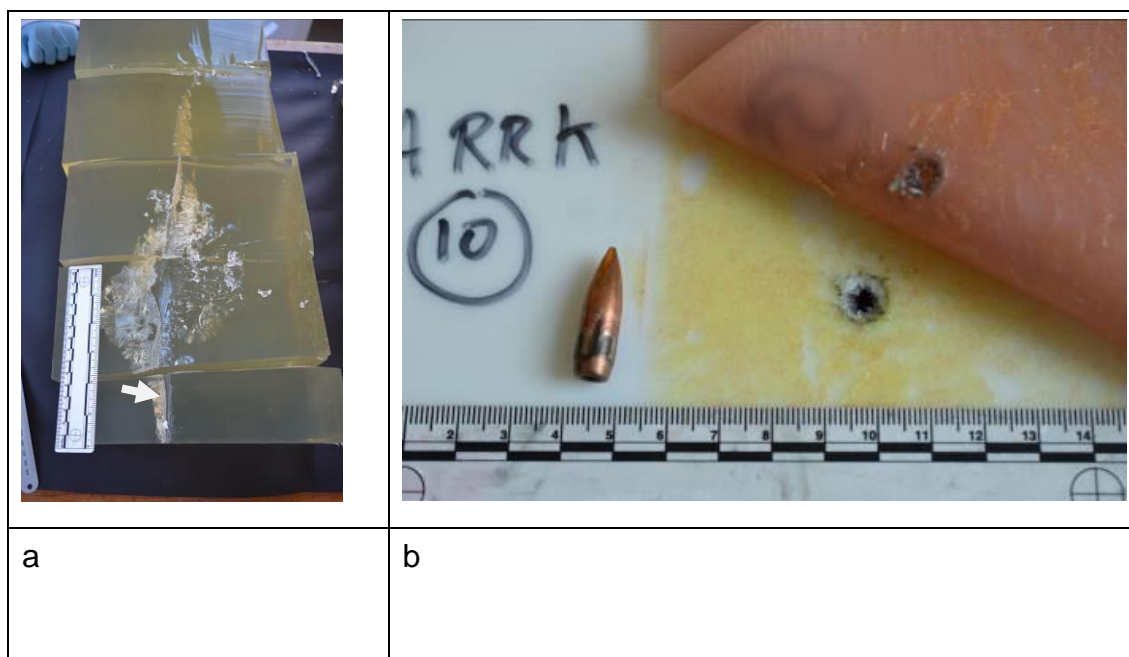


Figure 3-4 Post-impact assessments

(a) gelatine block dissection from which neck length, nL , (or 'narrow channel' [14]) was measured [arrowed] (bullet entry is into the horizontal face at the lower aspect of the figure; gelatine block has been cut in half lengthways to display the permanent cavity) (b) close up of synthetic skin 'exit wound' and ARRK/MU51 10 'entry wound' with associated bullet.

Measurements were taken from the high-speed video using the Phantom software (Visions Research, Phantom Camera Control Application 2.6). Each file was calibrated using a known length (forensic ruler) present in the image. As a check on the accuracy of the measurements from the images, the known lengths of the gelatin blocks and thickness of the synthetic bone plates were also measured from the images and compared with those of the actual objects and found to be within ± 0.5 mm) An example impact sequence for a scapula is shown in Figure 3-5 a-d.

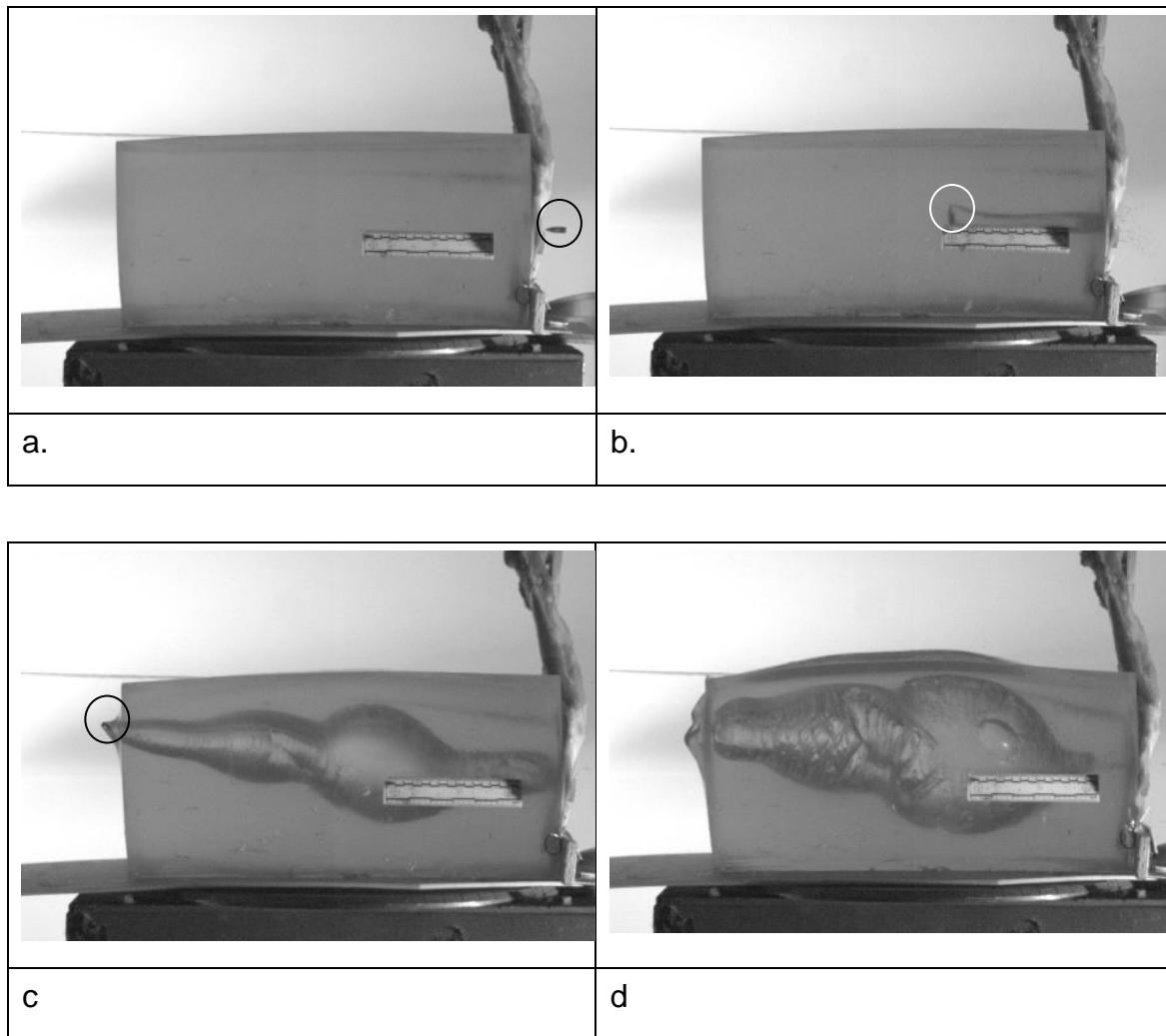


Figure 3-5 High speed video impact sequence scapula 1, side view

(a) immediately pre-bullet impact; bullet is visible in right hand side of image (b) bullet at 90° yaw within gelatine block (c) bullet visible on left hand side of image exiting gelatine block (d) cavity at maximum size after bullet exit (bullet circled in images a-c).

The area of interest for this work was the front half of the block- as the distance travelled by the bullet equates to that of a head wearing a helmet (Figures 3-1, 3-6, 3-7, 3-8 a & b).

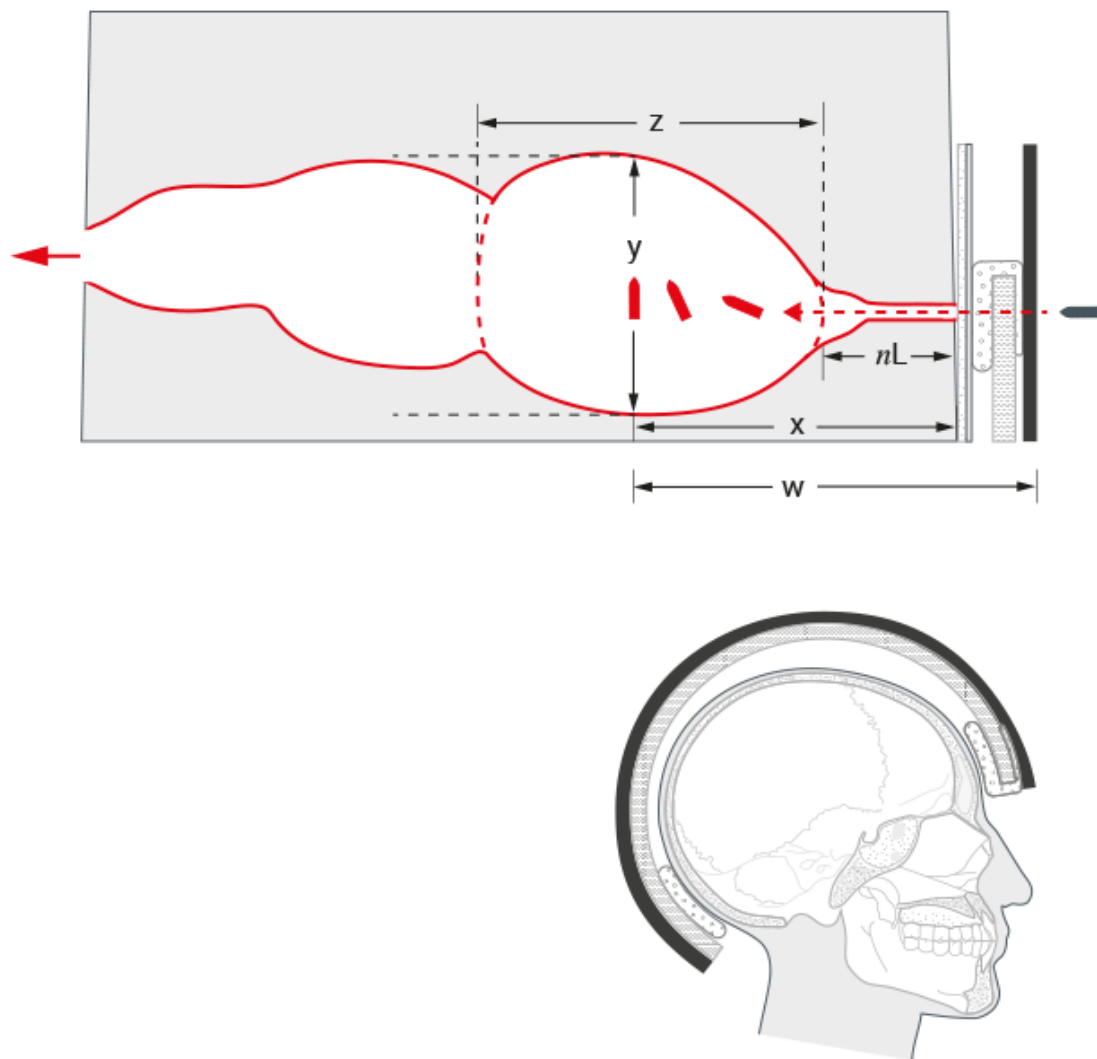


Figure 3-6 Measurements within gelatine blocks

(upper) representation of bullet path through full model and resulting temporary cavity (after references [12] and [14]) with measurements taken from the high-speed video

(lower) head wearing helmet (to scale). Material layers and scale are as labelled in Figure 3-1

w= bullet point of entry of external structures (synthetic bone etc) to bullet 90-degree yaw

x= bullet point of entry into block to 90-degree yaw

y= maximum height of first part of temporary cavity

z= maximum length of first part of temporary cavity

nL =Neck length; This was measured from the block dissections (Figure 3-5).

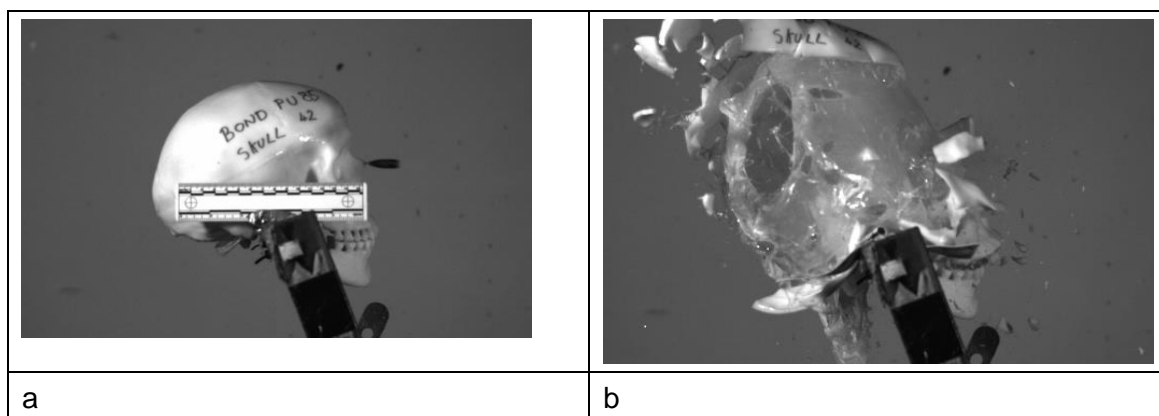
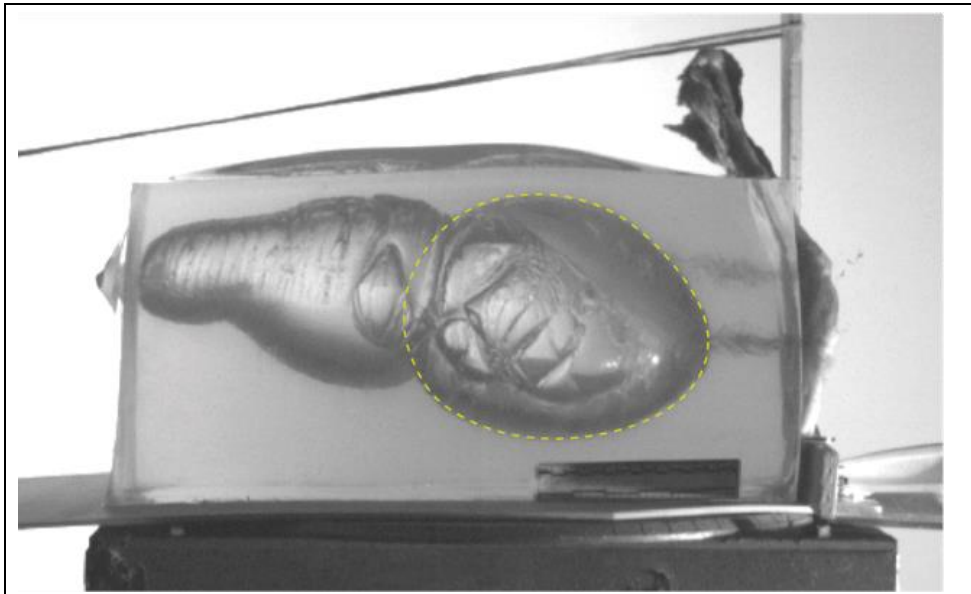


Figure 3-7 Temporary cavity within a skull model

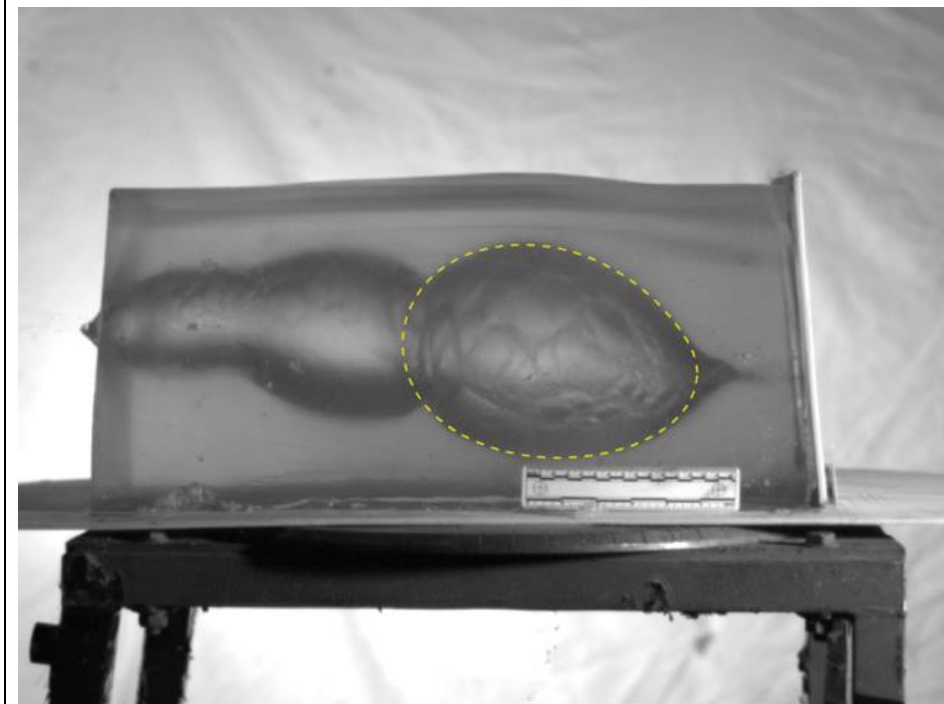
Image allows comparison with front half of the gelatine block in Figures 3-6 and 3-8 a & b (a) immediately pre-bullet impact (b) temporary cavity at maximum after bullet has passed through target; open end of cavity in 7b is 95 mm wide; forensic scale has been torn apart by fragments and the developing cavity; skull is same dimensions as that illustrated in Figures 3-1 and 3-6.

The distances measured are summarised in the International Business Machines Corporation's Statistical Package for Social Services version 24 (IBM SPSS v24) analysis section below (Table 3-1).

The effect of external layers on distances measured in the gelatine blocks was determined using analysis of variance (ANOVA); homogeneity and normality of data was checked and a significance level of 0.05 applied. Significant differences were identified using Tukey's honest significant difference (HSD) test.



a



b

Figure 3-8 Measurement of temporary cavity

The dimensions of the first part of the temporary cavity were estimated by drawing a best fit ellipse around the cavity and estimating where the left-hand border would lie (compare to Figures 3-6 & 3-7); gelatine blocks are the same dimensions as described in Figure 3-1; tracing the cavity from a photographic image is similar to the method described by Watkins et al. [26].

3.5 Results

Block temperature across all conditions was consistent (mean 7.8°C, SD 2.3°C) as was bullet impact velocity (mean 650 m/s, SD 9 m/s). Ball bearing impact velocity (mean 691 m/s, SD 19 m/s) and depth of penetration (DoP; mean 357 mm, SD 13 mm) was consistent with previous work [31] providing confidence within and among the groups of gelatine blocks tested (See Appendix A, Figure_A 3).

Mean Shore hardness of the synthetic skin was measured at 21.6 DU, SD 2 DU and mean tear strength 1.76 kN/m, SD 0.35 kN/m (See Appendix D, Table_A 3). In comparison with Reference [25], Shore hardness of the synthetic skin was similar to reported values for human skin, pig skin and some of the dental silicones, but tear strength was lower.

The bullets passed through all the intermediate layers and perforated the gelatine blocks. Where bullets were recovered after shooting (Figure 3-4b) they were intact other than some marking on the copper jacket and occasional minor deformity of the bullet tip. None of the bullets were seen to fragment on the high-speed images and no bullet fragments were recovered from the gelatine blocks.

One of the Synbone® sheets had cracked horizontally after the shot; all the rest appeared intact (apart from the hole from the bullet). There were no fragments of Synbone® material found in the gelatine blocks. Two of the six plain MU51 sheets produced plastic fragments within the permanent cavity of the corresponding gelatine blocks. Fragments were seen in the permanent tracts of all the gelatine blocks where MU51 sheets were shot with a synthetic skin layer and with the helmet material layers. None of the scapulae appeared cracked after the bullet impact, the only injury being the hole from the bullet. Bone fragments were present in five out of the six gelatine blocks from the scapula shots. Polymer and bone fragments were found between 50 to 340 mm within the gelatine blocks with no obvious link between distance and the type of intermediate layer. No helmet materials were found within the gelatine blocks.

For each of the different conditions listed the experiment was performed six times. High speed video data was lost from one of the MU51/Skin/Helmet experiments due to an onsite power failure but neck length (*nL*) data was still available from block dissection. Micro CT analysis of the bullet impacts on the different materials is presented in Appendix C.

3.5.1 IBM SPSS v24 analysis

IBM SPSS v24 was used to analyse the distances measured in the high-speed videos and block dissections (Figures 3-4, 3-6, 3-8 a & b, Table 3-1).

The different materials used did not significantly affect distance 'x' (bullet point of entry into block to 90-degree yaw), ($F_{5,29} = 2.0$, $p = NS$). The SD for plain blocks (19.3 mm) was much less than for blocks with intermediate layers. The greatest SD (37.8 mm) occurred with the MU51/Skin/Helmet combination. The mean value of 'x' for the MU51/Skin/Helmet group was different to that of the other groups, but due to the larger SD, ANOVA did not identify a statistically significant difference (Table 3-2).

Table 3-1 Measurements of the distances shown in Figure 3-6 for each block and material layer combination

Block number	x mm	y mm	z mm	w mm	<i>nL</i> mm	Material
1	183	179	201	183	110	plain
2	175	160	213	175	100	plain
3	225	179	228	225	100	plain
4	193	163	228	196	100	plain
5	173	181	233	173	90	plain
6	184	185	233	184	80	plain
7	231	171	232	237	140	MU51
8	217	200	219	223	120	MU51
9	190	175	227	197	100	MU51
10	150	146	206	156	80	MU51
11	182	172	208	187	130	MU51
12	212	150	213	218	130	MU51
13	246	196	209	253	130	Synbone®

Block number	x mm	y mm	z mm	w mm	nL mm	Material
14	210	210	242	217	130	Synbone®
15	213	228	240	219	164	Synbone®
16	171	162	210	177	170	Synbone®
17	173	164	210	180	150	Synbone®
18	186	168	212	193	150	Synbone®
19	192	185	205	198	110	Scapula
20	218	161	201	224	110	Scapula
21	238	158	212	245	140	Scapula
22	140	185	213	145	30	Scapula
23	180	188	229	187	120	Scapula
24	168	176	208	176	110	Scapula
25	161	170	210	171	60	MU51/Skin
26	124	177	218	132	70	MU51/Skin
27	189	194	221	197	80	MU51/Skin
28	216	165	225	225	120	MU51/Skin
29	221	186	246	231	150	MU51/Skin
30	181	164	210	189	80	MU51/Skin
31	130	183	227	176	30	MU51/Skin/Helmet
32#	-	-	-	-	45	MU51/Skin/Helmet
33	126	167	205	171	40	MU51/Skin/Helmet
34	104	169	203	158	50	MU51/Skin/Helmet
35	185	183	238	226	60	MU51/Skin/Helmet
36	188	164	216	238	100	MU51/Skin/Helmet

High speed video lost due to power cut

Table 3-2 Summary statistics for distance 'x'

Material	Mean value 'x' mm	SD mm	CV %
Plain	189.3	19.3	10.2
SYNBONE®	199.8	28.8	14.4
Horse	189.3	35.1	18.5
MU51	197.0	29.2	14.8
MU51/Skin	182.0	36.1	19.8
MU51/Skin/Helmet	146.6	37.8	25.8

Distance 'y' (maximum height of first part of temporary cavity) was not affected by intermediate layers ($F_{5,29} = 0.90$, $p = NS$). There was greatest variability in the Synbone® group followed by the MU51 layer. Distance 'y' is controlled by the radial pressure exerted by the bullet in the gelatine block (Table 3-3).

Table 3-3 Summary statistics for distance 'y'

Material	Mean value 'y' mm	SD mm	CV %
Plain	174.5	10.3	5.9
Synbone®	188.0	27.6	14.7
Horse	175.5	13.1	7.5
MU51	169.0	19.5	11.5
MU51/Skin	176.0	12.0	6.8
MU51/Skin/Helmet	173.2	9.1	5.3

Material did not affect the distance 'z' (maximum length of first part of temporary cavity), ($F_{5,29} = 0.6$, $p = NS$). The smallest value for 'z' was for the horse bones and the largest for the plain blocks, although there was very little variability in mean or CV across all conditions (Table 3-4).

Table 3-4 Summary statistics for distance 'z'

Material	Mean 'z' mm	SD mm	CV %
Plain	222.7	12.9	5.8
Synbone®	220.5	15.9	7.2
Horse	211.3	9.7	4.6
MU51	217.5	10.4	4.8
MU51/ Skin	221.7	13.3	6.0
MU51/Skin/Helmet	217.8	14.8	6.8

Distance 'w' (bullet point of entry to external structures to bullet 90-degree yaw) did not vary significantly among block groups ($F_{5,29} = 0.3$, $p = NS$). Plain gelatine was less variable than the blocks with intermediate layers (Table 3-5).

Table 3-5 Summary statistics for distance 'w'

Material	Mean 'w' mm	SD mm	CV %
Plain*	189.3	19.3	10.2
Synbone®	206.5	28.9	14.0
Horse	195.8	35.4	18.1
MU51	203.0	29.3	14.4
MU51/Skin	190.8	36.5	19.1
MU51/Skin/Helmet	193.8	35.7	18.4

***The values for distance 'x' and 'w' for plain blocks are identical as there are no additional layers**

Neck length (nL) was affected by intermediate layers ($F_{5,29} = 7.30$, $p \leq 0.001$),

Table 3-6. Tukey's HSD produced three overlapping groups:

Group 1 (Plain, Horse, MU51/Skin, MU51/Skin/Helmet)

Group 2 (Plain, Horse, MU51, MU51/Skin)

Group 3 (Horse, MU51, Synbone®).

This indicates that nL in the full model of MU51/Skin/Helmet is different to that with Synbone® as the intermediate layer.

Table 3-6 Summary statistics for 'nL'

Material	Mean 'nL' mm	SD mm	CV %
Plain	96.7	10.3	10.6
Synbone®	149.0	16.7	11.2
Horse	103.3	37.8	36.6
MU51	116.7	22.5	19.3
MU51/Skin	93.3	34.4	36.9
MU51/Skin/Helmet	56.0	27.0	48.2

In addition to the ANOVA a number of other observations can be made. With measurement 'x' (bullet yaw to 90 degrees), there is greater variability as the model becomes more complex. There is an effect of the external layers on distance 'w' (distance to bullet yaw to 90 degrees taking into account the external layers) but there is overlap across the different conditions. With

distance 'y' (temporary cavity height) there was greatest variability with the Synbone® and plain MU51 sheets, but less with the horse, MU51/skin, and the full helmet model. With neck length (nL) there was greatest variation with the horse, MU51/skin, and the full helmet model.

The horse and MU51/skin produced very similar results for distances 'w', 'x', y', and ' nL '.

3.6 Discussion

Ballistic head injury is complex and outcome is influenced by many factors [1-4]. Wearing military helmets is associated with reduced fatalities from ballistic impact [2]. Mechanisms include projectile deflection and energy dissipation by the helmet materials, although above a particular impact energy the helmet materials will be defeated.

The aim of this work was to simulate an overmatch ballistic event against a simplified model of a head wearing a helmet and understand how the intermediate layers of material influence the behavior of FMJ MSC 7.62 x 39 mm bullets. The main findings were that increased complexity in the model (i.e. additional layers) increased the variability (a) in distance from impact on the surface of the block to 90-degree yaw of the bullet (distance 'x') and (b) in neck length/narrow channel length within the gelatine block.

As noted above, Kneubuehl has described how the neck length depends on the form of the bullet tip, the bullet's gyroscopic stability and the angle of incidence at the point of impact with the target [14, p98]. The experiment reported in the current paper controlled for bullet tip variation by using rounds from the same manufactured batch. The angle of incidence was controlled as far as practical under the experimental conditions but as seen in Figures 3-3 b, 3-5 a & b, and 3-8 a & b there are very small differences in the impact angles presented by different targets.

On the high-speed video and at block dissection the initial bullet path (i.e. the neck) within all the gelatine blocks appeared horizontal after passing through the intermediate layers, thus intermediate layers did not affect bullet directionality along the horizontal centre axis. However, the results in Table 3-6 suggested that intermediate layers influenced gyroscopic stability i.e. intermediate layers appeared to affect the propensity of the bullet to start yawing.

The effects in our model are less clear cut than those described by Kieser et al. [29] (described in the helmet section of the introduction) where denim fabric draped on the gelatine impact surface caused 5.56 x 45 mm bullets to yaw more rapidly, produce larger cavities, and increase the risk of indirect fractures in the deer femur embedded in gelatine. The bullets used by Kieser et al. [29] tended to fragment within the gelatine blocks. This does illustrate how such interactions will vary with the bullet characteristics and material types. Even with the plain gelatine blocks without intermediate layers, there was variation in the temporary cavity measurements (as indicated by the CVs), despite factors such as bullet type, impact velocity, impact site on the gelatine, gelatine concentration and consistency, and temperature being controlled for. This supports Kneubuehl's view of the empirical nature of wound ballistics [14 p87].

Additional work is required to understand further how bullet interactions with helmet materials at overmatch influence wound profiles and how this relates to resulting clinical injury.

In terms of bullet damage, the scapulae and synthetic bone behaved in a similar fashion. For most targets, the only damage seen was the bullet hole, although one of the Synbone® sheets had cracked horizontally. The explosive effect illustrated in Figure 3-7 is a feature of the rapid rise in intracranial pressure from the temporary cavity within a filled skull model and is described further in references [9] and [23].

Previous work has been undertaken to find suitable synthetic tissue substitutes for skin [8, 24, 25] and bone [8, 9, 22, 23] so it is reassuring to find that the results for MU51/synthetic skin combination were very similar to those for the scapulae (with residual tissue layer) across a number of the measurements.

3.7 Conclusions

Using FMJ MSC 7.62 x 39 mm bullets there was an effect on neck length within the gelatine blocks when intermediate material layers were perforated suggesting an influence on bullet gyroscopic stability. Variability was observed in measurements within each experimental condition. The addition of material layers produced greater variability in the temporary cavity measurements under some of the conditions. Typically, variability increased with increasing complexity of the intermediate layers. One of the synthetic bone polymers with a synthetic skin layer produced similar results within the gelatine blocks to the horse scapulae (with residual tissue) and may be suitable for future ballistic experiments.

3.8 Limitations of the model

This model only used one type of ammunition at velocities chosen to overmatch the helmet materials. Different results might be obtained across a range of velocities and with alternative ammunition types.

3.9 Acknowledgements

1. Cranfield University, Defence Academy of the United Kingdom, Shrivenham, SN6 8LA.

Clare Pratchett, Art Director, CDS Learning Services.

Art work for Figures 3-1 and 3-6.

2. ARRK Europe Ltd, Gloucester Technical Centre, Olympus Park, Quedgeley, Gloucester, Gloucestershire GL2 4NF.

Craig Vickers. Head of Prototyping – Europe.

3. Morgan Advanced Materials, 473 Foleshill Road, Coventry, CV6 5AQ.

Stuart Bailey.

4. Royal Veterinary College, Royal College Street, London NW1 OUT.

Richard Prior and Andrew Mackie, Department of Pathology and Pathogen Biology.

5. Flexural Composites Research Laboratory, 107 Bonington Building, Nottingham Trent University, Dryden Street Nottingham, NG1 4GG.

Richard Arm, Research Fellow.

6. Royal Centre for Defence Medicine, CT Centre, Research Park Birmingham, B15 2SQ.

Yvonne Yau.

3.10 References

1. Keene DD, Penn-Barwell JG, Wood PR, Hunt N, Delaney R, Clasper J, Russell RJ, Mahoney PF (2016) Died of Wounds: a mortality review. *J R Army Med Corps* 162: 355-360
2. Carr DJ, Lewis E, Horsfall I (2017) A systematic review of military head injuries. *J R Army Med Corps* 163:13-19
3. Penn-Barwell JG, Sargeant ID (2016) Gun-shot injuries in UK military casualties- Features associated with wound severity. *Injury Int J Care Injured* 47: 1067-71
4. Smith JE, Kehoe A, Harrison SE, Russell R, Midwinter M (2014) Outcome of penetrating intracranial injuries in a military setting. *Injury Int J Care Injured* 45: 874-878
5. Humphrey C, Kumaratilake J (2016) Ballistics and anatomical modelling- a review. *Legal Medicine* 23: 21-29
6. Breeze J, Carr DJ, Mabbott A, Beckett S & Clasper JC (2015) Refrigeration and freezing of porcine tissue does not affect the retardation of fragment simulating projectiles. *Journal of Forensic and Legal Medicine* 32: 77-83
7. Falland-Cheung L, Waddell JN, Lazarjan MS, Jermy MC, Winter T, Tong D, Brunton PA (2017) Use of agar glycerol and agar/glycerol/water as a translucent brain simulant for ballistic testing. *Journal of the Mechanical Behaviour of Biomedical Materials* 65: 665-671
8. Thali MJ, Kneubuehl BP, Zollinger U, Dirnhofer R (2002) The 'skin-skull-brain model': a new instrument for the study of gunshot effects. *Forensic Science International* 125: 178-189

9. Mahoney PF, Carr DJ, Delaney RJ, Hunt N, Harrison S, Breeze J, Gibb I (2017) Does preliminary optimisation of an anatomically correct skull-brain model using simple simulants produce clinically realistic ballistic injury fracture patterns? *Int J Legal Med* 131: 1043-1053
10. Jussila J (2004) Preparing ballistic gelatine; review and proposal for a standard method. *Forensic Science International* 141: 91-98
11. Lazarjan MS, Geoghegan PH, Jermy MC, Taylor M (2014) Experimental investigation of the mechanical properties of brain simulants used for cranial gunshot simulation. *Forensic Science International* 239: 73-8
12. Fackler ML, Malinowski JA (1985) The wound profile: a visual method for quantifying gunshot wound components. *The Journal of Trauma* 25: 522-529
13. Berlin R, Gelin L, Janzon B, Lewis DH, Rybeck B, Sandegard J, Seeman T (1976) Local effects of assault rifle bullets in live tissue. *Acta Chir Scand Suppl* 459: 3-47
14. Kneubuehl BP (2011) General wound ballistics. In: Kneubuehl BP, Coupland RM, Rothschild MA, Thali MJ (Eds) *Wound Ballistics Basics and Applications*. Springer-Verlag, Berlin Heidelberg. pp 87-161
15. Ragsdale BD, Josselson A (1988) Predicting temporary cavity size from radial fissure measurements on ordnance gelatin. *The Journal of Trauma* 28: S5-9
16. Jussila J (2005) Measurement of kinetic energy dissipation with gelatine fissure formation with special reference to gelatine validation. *Forensic Science International* 150:53-62

17. Schyma C, Madea B (2012) Evaluation of the temporary cavity in ordnance gelatine. *Forensic Science International* 214: 82-87
18. Mabbot A, Carr DJ, Champion S, Malbon C (2016) Comparison of porcine thorax to gelatine blocks for wound ballistic studies. *Int J Legal Med* 130: 1353-62
19. De Boer HH, Van der Merwe AE, Soerdjbailie-Maikoe V (2016) Human cranial vault thickness in a contemporary sample of 1097 autopsy cases: relation to body weight, stature, age, sex and ancestry. *Int J Legal Med* 130:1371–1377
20. Patten Report Recommendations 69 and 70 relating to public order equipment. The Northern Ireland Office in consultation with the Association of Chief Police Officers. Third Report, December 2002. Page 92
21. Smith MJ, Brickley MB, Leach SL (2007) Experimental evidence for lithic projectile injuries: improving identification of an under-recognised phenomenon. *Journal of Archaeological Science* 34: 540-553
22. Smith MJ , James S, Pover T, Ball N, Barnetson V, Foster B, Guy C, Rickman J, Walton V (2015) Fantastic plastic? Experimental evaluation of polyurethane bone substitutes as proxies for human bone in trauma simulations. *Leg Med* 17: 427-35
23. Carr D, Lindstrom A-C, Jareborg A, Champion S, Waddell N, Miller D, Teagle M, Horsfall I, Kieser J (2015) Development of a skull/brain model for military wound ballistics studies. *Int J Legal Med* 129: 505-10
24. Jussila J, Leppaniemi A, Paronen M, Kulomaki E (2005) Ballistic skin simulant. *Forensic Science International* 150: 63-71

25. Falland-Cheung L, Pittar N, Tong D, Waddell JN (2015) Investigation of dental materials as skin simulants for forensic skin/skull/brain model impact testing. *Forensic Sci Med Pathol* 11: 552-557
26. Watkins FP, Pearce BP, Stainer MC (1988) Physical effects of the penetration of head simulants by steel spheres. *The Journal of Trauma* 28: S40-54
27. Carey ME, Herz M, Corner B, McEntire J, Malabarba D, Paquette S, Sampson JB (2000) Ballistic helmets and aspects of their design. *Neurosurgery* 47: 678-689
28. Carr D, Starling G, de Wilton T, Horsfall I (2014) Tensile properties of military chin-strap webbing. *Textile Research Journal* 84: 655-661
29. Kieser DC, Carr DC, Leclair SCJ, Horsfall I, Theis J-C, Swain MV, Kieser JA (2013) Clothing increases the risk of indirect ballistic fractures. *Journal of Orthopaedic Surgery and Research* 8: 42 DOI: 10.1186/1749-799X-8-42
30. Mabbott A, Carr DJ, Champion S, Malbon C, Tichler C (2013) Comparison of 10% gelatine, 20% gelatine and Permangel™ for ballistic testing. 27th International Symposium on Ballistics, Freiburg. pp 648-654
31. Mabbot A (2015) Wound ballistics: behind police body armour. PhD thesis Cranfield University UK

4 ASSESSMENT OF POLYURETHANE SPHERES AS SURROGATES FOR MILITARY BALLISTIC HEAD INJURY

Mahoney PF, Carr DJ, Delaney R, Hunt N

Publication: (2018) Int J Legal Med (2018) <https://doi.org/10.1007/s00414-018-1832-6>

4.1 Abstract

Synbone® spheres were shot with 7.62 x 39 mm mild steel core ammunition at a mean impact velocity of 654 m/s, SD 7 m/s, to simulate engagement distances of around 50-100 m. The wounds and fracture patterns were assessed by two forensic pathologists familiar with military cranial injury. The overall fracture pattern was assessed as being too comminuted when compared with actual injury. This suggests the Synbone® spheres have less utility for simulating military injury than other purposes described in the literature.

Key words

7.62 x 39 mm bullet, cranial fractures, ballistic trauma

4.2 Introduction

The aim of this project was to assess if Synbone® spheres (SYNBONE AG, Neugutstrasse 4, 7208 Malans, Switzerland) are suitable for simulating military ballistic head injury at engagement distances of 50 to 100 m.

Much of the ground work in simulating cranial gunshot injury with synthetic models has been done by Thali and colleagues [1-3]. In his initial paper [1], Thali expresses concern that the physical mechanisms behind ballistic trauma are poorly understood. To address this, the group built a synthetic head model using a layered polyurethane sphere (to simulate bone structure), a latex periosteum and a silicone cap to substitute for the scalp. 10% gelatine at 4°C was used as a 'brain' fill. The model was shot with a broad range of ammunition (including 7.62 x 51 mm and 7.62 x 39 mm, but mainly 9 x19 mm Full Metal

Jacket, FMJ, Luger) from 10 m and the authors concluded that the injuries created in the model were fully comparable to those seen in real incidents.

Further work with this model included impacting it with 9 mm Luger bullets to explore the underlying mechanisms for entrance wound characteristics [2] and a study of tangential gunshot head injury [3]. In the latter study, the bullets were fired directly at the synthetic skull with the latex periosteum layer (but not the silicone scalp) and found to produce realistic tangential injury and fracture patterns.

More recent work by Taylor and Kranioti has used Synbone® spheres to investigate execution style gunshot injuries [4]. The gelatine filled models were shot at a range of 30 cm with 7 different handgun ammunitions with the aim of detecting similarities and differences in wound characteristics for use in future investigations. The authors provide examples of two clinical cases (shot with .22LR and .45 ACP ammunition) that closely match the corresponding models. Smith et al. [5] carried out a detailed analysis of the differences between injuries inflicted on real bone compared to polyurethane bone substitutes. They used both flat plates of synthetic bone (5 mm thick) and spheres (5 and 7 mm wall thickness), and impacted them with a cross bow bolt, a ball fired from a black powder musket and modern rifle ammunition (.243" Winchester Soft Point, velocity 905 m/s, and 7.62 x 51 mm NATO FMJ, velocity 853 m/s). The weapons were fired from 2 m distance at the targets. They initially looked at impacts on flat plates and empty spheres to see if the different shapes affected the response to impact and compared these with shots into cattle scapulae. There were no gross differences between flat plates and spheres; both showed internal bevelling at the entry site. Differences between the synthetic and real bone are considered later in this paper.

Subsequent work involved spheres filled with 10% gelatine at 4°C. The secondary and tertiary fracture patterns produced by modern firearms were generally consistent with those seen in published examples of real cranial trauma [5].

4.3 Method

Nine Synbone® spheres (190 mm diameter, 6 mm wall thickness, thin rubber skin covering outer surface) were filled with ballistic gelatine of either 5, 7, or 10% by mass (Figure 4-1a). The gelatine was allowed to set at around 17 °C for 24 hours. Other work by our group has shown no difference in fracture patterns in a skull model when impacted at a series of temperatures from 4 to 25 °C [6] and no difference with the above gelatine % fills. Further data is presented in Appendix E.

The models were taken to the Small Arms Experimental Range, Cranfield University, Defence Academy of the UK (Figure 4-1b) and placed 10 m from a No 3 Enfield proof mount fitted with an accurate barrel and shot with 7.62 x 39 mm Ukrainian mild steel core (MSC) ammunition (Soviet State Factory, Lugansk, manufactured 1967), (mean impact velocity 654 m/s, SD 7 m/s). The ammunition was downloaded to achieve these velocities, simulating engagement distances of around 50-100 m) [7].

Bullet velocity was tracked using a Weibel Doppler (Figure 4-1c), and impacts filmed using two Phantom high-speed cameras (V12 from above, sample rate 20000 frames per second, exposure time 5 μ s, resolution 512 x 480; V1212 from the side, sample rate 34000 frames per second, exposure time 10 μ s, resolution 640 x 480).

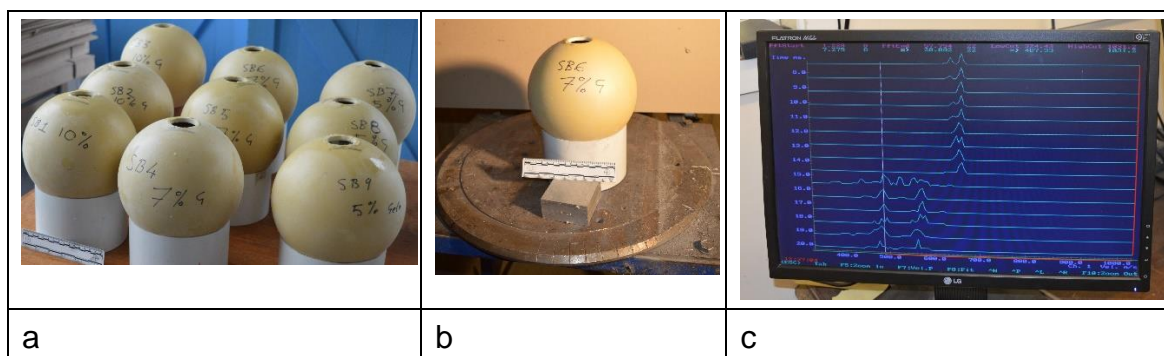


Figure 4-1 Synbone® spheres experimental preparation and set up

- (a) Synbone® spheres with range of gelatine fills (b) model 6 at the range pre-shooting (c) screen shot of Doppler radar read out for impact on model 6.

Models 1 to 3 were each shot twice to assess their suitability for simulating more than one gunshot injury and assessing if the order of shot impact could be determined as described by Thali [1]. Models 4 to 9 were each shot once to assess entry and exit fracture patterns from one impact sequence. The condition of the models insitu post impact was captured using a Nikon D3200 DSLR camera fitted with an AF-S NIKKOR 18-55mm lens.

The 9 models were then examined by two Home Office Forensic Pathologists with extensive experience of assessing ballistic injury. The pathologists were invited to score the entry wound, exit wound and overall fracture pattern using a 4-point Likert-type scale [8] (where 4 = exactly like a real injury, 3 = a lot like a real injury, 2= a bit like a real injury and 1= nothing like a real injury) and provide comment as needed. The scores are summarised in Table 4-1.

4.4 Results

4.4.1 High Speed Video (HSV)

Example impact sequences taken from the high-speed cameras are shown in Figures 4-1 to 4-4. All HSV triggered and captured the impacts except for the V1212 side view of model 4. The overhead view was recorded. There were two distinct series of events. For models 1,3,6, 8 and the first shot into model 2, the fractures developed as illustrated in Figures 4-2 and 4-3. Fractures spread from both the entry and exit sites but the main fragments were drawn back together by the extendable latex 'periosteum'. With models 4,5,7, 9 and the second shot into model 2, the sphere ruptured and the gelatine fill was expelled (Figure 4-4), imitating the 'Krönlein shot' [9]. From review of the high-speed videos the impact sites are not obviously different between the two groups and bullets can be seen to have yawed within the material and exited sideways (see Figures 4-2b,4-4b as examples from each group), although the fractures are more extensive and the integrity of the sphere lost in the models where the contents are completely expelled. There were also no obvious differences in the fracture

patterns seen on the HSV when the spheres with the different gelatine concentrations were compared.

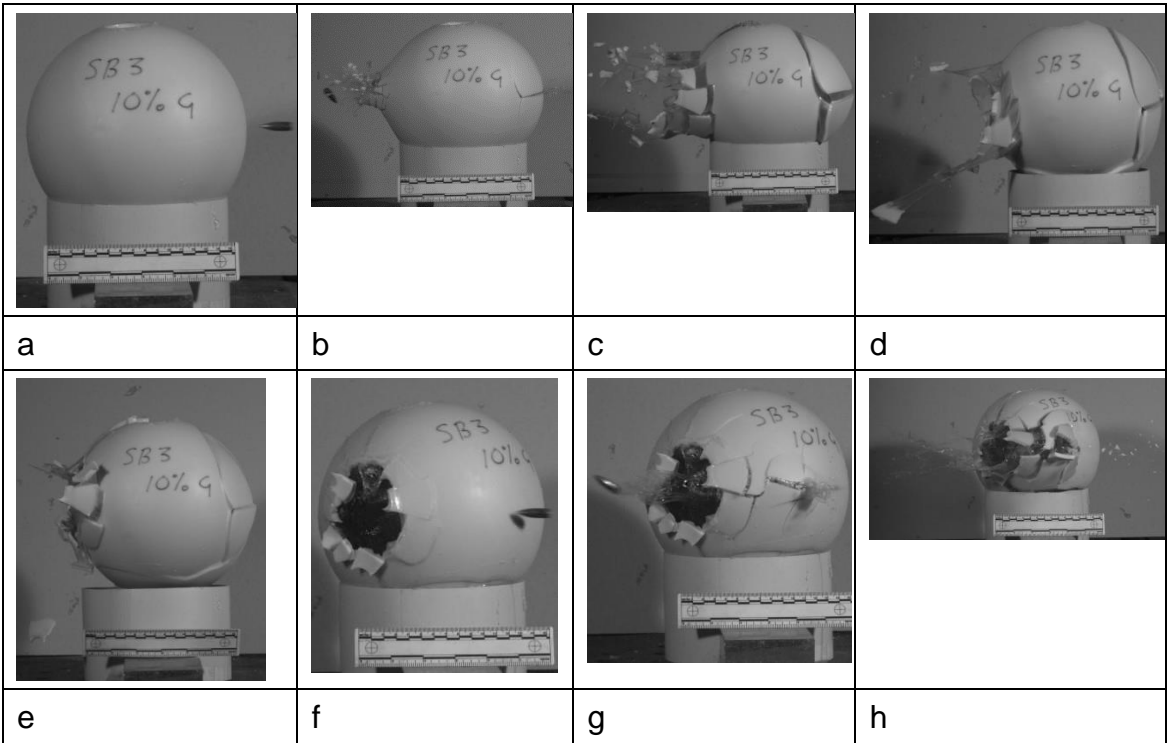


Figure 4-2 Model 3, 5% gelatine fill, V1212 Impact sequence (side view)

(a) pre-impact shot 1 (b) bullet exit, fractures developing entry and exit (c) further fracture development with temporary cavity expansion (d-e) fragments drawn back in by elasticity of the latex ‘periosteum’ (f) pre-impact shot 2 (g) bullet 2 exit (h) further fracture development.

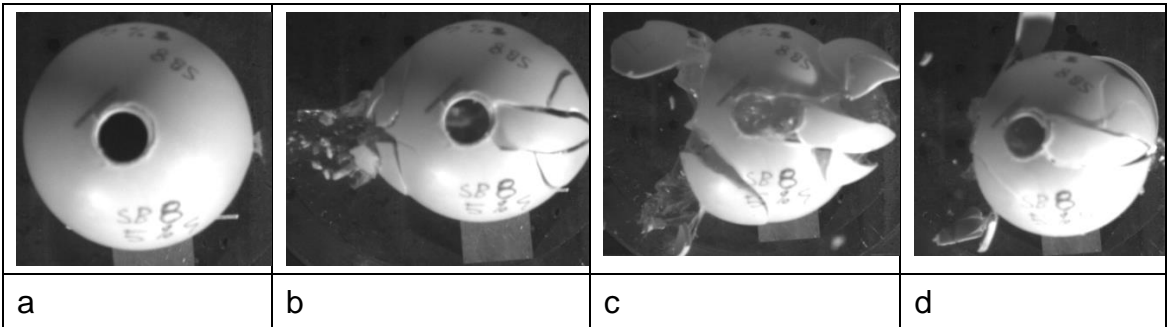


Figure 4-3 Model 8, 5% gelatine fill, V12 Impact sequence (from above)

(a) impact splash visible on right hand side of frame (b) bullet exit and fracture development, entry and exit sites (c) disruption of sphere with temporary cavity formation in the gelatine fill (d) collapse down of temporary cavity with many of the fragments having been retained by the latex ‘periosteum’ dropping back into place.

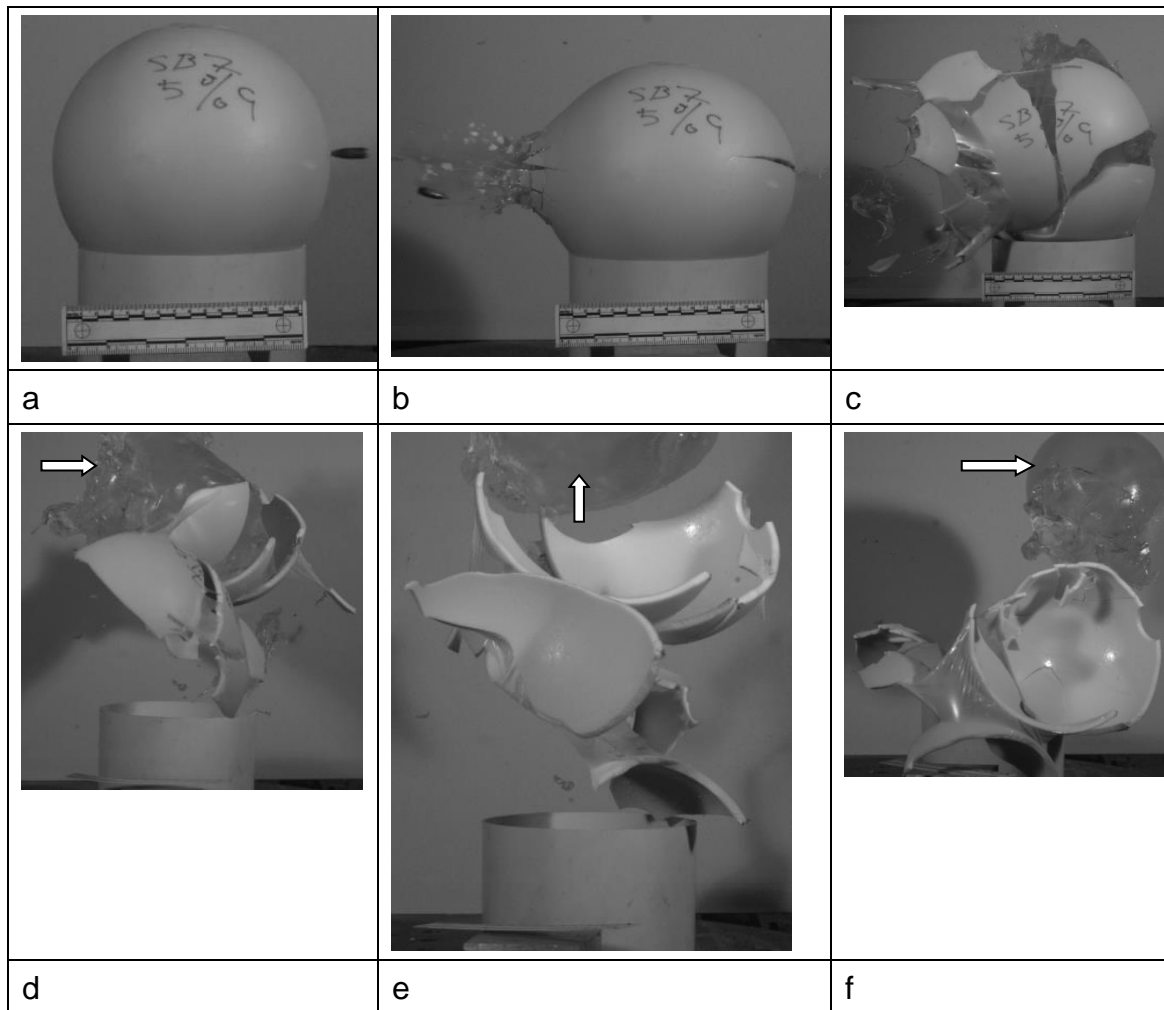


Figure 4-4 Model 7, 5% gelatine fill, V1212 Impact sequence (side view)

(a) pre-impact (b) bullet exit; fractures developing at both entry and exit sites (c) sphere breaks up, latex 'periosteum' holds majority of fragments together (d-f) gelatine fill ejected (arrowed) as the sphere breaks up.

4.4.2 Pathologists' assessment

From Table 4-1 it can be seen that the most of the entry wounds only scored 1. Although the entry sites displayed bullet wipe and six models had internal bevelling, the overall view was that they were too fractured when compared with real incidents and not realistic. The assessors were able to distinguish the different impacts in models 1-3 (model 3 was noted to have a good example of a key hole injury pattern from the second bullet impact) and the order in which they had occurred from the intersecting fracture lines.

The exit wounds scored marginally better but the overall view was that they were too comminuted. External bevelling was found in three models (3,7 and 9) but in others the exit elements were so fragmented this could not be assessed. The overall fracture patterns were judged as being too comminuted when compared with actual military head injury.

Table 4-1 Likert-type scores for Synbone ® sphere post-impact appearances

Model	% gelatine fill	Assessor	Entry wound	Exit wound	Overall fracture pattern
1	10	(a)	2	2	2
		(b)	2	2	2
2	10	(a)	1	2	1
		(b)	1	2	1
3	10	(a)	2	2	2
		(b)	1	2	2
4	7	(a)	1	1	1
		(b)	1	2	1
5	7	(a)	1	1	1
		(b)	1	2	1
6	7	(a)	1	2	1
		(b)	1	2	1
7	5	(a)	1	2	1
		(b)	1	2	1
8	5	(a)	1	2	2
		(b)	1	2	1
9	5	(a)	1	2	1
		(b)	1	2	1

The pathologists also noted that differences in bone thickness and structure within skulls (and anatomically correct models) does influence fracture patterns as discussed by Fenton et al. [10].

4.5 Discussion

Synbone® spheres have been successfully used to simulate ballistic injury by a number of authors. Smith [5] found that the models produced different fracture patterns when impacted by the three projectile types described above, and the black powder carbine did produce a realistic key hole defect from a tangential impact, similar to that described by Thali [3]. Taylor and Kranioti [4] noted differences in the entry wound characteristics between the ammunition types tested with *'entrance wound radius ...positively correlated with the caliber dimension'* and *'the number of radiating and concentric fractures is also increasing with the caliber dimension'* [4].

There have been a number of observations regarding how the models differ from real injury. Smith [5] noted that the exit fracture patterns were different from real bone and described *'stepped fractures where the radius of defect varied widely forming jagged corners around margins, unlike usually rounded/ovoid shapes in real bone'*

Taylor and Kranioti [4] also noted that the exit wounds in their model were larger than real injury.

The eviscerating injury seen in Figure 4 was first described by the Swiss Surgeon Rudolf Ulrich Krönlein in relation to close range gunshots with the 1889 Swiss repeating rifle [9]. This effect was also seen by Thali et al. [1].

Our experience using 7.62 x 39 mm ammunition at simulated engagement ranges is that the bony injuries produced in our models were too comminuted and fractured in comparison with contemporary military bony injuries reviewed by the pathologists. This suggests that the model has less utility for this purpose than when used in the tests described by others [1-5]. Of note, two of the 10% gelatine fill spheres had marginally higher scores when compared with the other fills, although the number of replicates for each experiment is small.

4.6 Conclusion

Synbone® spheres were assessed for their suitability in simulating military ballistic head injury at engagement distances of 50 to 100 m. Although the overall number of replicates was low (n=9) the impression was that the fractures produced were too comminuted when compared with recent military injury. Further work is ongoing to assess other materials for replicating these injuries.

4.7 Caveats

This experiment only used one ammunition type simulating a particular engagement range. Different results may be obtained with other ammunition and impact velocities.

4.8 Acknowledgements

Cranfield University, Defence Academy of the United Kingdom, Shrivenham, SN6 8LA.

David Miller and Michael Teagle, the Small Arms Experimental Range.

4.9 References

1. Thali MJ, Kneubuehl BP, Zollinger U, Dirnhofer R (2002) The 'Skin-skull-brain model': a new instrument for the study of gunshot effects. *Forensic Science International* 125 (2-3): 178-189
2. Thali MJ, Kneubuehl BP, Zollinger U, Dirnhofer R (2002) A study of the morphology of gunshot entry wounds in connection with their dynamic creation, utilizing the 'skin-skull-brain model'. *Forensic Science International* 125: 190-194
3. Thali MJ, Kneubuehl BP, Zollinger U, Dirnhofer R (2003) A high-speed study of the dynamic bullet-body interactions produced by grazing gunshots with full metal jacketed and lead projectiles. *Forensic Science International* 132: 93-98
4. Taylor SC, Kranioti EF (2018) Cranial trauma in handgun executions: Experimental data using polyurethane proxies. *Forensic Science International* 282: 157-167
5. Smith MJ, James S, Pover T, Ball N, Barnetson V, Foster B, Guy C, Rickman J, Walton V (2015) Fantastic plastic? Experimental evaluation of polyurethane bone substitutes as proxies for human bone in trauma simulations. *Legal Medicine* 17: 427-435
6. Mahoney PF, Carr DJ, Delaney R, Hunt N, Harrison S, Breeze J, Gibb I (2017) Does preliminary optimisation of an anatomically correct skull-brain model produce clinically realistic ballistic injury fracture patterns? *Int J Legal Med* 131: 1043-10537
7. Appendix A.10; Ballistics tables (metric system). In: Kneubuehl BP, Coupland RM, Rothschild MA, Thali MJ (2011) (Eds) *Wound Ballistics Basics and Applications*. Springer-Verlag, Berlin Heidelberg. pp 366-384

8. Clason, DL, Dormody, TJ (1994) Analyzing data measured by individual Likert-type items. *Journal of Agricultural Education* 35: 31- 35
9. Hildebrandt G, Stienen MN, Patzer J, Surbec W (2012) Neurosurgical contributions of the Swiss surgeon, Rudolf Ulrich Krönlein—A further pioneer in Swiss neurosurgery. *Acta Neurochir* 154:1923–1933 DOI 10.1007/s00701-012-1419-9 (accessed 16 January 2018)
10. Fenton TW, Stefan VH, Wood LA, Sauer NJ (2005) Symmetrical fracturing of the skull from midline contact gunshot wounds: reconstruction of individual death histories from skeletonized human remains. *J Forensic Sci* 50: 1-12

5 DOES PRELIMINARY OPTIMISATION OF AN ANATOMICALLY CORRECT SKULL-BRAIN MODEL USING SIMPLE SIMULANTS PRODUCE CLINICALLY REALISTIC BALLISTIC INJURY FRACTURE PATTERNS?

Mahoney PF, Carr DJ, Delaney RJ, Hunt N, Harrison S, Breeze J, Gibb I

Publication: (2017) Int J Legal Med 131: 1043-1053

5.1 Abstract

Ballistic head injury remains a significant threat to military personnel. Studying such injuries requires a model that can be used with a military helmet. This paper describes further work on a skull-brain model using skulls made from three different polyurethane plastics and a series of skull 'fills' to simulate brain (3, 5, 7 and 10% gelatine by mass and Permangel™). The models were subjected to ballistic impact from 7.62 x 39 mm mild steel core bullets. The first part of the work compares the different polyurethanes (mean bullet muzzle velocity of 708 m/s) and the second part compares the different fills (mean bullet muzzle velocity of 680 m/s). The impact events were filmed using high speed cameras. The resulting fracture patterns in the skulls were reviewed and scored by five clinicians experienced in assessing penetrating head injury. In over half of the models one or more assessors felt aspects of the fracture pattern were close to real injury. Limitations of the model include the skull being manufactured in two parts and the lack of a realistic skin layer. Further work is ongoing to address these.

Key words

Head, military helmet, assessment, 7.62 x 39 mm bullet, AK47

5.2 Introduction

Ballistic head injury remains a significant threat in modern conflict. Smith et al. [1] undertook a retrospective database review of patients presenting to UK field hospitals in Iraq and Afghanistan between 2003 and 2011. Eight hundred and thirteen patients on the database had suffered a penetrating head injury. Gunshot wound (GSW) was associated with a more severe injury and worse outcome than blast fragment injury. One of the study conclusions was that further work is needed to understand both the underlying anatomical lesions and the energy transfer distribution.

A further study [2] undertook a retrospective review of 71 casualties in Iraq and Afghanistan who had reached medical treatment facilities alive but subsequently died of their wounds. The most common cause of death (44 out of 71) was severe head injury from explosion, blast fragmentation and GSWs. Analysis of 42 of the patients (where full records were available) found that improved medical care would not have helped them and work should be concentrated on improving head protection.

All UK deaths on deployed operations are reviewed by a multidisciplinary panel [3]. A key output from these reviews has been identifying new injury patterns and informing the ongoing development of personal protective equipment.

Understanding and investigating these injury mechanisms, and potentially suggesting improvements in head protection requires suitable models.

There are many physical models used to assess head injury described in the literature. These include post-mortem human specimens [4], anaesthetised animals [5], animal material [6] and synthetic materials [7].

Thali et al. [7] described development of a 'Skin-skull-brain model' consisting of a 'scalp' made from silicon, a layered polyurethane sphere to represent the skull, and gelatine 10% at 4°C to simulate brain. The model was shot with a

series of ammunition types and the authors reported that '*injuries inflicted to this model are fully comparable to the morphology of equivalent real gunshot injuries*'.

Raymond and Bir [8] assessed a similar model against post mortem human specimens using blunt impacts (a 103g rigid impactor at 20 m/s) but found the fracture patterns to be different in the human bone compared to the polyurethane spheres.

Bir et al. [9] assessed two different synthetic femurs (Sawbones® and Synbone®) against post-mortem human material looking at both direct and indirect fractures from ballistic events and used a trained trauma surgeon to assess the injuries. The Synbone® produced similar fracture patterns to the human material but needed a higher direct impact velocity to create this. The Sawbones® fracture patterns were different to the human material. The authors concluded that the bone surrogates did not approximate to the cadaveric bone under the experimental conditions used.

There are ethical and practical issues around the use of cadavers and animals which makes synthetic bone substitutes an attractive and practical option [10]. Smith et al. [10] subjected Synbone® polyurethane bone substitute (flat plates and spheres) to a series of ballistic impacts (.243" Winchester Soft Point, 7.62 x 51 mm NATO Full Metal Jacket, 13.5 mm solid lead ball and 8.0 mm Perfectline alloy cross bow bolt) and compared both the macroscopic appearances and microscopic damage to experimental animal bone samples and published examples of human injury. They noted clear differences between real bone and the synthetic materials but felt the Synbone® spheres offered a useful approximation to the damage seen in bone.

Thali et al. [7] stated that they chose a Synbone® sphere rather than a more complex skull form as it would offer '*more reproducible and comparable results*'. A sphere is, however, not suitable for studies incorporating helmets.

Preliminary work to develop a suitable anatomically correct skull brain model for ballistic studies incorporating a helmet have been reported [11]. This model consisted of an anatomically correct polyurethane skull with a 10 % gelatine brain (by mass; 4 °C) impacted with 7.62 x 39 mm ammunition (M43 ball, Chinese, MSC, Factory 71, 1984) at a mean velocity of 675 m/s. Only six results were reported but the fracture patterns generated were compared to the limited forensic anthropology literature that exists and demonstrated macroscopic similarities [12, 13].

The aim of this subsequent work was to assess if the fracture patterns produced under a series of further experimental conditions using simple simulants would be assessed as realistic by clinical experts.

5.3 Method

The research described in this paper was carried out in a number of stages. Anatomically correct polymeric skulls were manufactured from rapid prototype data obtained by 3D mapping of both the internal and external surfaces of a human skull (ARRK Europe Ltd, Gloucester Technical Centre, Olympus Park, Quedgeley, Gloucester, Gloucestershire GL2 4NF).

5.3.1 Polymer comparison

The first stage (n = 9 skulls) involved a comparison of skulls made from different polymers (Table 5-1). The two parts of the skull were bonded using cyanoacrylate adhesive (Loctite, Henkel Corp, USA). A thin low-density polyethylene bag was inserted into the base of the skull and gelatine, 10% by mass, poured into the bag to fill the cranial cavity. The gelatine was allowed to

set for 24 hours at 17°C (laboratory temperature) and then conditioned at 4°C for a further 24 hours [11]. Further details of skull preparation are in Appendix F.

Table 5-1 Summary of synthetic skull material data

(Data from material manufacturers provided to ARRK Europe Ltd. Craig Vickers, Personal communication, January 2017)

Polymer	Hardness Shore D	Tensile Strength MPa	Bending Strength MPa	Impact Strength kJ/m ²	n
PU8098	85	70	75	10	3
UP5690	83	35	50	100	3
MU51	81	54	87	13	3

5.3.2 Skull fill and conditioning

The second stage (n = 30 skulls) involved a comparison of different fills and conditioning temperatures. With regard to simulating brain tissue, two of the authors (PM and SH) felt that gelatine 10% seemed too stiff when compared to living brain tissue in recently ballistically injured casualties. This was the incentive to explore the behaviour of different gelatine concentrations. Gelatine 10 % by mass has been used extensively in ballistic experiments but there is still uncertainty as to how it relates to biological tissue [14].

Skulls made of polymer MU51 were filled with either gelatine made by mass to 3, 5, 7 and 10 % or with Permangel™.

The skulls were filled as described above and again allowed to set overnight at 17 °C. The gelatine was then either:

- i. conditioned for a further 24 hours at 4°C and removed from the fridge just before being shot or
- ii. allowed to remain at 17 °C until shot or
- iii. kept in an oven at 25 °C until shot.

Permangel™ is reportedly a remeltable and reusable ballistic test material equivalent to 10 % gelatine, although ballistic testing with steel spheres has

suggested that Permangel™ is strain rate sensitive and its properties vary between 10 % and 20 % gelatine [15]. Permangel™ is melted at 110°C and therefore a thin oven ‘roasting bag’ was used to contain the molten Permangel™ rather than the polyethylene bag used for the liquid gelatine. Once poured into the skulls the Permangel™ was allowed to cool to 17°C (laboratory temperature) and remained at this temperature until shot.

The different fill and temperature combinations are summarised in Table 5-2.

Table 5-2 Summary of skull ‘fill’ (gelatine % by mass or Permangel™) and temperature of ‘fill’ immediately after ballistic impact

Skull ‘fill’	Temperature (rounded) °C	n=
Gelatine 10%	4	5
Gelatine 10%	17	3
Gelatine 7%	17	5
Gelatine 5%	17	3
Gelatine 3 %	4	2
Gelatine 3 %	17	3
Gelatine 3 %	25	3
Permangel™	17	6

5.3.3 Skull shooting

The first 9 skulls were shot with 7.62 x 39 mm Czech MSC ammunition (Sellier and Bellot, Prague; Factory in Zbrojovka Vlastim, manufactured 1983, mean muzzle velocity 708 m/s, SD =9 m/s). The next 30 were shot with 7.62 x 39 mm Ukrainian MSC ammunition (Soviet State Factory, Lugansk, manufactured 1967, mean muzzle velocity 680 m/s, SD = 24 m/s). The models were shot at a range of 10 m from a No 3 Enfield proof mount fitted with an accurate barrel

(Figure 5-2a). Prior to each shot the impact site on the model (Figure 5-2b) was confirmed using a sighting laser. Bullet velocity was tracked using a Weibel Doppler, and impacts filmed using two Phantom high-speed cameras (V12 and V1212) (Figure 5-2 c & d).

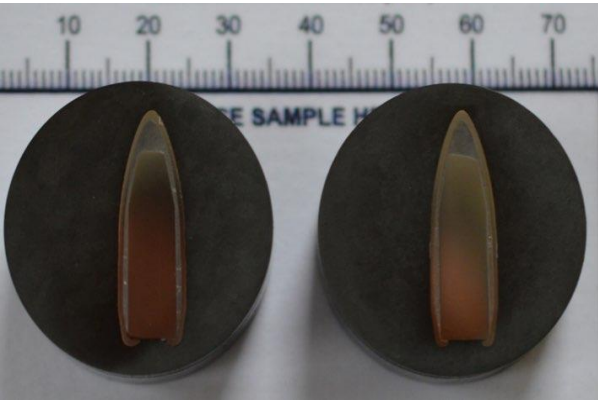


Figure 5-1 Sectioned 7.62 x 39 mm bullets. Left: Czech; Right Ukrainian

Bullets thickness is measured then bullet is enclosed in a container of Bakelite powder which is compressed and heated. The set Bakelite/bullet combination is then ground down to expose the bullet components as illustrated (See Appendix B).

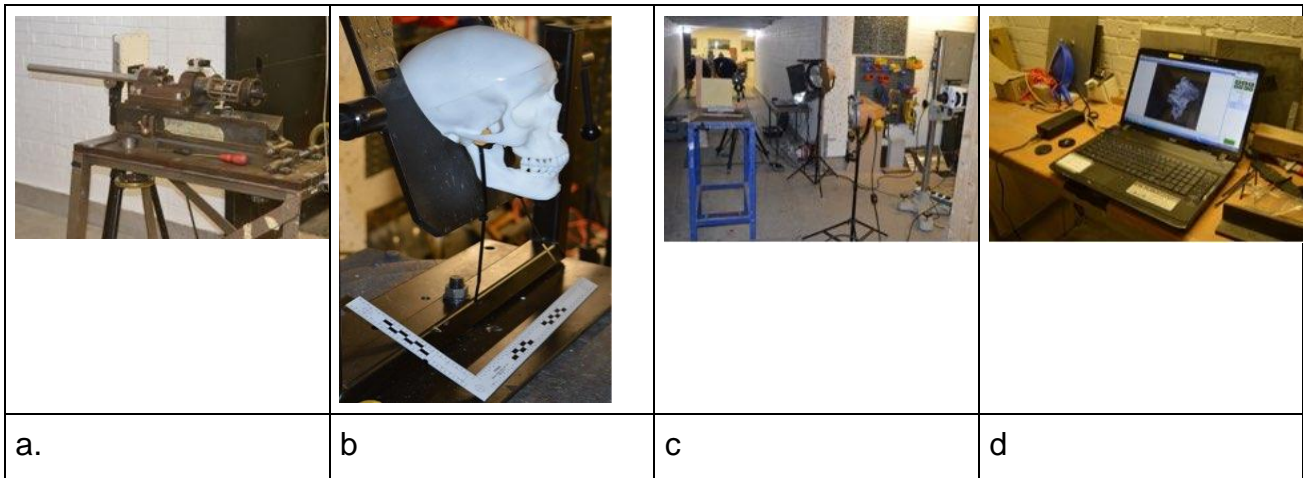


Figure 5-2 Experimental set up

(a) Enfield proof mount (b) skull-brain model (c) camera and lighting set up, looking towards the proof mount from target end of range (d) image capture on laptop.

The condition of the models insitu post impact was captured using a Nikon D3200 DSLR camera fitted with an AF-S NIKKOR 18-55mm lens. The fractured skull pieces and gelatine or PermagemTM contents were collected post impact and the extent of the damage recorded. The temperature of the gelatine and

Permagem™ was recorded immediately post impact using a calibrated digital thermometer (Table 5-2).

5.3.4 Clinician assessment

The third stage was inviting five military and civilian clinicians with extensive experience of managing and/or assessing ballistic head injury to individually review the fracture patterns in the skulls and score how clinically realistic they were using a 4-point Likert-type Scale [16] (Table 5-3).

Table 5-3 Likert-type scale for clinician assessments

1. This looks nothing like a real fracture pattern
2. This looks a bit like a real fracture pattern
3. This looks a lot like a real fracture pattern
4. This looks exactly like a real fracture pattern

The score sheet also included space for comments if the clinician wished to provide them (Figure 5-3 a & b). The clinicians invited to assess the skull models had either looked after casualties with ballistic head injury, reviewed x ray and CT images from such casualties or conducted post-mortem examinations of fatalities. Two had been regular members of the Mortality Peer Review Panel, a multidisciplinary group undertaking peer review of UK military deaths including the nature of the injuries and treatment given [3]. The current study was an opportunity to harvest this extensive collective knowledge.

The backgrounds of the clinicians were two Civilian Home Office Forensic Pathologists, and a military Radiologist, Neurosurgeon and Maxillofacial Surgeon. The clinicians were briefed on the bullet type used (i.e. 7.62 x 39 mm) and that different polymers/gelatine concentrations had been shot but were not given the details of the gelatine concentrations within individual skulls. The Permagem™ brains do not degrade the way gelatine does and were presented at the assessments with the skulls. No formal training in an assessment method

was given; the clinicians were invited to score the skulls based on their own prior experience.

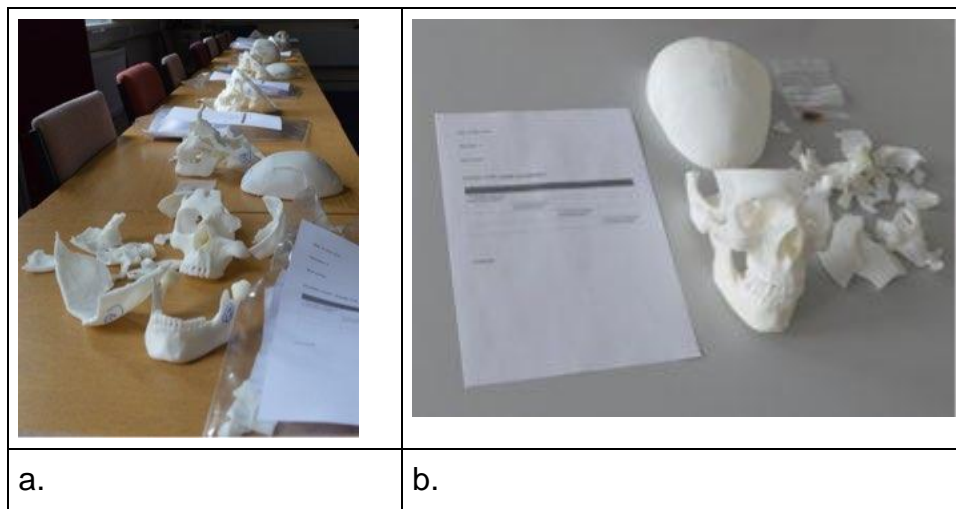


Figure 5-3 Shot skull assessment set up

(a) skull assessment stations (b) individual skull with score sheet.

5.4 Results

A typical fracture impact sequence is shown in Figure 5-4 a-d. The scores from the Likert-type scales were summarised in an Excel spreadsheet and analysed using International Business Machines Corporation's Statistical Package for Social Services (IBM SPSS) version 23.

The free text comments and notes made on the score sheets by the clinicians were also transcribed into an Excel spreadsheet so that comments about the wound characteristics and fracture patterns could be compared and assessed (see Appendix G for examples).

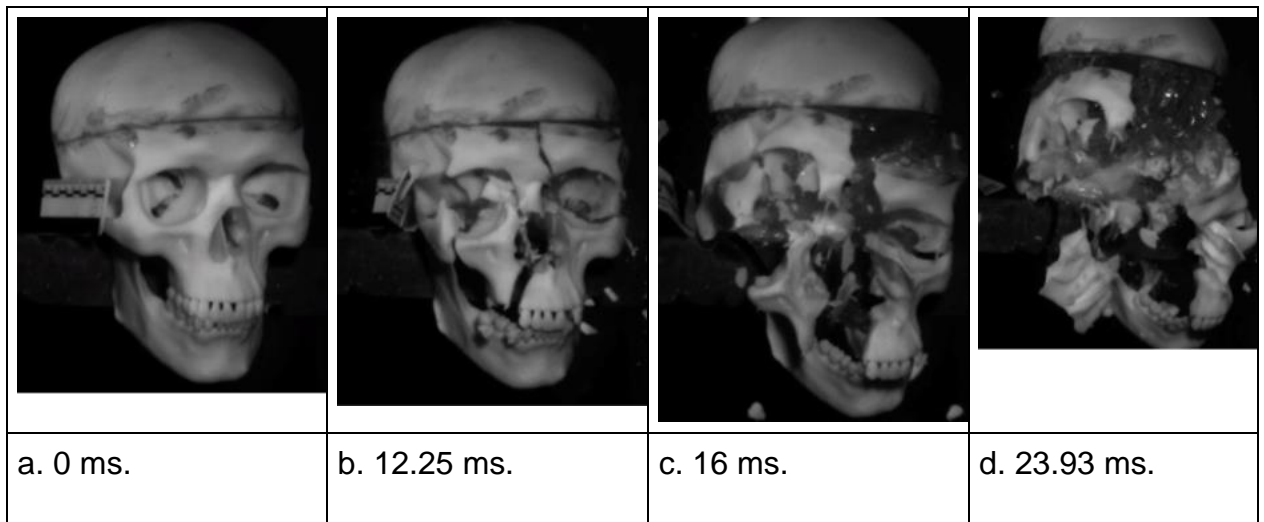


Figure 5-4 Frontal impact sequence captured with the V12 camera

5.4.1 IBM SPSS v23 analysis

The effect of polymer type on fracture score was determined using analysis of variance (ANOVA); homogeneity and normality of data was checked and a significance level of 0.05 applied. Significant differences were identified using Tukey's honest significant difference (HSD) test. Mean and standard deviation data are provided in Table 5-4.

Table 5-4 Descriptive statistics for the effect of polymer type on Likert-type score for fracture pattern

n= 15 assessor observations for each polymer

Polymer type	Mean Likert-type score for fracture pattern	SD
MU51	1.87	0.83
PU8098	1.93	0.70
UP5690	2.01	0.70

As shown there was minimal difference among the scores for the different polymer types and the ANOVA found that polymer type did not affect fracture score ($F_{2,42} = 0.28, p = NS$).

The effect of gelatine concentration (or use of PermagemTM) and temperature (rounded) on the fracture score was similarly assessed. For the purpose of analysis, temperatures between 17 and 19°C were rounded to 17°C. Mean and SD data are provided in Table 5-5.

ANOVA found that gelatine concentration (or use of PermagemTM) and temperature did not affect fracture score; gelatine/PermagemTM ($F_{4,142} = 1.21$, $p = \text{NS}$); temperature ($F_{2,142} = 0.01$, $p = \text{NS}$).

Table 5-5 Descriptive statistics for the effect of skull contents and temperature on fracture score

Gelatine %	Temperature °C	Mean Likert-type score for fracture pattern	SD	n (assessor observations)
10	17	2.47	0.83	15
10	4	2.12	0.78	25
3	17	1.87	0.52	15
3	25	2.00	0.53	15
3	4	2.20	0.92	10
5	17	2.13	0.52	15
7	17	2.40	0.71	25
Permagem TM	17	2.10	0.71	30

5.4.2 Summary of Likert-type scores and free text comments

Of the thirty-nine skulls assessed, twenty-three were given scores of 3 by at least one assessor and seven scores of 4 by at least one assessor. No skulls received the same scores from all five assessors.

Thirteen skulls had more than one score of 3 or 4 from separate assessors and are summarised in Appendix G. Assessor comments, where given, are included to demonstrate the elements that they felt were or were not representative of

real injury. In addition to their overall Likert-type fracture pattern score, assessors also commented on how realistic some of the entry and exit wounds appeared, along with the impact of the post mortem cut line. Examples of impacted skulls are shown in Figure 5-5. The frequency of comments is summarised in Table 5-6.

Table 5-6 Frequency of comments on entry and exit wound appearance plus influence of the post-mortem cut line

Assessor	Entry realistic	Entry unrealistic	Exit realistic	Exit unrealistic	Number of occasions cut line interferes with fracture pattern
1	2	8	7	3	8
2	15	20	21	14	1
3	5	9	5	10	21
4	6	19	6	9	13
5	3	26	22	14	27



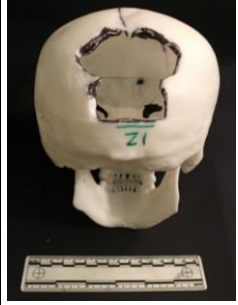

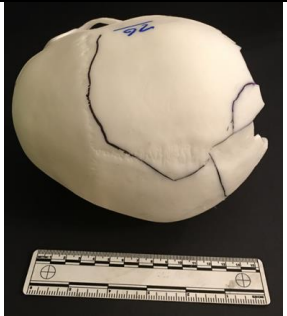



		
a (i) Skull 12 Entry wound and associated fracture lines.	a (ii) Skull 12. View from above. Fracture lines and exit site.	a (iii) Skull 12 Exit site, looking through to rear aspect of entry wound.
		
b (i) Skull 26. Entry site and associated fracture lines.	b (ii) Skull 26. View from above.	b (iii) Skull 26 Exit site, looking through towards rear aspect of entry wound.
		
c (i) Skull 28 Entry site.	c (ii) Skull 28 Exit site, looking through towards rear aspect of entry wound.	

Figure 5-5 Examples of impacted skulls, reconstructed where possible

Fracture lines highlighted with black ink; the skull numbers are the same as those in Appendix G.

5.5 Discussion

Smith et al. [10] found that spheres filled with ballistic gelatine produced damage patterns that compared well with published examples of real gunshot trauma, similar to the findings of both Thali et al. [7] using spheres and Carr et al. [11] using synthetic skulls. In this present work the overall fracture patterns in 23 of the 39 skulls (59 %) were considered close to reality by at least one of the five assessors.

There were differences of opinion. For example, in two skulls (numbers 8 and 11) non-pathologists commented that the fracture patterns were too extreme to reflect reality. These were both scored high by one pathologist and the radiologist. The published literature includes cases of similar devastating head injury [17]. The useful observation is that experts will interpret based on past experience which needs to be matched to the injury being investigated or modeled.

The majority view from the clinicians was that many of the entrance wounds were not realistic. The 'classical' appearances of gunshot wounds to the skull are described in a number of forensic science and pathology text books [18-20].

A bullet penetrating the skull typically creates a round to oval shaped hole in the outer table of the bone with a large bevelled out hole on the inner table. The outer table defect usually has sharp edges with a 'punched out' appearance and the inner table defect has an 'excavated' cone like appearance (Figure 5-6). If a bullet has sufficient energy to exit the cranial cavity a similar process occurs, except the inner table is now the 'entrance' surface and the outer table the 'exit'. Atypical appearances do occur including bevelling of entrance wounds [21].

Smith et al. [10] reported that the flat Synbone® samples and empty Synbone® spheres shot with both modern and obsolete ammunition types produced bevelled defects with similarities to those seen in real flat bone but lacked the

complexity produced in real crania and that this was unsurprising given the differences in structure between real bone and the polymers used in the artificial bones. The same effect is seen here where the polyurethane material used for the skulls does not reflect the complex structure of actual cranial bone.

The bullet strike may cause direct secondary radial fractures originating from the impact sites [22]. In addition, the rapid rise in intracranial pressure from the temporary cavity in the brain tissue can cause indirect tertiary concentric fractures. If the pressures are high enough an 'explosive' injury will be produced with skull comminution [18, 22]. These features are summarised in Figure 5-6. The secondary and tertiary fractures in high energy strikes can cause fragmentation of the original penetrating defects making assessment of which was the entry and exit wound complicated.

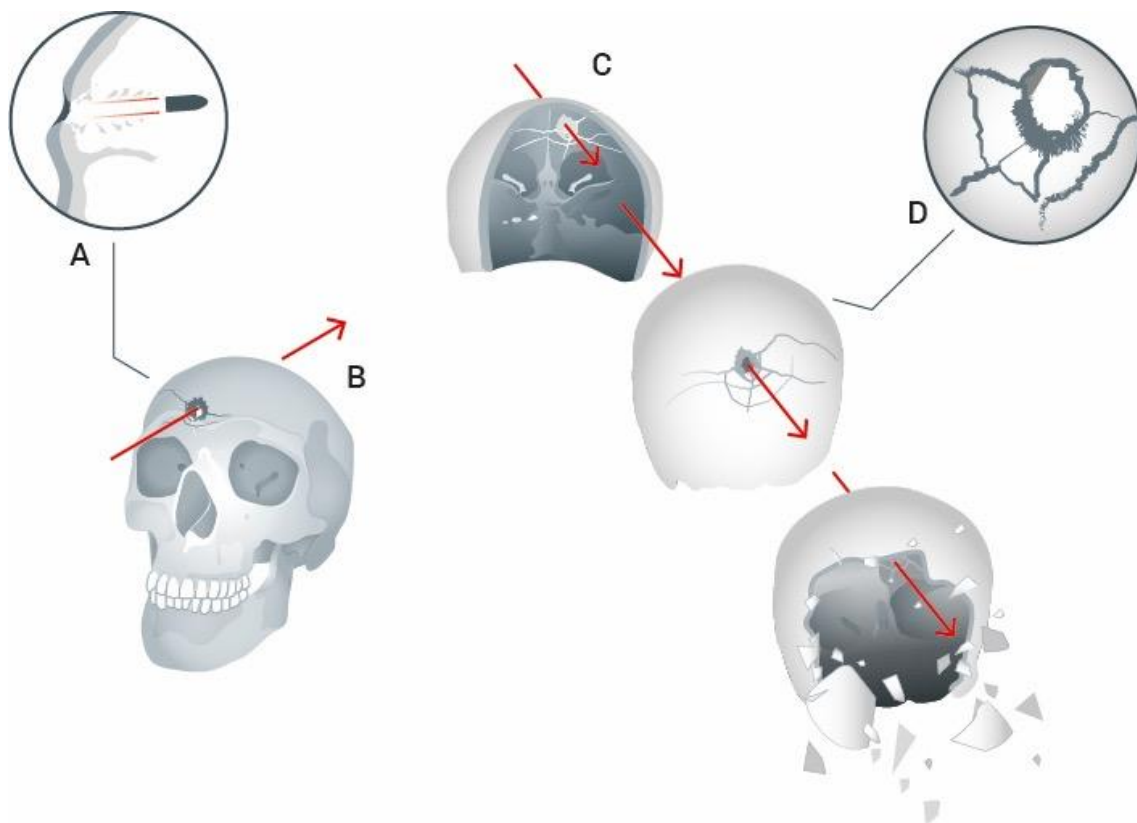


Figure 5-6 Characteristics of skull gunshot wounds

(A) detail of entry wound (after DiMaio [18]) (B) impact and passage of bullet through skull- front view (PFM) (C) passage of bullet through skull- rear view- and development of secondary and tertiary fractures plus explosive comminution. (PFM) (D) detail of exit from cranial cavity (after Karger [22]) .

5.5.1 Limitations of the model

As described by Thali [7] a synthetic model that produces realistic injury patterns would be very useful for forensic reconstructions and be free of the ethical issues and biological variation inherent in using animals and cadaveric specimens [10].

The model used in the current work does have the disadvantage of the post-mortem 'cut' line which is an inherent part of the manufacturing process (Email communication ARRK/Carr July 2016). As described by Viel et al. [23] applying *Puppe's rule* in relation to ballistic skulls fractures, the pre-existing cut line impacts on fracture propagation within the model. Approaches to managing this are being explored.

Unlike Thali's model [7], the one used in this work did not have a synthetic layer to simulate skin. A number of approaches to simulate skin have been reported in the literature [24] and work is ongoing to develop a suitable skin and soft tissue layers for this model.

5.6 Conclusions

The aim of this work was to see if optimisation of an anatomically correct skull-brain model using simple simulants (polyurethane and gelatine or PermagemTM) would produce clinically realistic ballistic injury fracture patterns. At least one assessor out of five felt the fracture pattern was close to real injury in over half of the models. Generally, the exit wounds were thought to be more realistic than the entry wounds. The model does have a number of limitations and future work is planned to address the bonding between the two parts of the skull along with building realistic skin and tissue layers.

5.7 Caveats

This paper only reports findings with two variants of one ammunition type. Other weapon systems or ammunition types may produce different results under these experimental conditions.

5.8 Acknowledgements

1.From Cranfield University, Defence Academy of the United Kingdom,
Shrivenham,

SN6 8LA:

Dr Trevor Ringrose (statistical advice).

David Miller and Michael Teagle, the Small Arms Experimental Range.

Clare Pratchett, Art Director, CDS Learning Services, (Art work for Figure 4.6).

2. ARRK Europe Ltd, Gloucester.

Craig Vickers, Head of Prototyping.

5.9 References

1. Smith JE, Kehoe A, Harrison SE, Russell R, Midwinter M (2014) Outcome of penetrating intracranial injuries in a military setting. *Injury Int J Care Injured* 45: 874-878
2. Keene DD, Penn-Barwell JG, Wood PR, Hunt N, Delaney R, Clasper J, Russell RJ, Mahoney PF (2016) Died of Wounds: a mortality review. *J R Army Med Corps* 162: 355-360
3. Russell R, Hunt N, Delaney R (2014) The mortality peer review panel: a report on the deaths on operations of UK service personnel 2002-2013. *J R Army Med Corps* 160:150-4
4. Sarron JC, Dannawi M, Faure A, Caillou J-P, Da Cunha J, Robert R (2004) Dynamic effects of a 9mm missile on cadaveric skull protected by aramid, polyethylene or aluminium plate: an experimental study. *The Journal of Trauma, Infection and Critical Care* 57: 236-243
5. Lu H, Wang L, Zhong W, Rongfeng Q, Li N, You W, Su X, Zhuang Z, Cheng H, Shi J (2015) Establishment of a swine-penetrating craniocerebral gunshot wound model. *Journal of Surgical Research* 199: 698-706
6. Puskas CM, Rumney DT (2003) Bilateral fractures of the coronoid processes: differential diagnosis of intra-oral gunshot trauma and scavenging using a sheep crania model. *J Forensic Sci* 48: 1-7
7. Thali MJ, Kneubuehl BP, Zollinger U, Dirnhofer R (2002) The 'Skin-skull-brain model': a new instrument for the study of gunshot effects. *Forensic Science International* 125: 178-189
8. Raymond DE, Bir CA (2015) A biomechanical evaluation of skull-brain surrogates to blunt high-rate impacts to post mortem human subjects. *J Forensic Sci* 60: 370-3

9. Bir C, Andreovich C, Di Maio VJM, Dougherty PJ (2016) Evaluation of bone surrogates for indirect and direct ballistic fractures. *Forensic Sci Int* 261: 1-7
10. Smith MJ, James S, Pover T, Ball N, Barnetson V, Foster B, Guy C, Rickman J, Walton V (2015) Fantastic plastic? Experimental evaluation of polyurethane bone substitutes as proxies for human bone in trauma simulations. *Legal Medicine* 17: 427-435
11. Carr D, Lindstrom A-C, Jareborg A, Champion S, Waddell N, Miller D, Teagle M, Horsfall I, Kieser J (2015) Development of a skull/brain model for military wound ballistics studies. *Int J Legal Med* 129: 505-10
12. Betz P, Steiefel D, Hausmann R, Eisenmenger W (1997) Fractures at the base of the skull in gunshots to the head. *Forensic Sci Int* 86: 155-161
13. Fenton TW, Stefan VH, Wood LA, Sauer NJ (2005) Symmetrical fracturing of the skull from midline contact gunshot wounds: reconstruction of individual death histories from skeletonized human remains. *J Forensic Sci* 50: 1-12
14. Mabbott A, Carr DJ, Champion S, Malbon C (2016) Comparison of porcine thorax to gelatine blocks for wound ballistics studies. *Int J Legal Med* 130: 1353–1362
15. Mabbott A, Carr DJ, Champion S, Malbon C, Tichler C (2013) Comparison of 10% gelatine, 20% gelatine and PermaganTM for ballistic testing. 27th International Symposium on Ballistics, Freiburg. pp 648-654
16. Clason, DL, Dormody, TJ (1994) Analyzing data measured by individual Likert-type items. *Journal of Agricultural Education* 35: 31- 35
17. Hejna P, Safr M, Zatopkova L (2011) Reconstruction of devastating head injuries: a useful method in forensic pathology. *Int J Legal Med* 125: 587-590

18. Di Maio VJM (2016) Gunshot wounds. Practical Aspects of Firearms, Ballistics and Forensic Techniques (3rd Edn). CRC Press, Taylor and Francis Group, Boca Raton
19. Leestma IE, Kirkpatrick JB (2014) Gunshot, penetrating and blast related injuries to the nervous system. In: Leestma JE (Ed). Forensic Neuropathology, 3rd Edn. CRC Press, Taylor and Francis Group, Boca Raton. pp 655-697
20. Saukko P, Knight B (2016) Gunshot and explosion deaths. In: Knights Forensic Pathology (4th Edn). CRC Press, Taylor and Francis Group, Boca Raton. pp 241-275
21. Coe JI (1982) External bevelling of entrance wounds by handguns. Am J Forensic Med Pathol 3: 215-220
22. Karger B (2008) Forensic Ballistics. In: Tsokos M (Ed). Forensic Pathology Reviews Volume 5. Humana Press, Totowa. pp 139-172
23. Viel G, Gehl A, Sperhake JP (2009) Intersecting fractures of the skull and gunshot wounds. Case report and literature review. Forensic Science, Medicine, and Pathology 5: 22-7
24. Falland-Cheung L, Pittar N, Tong D, Waddell NJ (2015) Investigation of dental materials as skin stimulant for forensic skin/skull/brain model impact testing. Forensic Science, Medicine and Pathology 11: 552–557

6 BALLISTIC IMPACTS ON AN ANATOMICALLY CORRECT SYNTHETIC SKULL WITH A SURROGATE SKIN/SOFT TISSUE LAYER

Mahoney PF, Carr DJ, Arm R, Gibb I, Hunt N, Delaney R

Publication: (2018) Int J Legal Med 132: 519-530

6.1 Abstract

The aim of this work was to further develop a synthetic model of ballistic head injury by the addition of skin and soft tissue layers to an anatomically correct polyurethane skull filled with gelatine 10% by mass. Six head models were impacted with 7.62 x 39 mm full metal jacket mild steel core (FMJ MSC) bullets with a mean velocity of 652 m/s. The impact events were filmed with high speed cameras. The models were imaged pre- and post-impact using Computed Tomography. The models were assessed post impact by two experienced Home Office pathologists and the images assessed by an experienced military radiologist. The findings were scored against real injuries. The entry wounds, exit wounds and fracture patterns were scored positively but the synthetic skin and soft tissue layer was felt to be too extendable. Further work is ongoing to address this.

Key words: Head injury, CT Scanning, Ballistic images, synthetic skin

6.2 Introduction

Ballistic head injury is a significant threat to troops in combat [1] and ongoing research is needed to assist designers of military helmets and associated personal protective equipment [2].

The Impact and Armour Group at Cranfield University, Defence Academy of the UK are working on an anatomically correct synthetic model of ballistic head injury for this purpose. Preliminary work has been reported [3] along with a

further development assessing the fracture patterns produced in the model under ballistic impact for clinical realism [4].

An acknowledged limitation of the model to date has been the lack of skin and soft tissue layers around the synthetic skull.

Thali et al. [5] developed a 'Skin-skull-brain model' made of a silicone scalp, a layered polyurethane sphere to represent the skull, and gelatine 10% at 4°C to simulate brain. After shooting the model with a series of ammunition types (9mm Luger Full Metal Jacket, FMJ, 22LR, .38Spl, .44 Rem Mag, 7.62 x 51 mm NATO FMJ, 7.62 x 39 mm FMJ and 12/70 Brenneke Slug), the authors reported that the results were comparable to those of real gunshot injuries.

6.2.1 Gunshot wound characteristics

The appearance and characteristics of gunshot wounds depend on a number of factors. These include (i) weapon type (ii) projectile type (iii) projectile velocity (iv) distance of the weapon from the person when fired (v) the effect of intermediate targets such as clothing or armour and (vi) where on the body the person was struck. Bullets impacting on soft areas such as muscle may produce different appearances to those impacting hard areas (e.g. where bone is close to the body's surface such as the head). This is explored in standard forensic textbooks, e.g. [6].

Thali et al. [7] used their model to look at the characteristics of (non-contact) gunshot entrance wounds produced by 9 mm Luger FMJ fired 10m from the target with a muzzle velocity of 350 m/s. These characteristics are summarised in Figure 6-1. Thali et al. [7] noted that the terminology is not uniform among different authors and Figure 6-1 is an attempt to reconcile this.

Figure 6-1 is explained in detail in the following text.

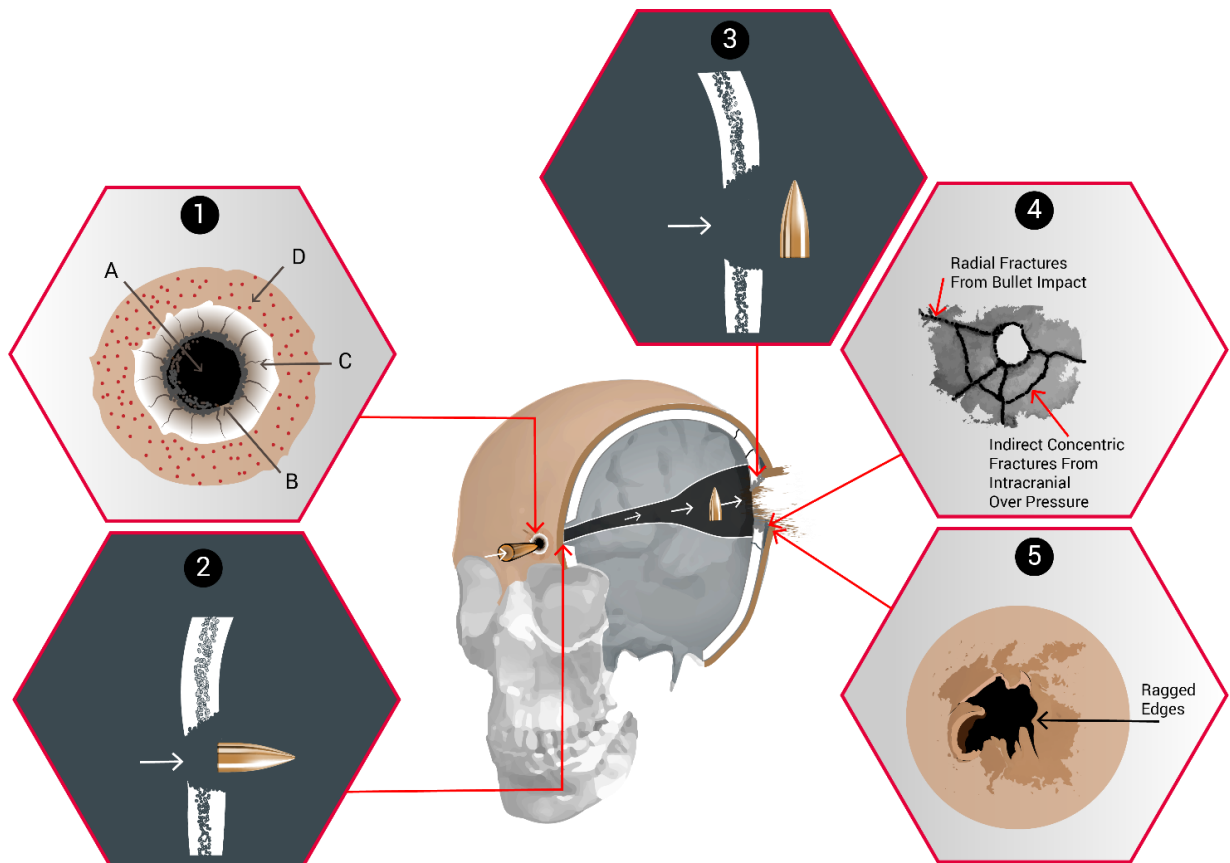


Figure 6-1 Head injury gunshot characteristics

(1) skin and soft tissue entry wound, after Thali et al. [7]; for explanation of letters A-D please see text below **(2) bone entry wound, internal bevelling** **(3) bone exit wound, external bevelling**, (2 and 3 after Di Maio [8]) **(4) additional bone fractures** (after Karger [9]) **(5) skin and soft tissue exit wound**.

6.2.1.1 Skin and soft tissue gunshot entry wound

(After Thali et al. [7], hexagon 1 in Figure 6.1).

A. *Central 'defect'* due to (i) tissue destruction by the bullet and (ii) tissue compression as the skin is spread radially by the impact.

B. *'Bullet wipe'*, a ring of contamination, due to materials on the head of the projectile (e.g. dirt, oil, propellant) being transferred to the skin (Bullet wipe may also be found on the underlying bone).

C. *Abrasion collar / Contusion ring* [6, p258], which has different mechanisms proposed for its creation [6, 7, 10]. Thali proposes it is due to temporary over extension of the skin adjacent to the impact area, and the skin

subsequently drying out. Rothschild [11, p258] describes radial stretching cracks and tears in the epidermis.

D. *Margin of distension*. Rothschild [11, p258] refers to this as being the boundary of the skin stretched by the radial acceleration forces and is associated with petechial haemorrhage.

6.2.1.2 Entrance wound bone damage

(After Di Maio [8], hexagon 2 in Figure 6.1).

The bone of the cranial vault is made up of outer and inner cortical tables joined by thin cancellous bone (the Diploë) [12, p673]. The 'typical' appearance of an entry wound is that of a 'broadening cone' [12, p674] or crater [6, p261]. This is described as 'internal bevelling' [8]. In a review of the skeletal remains of twenty-one gunshot victims, Quatrehomme and Işcan [13] found internal bevelling in the bone entry wounds of twenty skulls but noted external bevelling in one.

6.2.1.3 Exit wound bone damage

(After Di Maio [8], hexagon 3 in Figure 6.1).

If the bullet has sufficient energy to cross the skull and perforate bone again a similar action occurs but with the broader aspect of the wound on the outside of the skull ('external bevelling') [12, p674]. In the central image of Figure 6-1 the bullet has 'yawed' within the brain tissue and exited side on causing the bone exit wound to be larger than the entrance. Quatrehomme and Işcan [13] noted bone exit wounds to be more irregular than bone entry wounds and found external bevelling in most vault injuries but not those of the orbit, maxilla, temporal, greater wing of the sphenoid or left occipital bone.

6.2.1.4 Additional fractures

(After Karger [9], hexagon 4 in Figure 6.1).

The bony injury seen may be complicated by further fractures. Karger [9, p151] describes how secondary radial fractures are induced by the bullet's impact and originate at the entry and exit sites. Karger also describes how the brain is vulnerable to cavitation [9, p149] but the intact skull doesn't allow expansion,

resulting in high pressures within the cranial cavity. If the overpressure exceeds the skull's capacity to elastically extend, indirect concentric fractures result. Sufficiently high pressures will result in fractures combining to produce an 'explosive' type of injury [6, 9, 11, 14].

6.2.1.5 Skin and soft tissue exit wounds

(Hexagon 5 in Figure 6.1).

Rothschild [11, p260] notes that exit wounds show a high degree of variation. In a perforating injury, the skin bulges out before breaking, producing an irregular, slit-like or stellate wound with everted edges. Deformed bullets and fragmented bullets are associated with more skin tearing [11, p261]. The exit wound associated with a high energy round producing a temporary cavity will vary with the length of the wound tract and whether the exit point occurs within or after the temporary cavity [6, p262; 11, p261].

6.2.2 Imaging in ballistic investigations

Thali et al. also described using their model to look at fracture pattern development from a 9mm bullet impact [15]. The impact sequence was captured with high speed photography and the model underwent radiographic Computed Tomography (CT) examination to visualise the wound tracts and fractures. The images were, in turn, compared to the findings when the model underwent 'autopsy'. The authors concluded that the model produced realistic features of gunshot injury and that the CT examination and the 'autopsy' revealed very similar data. They also postulated the role of imaging for 'virtual' autopsies [15].

Imaging studies have gone hand in hand with experiments to understand ballistic injury mechanisms.

Butler et al. [14] describe using x-ray apparatus with an exposure time of one microsecond to capture temporary cavity formation in the brains of

anaesthetised animals (cats and dogs) impacted by steel spheres at between 3,800 and 4000 fps.

Watkins et al. [16] used a model consisting of dried human skulls filled with 20% gelatine and covered with two layers of gelatin soaked chamois leather. The models were impacted with either 3 mm or 6 mm diameter ball bearings (with velocities between ~200 to 1300 m/s, [16 p S43, Table III]) in a series of twelve experiments. In the later experiments, a pulsed X-ray source was used to produce a train of 50 images at millisecond intervals during the impact events and a cine camera used to capture the resulting images.

Other authors have used CT imaging for ballistic experiments. Schyma et al. [17] constructed four head models using hollow spheres filled with 10% gelatine. Thin foil bags containing a mixture of acrylic paint and barium meal were glued onto each sphere and the assembly coated with a layer of silicone. The models were shot through the foil bag with 9 x 19 mm pistol ammunition and the following day underwent CT examination. The barium within the wound tract allowed reconstructed 3-D images of the damage to be created. They also removed the gelatine cores from the models after shooting, cut them into 1 cm slices and scanned the slices on a flat bed scanner to produce images of the bullet tract. They found the correlation of the optical and radiological measurements to be 'satisfactory' [17].

Bollinger et al. [18] used CT imaging to assess damage in a Synbone® pelvis embedded in 10% gelatine and impacted with 9 mm and .45 in pistol ammunition. The authors felt that CT imaging offered advantages over dissecting the model as (i) the distribution of osseous fragments within the gelatine could be observed more accurately and (ii) the crack lengths within the damaged gelatine could be measured allowing assessment of energy transfer along the bullet's course.

Karger et al. [19] had a licensed veterinarian shoot ten live New Jersey calves (destined for the slaughter house) with either 9 x19 mm FMJ or 9 x19 mm hollow point ammunition in the right temple. The heads underwent full autopsy and the brains were removed and fixed in formaldehyde. The fixed brains were imaged using plain x-ray, CT and magnetic resonance imaging (MRI). Each brain was also examined and histology performed. Key features of the brain injury included wound tracts due to direct tissue crushing by the bullet, cortical contusions from the brain impacting against the inside of the skull, shearing of brain tissue from the intracranial temporary cavitation, associated oedema and bruising, and bone fragments both within the wound tracts and driven into brain tissue.

Oehmichen et al. [20] studied forty-seven cases of lethal gunshot injury to the brain from civilian practice. In seventeen of these CT and MRI were performed either prior to autopsy or on the isolated formalin fixed brain, and the imaging correlated with the autopsy findings [21]. They reported that imaging was able to distinguish entrance from exit wounds, determine the missile track and demonstrate aspects of the brain injury. CT was particularly useful in localizing foreign objects within the brain (e.g. bone and bullet fragments) which can be difficult to locate during autopsy [21].

6.2.3 This project

The aim of this current work was to assess the effect of synthetic facial skin and tissue on the fracture development in our model and assess the overall realism of the entry wounds, exit wounds, wound tract, fractures and tissue characteristics using both modern CT scanning and formal 'autopsy', building on the approach of Thali and colleagues [15]. Assessment of entry and exit wound characteristics was felt to be a key observation given the reported variation of wound appearances in both forensic [22] and experimental [23] cases.

6.3 Method

The research described in this chapter was carried out in a number of stages.

6.3.1 Skulls

Synthetic bone surrogates have been assessed by other authors for ballistic testing [24,25] and synthetic skulls produced realistic fracture patterns in our previous work as described in chapter 5 and [3,4]. This work uses the same skulls described in chapter 5 made from the MU51 polymer [4].

MU51 is a two-part thermoset polyurethane plastic mixed in the correct ratios within a vacuum casting chamber (Craig Vickers, ARRK Europe Ltd, personal communication). The skulls are in turn produced in two parts (above and below the post mortem cut line) and need to be bonded prior to ballistic tests. The glue line was noted to be a weak point in previous work [4] so a number of adhesives were assessed for suitability under ballistic strain conditions. Pro-Flex 50, a 50 Shore A fast curing rubber has, to date, proved the most effective (<http://www.mouldlife.net/ekmps/shops/mouldlife/resources/Other/pro-flex-50-data-sheet.pdf>). The two parts of the skulls were bonded using Pro-Flex 50 at the Flexural Composites Research Laboratory, Nottingham Trent University (FCRL NTU).

6.3.2 Faces

Sheets of polydimethylsiloxane (PDMS) composite prepared as a surrogate skin/subcutaneous tissue were produced by FCRL NTU for a previous set of ballistic experiments [26]. Samples of the surrogate skin/subcutaneous tissue were assessed using the BS ISO3-1:2015 Trouser Tear test and by measuring Shore hardness. This is detailed in Appendix D. The Shore hardness was similar to reported values [27] for human skin, pig skin and dental silicones but tear strength was lower [26].

The PDMS surrogate skin/subcutaneous tissue was derived from part of a larger work strand to build realistic artificial skin and organs to support military surgical training [28]. This project involved creating surrogate samples to mimic the tactile qualities of real living tissues such as muscle, liver and lung. Surgeons and other clinicians were invited to comment on how 'real' particular synthetic tissues appeared to them and the synthetic materials adjusted accordingly [29]. Previous work within the Impact and Armour Group has used food grade swine tissue for ballistic experiments [30] and assessing the PDMS against this was felt to be a useful comparison.

When impacted by the same Ukrainian 7.62 x 39 mm Mild Steel Core (MSC) rounds as selected for the current experiment, a combination of the PDMS surrogate with sheets of MU51 polymer produced very similar results to horse scapulae with a residual layer of tissue [26]. The same combination of materials was therefore chosen for this experiment as a suitable skin/soft tissue/polymer bone substitute, while accepting that the polymer skull lacks the complex structure of real bone [24].

Using anatomical data [31] the facial tissues were built up layer by layer on one of the synthetic skulls using a waxed based polymer clay. The final model was the base from which moulds were created for the PDMS tissue structures used to form faces and scalps to place over the skulls [32] (Figure 6-2).



Figure 6-2 MU51 Polymer skulls with moulded PDMS faces and scalps

6.3.3 Complete model

A thin low-density polyethylene bag was inserted into the base of the face/skull model and gelatine, 10% by mass, poured into the bag to fill the cranial cavity. The gelatine was allowed to set for 24 hours at around 17°C. Our previous work (chapters 5) did not find a difference in the fracture patterns generated in a skull model filled with gelatine 10% at a series of temperatures [4] and therefore no further temperature conditioning was used. While accepting that 10% gelatine is not a completely biofidelic brain simulant [33], its use for the current project allows reference to our previous work [4, 26]. Jussila [34] notes that the properties of tissue simulants do not need to be exactly the same as living tissue '*provided the results can be measured and appropriately extrapolated or scaled*' [34].

6.3.4 First set of CT scans

The complete face/skull models with gelatine fill were taken to the Centre for Defence Imaging (Royal Centre for Defence Medicine, Queen Elizabeth Hospital, Birmingham) and underwent CT scans (SOMATOM Definition CT scanner, Siemens Health Care Ltd, Camberley, UK) using both Dual Energy Head Angiogram and Spiral Head protocols (Window Level 100/35, 1mm slice thickness). The models were given designations using the NATO Phonetic Alphabet [35] Golf (Face 1) through to Lima (Face 6) to allow images to be catalogued and filed.

The CT scans produced pre-impact images for each model, allowing any filling defects in the gelatine to be identified and distinguished from later bullet tracts.

6.3.5 Ballistic testing

The following day the models were shot at a range of 10 m from a No 3 Enfield proof mount fitted with an accurate barrel using 7.62 x 39 mm Ukrainian mild

steel core (MSC) ammunition (Soviet State Factory, Lugansk, manufactured 1967) (mean impact velocity 652 m/s, SD 6 m/s; Figure 6-3). This ammunition type was chosen as representative of those faced by UK armed forces and allies [36, 37, 38, 39].

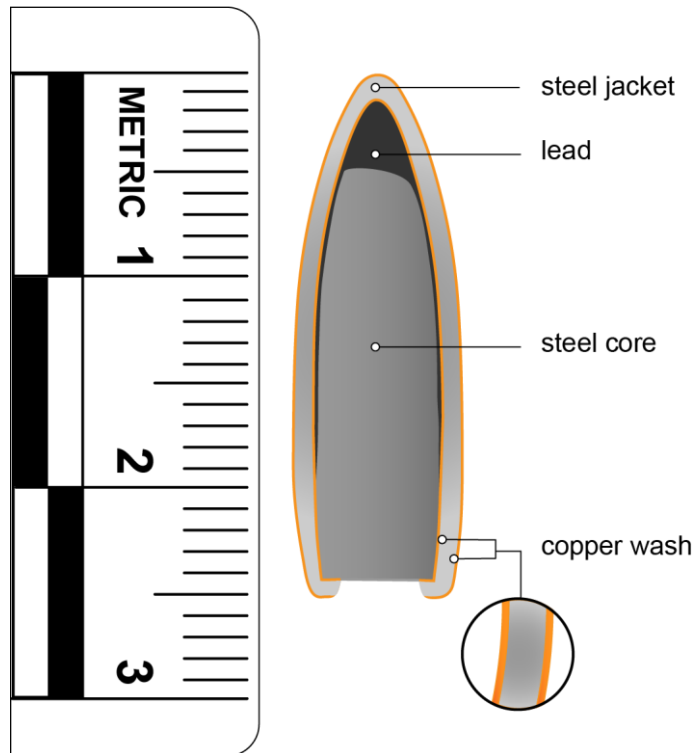


Figure 6-3 Details of Ukrainian MSC 7.62 x 39 mm ammunition

(1) Composition confirmed using Hitachi SU3500 scanning electron microscope with EDAX microanalysis system & TEAM software version 4.4.

(2) Microhardness of core and jacket measured using Indentec HWDM-7 apparatus with diamond indenter (Indentec, Unit 30 Navigation Drive, Hurst Business Park, Brierly Hill, West Midlands, DY5 1UT UK). Mean hardness of core* 207HV, SD 18HV; of jacket 199HV, SD 9 HV. Lead hardness 3.9HV.

(*from n=3 bullets using n=3 measurement points from each core and n=5 measurement points from each jacket; see Appendix B).

Prior to each shot the impact site on the model was confirmed using a sighting laser. The intended impact site was central into the frontal bone, below the post-mortem cut line, and around the level of the supraorbital margin. Projectile velocity was tracked using a Weibel Doppler, and impacts filmed using two

Phantom high-speed cameras (from the front a V12, sample rate 28,000 frames per second, exposure 4 μ s resolution 512 x 384; from the side a V1212, sample rate 37,000 frames per second, exposure 4 μ s, resolution 512 x 384). Experimental set up and typical images from an impact event are shown in Figure 6-4.

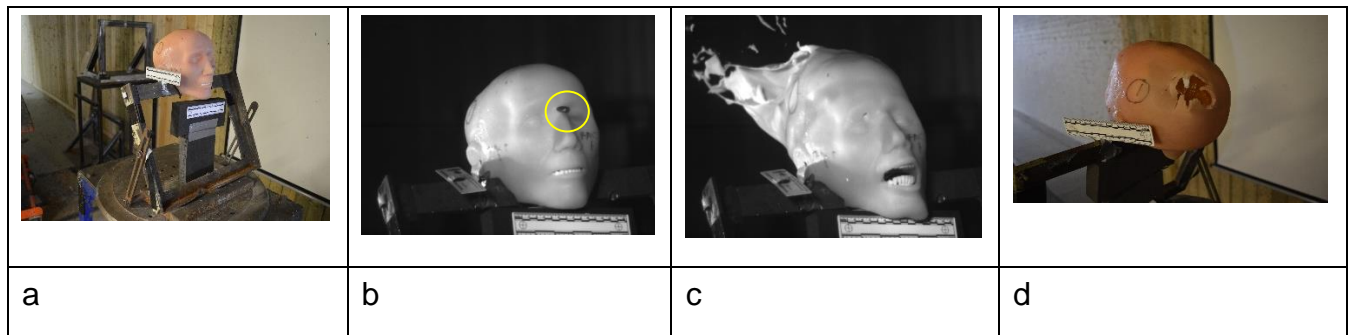


Figure 6-4 Face 1/Golf at range

(a) in situ at the range (b) image from V12 High Speed Video immediately prior to bullet impact, bullet circled (c) impact event, bullet has exited the model; the temporary cavity develops within the gelatine and the skin is extended (d) resulting exit wound in model.

The condition of the models in situ post impact was recorded using a Nikon D3200 DSLR camera fitted with an AF-S NIKKOR 18-55 mm lens. The temperature of the gelatine was taken immediately post impact using a calibrated digital thermometer.

6.3.6 Second set of CT scans

That evening the shot models were re-imaged at the Centre for Defence Imaging using the same CT protocols as for the first set of scans (Figure 6-5). Each model was scanned both without and with contrast material (Omnipaque™ 300, Iohexol, GE Healthcare Inc) injected into the wound tract. A pilot project imaging a series of 20 ml syringes filled with Omnipaque™ 300 diluted with different amounts of 0.9% saline found a mixture of 40% contrast and 60% saline produced the clearest images with the least artefact (See

Appendix F, Figure_A 19). For this study 20 ml of this mixture was gently introduced into wound tract using a syringe and a soft catheter, split 10 ml into the entry wound and 10 ml into the exit wound.

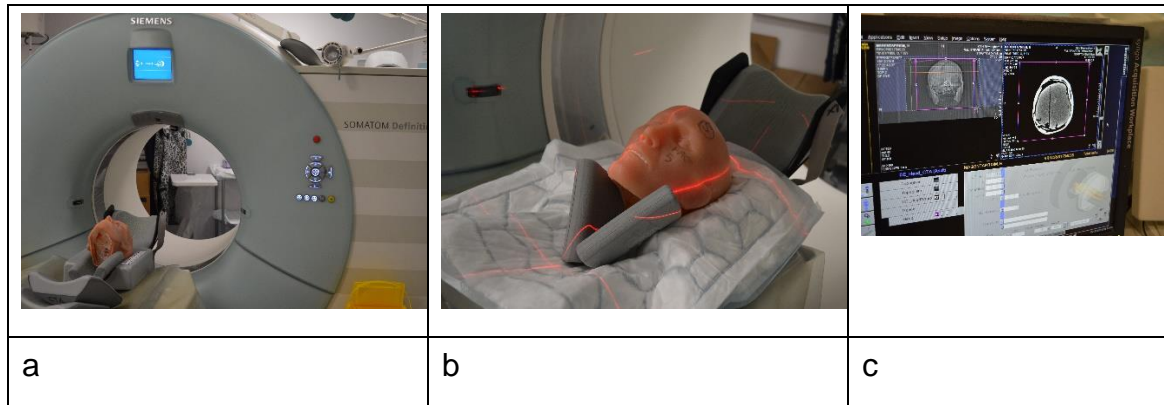


Figure 6-5 CT scanning at Queen Elizabeth Hospital Birmingham

(a) Face 1/Golf in the CT scanner (b) detail of Face 5 /Kilo in the CT scanner (c) CT work station displaying images from Face 2 / Hotel; bullet path and fractures are visible in right hand image on the screen.

6.3.7 Pathologists' examination

The six models were then examined by two Home Office Forensic Pathologists with extensive experience of assessing ballistic injury. The pathologists were invited to conduct a formal 'post mortem' examination of each model (Figure 6-6) and score them using a 4-point Likert-type scale [40] similar to that used in our earlier work (chapter 5 and [4]) but looking at more parameters (i.e. skin and soft tissue characteristics, entry wound, exit wound, fractures, wound tract, imaging). The score sheet also included space for comments if the pathologists wished to provide them. These are summarised in the results section below.

6.3.8 Radiologists' examination

The pre- and post- shot CT scans were viewed by a Military Consultant Radiologist with extensive experience of ballistic injury imaging using OsiriX DICOM viewer (<http://www.osirix-viewer.com>, Pixmeo SARL, 266 Rue de

Bernex, CH-1233 Bernex, Switzerland). Tissue layers were removed from the images using Phillips Brilliance Extended Work Station (Koninklijke Phillips N.V., Amstelplein 2, 1096 BC Amsterdam, The Netherlands) and the underlying damage assessed as described by Myers et al. [41] and scored using the same sheets referenced above. Examples of the CT scans are shown in Figure 6-7.

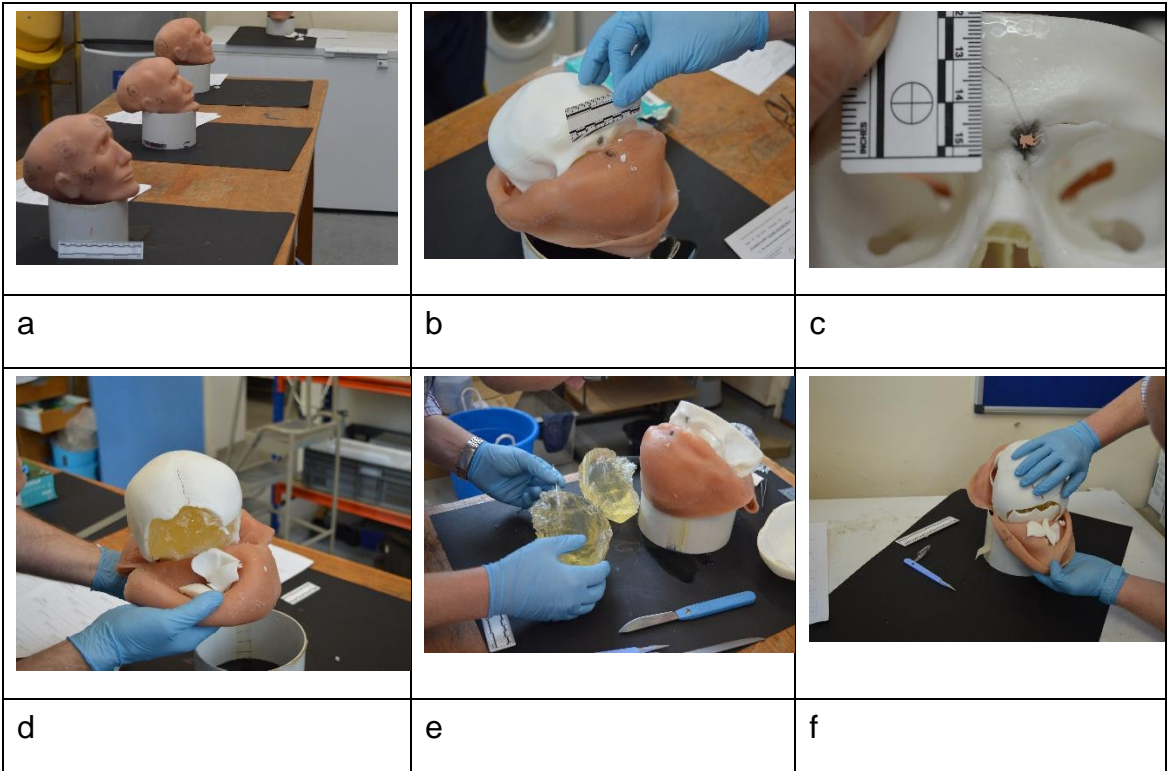


Figure 6-6 Pathologists' examination

(a) set up of examination room **(b)** entry wound in Face 3/India and underlying skull **(c)** detail of entry wound Face 6/Lima showing bullet wipe and radial fractures **(d)** corresponding exit wound, Face 6 **(e)** examination of gelatine brain, Face 6 **(f)** exit wound Face 2/Hotel.

6.3.9 High Speed Video (HSV) examination

The HSV images were reviewed to track the bullet trajectory through each of the models, assess if the impacts differed from one another and look for evidence of damage to the bullets.

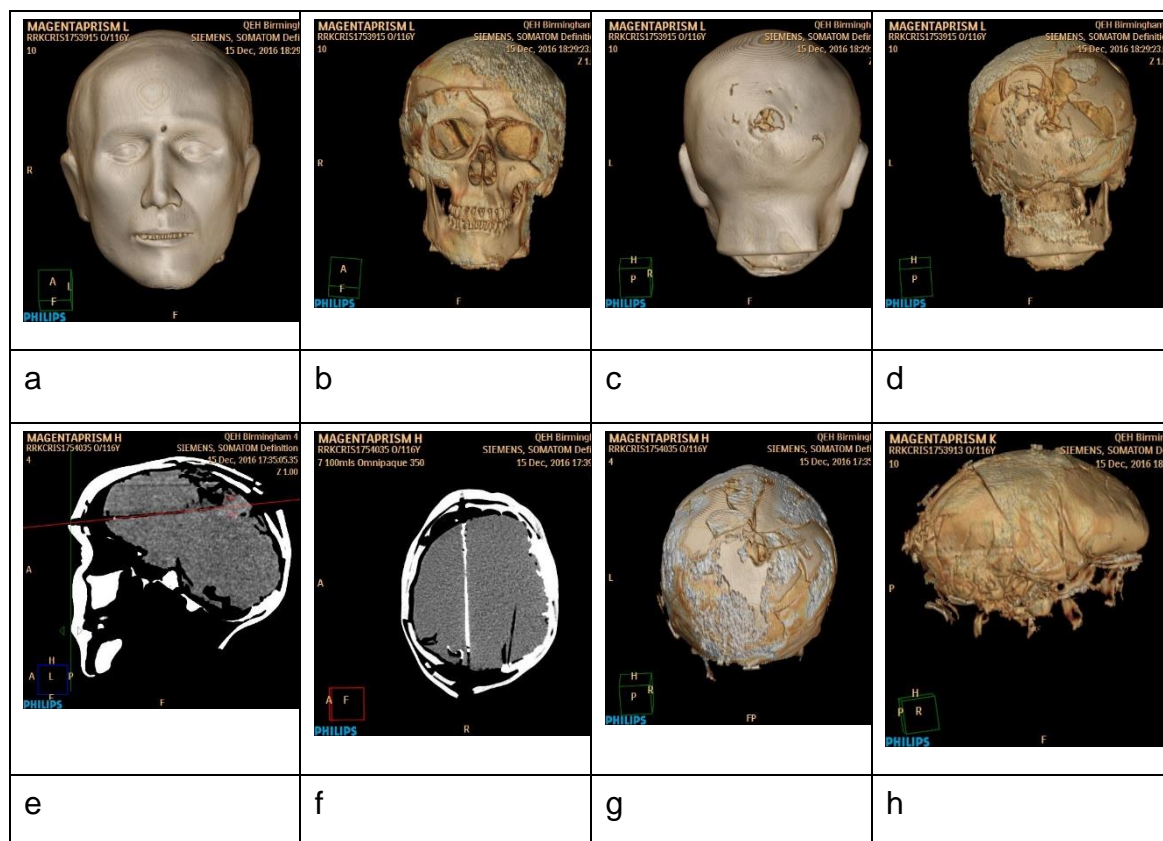


Figure 6-7 CT reconstruction images

a-d show Face 6/Lima

(a) entry wound (b) fracture patterns underlying entry site (c) exit wound (d) fracture patterns under exit site.

e-g show Face 2/Hotel

(e) sagittal view of bullet trajectory with fractures and exit wound (f) cross sectional view of same features; Omnipaque™ 300 contrast present in the bullet tract (g) 3D reconstruction of fractures (h) Face 5/Kilo; 3D reconstruction of gelatine brain with posterior damage post shot. Images from Phillips Brilliance Extended Work Station.

6.4 Results

6.4.1 HSV

Review of the HSV found that the bullets followed four slightly different trajectories. These are summarised in Figure 6-8. All the bullets with the

exception of the one impacting Face 4 emerged intact from the models. Face 4 is considered further below under 'Fracture Patterns'.

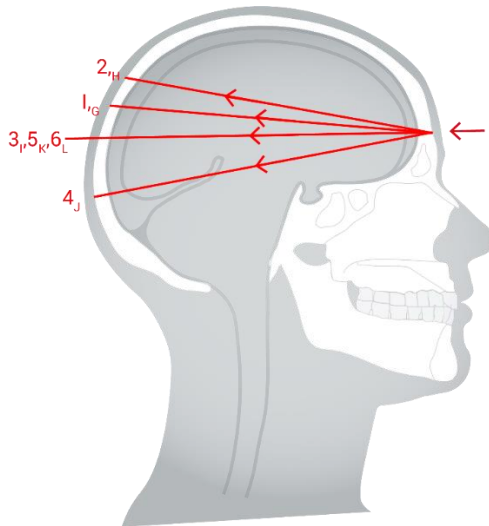


Figure 6-8 Summary of bullet trajectories

6.4.2 Likert-type scores

The scores from the Likert-type scales were collated in an Excel spreadsheet. These are summarised in Figure 6-9. The free text comments and notes made on the score sheets by the clinicians were also transcribed into an Excel spreadsheet so that comments about the wound characteristics and fracture patterns could be compared and assessed.

Each parameter (apart from imaging) could achieve a maximum score of 72 (i.e. 6 models, 3 assessors, maximum score of 4 from each assessor). The actual score obtained for each parameter was divided by 72 and multiplied by 100 to give an indication of how 'real' the combined assessors regarded each parameter to be as a percentage score. Imaging assessment was undertaken by only one assessor (IG) with a maximum possible score of 24.

No parameter scored the maximum 4 from any of the assessors.

With the small number of observations being considered more complex statistical analysis was not appropriate.

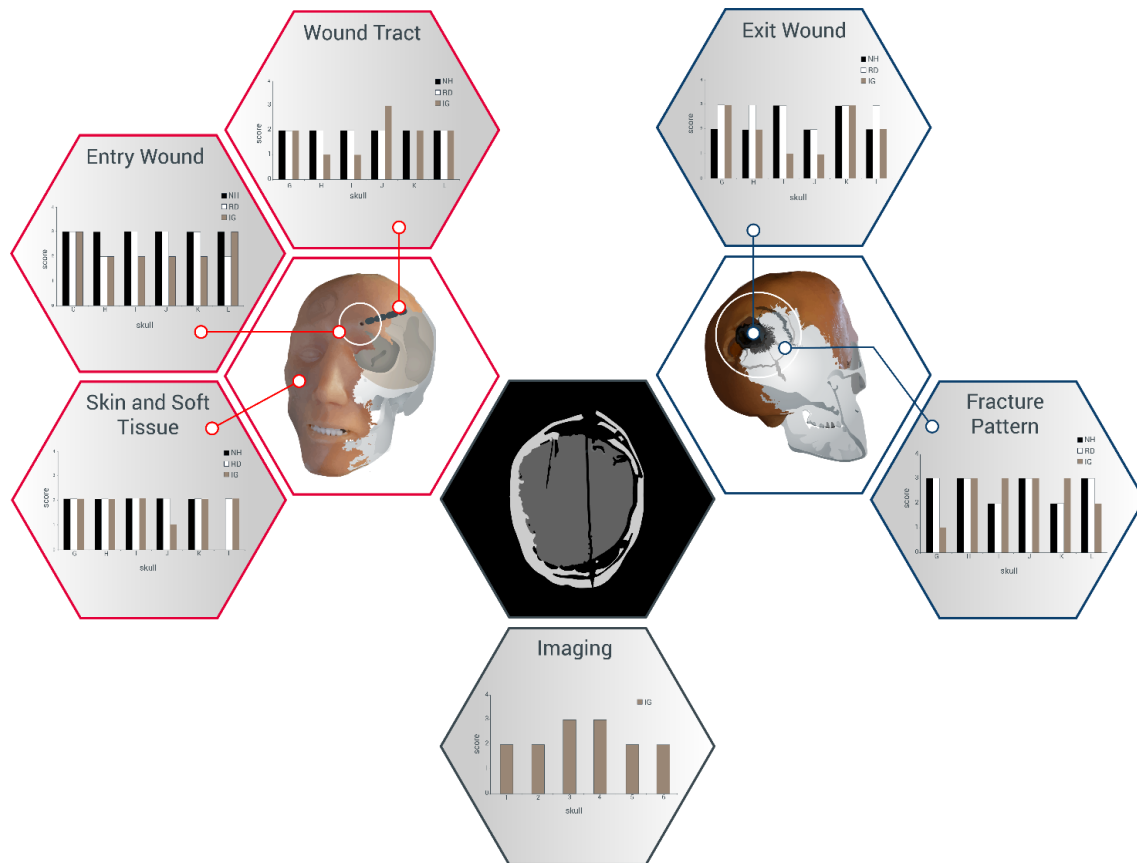


Figure 6-9 Summary of Likert-type score sheets as graphs.

Assessors are designated by initials and colours (NH = N Hunt, black; RD = R Delaney, white; IG = I Gibb, brown). Scores from NH and RD done from physical examination of models. Scores from IG done by examination of the CT scans.

6.4.2.1 Skin/soft tissue appearance and feel

Score 33/72 = 46%. The skin/soft tissue was mainly give a score of two by each assessor for each model, other than one which was not scored by one of the pathologists and another (Face 4) given a score of one based on the CT images by the radiologist. The radiology comment for Face 4 was the soft tissue over the frontal bones was too thick, which in turn exaggerated the wound tract through the soft tissue.

6.4.2.2 Entry wounds

Score 48/72 = 67%. Five of the tissue entry wounds (Faces 1 to 5) were described as 'too small for 7.62 mm bullet' by the pathologists. All were noted by the pathologists to have visible bullet wipe; abrasion collar and radial splits were present but required additional lighting and magnification to be seen well. On CT reconstruction, the bullet entry wound was described as 'gaping open' with the comment that real wounds often close down to a slit. The impact site on Face 6/Lima was more elliptical than expected and one of the pathologists (NH) felt this was due to its location over the medial aspect of the supraorbital ridge.

6.4.2.3 Exit wounds

Score 43/72 = 60%. Comments from all assessors were that the exit wounds in the soft tissue were generally more realistic than the entry wounds, although the overall score was lower. The larger wounds were regarded as more realistic (Faces 1, 2 and 5). Five wounds were noted to have everted margins and irregular edges, as is commonly seen in real wounds. Both Faces 3 and 4 were scored very low on CT examination with the comment that the exit wound in the soft tissue was not consistent with the underlying fractures, although Face 3 was described as realistic by the pathologists and scored well.

6.4.2.4 Wound tracts

Score 33/72 = 46%. Only one wound tract (Face 1) was described as realistic by one pathologist (RD). Two wound tracts (Faces 1 and 4) had fragments of bone and skin within the tract; features which are seen in real incidents. Bullets were noted to yaw at distances between 50 and 110 mm from entry into the gelatine. In five tracts, the damage to the distal end of the tract from the bullet yaw was such that detailed assessment was not possible by the pathologists (Faces 2, 3, 4, 5, and 6). From viewing the CT scans IG noted that the spread of contrast within the gelatine was very different to real brain. The pathologists stated that where folds were present in the gelatine (due to the thin

polyethylene bag in the skull, see Methods section 6.3.3 above) tract assessment was impeded and that as the ballistic injury features in real brain are very different to those in gelatine [19] direct comparison was not possible.

6.4.2.5 Fracture patterns

Score 47/72= 65%. Five of the entry sites had associated radial fractures, although these were found more often by the pathologists than from the CT scans due to the soft tissue CT appearance being close to that of the synthetic bone as described above (Faces 1, 2, 3, 4, and 6). From the pathologists' examinations, three of the entry sites (Faces 3, 5 and 6) had both internal and external bevelling at the entry site. Two of the exit sites had external bevelling (Faces 1 and 3) but for others loss of material at the exit site made bevelling assessment not possible. Three faces were described as 'realistic' by at least one pathologist (Faces 3, 4, 6). Face 4 was described as 'realistic for the trajectory, including the palpable mid-face fracturing'. The pathologists noted the round had struck the right petrous ridge. On the high-speed video, this is the only round seen to have fractured on exit from the model (Figure 6-10). As with previous work, (chapter 5 and [4]), the post-mortem cut present in the model impacted on some of the fracture propagation and was noted to be an issue in two of the models (Faces 5 and 6).

6.4.2.6 Imaging

Score 14/24 = 58%. While the CT images were able to produce good surface reconstructions, the skin/soft tissue properties were very close to those of the synthetic bone making reconstruction of the underlying structures difficult (e.g. Figure 6-7). The key observation from the overall assessment of the CT reconstructions was that the exit fractures were most realistic while the skin wounds and wound tract were less so.

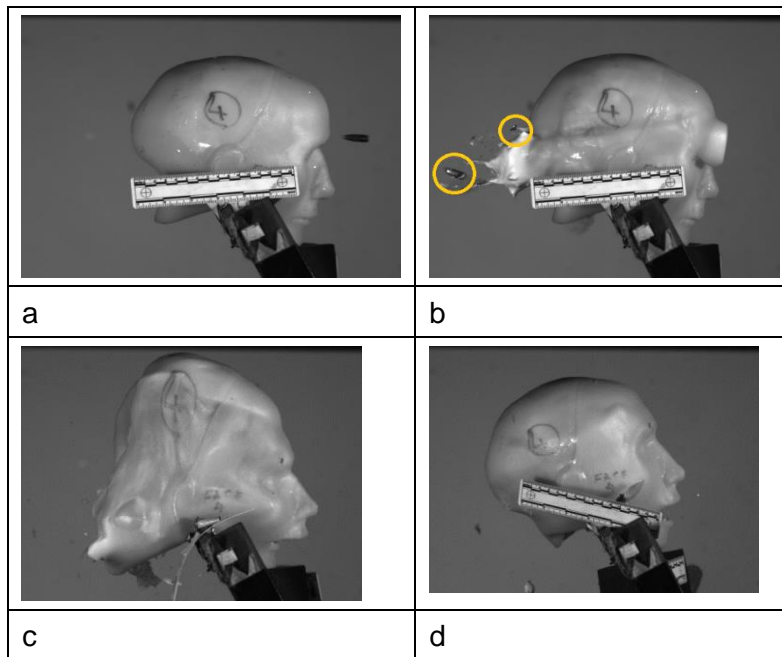


Figure 6-10 HSV Impact sequence Face 4

(a) Face 4, immediately before impact (b) bullet has exited damaged (left hand circle); bullet tip is visible separately (right hand circle); entry wound is still expanding (c) temporary cavity expansion (d) resting position after temporary cavity has collapsed down; skull fractures are visible through the synthetic skin and soft tissue.

6.5 Discussion

As far as possible the models used in the current work were constructed to be identical but inevitably there were minor differences (such as with the creases in the gelatine fill). The bullet ‘strike’ point was consistent for each model but there was variation in the trajectories (Figure 6-8), fracture patterns and entry/exit wound appearances as shown by the assessments. Schyma et al. [17] also noted differences among their four models and suggested this might be due to heterogeneity in the silicone coatings on the spheres.

Previous authors have suggested a high degree of authenticity for their ballistic injury models compared to actual wounds [3, 5, 7, 15]. Based on clinical experience in Afghanistan (2007-2014) of managing casualties soon after injury

during battlefield evacuation, one of the authors of the current study (PFM) felt that the overall look and feel of our model after shooting (particularly the exit wound and fracture complex) was realistic (see chapter 1).

None of the models scored a '4' ('exactly like a real injury') in any of the parameters assessed, unlike our previous study which did not include soft tissue [4]. In chapter 5 and [4], twenty three of the thirty-nine skulls assessed for fracture patterns were given a score of three by at least one of the five assessors and seven were given a score of four by at least one assessor. No skulls received the same scores from all five assessors. Figures 5-6 and 6-1 show the 'ideal' characteristics of gun shot injuries to the head but as noted in the introduction to this paper, the literature demonstrates that there are exceptions reported to these appearances in both experimental work and actual cases.

The main critical comment from the pathologists was that the skin/soft tissue was 'too stretchy'. The characteristics of the synthetic skin and soft tissue have major influences on the appearance of the entry and exit wounds. Rothschild [11, p257] states that the diameter of the central skin defect (Figure 6-1, A) is generally smaller than that of the bullet as, after being extended, the skin recovers elastically following the bullet perforation. Even allowing for this, and the reported bullet hole variation in experimental cases [23], our entry wound defects are smaller than real injuries (around 2 to 3 mm diameter skin defect). Previous work at the Impact and Armour group has used food-grade swine tissue for ballistic experiments; mean entrance holes using similar ammunition were 4.8 x 5.1mm (n=3) [30]. The skin entry wounds do show many features of real gunshot wounds (including bullet wipe, abrasion collar and radial tears) but to a varying degree. The properties of the skin/soft tissue surrogate are suitable for clinical training (see methods section above) but at ballistic strain rates behave differently to real skin. The similarity of the skin to synthetic bone on CT imaging also made aspects of the CT assessment challenging.

A key function of the surrogate soft tissues was containing the majority of the fragments associated with the bone exit wound. Even with this some of the material was lost making assessment of the exit characteristics difficult. In real cases wound assessment can also be frustrated by lost fragments, surgical treatment and scavenger activity [6].

Smith et al. [24] compared ballistic impacts on polyurethane bone substitute [Synbone®] with those on cattle scapulae. Impacts on the synthetic bone with modern rifle bullets (7.62 x 51 mm NATO FMJ and .243" Winchester jacketed soft point) produced the expected bevelled margins. The bone surrogate used in the current work showed some of the elements of real bone injury although bevelling at the entrance and exit sites was inconsistent, as can be the case in real ballistic events [13]. Overall, the reviewer response to the macroscopic fracture pattern in this work and the previous studies [3,4] was positive, likely due to the anatomically correct features of the skull model used.

Gelatine 10% is a very different material to living brain and the wound tract produced in the model is not as complex as actual injuries. As noted above (6.2.2, Imaging in ballistic investigations), real brain injury includes cortical contusions and bleeding from tissue shearing with associated oedema. Gelatine 10% does allow the formation of a temporary cavity and the production of realistic additional fractures as shown in Figure 6-4.

Our current study used a combination of physical assessments by pathologists and imaging assessments by a radiologist. Although Bollinger et al. [18] felt that imaging offered advantages over dissection, we agree with Karger [19] that the combination of methods is best as each can inform the other in searching out particular information (such as accurately locating intracranial fragments [21]).

A significant test for our model will be using it to recreate actual ballistic incidents and assessing how the CT images and injury patterns from the

models compare with those from real cases, allowing '*measurement and extrapolation*' as stated by Jussila [34].

6.6 Conclusion

An anatomically correct synthetic skull with a surrogate skin/soft tissue layer was impacted with 7.62 x 39 mm bullets and the damage assessed by two pathologists and a radiologist with experience of real gunshot wounds caused by similar ammunition. Drawing on two different clinical specialities has offered both contrasting and complementary views of the realism of the model.

The assessment was undertaken both by physical examination and CT imaging. The model showed some of the features of real wounds including entry and exit wound characteristics and macroscopic fracture patterns - but individual elements (including the size of bullet holes in the skin and synthetic bone bevelling) need refinement. Testing the model against data from actual incidents will allow us to critically assess it further and undertake these refinements.

6.7 Caveats

This paper only reports findings with one ammunition type fired at approximately 650 m/s. Other weapon systems or ammunition types may produce different results under these experimental conditions.

6.8 Acknowledgements

1.Cranfield University, Defence Academy of the United Kingdom, Shrivenham, SN6 8LA.

Clare Pratchett, Art Director, CDS Learning Services (Artwork for Figures 6-1, 6-3, 6-8 and 6-9).

David Miller and Mike Teagle, the Small Arms Experimental Range.

Adrian Mustey and Dr Jon Painter, Cranfield Forensic Institute.

2.Royal Centre for Defence Medicine, Research Park, Birmingham B15 2SQ.

Dr Amarjit Samra, Director of Research.

Ms Yvonne Yau.

3. Centre for Defence Imaging, Queen Elizabeth Hospital Birmingham, Mindelsohn Way, Birmingham B15 2TH.

Suzanne Elliott and Anthony Barnett, Military CT Specialist Radiographers.

6.9 References

1. Keene DD, Penn-Barwell JG, Wood PR, Hunt N, Delaney R, Clasper J, Russell RJ, Mahoney PF (2016) Died of Wounds: a mortality review. *J R Army Med Corps* 162: 355-360
2. Carr DJ, Lewis E, Horsfall I (2017) A systematic review of military head injuries. *J R Army Med Corps* 163:13-19
3. Carr D, Lindstrom A-C, Jareborg A, Champion S, Waddell N, Miller D, Teagle M, Horsfall I, Kieser J (2015) Development of a skull/brain model for military wound ballistics studies. *Int J Legal Med* 129: 505-10
4. Mahoney PF, Carr DJ, Delaney R, Hunt N, Harrison S, Breeze J, Gibb I (2017) Does preliminary optimisation of an anatomically correct skull-brain model produce clinically realistic ballistic injury fracture patterns? *Int J Legal Med* 131: 1043-1053
5. Thali MJ, Kneubuehl BP, Zollinger U, Dirnhofer R (2002) The 'skin-skull-brain model': a new instrument for the study of gunshot effects. *Forensic Science International* 125 (2-3): 178-189
6. Saukko P, Knight B (2016) Gunshot and explosion deaths. In: *Knights Forensic Pathology* (4th Edn) CRC Press, Taylor and Francis Group, Boca Raton. pp 241-275
7. Thali MJ, Kneubuehl BP, Zollinger U, Dirnhofer R (2002) A study of the morphology of gunshot entry wounds in connection with their dynamic creation, utilizing the 'skin-skull-brain model'. *Forensic Science International* 125: 190-194

8. Di Maio VJM (2016) Gunshot Wounds: Practical Aspects of Firearms, Ballistics and Forensic Techniques (3rd edn) CRC Press, Taylor and Francis Group, Boca Raton
9. Karger B (2008) Forensic Ballistics. In: Tsokos M (Ed) Forensic Pathology Reviews Volume 5. Humana Press, Totowa. pp139-172
10. Sellier K (1969) Bullet entry studies of the skin. Beitr Gerichtl Med 25:265-270
11. Rothschild, M (2011) Conventional Forensic Medicine. In: Kneubuehl BP (Ed), Coupland RM, Rothschild MA, Thali MJ. Wound Ballistics Basics and Applications. Translation of the revised third German edition. Springer -Verlag Berlin Heidelberg. pp 253-285
12. Leestma JE, Kirkpatrick JB (2014) Gunshot, penetrating and blast related injuries to the nervous system. In: Leestma JE (Ed) Forensic Neuropathology (3rd edn) CRC Press, Taylor and Francis Group, Boca Raton. pp 655-697
13. Quaterhomme G, İşcan MY (1999) Characteristics of gunshot wounds to the skull. J Forensic Sci 44: 568-576
14. Butler EG, Puckett WO, Newton Harvey E, McMillen JH (1945). Experiments on head wounding by high velocity missiles. Journal of Neurosurgery 2: 358-363
15. Thali MJ, Kneubuehl BP, Vock P, Allmen G, Dirnhofer R (2002) High speed documented experimental gunshot to a skull-brain model and radiological virtual autopsy. Am J Forensic Med Pathol 23: 223-228

16. Watkins FP, Pearce BP, Stainer MC (1988) Physical effects of the penetration of head simulants by steel spheres. *The Journal of Trauma* 28: S40-54
17. Schyma C, Greschus S, Urbach H, Madea B. (2012) Combined radio-colour contrast in the examination of ballistic head models. *Int J Legal Med* 126: 607-613
18. Bollinger SA, Ampanozi G, Kneubuehl BP, Thali MJ (2014) Gunshot to the pelvis- experimental ballistics and forensic radiology. *Journal of Forensic Radiology and Imaging* 2: 17-19
19. Karger B, Puskas Z, Ruwald B, Teige K, Schuirer G (1998) Morphological findings in the brain after experimental gunshots using radiology, pathology and histology. *Int J Legal Med* 111: 314-319
20. Oehmichen M, Meissner C, König HG, Gehl H-B (2004) Gunshot injuries to the head and brain caused by low-velocity handguns and rifles. A review. *Forensic Science International* 146: 111-120
21. Oehmichen M, Gehl H-B, Meissner C, Petersen D, Höche W, Geeling I, König HG (2003) Forensic pathological aspects of post-mortem imaging of gunshot injury to the head: documentation and biometric data. *Acta Neuropathol* 105: 570-580
22. Berryman HE, Smith OC, Symes SA (1995) Diameter of cranial gunshot wounds as a function of bullet caliber. *Journal of Forensic Sciences* 40: 751-754
23. Rainio J, Lalu K, Ranta H, Penttilä A (2003) Morphology of experimental assault rifle skin wounds. *Int J Legal Med* 117:19-26

24. Smith MJ , James S, Pover T, Ball N, Barnetson V, Foster B, Guy C, Rickman J, Walton V (2015) Fantastic plastic? Experimental evaluation of polyurethane bone substitutes as proxies for human bone in trauma simulations. *Legal Medicine* 17: 427-435
25. Bir C, Andreovich C, Di Maio VJM, Dougherty PJ (2016) Evaluation of bone surrogates for indirect and direct ballistic fractures. *Forensic Sci Int* 261: 1-7
26. Mahoney PF, Carr D, Miller D, Teagle M (2017) The effect of helmet materials and simulated bone and tissue layers on bullet behavior in a gelatine model of overmatch penetrating head injury. *Int J Legal Med* 131:1765-1776
27. Falland-Cheung L, Pittar N, Tong D, Waddell JN (2015) Investigation of dental materials as skin simulants for forensic skin/skull/brain model impact testing. *Forensic Sci Med Pathol* 11: 552-557
28. www.bbc.co.uk/news/uk-england-nottinghamshire-37497182 accessed 23 August 2017
29. Arm R (2015) Development of a Thoracic Trauma Trainer for the advancement of military operational surgical training. DMS RSG 20140911 [Internal Report]
30. Defriend JP (2015) Overmatching of military soft body armour. MSc Thesis Cranfield University
31. Wilkinson C (2004) *Forensic facial reconstruction*. Cambridge University Press, Cambridge, UK
32. Arm R (2017) A PDMS Soft tissue model for ballistic testing. Internal Report for Cranfield University. Purchase order 5146084

33. Lazarjan MS, Geoghegan PH, Jermy MC, Taylor M (2014) Experimental investigation of the mechanical properties of brain simulants used for cranial gunshot simulation. *Forensic Science International* 239: 73-8
34. Jussila J (2004) Preparing ballistic gelatine- review and proposal for a standard method. *Forensic Science International* 141: 91-98
35. http://nato.int/cps/en/natohq/declassified_136216.htm. Accessed 23/8/2017
36. Surveying the Battlefield: illicit small arms in Afghanistan, Iraq and Somalia. In: *Small Arms Survey 2012*. Cambridge University Press, New York. pp313-355
37. Threats, head injuries and test methodologies. In: *Review of Department of Defense Test Protocols for Combat Helmets (2014)* Committee on review of test protocols used by DoD to test combat helmets, Board on Army Science and Technology; Division on Engineering and Physical Sciences; National Research Council, National Academies of Science. ISBN 978-0-309-29866-7. pp15-24.
38. NATO Standard AEP-2920 (2015) Procedures for the evaluation and classification of personal armour. Bullet and fragmentation threats. Edition A Version 1. NATO Standardisation Office
39. Penn-Barwell JG, Sargeant ID (2016) Gun-shot injuries in UK military casualties- Features associated with wound severity. *Injury* 47: 1067-71
40. Clason DL, Dormody TJ (1994) Analyzing data measured by individual Likert-type items. *Journal of Agricultural Education* 35(4): 31- 35
41. Myers JC, Okoye MI, Kiple D, Kimmerle EH, Reinhard KJ (1999) Three-dimensional (3-D) imaging in post mortem examinations: elucidation and identification of cranial and facial fractures in victims of homicide utilizing 3-D computerized imaging reconstruction techniques. *Int J Legal Med* 113: 33-37

7 FORENSIC RECONSTRUCTION OF TWO MILITARY COMBAT RELATED SHOOTING INCIDENTS USING AN ANATOMICALLY CORRECT SYNTHETIC SKULL WITH A SURROGATE SKIN/SOFT TISSUE LAYER

Mahoney PF, Carr DJ, Harrison K, McGuire R, Hepper A, Flynn D, Delaney R, Gibb I

Publication: Int J Legal Med (2018) DOI 10.1007/s00414-018-1802-z

7.1 Abstract

Six synthetic head models wearing ballistic protective helmets were used to recreate two military combat related shooting incidents (three per incident, designated 'Incident 1' and 'Incident 2'). Data on the events including engagement distances, weapon and ammunition types was collated by the Defence Science and Technology Laboratory. The models were shot with 7.62 x 39 mm ammunition downloaded to mean impact velocities of 581 m/s (SD 3.5 m/s) and 418 m/s (SD 8 m/s) respectively to simulate the engagement distances. The damage to the models was assessed using CT imaging and dissection by a forensic pathologist experienced in reviewing military gunshot wounds. The helmets were examined by an MoD engineer experienced in ballistic incident analysis. Damage to the helmets was consistent with that seen in real incidents. Fracture patterns and CT imaging on two of the models for 'Incident 1' (a frontal impact) were congruent with the actual incident being modelled. The results for 'Incident 2' (a temporoparietal impact) produced realistic simulations of tangential gunshot injury but were less representative of the scenario being modelled. Other aspects of the wounds produced also exhibited differences. Further work is ongoing to develop the models for greater ballistic injury fidelity.

Key words: Ballistic, helmet, human head surrogate, cranial trauma, simulation

7.2 Introduction

Reconstructions are used in forensic investigation to try and understand what happened during an incident. Shooting incident reconstructions can vary in complexity from a single shot being fired from a single weapon to multiple weapons firing many shots [1]. Reconstructions can range from scale models and computer animations through to full sized re-enactments [1]. The aim of this project was to attempt to reconstruct two examples of combat related ballistic head injury.

Gunshot injury in humans can take a multitude of forms as detailed by Di Maio [2] and vary according to weapons system used, bullet construction and area of the body impacted. These factors need to be considered when contriving a reconstruction, particularly as different ammunition types can produce different bone fracture patterns [3] and injuries [4].

Reconstructions of ballistic events on humans have been undertaken with a range of models as described in Humphrey and Kumaratilake's recent (2016) review [5] this includes cadavers, animal models, simulated bone and tissue and computer models. Raino et al. [6] used anaesthetised pigs to study the morphology of assault rifle gunshot wounds and subsequent post mortem changes as part of their investigation into shootings in Kosovo. They commented that the work was helpful for clarifying injury mechanism but that *'the reproducibility of ballistic experiments using live animals is extremely difficult'* [6]. Issues included both variability in the appearance of different wounds, despite being inflicted by the same weapons and ammunition, and the effect of post mortem changes on the wounds as the experiment progressed.

Smith et al. [7] assessed Synbone®, a polyurethane synthetic bone substitute against real bone in a series of ballistic experiments. The advantage of using a manufactured proxy is that each should be identical. They concluded that the Synbone® responded similarly to bone on a macroscopic level but,

unsurprisingly, was less comparable when examined in detail due to the structural differences between the materials. The Synbone® spheres shot with modern rifles (.243" Winchester and 7.62 mm calibres) were noted to '*compare favourably with published examples of modern cranial gunshot injury*' [7]. Carr et al. [8] reported similar findings using an anatomically correct skull model which has been the basis for our subsequent experiments [9, 10].

Much of the groundwork on simulating ballistic head injury has been done by Thali et al. [11] who developed a 'Skin-skull-brain model' made of a silicone scalp, a layered polyurethane sphere to represent the skull, and gelatine 10% at 4°C to simulate brain. After shooting the model with a series of ammunition types the authors reported that the results were comparable to those of real gunshot injuries. Thali et al. [12] went on to use their model in a series of experiments, including researching the behaviour of 'glancing' head gunshots. They concluded that the model could be used for answering questions in real forensic cases where this was the underlying injury mechanism, i.e. it would provide a faithful platform for reconstructions in casework.

In more recent work Synbone® polyurethane spheres have been used to model close range (30 cm) 'execution' style head gunshots. The authors used six different calibres and provide photographs of two clinical cases (.22 LR and .45 ACP) where the bony injury and the model look very similar [13]. The model also performed well in a reconstruction of a blunt impact on a Neolithic skull using a replica contemporary club [14].

In modern combat injury the effect of protective helmets needs to be considered when modelling ballistic wounds [15]. In our previous work [16] the addition of material layers (including simulated bone, skin and sheets of helmet material) in front of a 10% gelatine block tended to increase the variability in bullet behaviour between different shots. This suggests that reconstructing a bullet impact on a head wearing a helmet is likely to be more complex than one without. Impact with intermediate targets (such as bone or helmet material) may

also cause bullets to destabilise and fragment [17], adding further to the complexity. Impacts on clothing [18] can also influence bullet stability.

It is not possible to place a combat helmet on a Synbone® sphere. In order to reconstruct impacts on a head wearing a modern combat helmet we have been developing a surrogate around an anatomically correct polyurethane skull [8] which, under ballistic impact, produces realistic fracture patterns [9] (chapters 5 and 6). Differences in bone thickness and structure within the skull accounting for fracture patterns from contact gunshot wounds are discussed by Fenton et al. [19] which lends further weight to using anatomically correct models for complex reconstructions.

Studies investigating Behind Helmet Blunt Trauma (BHBT) have looked at the interaction between ballistic impact, protective materials and head injury. Sarron et al. [20] undertook two sets of experiments using initially dry skulls, and later cadaveric heads, both protected by plates of helmet materials. The models were also instrumented with pressure sensors. The helmet materials were placed 12 to 15 mm from the skulls and impacted with 9 mm bullets at around 400 m/s. The aim was to produce a non-penetrating impact on the plates and assess the damage to the skulls and cadaveric heads from the plate deformation. For the cadaveric heads a 4-point scale was used to assess damage (0, nothing, to 3, severe). Greater plate deformation, and plates placed closer to the models, were associated with more damage to the models.

Freitas et al. developed a '*Human Head Surrogate*' [21] (HHS) by combining human crania with synthetic soft tissues and brain mounted to a Hybrid III ('crash test dummy') neck assembly. A stated intent was to '*fill the void between post mortem human subject testing (which have biofidelity but are subject to handling restrictions) and commercial ballistic head forms (easy to use but lack biofidelity)*' [21]. The models were instrumented with pressure transducers. The surrogates were fitted with a protective helmet and impacted with a series of ammunition types. As the intent of the study was to look at BHBT and, as with

Sarron et al. [20], produce a non-penetrating impact, a ceramic applique was fitted to the front of the helmet for high energy ammunition (7.62 x 39 mm and 7.62 x 51 mm). Flash x-ray was used to capture the maximum back face deformation of the helmets. The extent of the resulting fractures was assessed and graded as none, minor, moderate or critical, descriptors which had been discussed earlier in the study in relation to associated clinical injury.

In contrast to these BHBT studies we wanted to assess a completely synthetic surrogate and test it against a penetrating head injury.

7.3 Method

7.3.1 Ethics and permissions

Ethical approval for developing and testing a ballistic injury surrogate was obtained from Cranfield University.

Permission to view anonymised Computer Tomography (CT) images of deceased coalition service personnel was granted by the Coroners of Oxford and Wiltshire. The request to the coroners stated that the purpose of this was to develop a synthetic model of ballistic head injury to improve future protection.

7.3.2 Defence Science and Technology Laboratory

The Joint Theatre Trauma Registry (JTTR) is a data base of major trauma casualties from recent conflicts [22]. Permission was granted to search JTTR for fatal gunshot head injuries, building on previous work [23]. The review of JTTR took place at the Defence Science and Technology Laboratory (DSTL) and identified sixty casualties who had suffered a fatal gunshot wound to the head during the period 2006 and 2013.

Each case was then assessed for additional information about the events using incident reporting, contemporary accounts, equipment and threat analyses, and operational learning reports held at DSTL. This included likely engagement ranges, weapon systems used and bullet types (where known). If engagement ranges were not specifically stated these were calculated from maps and satellite images of the ground where the shooting took place. All reviews were conducted using incident reference numbers and no personal data was released in accordance with data protection requirements.

In order to allow comparison with our previous work (chapters 3, 5 and 6 and [9, 10, 16]) casualties were identified where 7.62 mm bullets were confirmed responsible for the injuries (this included 7.62 x 39 mm, 7.62 x 51 mm and 7.62 x 54R mm). Seven casualties were confirmed as such. While it is highly likely that other casualties were struck by 7.62 mm bullets this could only be confirmed with certainty where either bullets or enemy weapon systems were recovered.

DSTL uses a software package called IMAP (Interactive Mapping Analysis Platform, IMAP v1.3.3.0, developed under contract to DSTL) to map bullet and fragment strikes, trajectories and resulting injuries on casualties. The IMAP images for the seven casualties with 7.62 mm bullet injuries were reviewed and confirmed to involve the casualties' helmet and head (Figure 7-1 a-e).

Casualties where bullets had hit an intermediate target prior to striking the helmet were removed from the group. As noted above this makes bullet behaviour more unpredictable. Casualties whose injury predated the UK policy of post-mortem CT scanning were also removed from the group. This left two casualties, identified only by an incident number. The incident number was used to retrieve the post mortem CT scans and selected images from these were made by Defence Radiology with all identifying data removed (Figure 7-1f).

The anonymised CT images and summary of the incidents (engagement range, calculated impact velocity of the bullet and selected IMAP images) were collated as laminated A4 sheets, one set for each shooting, and labelled ‘Incident 1’ and ‘Incident 2’.

7.3.3 Model construction

Six head models were built from a synthetic skull [8, 9, 10], face and scalp (made from polydimethylsiloxane, PDMS, Flexural Composite Research Laboratory, Nottingham Trent University) with a 10% by mass gelatine fill (Figure 7-2 a, b). The full methodology is described in chapter 6 and [10].

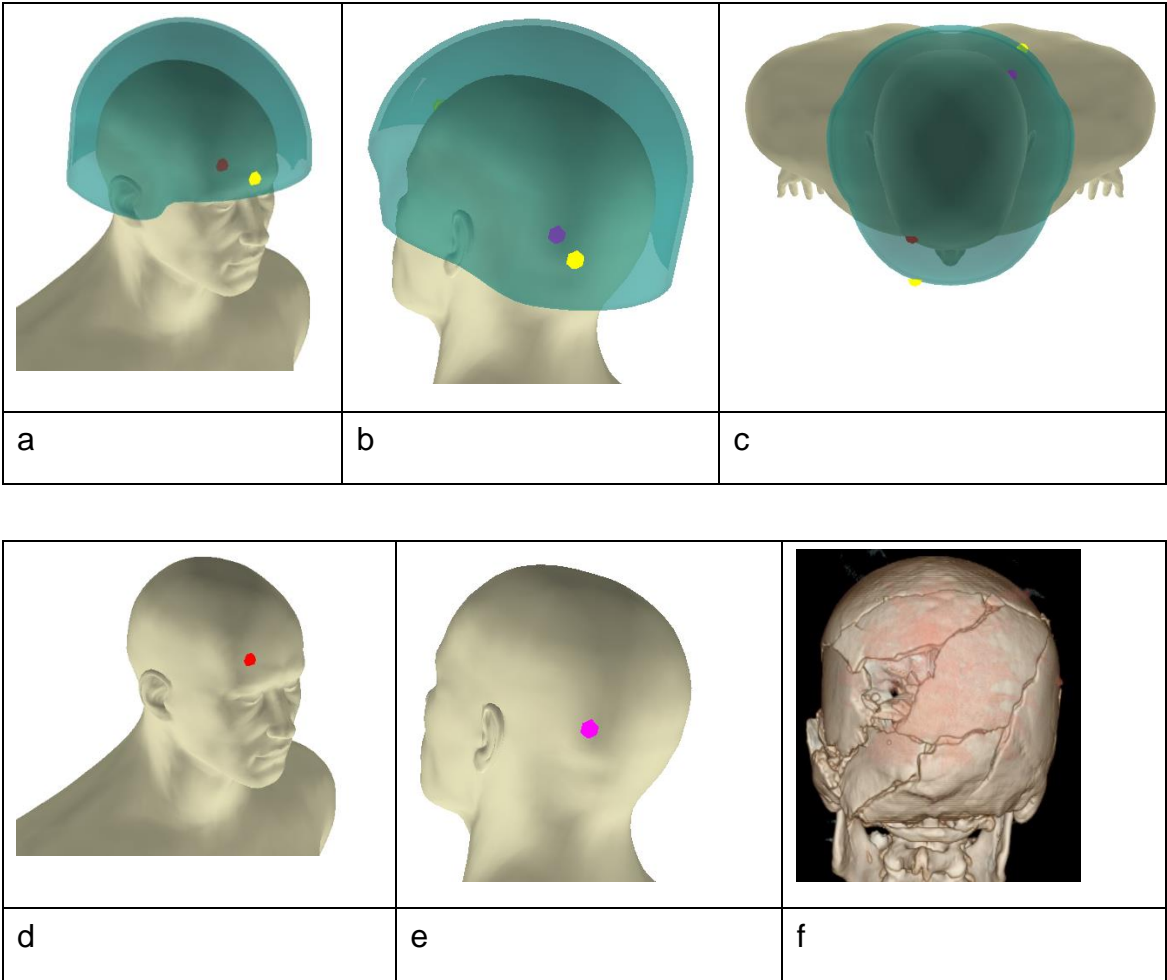


Figure 7-1 IMAP and CT Images Incident 1

(a) entry wounds, helmet in situ (b) exit wounds, helmet insitu (c) view from above, helmet in situ (d) entry wound site on skin (e) exit wound site on skin (f) anonymised CT scan showing exit wound left parietal bone, posterior aspect.

Each head model was fitted with a commercially purchased ballistic helmet (Figure 7-2c). The helmet consisted of an outer protective shell made of multiple layers of resin bonded para-aramid and an impact absorbing liner. For security reasons this was not a current in-service military helmet but one with a similar construction and performance to allow a valid comparison.

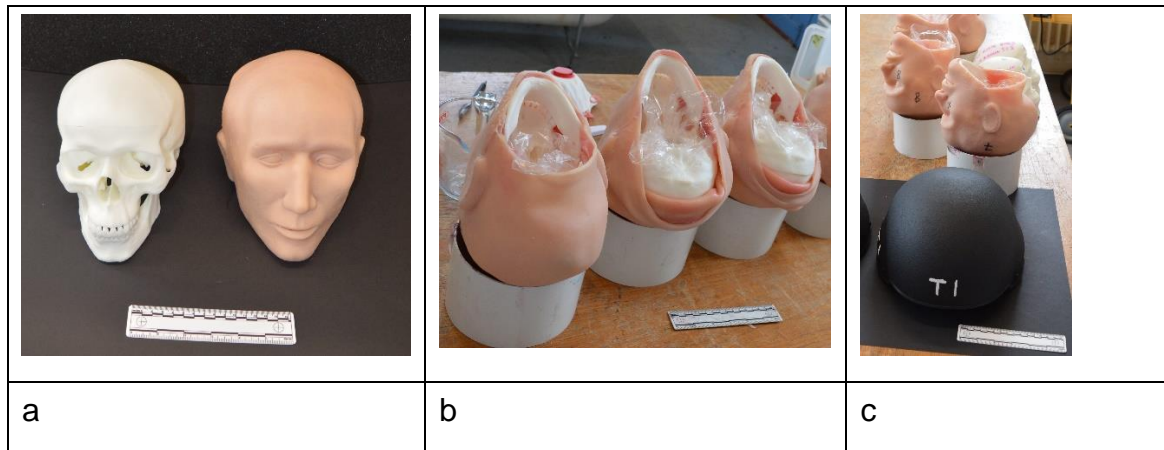


Figure 7-2 Model construction

(a) polyurethane skull and corresponding skin layer (b) models being filled with 10% gelatine (c) ballistic helmet in foreground.

7.3.4 Range and flash x-ray

The models were placed in turn 9.6 m from a No 3 Enfield Proof Mount fitted with an accurate barrel (length 72.5 cm, 1:9.45 twist rate) at the Cranfield Ordnance Testing and Evaluation Centre (COTEC, Gore Cross, West Lavington, Devizes, Wiltshire, SN10 4NA, UK).

Each model was shot once with 7.62 x 39 mm Mild Steel Core Ukrainian Ammunition (chapter 5, Figure 5-1; chapter 6, Figure 6-3, Appendix B). Using data from Kneubuehl [24] and data from previous work at the Impact and Armour Group [25], ammunition was reloaded with Vivhtavuori N140 smokeless propellant (Nammo Lapua Oy, Vivhtavuori Site, Ruutitehaantie 80, FI-41330

Vihtavuori, Finland) to recreate the bullet impact velocities from the actual incidents. Models one to three were used to recreate 'Incident 1' (entry and exit wounds as shown in Figure 7-1) and Models four to six to recreate 'Incident 2' (entry wound left temporoparietal region; exit wound lower left occiput). Models for 'Incident 1' were impacted at a mean velocity of 581 m/s (SD 3.5 m/s) and models for 'Incident 2' at a mean velocity of 418 m/s (SD 8 m/s).

The impacts were captured with high speed video (HSV) cameras (V12; sample rate 41000 fps, exposure 10 μ S, resolution 512 x 256; and V1212; sample rate 37000 fps, exposure 6 μ S, resolution 384 x 288). Just prior to impact each bullet penetrated a thin foil located in front of the model triggering the Scandiflash 150 x-ray system (Scandiflash AB, Palmbladsgatan 1A, S-754 50 Uppsala, Sweden). The distance from the foil to the centre of the model was measured and, with the expected impact velocity of the bullet, used to calculate the likely time lapse in microseconds from the bullet cutting the foil to reaching the required point in the model. This was input into the x-ray system's delay generator with the aim of delivering the x-ray exposure at the correct point in the bullet's pathway. Each exposure was delivered over a period of 35 nanoseconds. To ensure adequate penetration of the model the maximum output voltage of 150 kV was used. The experimental set up is summarised in Figure 7-3.

7.3.5 CT Scans

After shooting each model was handled carefully to minimise any disruption to the underlying bullet damage and taken in padded cool boxes to the Department of Radiology at the Queen Elizabeth Hospital Birmingham for CT Scanning by military radiographers using SOMATOM Definition CT scanner, (Siemens Health Care Ltd, Camberley, UK) using Spiral Head protocols (Window Level 100/35, 1 mm slice thickness).

The scans were sent to an experienced military radiologist for reporting and comparison with the actual incidents. Tissue and helmet layers were removed

from the images using Phillips Brilliance Extended Work Station (Koninklijke Phillips N.V., Amstelplein 2, 1096 BC Amsterdam, The Netherlands).

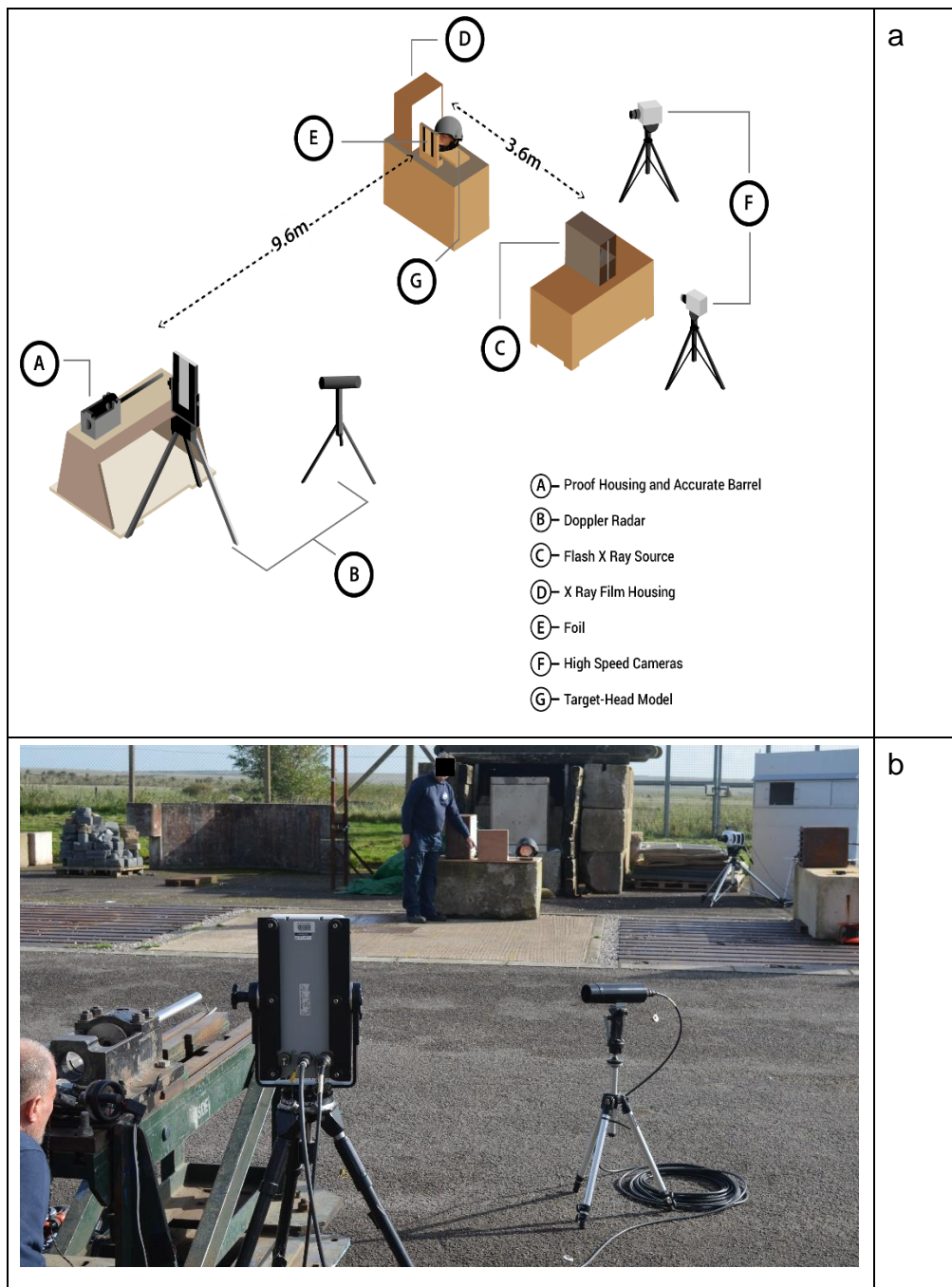


Figure 7-3 Experimental set up at COTEC

(a) schematic (b) ballistic range.

7.3.6 Pathologist and engineer examination

The models were then taken back to the Impact and Armour Group at the Defence Academy, Shrivenham for examination by a Home Office pathologist and an MoD engineer experienced in post incident analysis of ballistic events (Figure 7-4).

As shown in Figure 7-4 (a & b) and Figure 7-9 (b) the helmets had all been moved by the bullet impact from the position in which they would be correctly worn on the head. The radiologist and pathologist were invited to score their findings using a Likert-type scale [26] (Table 7-1, *Results*) against the actual incidents being recreated (Table 7-2, *Results*). They were also asked to comment on how the models compared to other incidents they had been involved with. The MoD engineer was invited to write up the findings in the format that would be used in actual investigations.

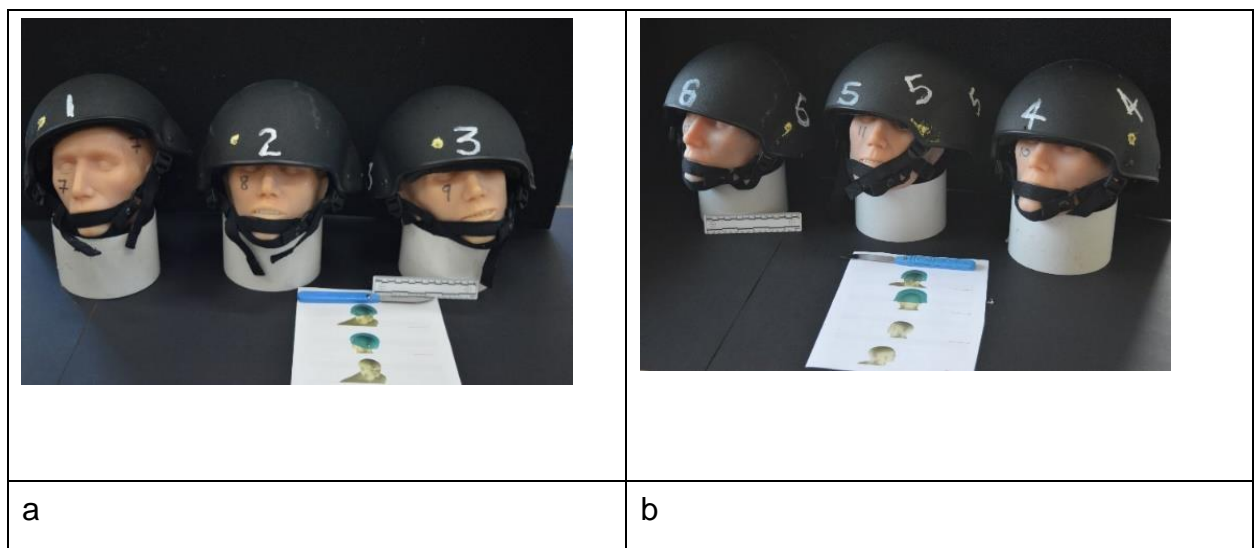


Figure 7-4 Models awaiting examination after shooting

(a) Incident 1, models 1-3, frontal impact (b) Incident 2, models 4-6 side impact; hard copy of the relevant IMAP images (described above) are visible in the foreground. Models are described in the text by the helmet number shown in white. The black numerals on the faces indicate that they are sequential to those described in [10] and chapter 6.

7.4 Results

7.4.1 Impact event HSV and flash x-ray

Impact events were captured on HSV (V12 and V1212) for all six models. Flash x-ray imaged the bullet passage in models 2,3 and 5. Bullets perforated all the head models except 5 where the bullet passed between the inside of the helmet and the head, impacting on the inner aspect of the rear of the helmet. The forward-facing surface of each helmet was perforated by the bullet entry impact (Figure 7-5 b).

None of the rear surfaces of the helmet were perforated after the bullet exited the head model, although damage is visible on the CT scans (Figure 7-9). Example images from the HSV and flash x-ray, plus model 5 in situ after shooting are shown in Figure 7-5. Of note the bullets can be seen to have yawed through 180 degrees in the flash x-ray images (Figure 7-5 g & h).

7.4.2 Summary of bullet trajectories

The entry points in the helmets and entry and exit points in the head model were plotted to allow comparison with the actual incidents. These are summarised in Figures 7-6 and 7-7. Of note the experimental gunshots tended to track in a more upward direction than the actual wounds in both incidents.

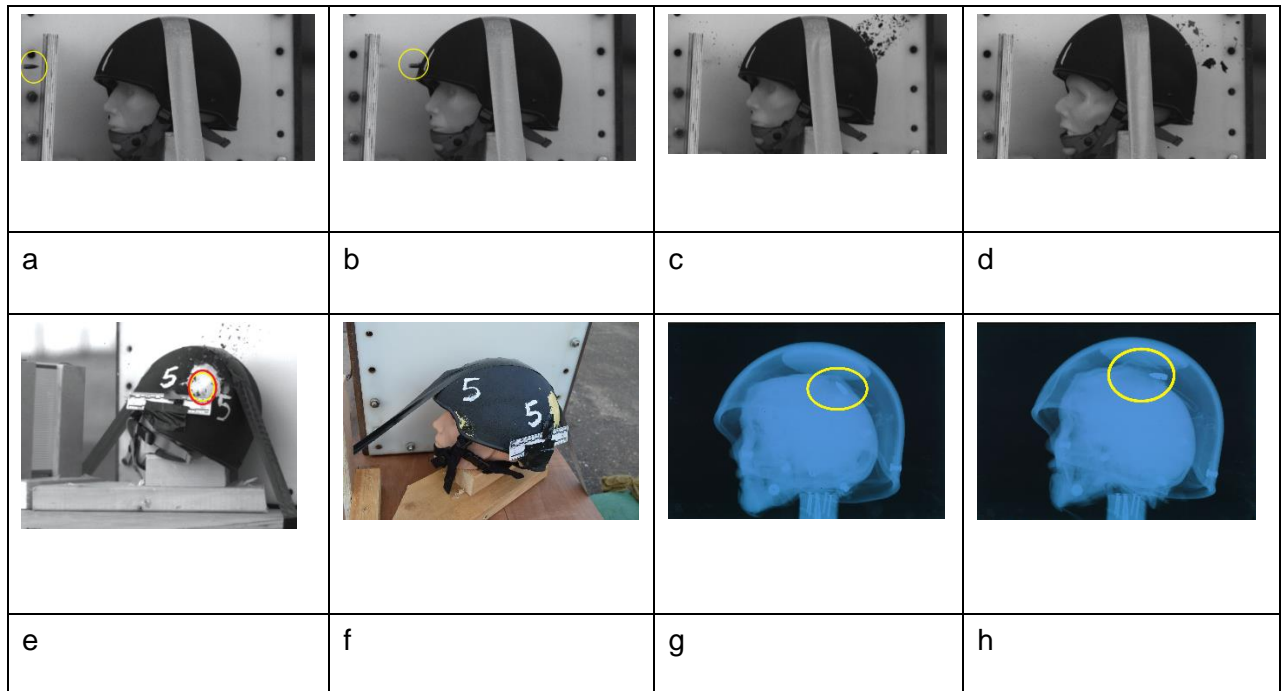


Figure 7-5 Impact events and flash x-ray

(a-d) Impact sequence model 1, frames from V12 camera

(a) bullet (circled) prior to cutting foil (b) helmet impact, bullet circled (c) shower of paint from bullet impact inside rear of helmet (d) distortion of face due to stretching from temporary cavity development (e) impact of bullet inside rear of helmet 5. Distortion of helmet material from bullet impacting sideways circled. Frame from V1212 camera (f) model 5 insitu after shooting

(g-h) Flash x-ray images

(g) model 3 (h) model 2

Bullets circled in frames a, b, e, g and h; forensic scale visible in (e) and (f).

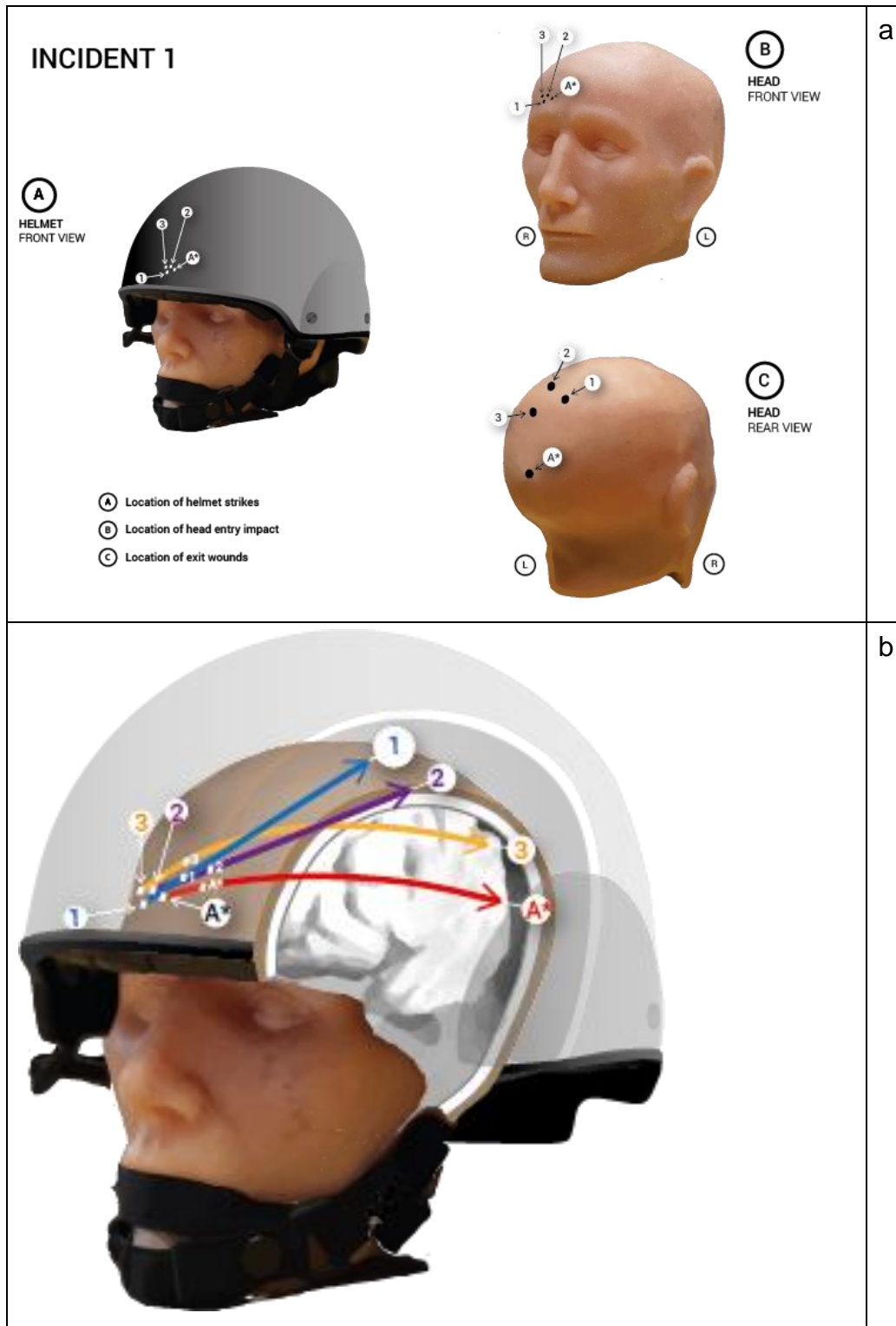


Figure 7-6 Location of strikes and trajectories models 1 to 3

(a) location of bullet strikes in models 1,2,3. The A* symbol designates the actual strike points in Incident 1 (b) summary of bullet trajectories within models 1,2,3 compared with the actual trajectory, A*.

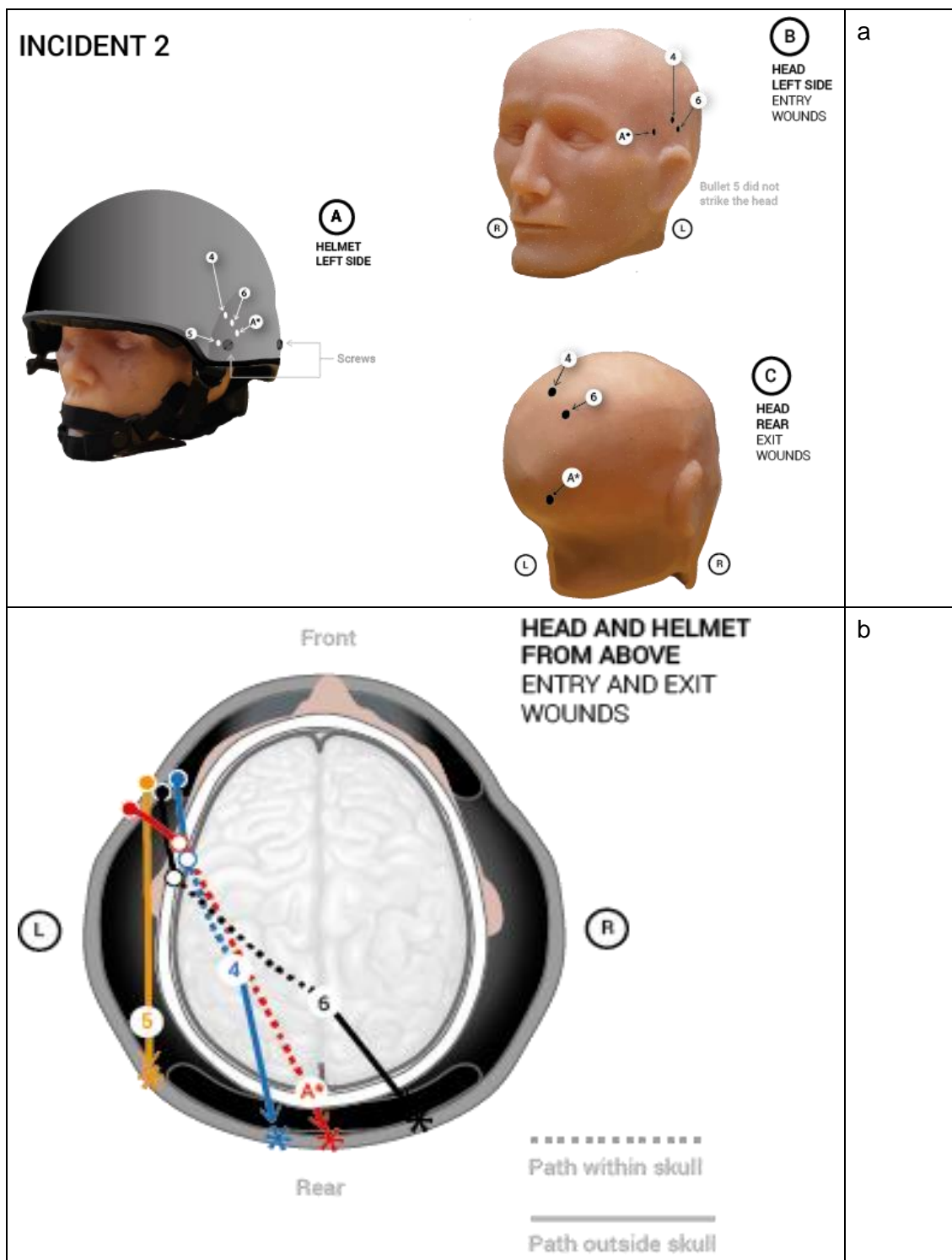


Figure 7-7 Location of strikes and trajectories models 4 to 6

(a) location of bullet strikes in models 4, 5, 6; the A* symbol designates the actual strike points in Incident 2 (b) summary of bullet trajectories within models 4, 5, 6 compared with the actual trajectory, A*.

7.4.3 Engineering helmet assessment

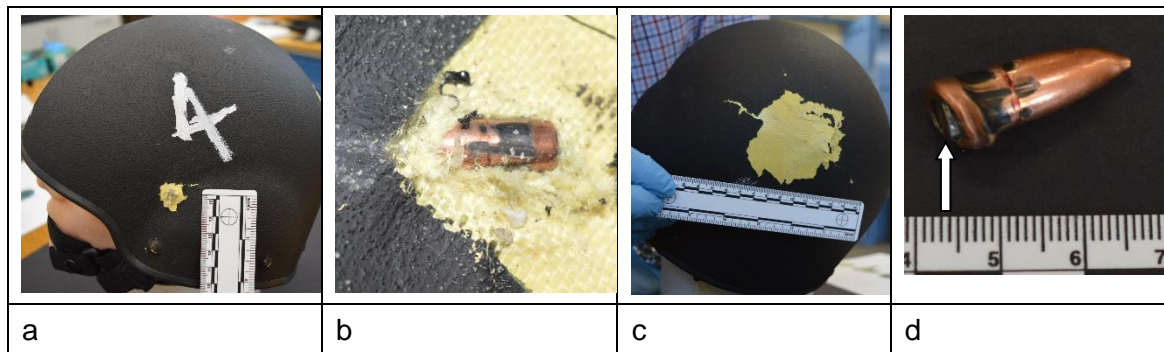


Figure 7-8 Engineering helmet assessment

(a) assessment of entry site, helmet 4; four mm perforating entry hole surrounded by area of paint loss (b) bullet embedded in composite shell of helmet 2 (c) area of damage rear of helmet 1 (d) distorted bullet from helmet 3; copper jacket twisted to reveal mild steel core (arrowed).

All helmets had a perforating entry hole (all six were 4 mm diameter) marked by bullet wipe, on the outer face of the helmet shell (Figures 7-5b, 7-8a). The helmets were dismantled removing the inner net liner, foam impact liner and comfort pads to allow full inspection of the composite para-aramid shell. The inner face of the entry holes had fibres of the composite shell distorted inwards towards the head model. Helmets 1, 2, 3, 4 and 6 had fragments of simulated bone and tissue evident inside the helmet, consistent with a bullet passing through the head model.

A bullet was found lodged between the para-aramid shell and foam impact liner in helmets 1, 4 and 6. A bullet fell free from helmet 3 during examination (Figure 7-8d). The bullets from helmet 2 and helmet 5 were embedded in the para-aramid shell (Figure 7-8b).

On each of the helmets there was an area of loss of the outer gel coat and black paint (Figures 7-5 c-f, 7-8c) (mean diameter 65 mm; SD 13 mm) with distortion of the para-aramid shell outwards (Figure 7-5e, 7-8c).

Overall the damage to the ballistic helmets was assessed to be representative of that seen in actual incidents.

7.4.4 Forensic Pathologist and Military Radiologist assessment

The Likert-type scores from the forensic pathologist (FP) and military radiologist (MR) are summarised in Table 7-2. As shown in the table there were differences in the scores awarded by the pathologist and radiologist to the considered features.

The CT imaging of the damaged helmets scored high, which is consistent with the engineering assessment given above. Model 5 only involved helmet damage so is not part of the further assessment of the simulated injuries. Examples of the simulated injury assessments and related CT images are shown in Figure 7-9.

For 'Incident 1' models 2 and 3 scored 'quite like the real incident' for both the CT images and pathology assessments. The comment on the lower scoring model 1 was that the fracture patterns and fragments along the vertex did not seem quite right.

The skin entry wound was described a 'slit like' and too narrow in models 1-3 by the pathologist but 'gaping' by the radiologist. Synthetic bone fragments were noted to be protruding through the skin in models 2 and 3 in the area between the bullet entry and exit wounds.

For 'Incident 2' models 4 and 6 produced very superficial bullet paths compared to the actual incidents and were scored low by the pathologist accordingly. The imaging scores were generally higher. The models did, however, produce realistic tangential injury patterns of the type described by Thali [12] which is noted by the scores in brackets in Table 7-2. A key feature of model 6 was a good fracture propagation seen in the CT images.

Mean neck length (distance from entry into the gelatine to beginning of yaw) of the permanent cavity in the gelatine 'brains' of models 1-3 was 60 mm (SD 5 mm). The bullet path in the gelatine brains of models 4 and 6 was too small due to the tangential strikes to make meaningful measurements. The mean neck length in gelatine blocks with sheets of the same synthetic materials as intermediate targets described in [16] was 56 mm (SD 27 mm) but the SD was much greater.

7.5 Discussion

The aim of this work was to attempt to replicate the injuries seen in two cases of combat related ballistic head injury, building on our previous model development [8, 9, 10, 16] and chapters 3 to 6.

Hueske [1] describes how shooting incident analysis and reconstruction requires the input of a number of different scientific disciplines. Our current work illustrates this when compared with our earlier projects by the input needed from DSTL to gather basic data about the events (engagement range, weapon type, ammunition type, etc).

Two of the models representing Incident 1 achieved an overall score of 3 by at least one of the two assessors ('quite like the real incident') although as noted in the Results, the bullets in the models followed an upward path compared with those in the actual incident. Hueske [1] also notes that some variables about an incident will not be known including exact position of the shooter and the victim at the time. Small changes in the positioning of the models could alter the bullet path through the simulants significantly. In addition, as shown in our earlier work (Figure 6-8) there is often a degree of variation in trajectories.

From analysis of the HSV, the foil used to trigger the flash x-rays does not appear to alter the bullet flight prior to impact on the model. While bullet behaviour within the models could be inferred from the permanent cavity in the

gelatine 'brain', the exit fracture patterns and the resting place of the bullet within the helmet structure, the flash x-ray images were helpful to confirm this. While the mean neck length in the gelatine brains of models 1,2 and 3 (see *Results 7.4.4* above) was similar to that of gelatine blocks in our earlier work (chapter 3 and [16]), with intermediate targets of sheets of the same helmet material, synthetic skin and synthetic bone), there was greater variability in the blocks. Further work is needed to understand how comparable the models are.

The presence of synthetic bone and tissue within the helmets is consistent with post-shooting artefacts seen in actual incidents.

The models representing Incident 2 scored less well than those of Incident 1. The bullet pathway in synthetic head models 4 and 6 was very superficial. While these did not replicate the injuries from the actual incident, they did produce a good representation of tangential head gunshot wounds as described in Thali's work [12] and illustrated in real examples by Di Maio [2].

Post hoc matching of damage to a model with historical clinical images is a useful process when establishing if a simulation has any clinical congruence [7, 8, 9, 11, 12], but when undertaking a reconstruction caution and care are needed to ensure incorrect conclusions are not drawn.

As shown in Figure 7-7b, the bullet in model 5 perforated the helmet, missed the head and impacted in the rear of the helmet. The head model was undamaged. Within our military data set there are at least two confirmed incidents of bullets entering helmets and missing the head. One bullet was retained in the helmet, one exited. In neither case was the skin penetrated but both cases were associated with a traumatic subarachnoid haemorrhage and one with a calvarial fracture.

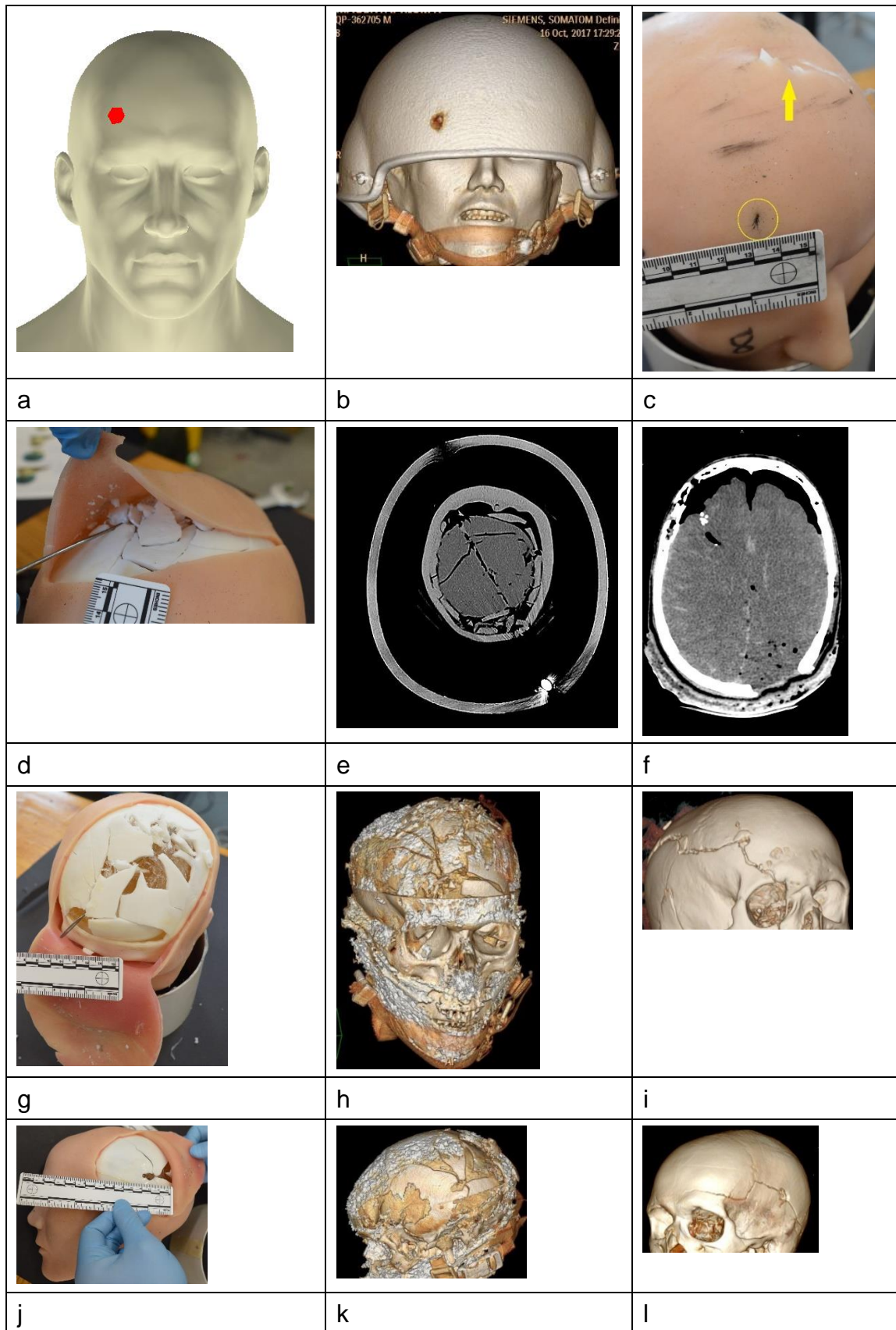


Figure 7-9 Simulated injuries and corresponding CT images

3D CT reconstructions from actual incidents as detailed below.

(a) IMAP image for incident 1

(b-e, g-h) model 2, Incident 1

(b) 3D CT scan reconstruction with helmet in situ; entry site visible, for comparison with (a). Note helmet has been moved from correct wear position by bullet impact- see Figure 7-4

(c) 'slit like' skin entry wound (circled), and synthetic bone fragments protruding through the skin (arrow)

(d) underlying fractures

(e) corresponding CT scan of the Model, helmet insitu

(f) CT scan of the actual incident, no helmet

(g) model 2, fractures exposed, probe marks path of bullet through gelatine brain

(h) corresponding 3D CT reconstruction

(i) 3D CT reconstruction of actual Incident 1

(j-k) Model 6, Incident 2

(j) tangential bullet strike; left parietal area

(k) corresponding 3D reconstruction of the fractures in model 6

(l) 3D CT reconstruction, actual incident 2.

Table 7-1 Explanation of Likert-type scores

(4) Exactly like the real incident	(3) Quite like the real incident	(2) A bit like the real incident	(1) Nothing like the real incident
------------------------------------	----------------------------------	----------------------------------	------------------------------------

Table 7-2 Likert-type scores, Forensic Pathologist (FP) and Military Radiologist (MR)

	Helmet CT imaging	CT Imaging of head model	Skin Entry	Bone Entry	Bullet Path in brain	Bone exit	Skin exit	How close is the model taken as a whole to the incident?
INCIDENT 1								
Model 1								
FP	-	-	2	2	3	3	2	2
MR	4	2	3	2	3	3	2	2
Model 2								
FP	-	-	2	2	3	3	2	3
MR	4	3	3	3	3	2	1	3
Model 3								
FP	-	-	2	2	3	3	1	3
MR	4	3	3	3	3	3	1	3
INCIDENT 2								
Model 4								
FP	-	-	2	1 (3)#	1 (3)#	1(3)#	2	1 (3)#
MR	3	3	3	3	2	3	1	3
Model 5*								
FP	-	-	-	-	-	-	-	-
MR	4	-	-	-	-	-	-	Helmet damage only
Model 6								
FP	-	-	2	3	2 (3)#	3	3	2 (3)#
MR	4	4	3	3	3	4	2	(4)# (excluding skin)

FP scores based on examining the models which did not include the helmet which was being assessed by the MoD Engineer or the CT scans

MR scores based on examining the CT scans

***Model 5 was helmet damage only**

Number in brackets indicates how well these models represent a tangential bullet strike; number outside brackets assesses the model against the actual incident (see text)

There are acknowledged limitations to our model. One of these is the post-mortem cut line in the skull, discussed in [9, 10] and chapters 5 and 6. Another is the extendable nature of the synthetic skin, discussed in [10] and chapter 6. Work is ongoing to address the skin properties but we elected to shoot these models with the known skin material to assess if the presence of the helmet altered the skin wounding appearances. The skin entry wounds were described as ‘slit like’ by the pathologist (Figure 7-10a) but could be stretched to resemble the round entry wounds seen in models shot without helmets [10], (Figure 7-10c).

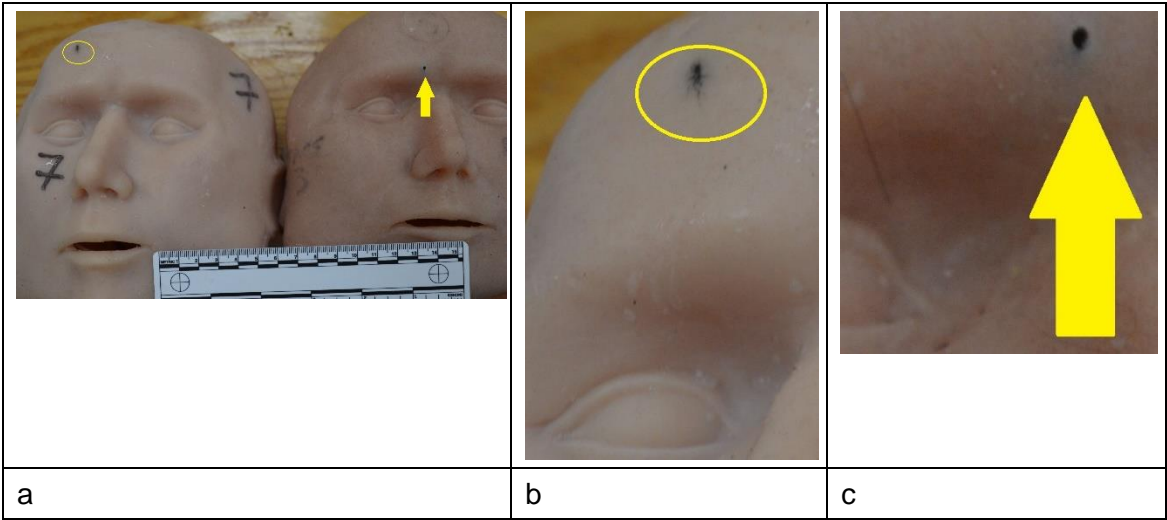


Figure 7-10 Comparison of skin entry wounds

(a) left hand ‘face’ model 1, this study; slit like entry circled; right hand ‘face’ model 3, study [10] & chapter 6; shot without helmet; circular entry arrowed; forensic scale visible (b) close up entry wound from left hand face in (a), this study (c) close up entry wound, study [10] & chapter 6, right hand face from 7-3a.

One explanation is that the synthetic skin underwent a degree of compression with the helmet insitu. The skin exit wounds scored lower in models 1-4 when compared with the models shot without helmets [10], chapter 6. The wounds in the models without helmets tended to be larger with a more ‘ragged’ appearance (Figure 6-4d and [10]). Observations from one of our authors (RD, forensic pathologist) is that the exit wound appearances in real casualties are variable but with helmets in place there may be less stellate type tearing than expected, presumably due to the support provided by the helmet to the tissues.

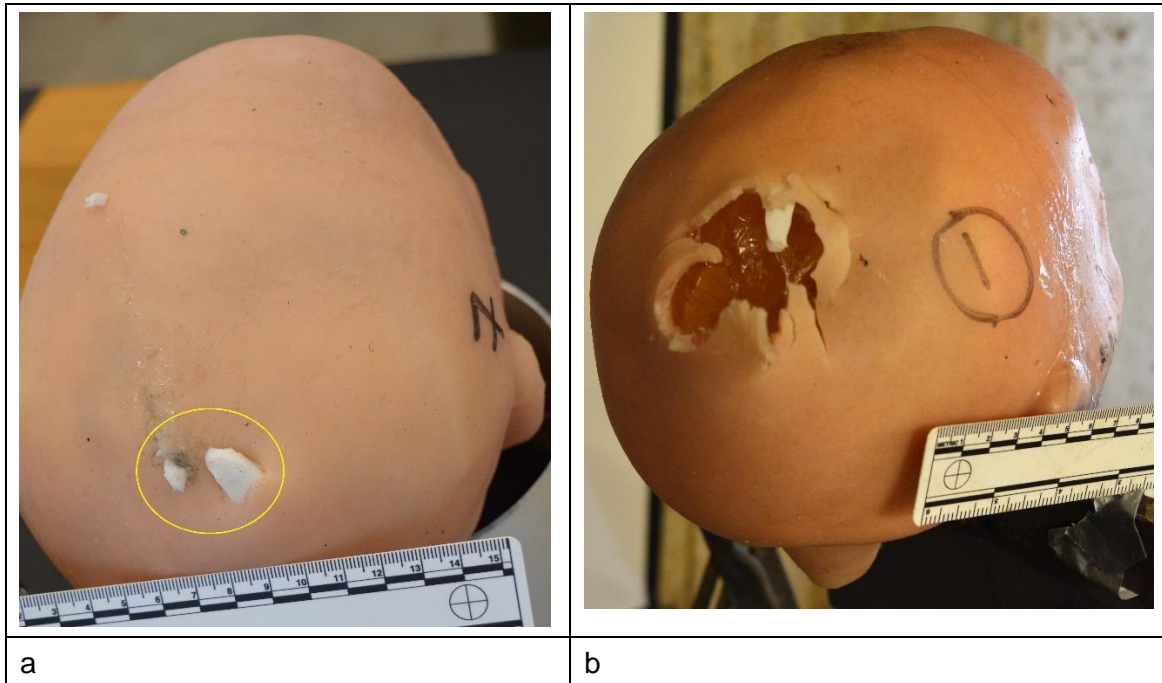


Figure 7-11 Exit wounds, rear of head models

(a) model 1, this study, shot with helmet insitu; example exit wound with synthetic bone fragments protruding (circled) (b) model 1 from study in [10] shot without helmet; exit wound is gaping with ragged edges.

A question that needs further consideration is to what extent anatomically accurate models are needed for ballistic experiments or whether simple spheres suffice (Other than the need for anatomical accuracy when placing helmets onto surrogates). Synbone® spheres have been successfully used for a variety of impact scenarios both ballistic [11-13] and blunt [14] but as described in chapter 4 did not replicate military injury at the simulated engagement distances tested. The internal structure of the skull does, however, influence the fractures that develop with ballistic impact as described by Fenton et al. [19], an effect that is seen in our skull model when fracture lines run through the skull base. How our models compare with the more biofidelic surrogates of Sarron et al. [20] and Freitas et al. [21] is a subject for future work.

7.6 Conclusions

Six surrogate head forms were shot with 7.62 x 39 mm ammunition in an experiment to reconstruct two military shooting incidents of individuals wearing ballistic protective helmets, (3 models used per incident). Both sets of models exhibited a range of bullet trajectories despite factors such as bullet manufacturer, batch and propellant load being controlled.

The wounds, fracture patterns and CT images were compared with those from the actual incidents.

Two of the models used for 'Incident 1', a frontal impact, produced injuries closer to the actual event than did the models for 'Incident 2', a left temporoparietal impact.

Two of the models for 'Incident 2' did produce good reproductions of tangential gunshot wounds but this was not the mechanism being reconstructed. Post hoc matching of clinical images to synthetic ballistic injury models is suitable for proof of concept but care is needed in reconstructions to ensure incorrect conclusions are not drawn where the features produced in models do not match the circumstances of the incident.

Skin wound appearances on models shot wearing a helmet are very different from the same models shot without a helmet.

Positive features of the model include realistic internal fracture lines and the ability to place a helmet to reproduce military scenarios.

7.7 Caveats

This work has only used one ammunition type simulating a particular engagement distance. Different results may be obtained with different ammunition or different ranges.

7.8 Acknowledgements

1.Cranfield University, Defence Academy of the United Kingdom, Shrivenham, SN6 8LA.

Clare Pratchett, Art Director, CDS Learning Services (Artwork for Figures 7-3a, 7-6, 7-7).

David Miller and Mike Teagle, the Small Arms Experimental Range.

Jim Clements, Senior Research Fellow, Test and Evaluation Group.

2.Royal Centre for Defence Medicine, Research Park, Birmingham B15 2SQ.

Dr Amarjit Samra, Director of Research.

Ms Yvonne Yau, Operations Manager.

Paula Dalton-Kirby, JTTR Data access.

3. Centre for Defence Imaging, Queen Elizabeth Hospital Birmingham, Mindelsohn Way, Birmingham B15 2TH.

Catherine Bean

Thomas Maffia

Lauren Potts

Military CT Specialist Radiographers.

4. Cranfield Ordnance Testing and Evaluation Centre (COTEC), Gore Cross, West Lavington, Devizes, Wiltshire, SN10 4NA, UK.

Trevor Lawrence, Director

Andrew Fenwick

Ray Hampshire

John Hampshire

Jerry Pennell

Luke Stockford

5. Nottingham Trent University, Flexural Composites Research Laboratory, 107 Bonington Building, Dryden Street, Nottingham, NG1 4GG, UK.

Richard Arm, Research Fellow.

7.9 References

1. Theory and practice of shooting reconstructions In: Hueske EE (2016) Practical Analysis and Reconstruction of Shooting Incidents (2nd edn). CRC press, Taylor & Francis Group, Boca Raton. pp 31-53
2. Introduction to the classification of gunshot wounds. In: Di Maio VJM (2016) Gunshot Wounds; Practical Aspects of Firearms, Ballistics and Forensic Techniques (3rd edn). CRC press, Taylor & Francis Group, Boca Raton pp 57-108
3. Fragkouli K, Al Hakeem E, Bulut O, Simmons T (2018) The effect of range and ammunition type on fracture patterns in porcine post cranial flat bones. Journal of Forensic and Legal Medicine 53: 1-12
4. Jorgensen JJ, Aksel-Ness P, Gaarder C (2016) Injuries caused by fragmenting rifle ammunition. Injury, Int J Care Injured 47:1951-1954
5. Humphrey C, Kumaratilake J (2016) Ballistics and anatomical modelling- a review. Legal Medicine 23: 21-29
6. Rainio J, Lalu K, Ranta H, Penttila A (2003). Morphology of experimental assault rifle skin wounds. Int J Legal Med 117: 19-26
7. Smith MJ , James S, Pover T, Ball N, Barnetson V, Foster B, Guy C, Rickman J, Walton V (2015) Fantastic plastic? Experimental evaluation of polyurethane bone substitutes as proxies for human bone in trauma simulations. Legal Medicine 17: 427-435
8. Carr D, Lindstrom A-C, Jareborg A, Champion S, Waddell N, Miller D, Teagle M, Horsfall I, Kieser J (2015) Development of a skull/brain model for military wound ballistics studies. Int J Legal Med 129: 505-10

9. Mahoney PF, Carr DJ, Delaney R, Hunt N, Harrison S, Breeze J, Gibb I (2017) Does preliminary optimisation of an anatomically correct skull-brain model produce clinically realistic ballistic injury fracture patterns? *Int J Legal Med* 131: 1043-1053
10. Mahoney P, Carr D, Arm R, Gibb I, Hunt N, Delaney RJ (2017) Ballistic impacts on an anatomically correct synthetic skull with a surrogate skin/soft tissue layer. *Int J Legal Med* 132: 519-530
11. Thali MJ, Kneubuehl BP, Zollinger U, Dirnhofer R (2002) The 'skin-skull-brain model': a new instrument for the study of gunshot effects. *Forensic Science International* 125 (2-3): 178-189
12. Thali MJ, Kneubuehl BP, Zollinger U, Dirnhofer R (2003) A high-speed study of the dynamic bullet-body interactions produced by grazing gunshots with full metal jacketed and lead projectiles. *Forensic Science International* 132: 93-98.
13. Taylor SC, Kranioti EF (2018) Cranial trauma in handgun executions: Experimental data using polyurethane proxies. *Forensic Science International* 282: 157-167
14. Dyer M, Fibiger L (2017) Understanding blunt force trauma and violence in Neolithic Europe; the first experiments using a skin-skull-brain model and the Thames Beater. *Antiquity* 91: 1515-1528
15. Carr DJ, Lewis E, Horsfall I (2017) A systematic review of military head injuries. *J R Army Med Corps* 163:13-19
16. Mahoney PF, Carr D, Miller D, Teagle M (2017) The effect of helmet materials and simulated bone and tissue layers on bullet behaviour in a gelatine model of overmatch penetrating head injury. *Int J Legal Med* 131:1765-1776

17. Farrugia A, Raul JS, Geraut A, Tortel MC, Ludes B (2009). Destabilisation and intracranial fragmentation of a full metal jacket bullet. *Journal of Forensic and Legal Medicine* 16: 400-402
18. Kieser DC, Carr DC, Leclair SCJ, Horsfall I, Theis J-C, Swain MV, Kieser JA (2013) Clothing increases the risk of indirect ballistic fractures. *J Orthop Surg Res* 8: 42 DOI: 10.1186/1749-799X-8-42
19. Fenton TW, Stefan VH, Wood LA, Sauer NJ (2005) Symmetrical fracturing of the skull from midline contact gunshot wounds: reconstruction of individual death histories from skeletonized human remains. *J Forensic Sci* 50: 1-12
20. Sarron JC, Dannawi M, Faure A, Caillou J-P, Da Cunha J, Robert R (2004) Dynamic effects of a 9 mm missile on cadaveric skull protected by aramid, polyethylene or aluminium plate: an experimental study. *J Trauma* 57: 236-247
21. Freitas CJ, Mathis JT, Scott N, Bigger RP, MacKiewicz J (2014) Dynamic response to a behind helmet blunt trauma measured with a human head surrogate. *Int J Med Sci* 11: 409-425 DOI: 10.7150/ijms.8079 (Accessed 23/03/2016)
22. Smith JE, Kehoe A, Harrison SE, Russell R, Midwinter M (2014) Outcome of penetrating intracranial injuries in a military setting. *Injury Int J Care Injured* 45: 874-878
23. Keene DD, Penn-Barwell JG, Wood PR, Hunt N, Delaney R, Clasper J, Russell RJ, Mahoney PF (2016) Died of Wounds: a mortality review. *J R Army Med Corps* 162: 355-360
24. Appendix A.10: Ballistics tables (metric system). In: Kneubuehl BP, Coupland RM, Rothschild MA, Thali MJ (2011) (Eds) *Wound Ballistics Basics and Applications*. Springer-Verlag, Berlin Heidelberg. pp 366-384

25. Defriend JP (2015) Overmatching of military soft body armour. MSc Thesis Cranfield University
26. Clason, D. L., & Dormody, T. J. (1994) Analysing data measured by individual Likert-type items. *Journal of Agricultural Education* 35(4): 31- 35

8 FURTHER ASSESSMENT OF A SURROGATE HEAD MODEL FOR MILITARY BALLISTIC INJURY WITH CASE STUDIES

Mahoney PF, Carr DJ, Delaney R, Gibb I

8.1 Abstract

A synthetic head model developed to reproduce military injuries was assessed in two different scenarios. The first was an impact with 5.56 x 45 mm ammunition at contact distance. The second involved shooting through intermediate targets (a laminated windscreen in one experiment and a helicopter window in another) with 7.62 x 39 mm MSC ammunition. The injury patterns resulting from the two scenarios were assessed by a military radiologist and a forensic pathologist and in the case of the 5.56 x 45 mm impact compared with an actual incident. Areas for further model development have been identified.

Key words: windscreen shooting; 7.62 x 39 mm MSC ammunition; contact gunshot

8.2 Introduction

Chapters 5, 6 and 7 of this thesis have described the sequential development and testing of a synthetic head model based around an anatomically correct skull with PDMS skin/soft tissue layers and a gelatine or Permagel™ fill. A caveat for the work so far is that the model has only been tested against one ammunition type (7.62x 39 mm MSC) although in chapter 7 different simulated engagement ranges were used. Di Maio [1] divides gunshot wounds into four categories based on the distance between the muzzle of the weapon and the target. These are contact wounds (where the muzzle on the weapon is held in contact with the target), near-contact wounds (muzzle is a short distance from the skin and the discharge causes a wide zone of skin searing and soot

contamination), intermediate range wounds (muzzle is held away from the target but is close enough for powder tattooing of the victim's skin to occur) and distant wounds (where the only marks on the victim are from the bullet impact). The work described to date would come under the 'distant' wound group.

Intermediate wounds have been simulated by Taylor and Kranioti [2] firing at Synbone® spheres from a distance of 30 cm.

At the request of a Forensic Pathologist, the surrogate model developed in this thesis was used to recreate a contact gunshot injury. The features of a contact gunshot injury may include radial tears around the entry wound, burning of the tissue from both flash and hot propellant gases, and an imprint of muzzle shape [1, 3-6].

A similar reconstruction is described by Kneubuehl and Thali [7] using polyurethane spheres.

An additional area that needed assessment was the influence of intermediate targets (such as glass) on the wounds produced in the model, as military personnel may be attacked within vehicles and buildings. Intermediate targets such as clothing [8] can influence bullet stability, and bone [9] may cause a round to fragment. Previous work (chapter 4, and [10]) found that the variability in 7.62 x 39 mm MSC bullet behaviour between shots was increased by the presence of intermediate target layers.

Harper [11] described how police officers may be required to fire through the windows of buildings or automobiles in the course of their duties. Anticipated effects on bullets included deformation, loss of energy, and deflection. To study bullet deflection, he conducted experiments where pistol ammunition was fired at window glass, plate glass and automobile safety glass. The experiments showed significant deflection of the bullets at ranges of 25 to 75 yards, greatly reducing the accuracy of fire. Thick glass (plate or safety) absorbed sufficient energy from lead bullets that fire could be deemed ineffective.

Building on Harper's work, Lambert [12] looked at .308" FMJ bullet deflection, citing an incident in 1991 where elimination of hostage takers was delayed as a bullet fired by a marksman was deflected by glass. The delay meant that three hostages were killed before the incident could be contained. His MSc project aimed to quantify these deflections and provide a mathematical model to calculate them at future incidents. An issue noted in the project was that many bullet types fragment on impact with glass [12].

Di Maio [1] describes how deformed, destabilised and fragmented bullets may cause larger and more irregular wounds than expected. Bullets perforating glass will produce a cloud of fragments and these in turn can cause pseudo tattooing (i.e. mimicking the tattooing and soot deposition of close range gunshots) on the skin of a victim if close enough [1, 13].

To minimise duplication, generic aspects of the method for all the models will be described together and any variations in the individual experiments given separately.

8.3 Method-general

Four surrogate head models were assembled from MU51 polymer anatomically correct skulls with PDMS skin/soft tissue faces. The full methodology is described in chapters 6 (sections 6.3.1 and 6.3.2) and 7 (section 7.3.3). Because of an anticipated delay in CT scanning and examining the models after shooting the decision was made to use Permangel™ rather than gelatine as the brain 'fill'. (see section 5.3.2) because gelatine degrades within days, even when refrigerated. Although blocks of both Permangel™ and Clear Ballistics Synthetic Gelatine (<https://www.clearballistics.com/>) have been found to burn along the bullet path by the Impact and Armour Group at Shrivenham when shot with 7.62 x 39 mm ammunition (see Appendix H) it was decided that this was an acceptable risk for this project.

8.3.1 Ranges

8.3.1.1 Case study 1: Contact wound reconstruction

Two head surrogate models were marked up with black circular stickers to indicate the entry and exit points in the case under consideration (Figure 8-1a). The models were placed in turn in contact with the muzzle of the barrel from a current in-service 5.56 mm calibre rifle secured to an Enfield proof mount (Figure 8-1c). The ammunition used was unmodified in-service 5.56 x 45 mm rifle ammunition (Figure 8-1b).

Model 13 (sequential to the models described in chapters 6 and 7) was fitted with the same PDMS skin/soft tissue used in the previous experiments to allow a direct comparison of the wounds produced.

Model 14 was fitted with a less extendable version of the PDMS skin/soft tissue material, developed in an ongoing project with Nottingham Trent University.

Impacts were filmed using Phantom V12 (21,000 fps, exposure 4 μ S, resolution 512 x 512, filming front view of model) and V1212 (30,000 fps, exposure 6 μ S, resolution 768 x 480, filming side of model) cameras. The condition of the model pre- and post-impact was recorded using a Nikon D3200 DSLR camera fitted with an AF-S NIKKOR 18-55 mm lens. The experimental set up for both models is summarised in Figure 8-1c & d.

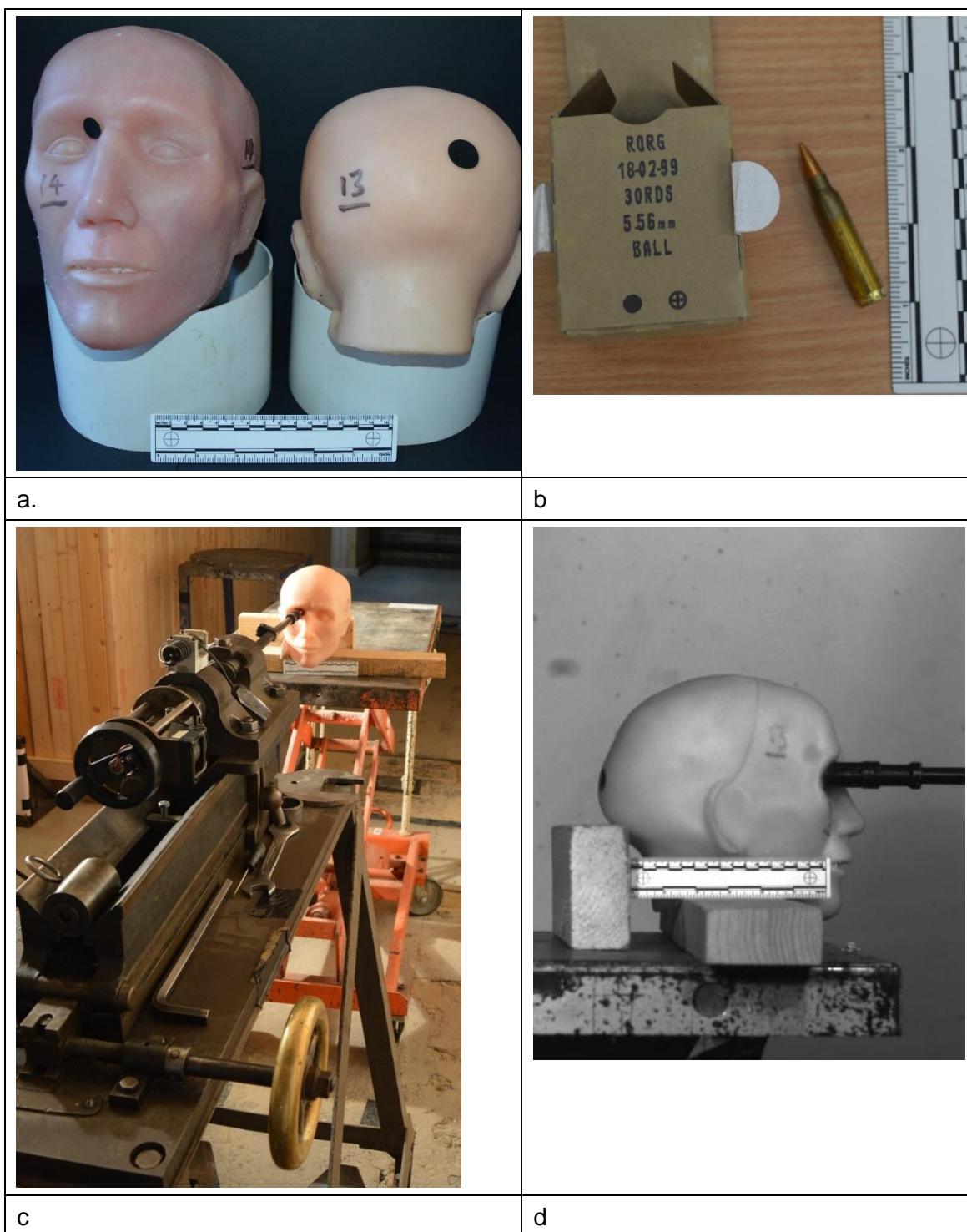


Figure 8-1 Experimental set up models 13 and 14

(a) bullet entry and exit sites marked up (b) ammunition used for the experiment (c) model 13 in situ at the SAER, Shrivvenham Campus (d) pre-impact image from the V1212 HSV. In both panels (c) and (d) the rifle barrel can be seen in contact with the model.

Impact velocity could not be measured using the Doppler radar as this was a contact wound and there was therefore no projectile visible to the radar for tracking.

8.3.1.2 Case study 2: The influence of intermediate targets

8.3.1.2.1 Laminated windscreen

Model 15, fitted with the less extendable PDMS face/soft tissues, was placed 10 m from an Enfield proof mount fitted with an AK 47 barrel. A laminated windscreen was placed 50 cm in front of the model to simulate the distance between a driver and a windscreen. The model was shot with unmodified Russian MSC ammunition (impact velocity 670 m/s measured by Weibel Doppler radar). HSV and DSLR images were recorded as described above.

The experimental set up is summarised in Figure 8-2.

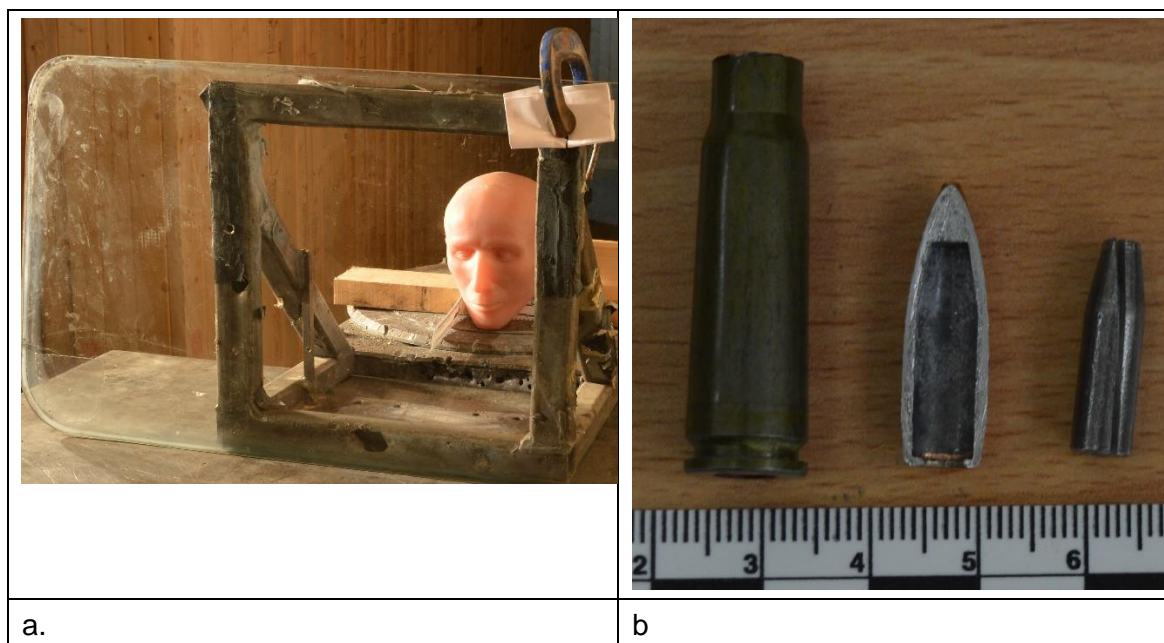


Figure 8-2 Experimental set up laminated windscreen impact

(a) model 15 placed 50 cm behind a laminated windscreen secured to a frame (b) example Russian 7.62 x 39 mm MSC ammunition showing (left to right) cartridge case, steel jacket with lead lining and MSC.

8.3.1.2.2 Helicopter window

Model 16, also with the less extendable PDMS skin/soft tissue was fitted with a military aviation helmet and placed 50 cm behind a transparent thermoplastic helicopter window, 10 m from an Enfield proof mount as described above and impacted with the same ammunition (impact velocity 691 m/s). HSV and DSLR images were recorded as described above. The experimental set up is summarised in Figure 8-3.

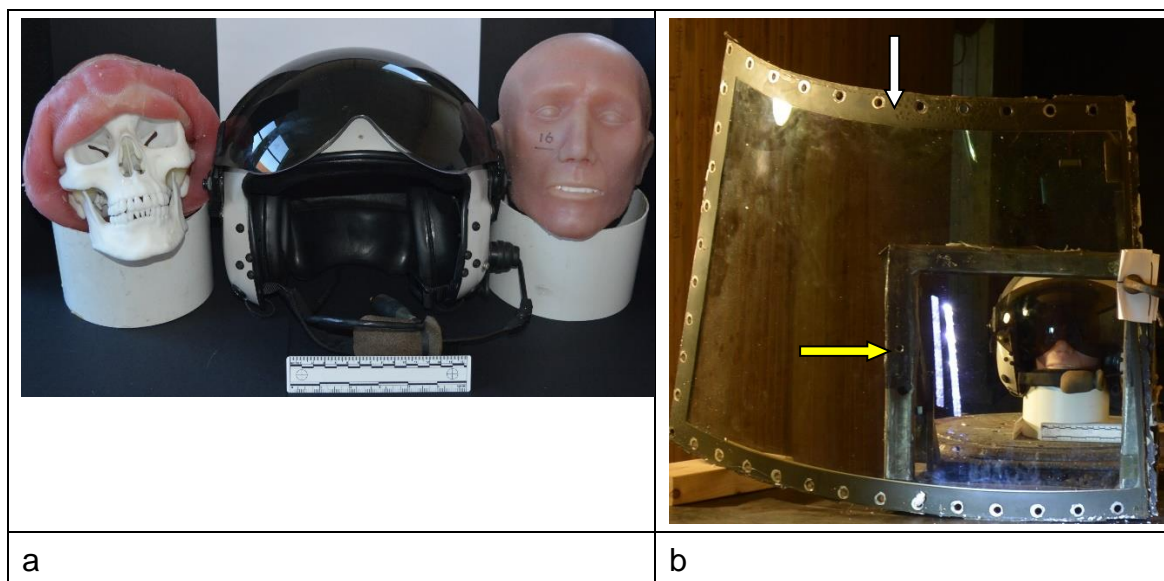


Figure 8-3 Components of the 'aviation' head model

(a) models 15 and 16 plus military aviation helmet; face on 15 has been peeled back to show the anatomically accurate synthetic skull underneath (b) experimental set up; helicopter window (white arrow) clamped to a metal frame (yellow arrow) is 50 cm in front of face 16 wearing the helmet.

8.3.2 CT scanning and radiology examination

After shooting, each model was wrapped in clear plastic film to preserve any bullet fragments or glass fragments on the surface of the model and taken to the Centre for Defence Imaging at the Queen Elizabeth Hospital Birmingham for CT Scanning by military radiographers using a SOMATOM Definition CT scanner, (Siemens Health Care Ltd, Camberley, UK) with Spiral Head protocols (Window Level 100/35, 1 mm slice thickness). The scans were sent to an

experienced military radiologist for reporting and, in the case of the contact wounds, comparison with the actual incident. Tissue layers (and helmet for the 'aviation' incident) were removed from the images using Phillips Brilliance Extended Work Station (Koninklijke Phillips N.V., Amstelplein 2, 1096 BC Amsterdam, The Netherlands).

8.3.3 Pathology examination

The models were then taken to the Royal Centre for Defence Medicine for examination by a Home Office pathologist familiar with military ballistic injury [14]. The pathologist was requested to compare the appearances of the model with those of the actual incident. The combined assessment by a pathologist and radiologist is in line with the views of Karger [15] and Oehmichen [16] on multidisciplinary assessment as discussed in chapter 5, and the methodology of the UK military mortality review panel [14].

8.4 Results

Images have been selected to illustrate the difference between these experiments and those described earlier in the thesis and minimise duplication.

8.4.1 Case study 1: Contact wound reconstruction

Both head models were noted to have smoke coming from the entry and exit wounds immediately after shooting.

8.4.1.1 HSV

Impact sequences from model 13 are shown in Figure 8-4.

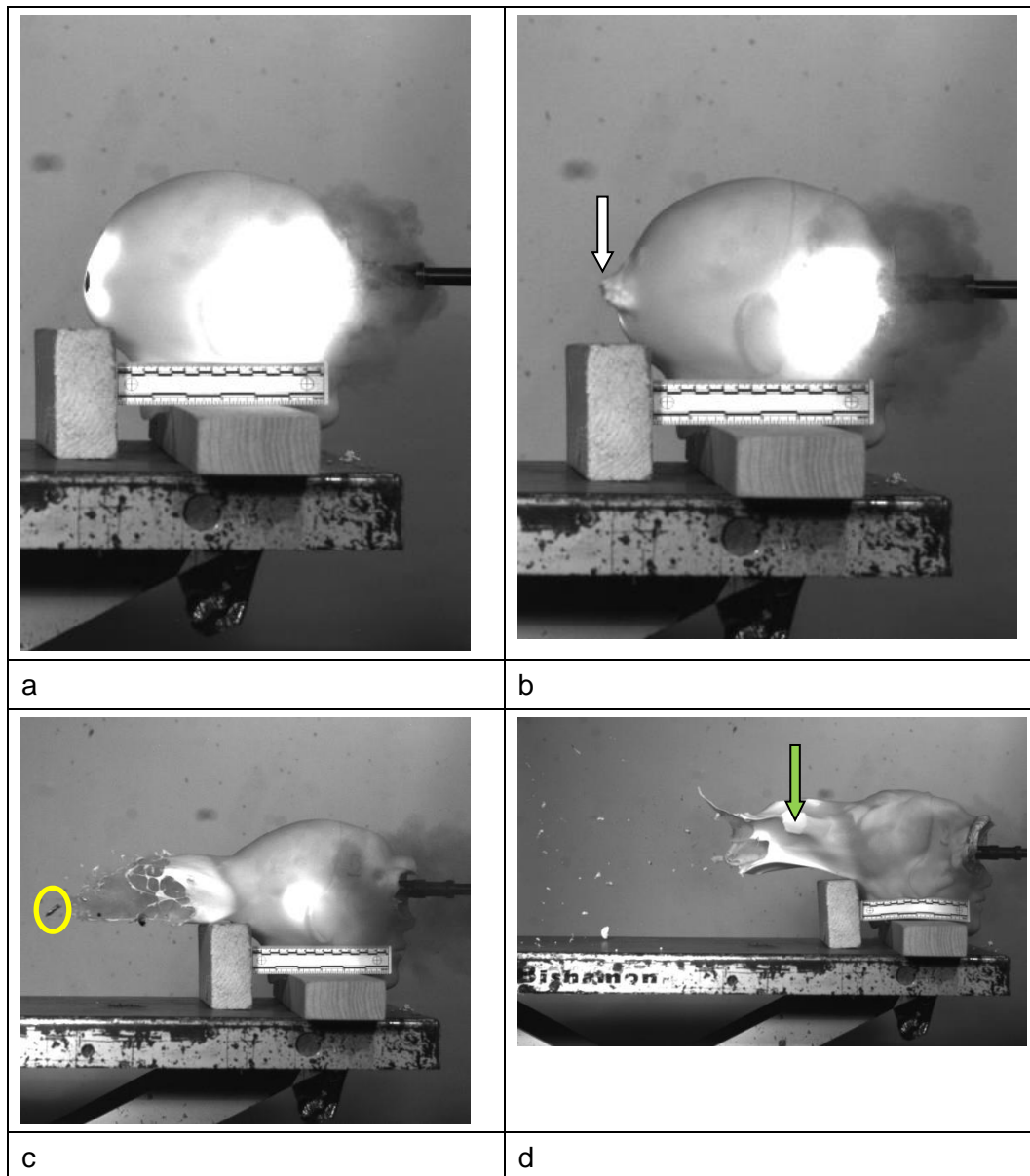


Figure 8-4 V1212 Impact sequence model 13

(a) moment of impact; muzzle flash and gases visible (b) bullet about to emerge from rear of the model (white arrow) (c) bullet (circled) emerges intact from the model; entrance wound continues to expand and exit wound complex visible (d) fractures visible within the head model and detached bone fragments visible near the exit (green arrow).

Impact sequences from model 14 are shown in Figure 8-5.

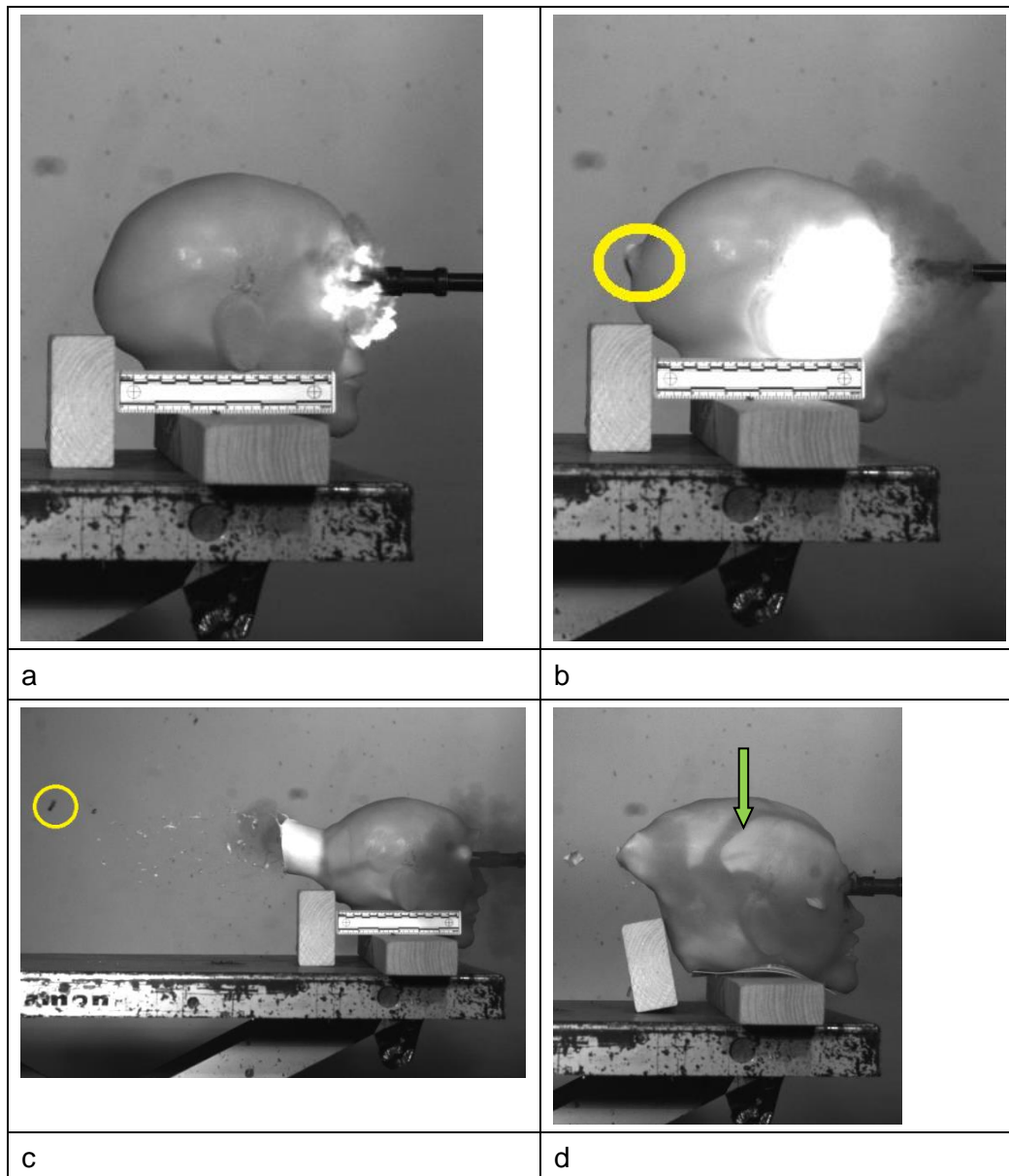


Figure 8-5 V1212 impact sequence model 14

(a) moment of impact (b) bullet (circled) about to emerge from rear of model (c) undamaged bullet visible behind model; exit wound less extended than with model 13 shown in Figure 8-4 c & d (d) PDMS skin/soft tissue retracting; extensive fractures visible within the model (green arrow).

The main results from the HSV images are that:

- (1) at ballistic strain rates the 'new' PDMS skin/soft tissue is less extendable than the original formulation but still more so than real tissue.
- (2) the bullet emerges intact from the model whereas it shattered within the head of the casualty in the actual incident.

8.4.1.2 Pathologist assessment

Entry wounds

The stellate soot contamination from the vents of the barrel's flash suppressor was reproduced well (Figure 8-6a) although the extendable skin produced a smaller entry wound than the actual case (entry wound in model 13 was 15 mm long and 12 mm wide; that of model 14 was 12 mm long and 12 mm wide, Figure 8-9a). The underlying bone damage was described as realistic (Figures 8-6b, 8-9b).

Exit wounds

The tissue exit wounds were smaller than expected for both models and both models had substantial bone loss around the exit site (Figures 8-6c, 8-9d). The 'new' PDMS skin on model 14 produced a less torn exit wound (Figure 8-9c) than that on face 13 (Figure 8-7a). Model 13's wound exit wound was 25 mm long with additional tears of 25mm (Figure 8-7a); Model 14's was also 25 mm long with tears of around 5 mm (Figure 8-9c).

Fracture patterns

The fracture pattern across the skull base and vault was judged to be more realistic in model 14 and not comminuted enough in model 13 (Figure 8-6d), possibly influenced by lack of fracture propagation across the post-mortem cut line, a recognised issue with the surrogate [17].

Brain Injury

There was no evidence of bullet yaw in either of the Permangel™ brains which contrasts with the 7.62 x 39 mm bullets fired at 10 m distance in earlier experiments [17] where yaw was seen at around 70 mm in some of the models with a Permangel™ fill.

Images from the pathology examination are shown in Figures 8-6 to 8-9.

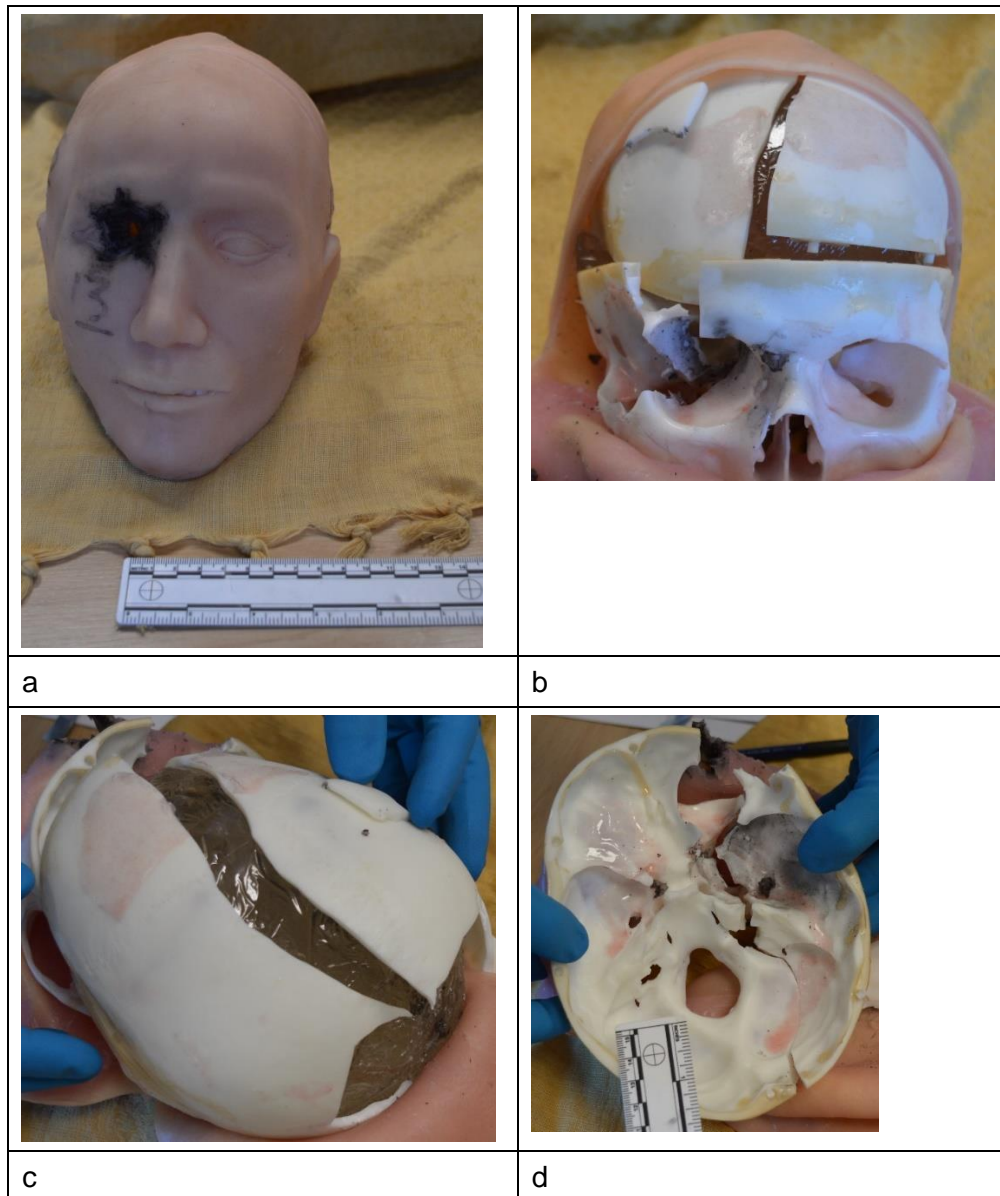


Figure 8-6 Model 13 pathologist examination (1)

(a) stellate entry wound with soot contamination (b) underlying entry wound fractures (c) calvarial fractures (d) base of skull fractures.

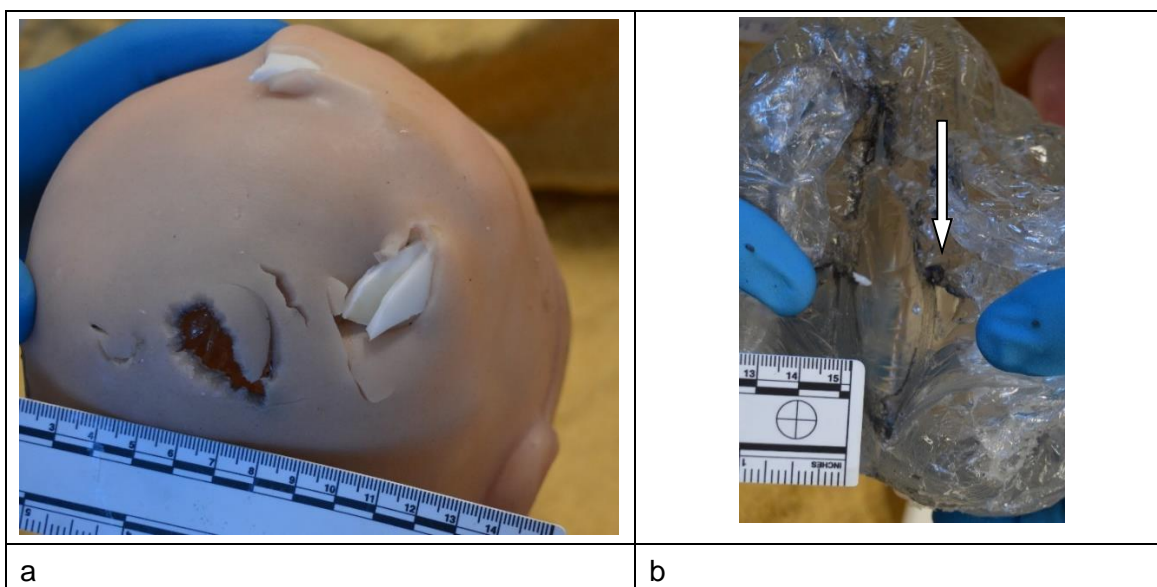


Figure 8-7 Model 13 pathologist examination (2)

(a) exit wounds, protruding bone fragments visible (b) bullet path within Permugel™ brain; note areas of soot contamination (arrowed).



Figure 8-8 Model 14 pathologist examination (1)

Section of right hand side temporoparietal synthetic bone fragment; of note the bond for the post-mortem cut line has held.

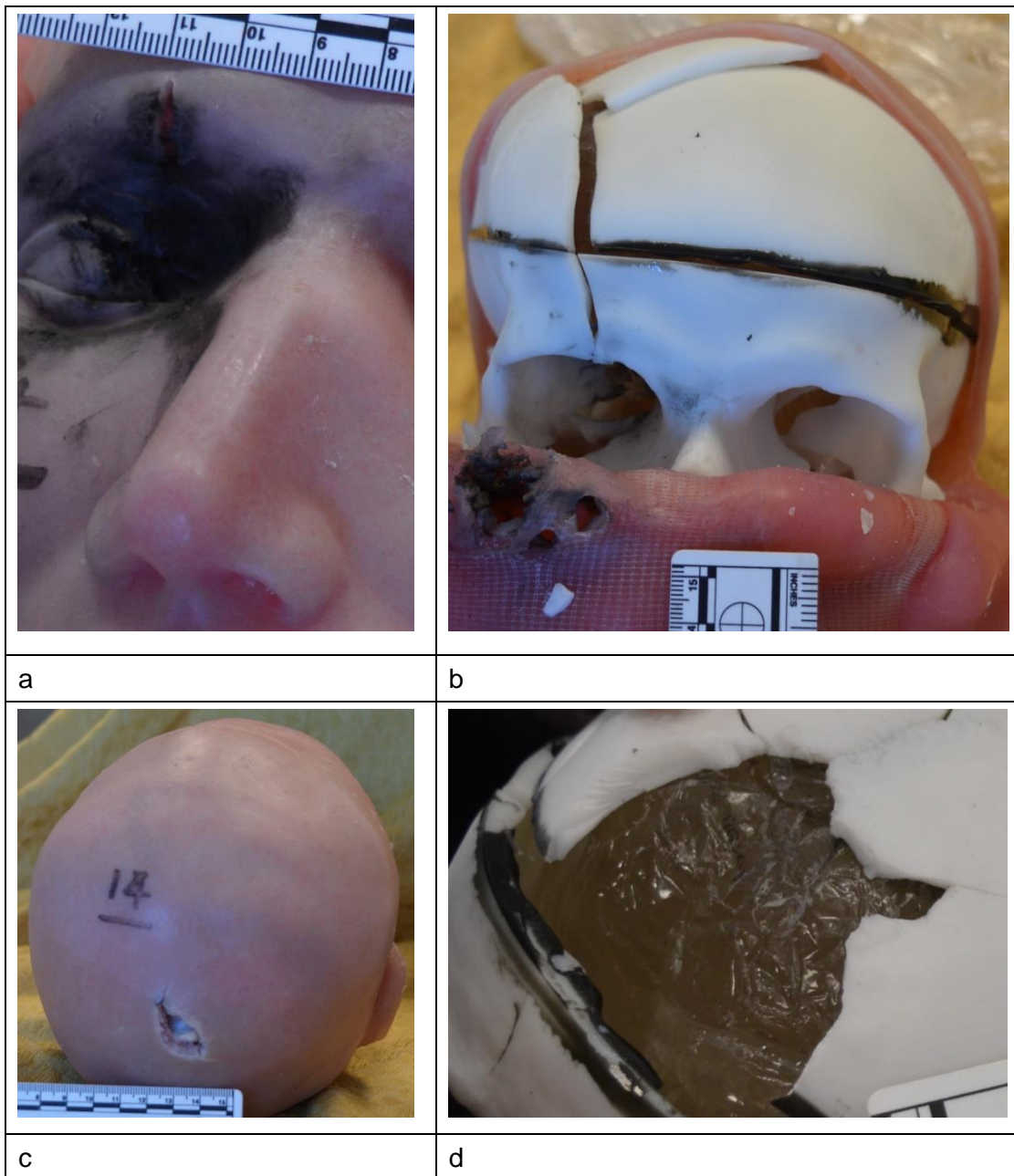


Figure 8-9 Model 14 pathologist examination (2)

(a) skin entry wound with soot contamination (b) underlying frontal fractures; the PDMS/skin soft tissue has been peeled back demonstrating its different structure compared to the original version (Appendix D) (c) small exit wound (compare with exit wound for model 13, Figure 8-7a) (d) exit fracture complex.

8.4.1.3 Radiologist assessment

Entry wounds

Both entry wounds were noted to be more over the orbit than in the actual case and irregular in appearance (Figure 8-8a).

Exit wounds

In model 13 the exit wound appearance was more extensive than in the actual case (Figure 8-9a). In model 14 the wound was smaller but irregular with marginal tears.

Fractures

In model 13 the calvarial deformity was more extensive than in the actual case (Figures 8-8b, 8-9b), although the overlapping calvarial fragments were realistic. Fracture propagation was described as good with progression through the base of skull and occiput.

For model 14 the posterior bone comminution was again noted to be more extensive than the actual case but the calvarial disruption was reasonable. There was less fracture propagation into the face and base of skull than in the real case.

Brain injury

A few small 'bone' fragments were seen on the brain surface of model 13 and one within the wound tract. There were several small fragments seen within the brain of model 14 (one fragment visible on the CT slice shown in Figure 8-11).

The fact that the bullet had not shattered inside the model, unlike the real case, was also noted.

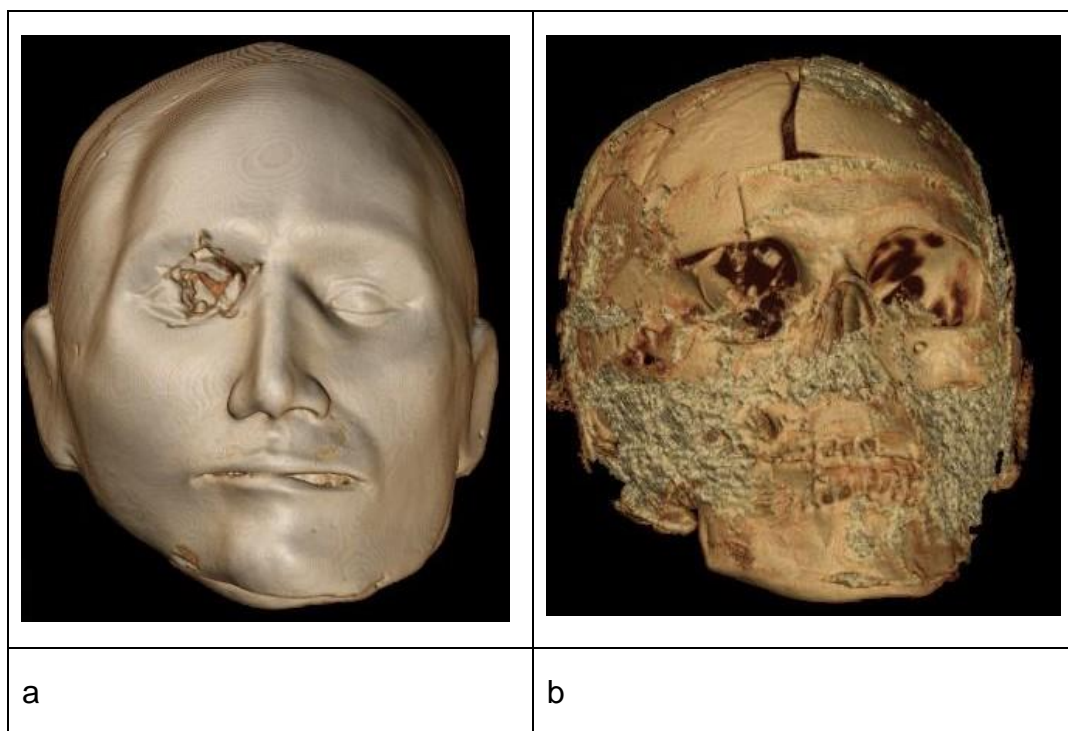


Figure 8-8 Model 13 CT 3D reconstruction entry wounds

(a) skin/soft tissue (b) underlying fractures.

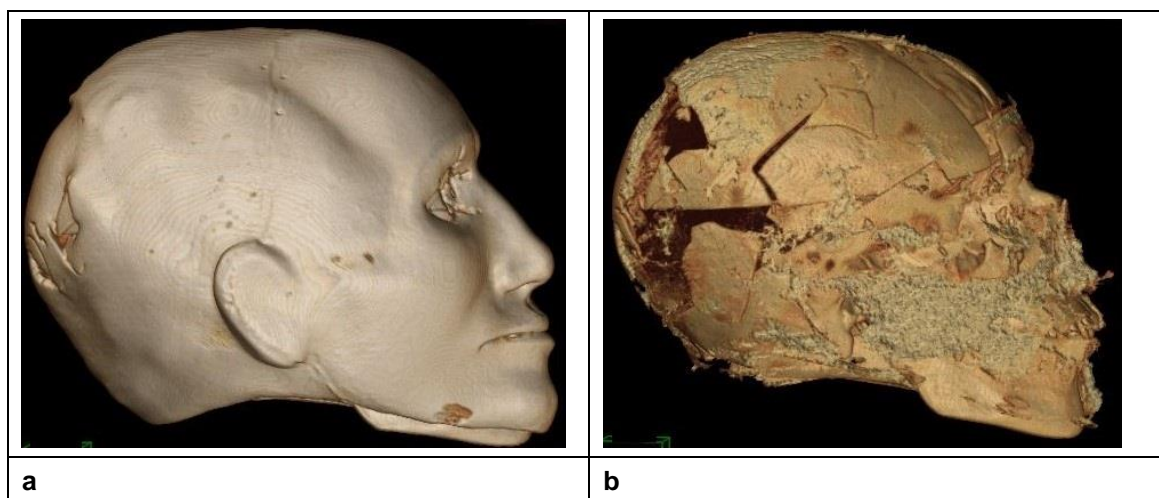


Figure 8-9 Model 13 CT 3D reconstruction lateral view

Lateral view shows head distortion post impact (a) skin and soft tissue (b) underlying fractures.

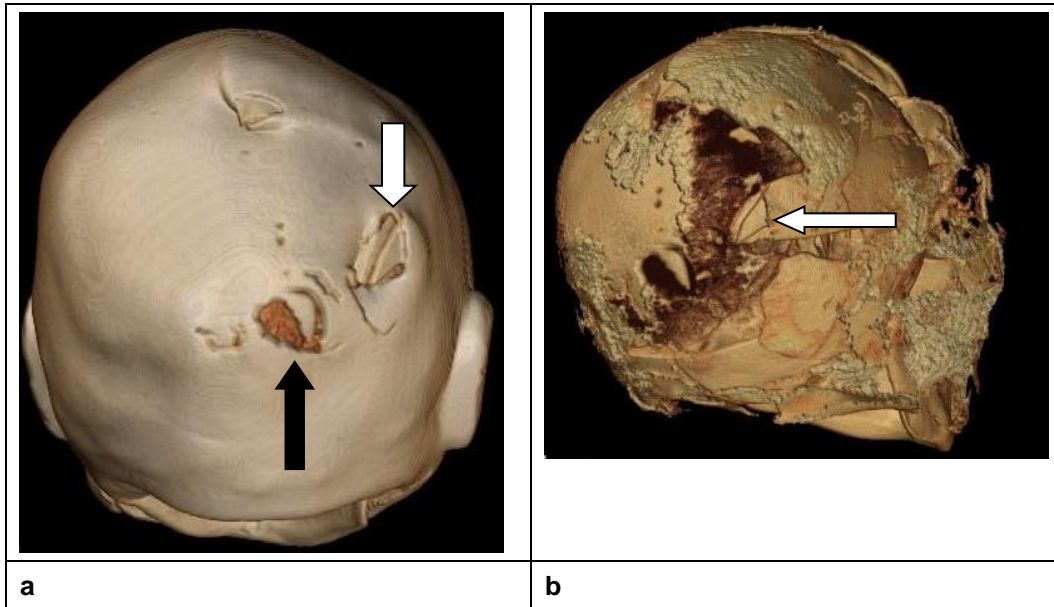


Figure 8-10 Model 13 CT 3D reconstruction exit wounds

(a) skin and soft tissue, (exit wound black arrow, bone fragments white arrow)

(b) underlying fractures, rear oblique view; white arrow points to bone fragments visible in panel (a).

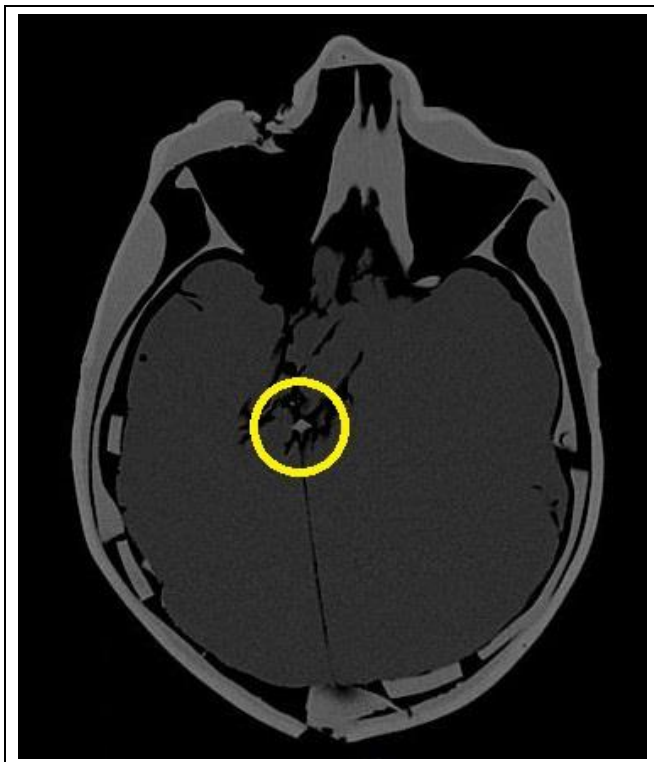


Figure 8-11 Transverse cut through model 14

'bone' fragment within bullet path circled.

8.4.2 Case study 2: The influence of intermediate targets on wounding patterns in the models

8.4.2.1 Laminated windscreen impact

8.4.2.1.1 HSV

Impact sequences from model 15 are shown in Figures 8-12 and 8-13. Bullet yaw is visible in Figure 8-13b

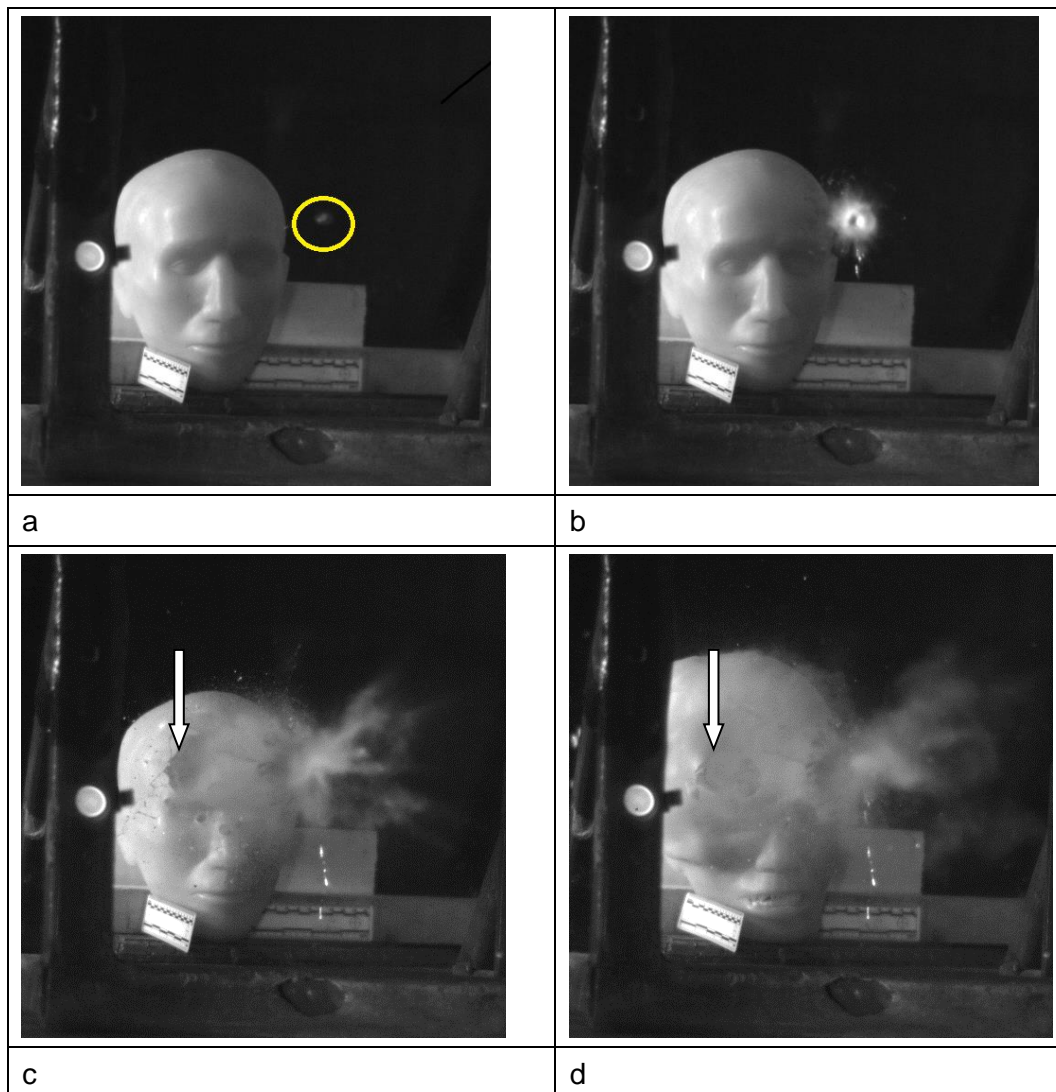


Figure 8-12 Model 15 V12 HSV front view

(a) pre-impact, bullet circled (b) windscreen impact (c) cloud of glass fragments plus crack forming in windscreen; entry wounds visible on the model (d) model distortion due to temporary cavity formation; white arrow in panels c & d points to main entry wound.

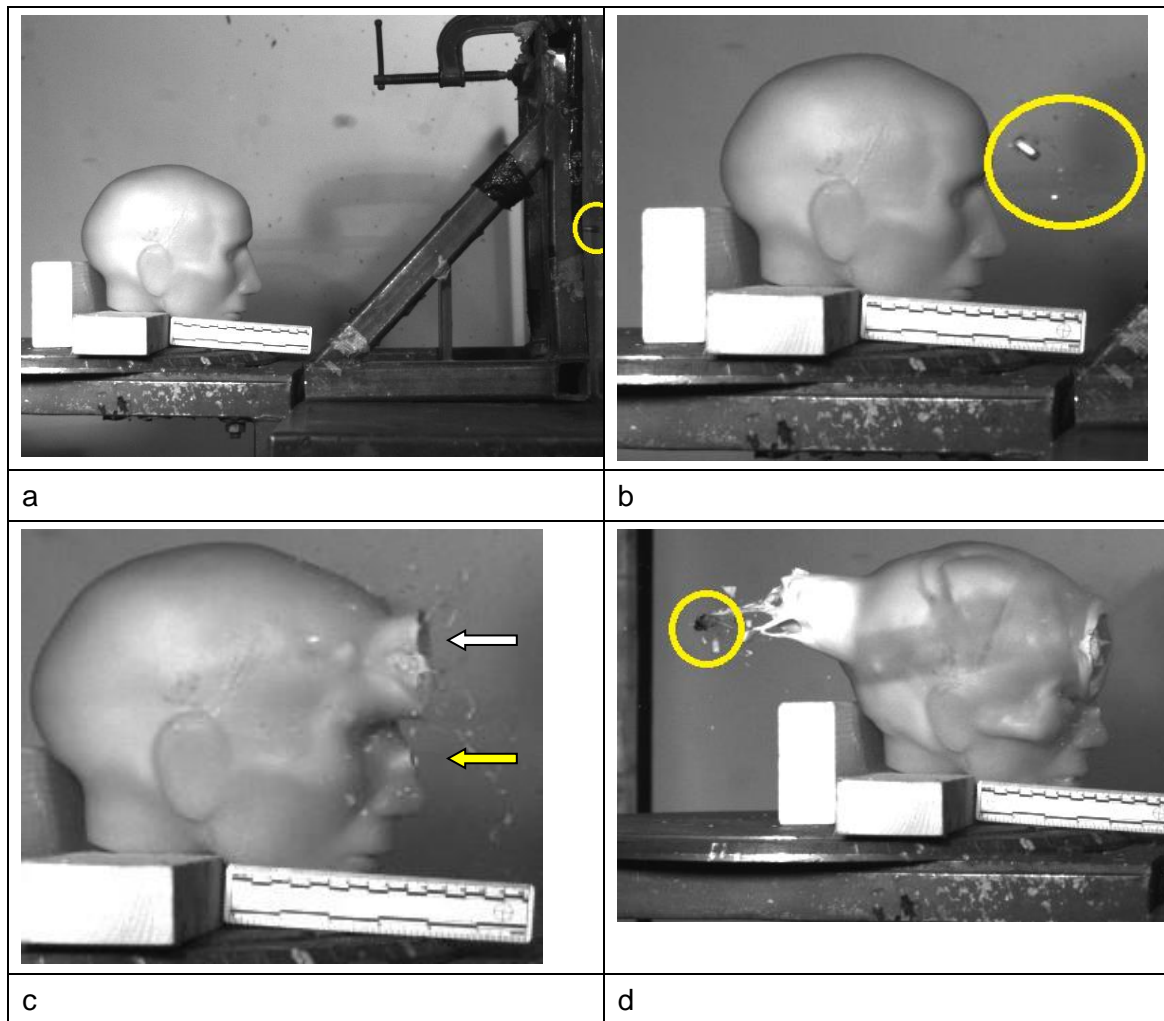


Figure 8-13 Model 15 V1212 HSV side view

(a) pre-windscreen impact, bullet circled (b) pre-head impact, bullet (circled) has emerged from windscreen and is damaged and yawing (c) impact from both bullet (forehead, white arrow) and glass fragments (nose and face, yellow arrow) (d) bullet exit, bullet circled; fractures visible within the model and temporary cavity developing.

8.4.2.1.2 Pathologist assessment

Entry wounds

The base of the skin/soft tissue entry wound was 13 mm long and between 2 and 6 mm wide (Figure 8-14a). There was 'tissue' loss on the outer aspect of the wound with appearances similar to an abrasion collar. Glass fragment wounds (up to 4 mm wide) peppered the face (Figure 8-14a). The skull had an

entry wound just above the right orbit with shattering of the superior orbit and frontal area (below the post-mortem cut line) and fractures visible above the cut line (Figure 8-14b).

Exit wounds

The skin/soft tissue wound consisted of 3 main lacerations (length 15 mm, 10 mm and gaping 15 mm up to 10 mm wide with short splits above. The wound edges were everted in places (Figure 8-14d). The underlying bone was shattered into multiple tiny fragments.

Fracture patterns

The post-mortem cut line interfered with the entrance fracture pattern. The skull base was shattered.

Brain injury

The wound track had variable width indicating bullet yaw (yaw is visible on the HSV frames between the windscreen and the model, Figure 8-13b). There were multiple bone fragments within the track along the whole length but no visible glass or bullet fragments (Figure 8-14c).

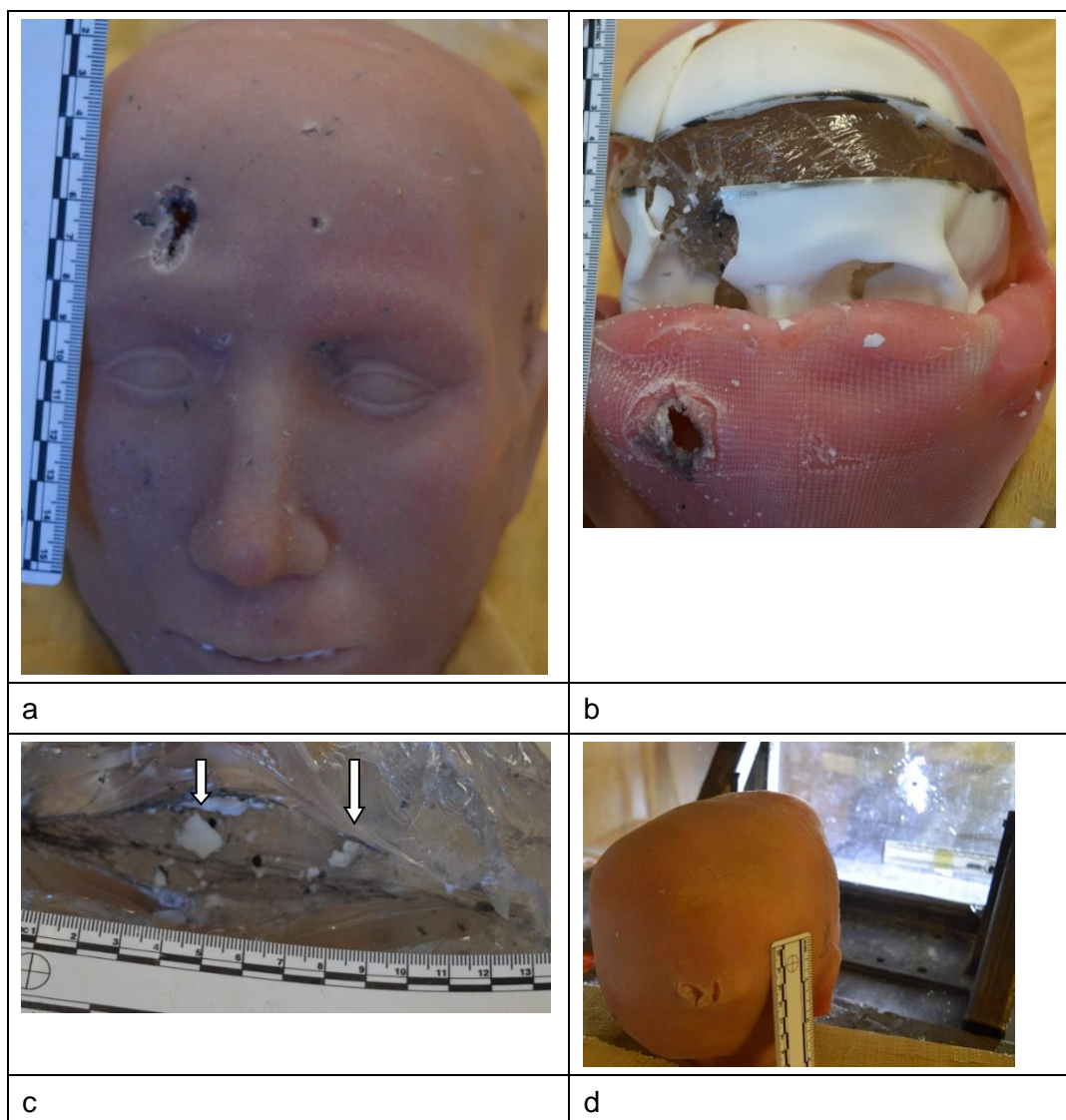


Figure 8-14 Model 15 pathologist examination

(a) entry wound skin/soft tissue (b) underlying entry wound fractures (c) ‘bone’ fragments within the Permagan™ brain (arrowed) (d) exit wound skin/soft tissue (image from the range, windscreen with bullet hole visible in background).

8.4.2.1.3 Radiologist assessment

Extensive peppering of the face with glass fragments was noted (Figure 8-15a). Glass and metal fragments were seen within the Permugel™ brain (Figure 8-17c).

Entry wound.

There was a large irregular entry wound typical of an unstable bullet with maximum dimensions of 22 mm x 12 mm (Figure 8-15a).

There was good fracture propagation from the bone entry wound into the face with minimal displacement (visible in Figure 8-15c).

Exit wound

The soft tissue exit wound was slightly larger (26 mm x 14 mm) and more irregular with tears. There was less tearing that might be seen in a real case but it was otherwise described as a 'very good representation'.

Fracture pattern

There was base of skull disruption without massive displacement but significant displacement and disruption of the posterior calvarium (visible in Figure 8-17c).

Brain injury

There was a good wound profile within the brain (Figure 8-17c) and a 'snow storm' of fragments from the bullet and the windscreen along the track (Figures 8-15 b & c, 8-16 b & c, 8-17 a-c).

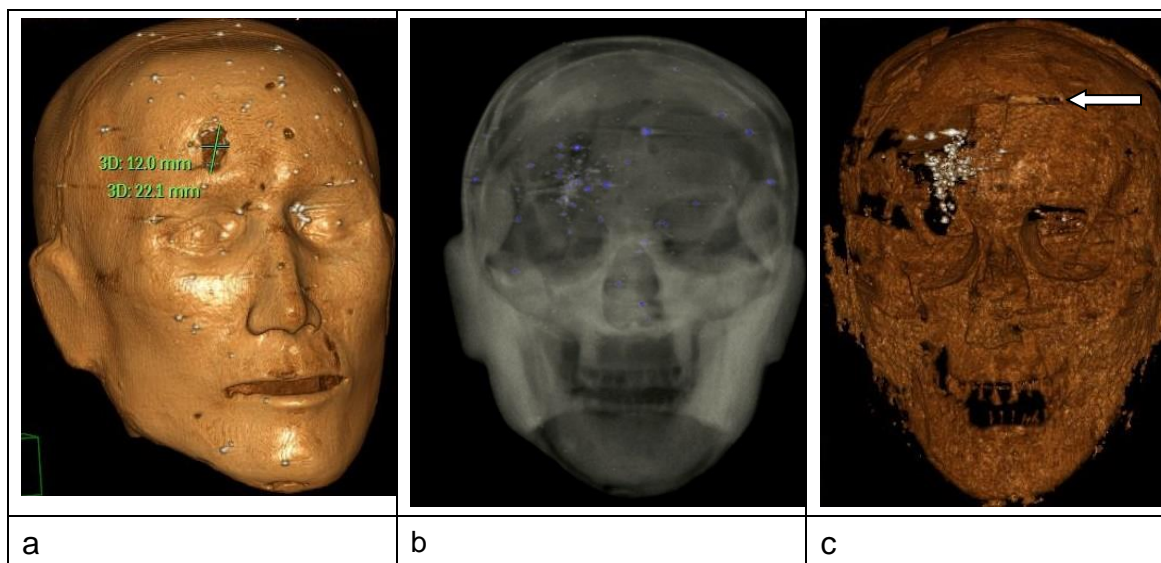


Figure 8-15 Model 15 CT 3D reconstruction front view

(a) surface image, multiple fragments visible on skin; markers for measuring entry wound visible (b) image optimised for dense fragments; metal fragments appear blue (c) soft tissue removal to show cluster of fragments along bullet path; fractures arrowed.

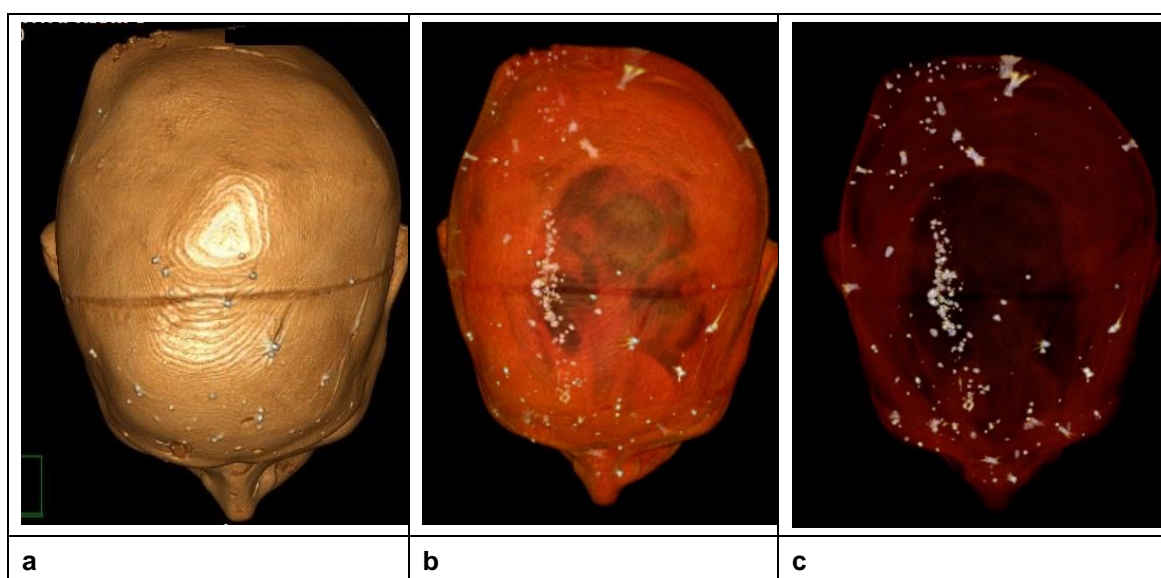


Figure 8-16 Model 15 CT 3D reconstruction from above

(a) surface image of multiple fragments (b) & (c) images optimised for fragments; metallic objects appear brightest.

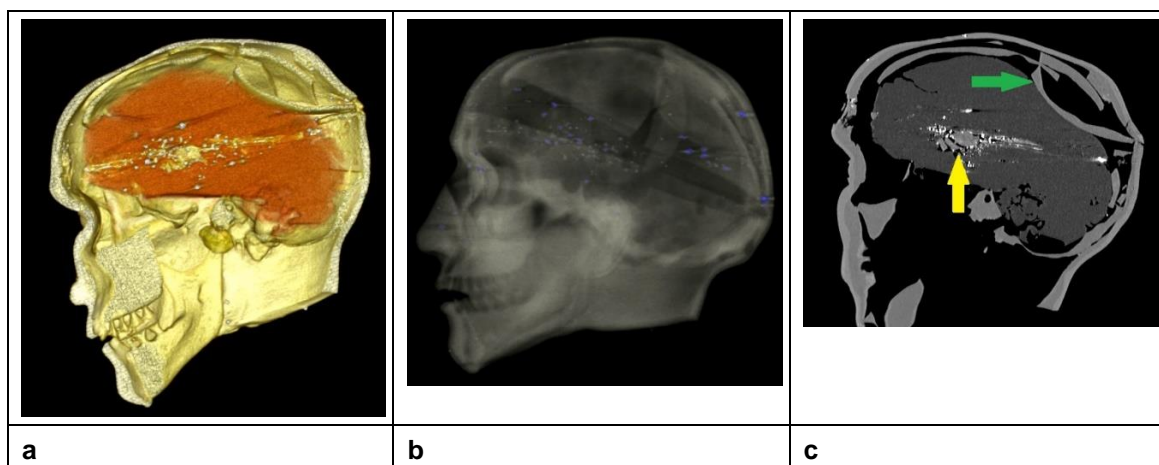


Figure 8-17 Model 15 CT 3D reconstruction sagittal cut

(a) demonstrating bullet path through brain (b) optimised for dense fragments-metal appears blue (c) optimised for bone; note bone fragments deep within wound (yellow arrow) and inverted calvarial fragment (green arrow).

8.4.2.2 Helicopter window impact

8.4.2.2.1 HSV

Impact sequences from model 16 are shown in Figures 8-18 and 8-19. Of note the bullet jacket had been stripped off the MSC within the helmet/head model. The MSC can be seen to exit in Figure 8-19d, and the damaged jacket is shown in Figure 8-20b.

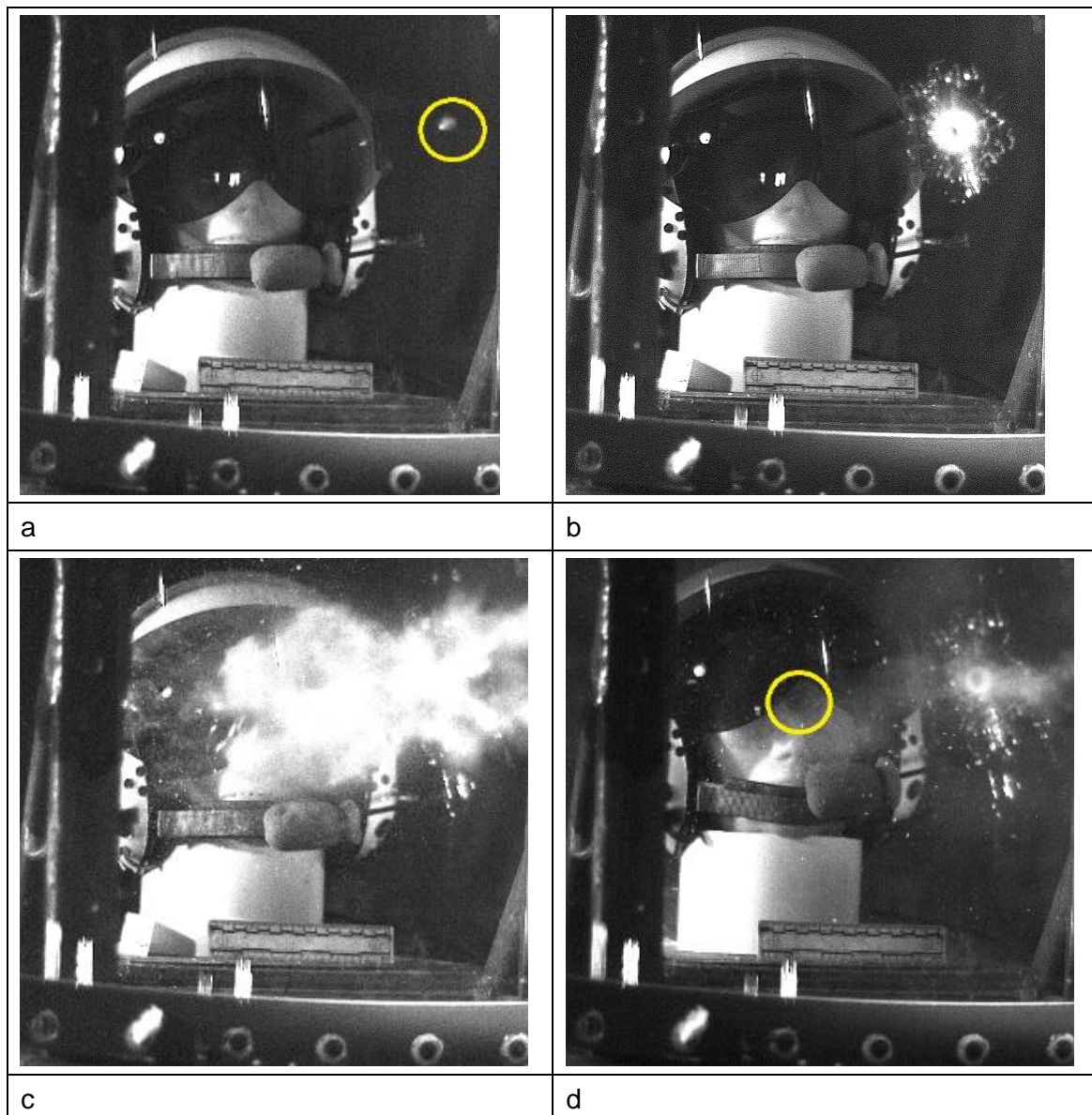


Figure 8-18 Model 16 V12 HSV, frontal view

(a) pre-impact, bullet circled (b) impact with window (c) cloud of fragments produced (d) bullet impact into face, bullet circled.

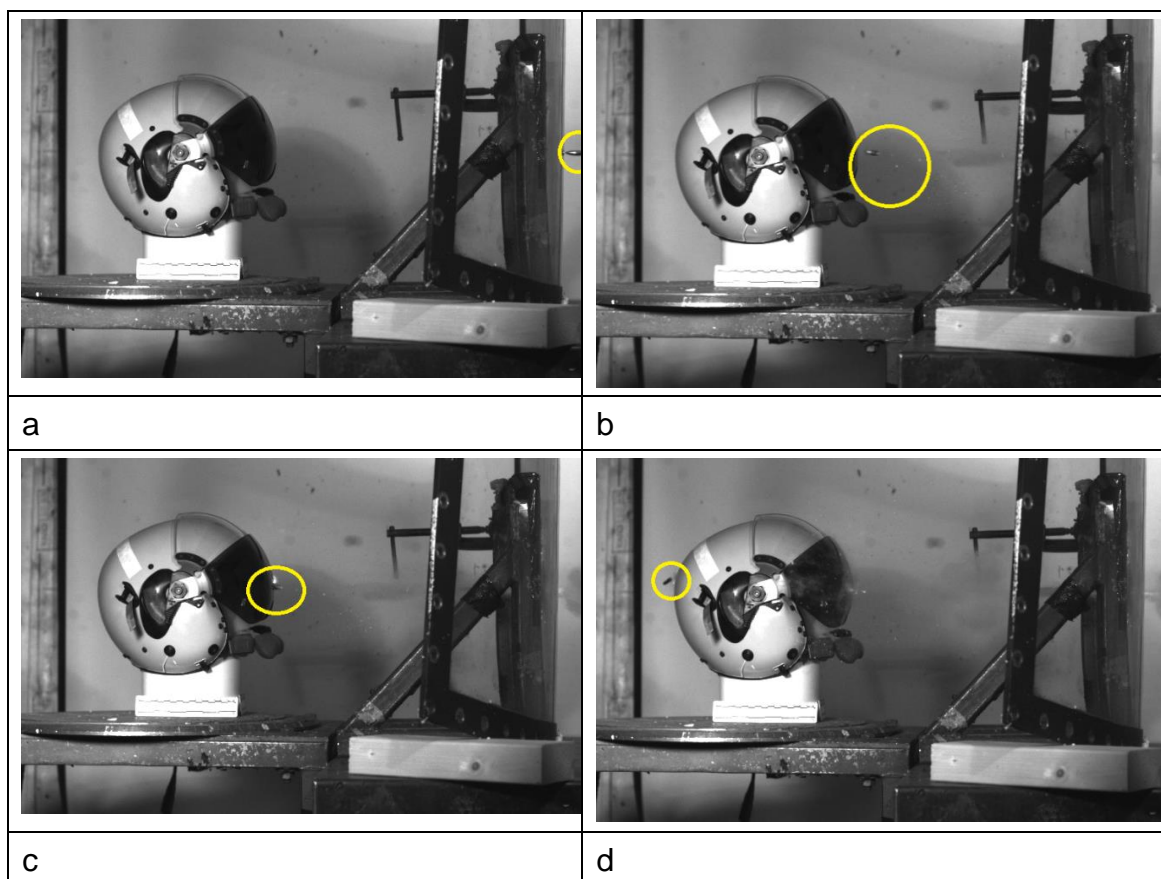


Figure 8-19 Model 16 V1212 HSV, side view

(a) pre-impact on window (b) pre-impact on visor (c) impact on visor (d) MSC exit, rear of helmet (bullet/MSV circled in all frames).

8.4.2.2.2 Pathologist assessment

Entry wound

A 15 mm x 6 mm horizontal defect was present medial to the left eye (Figure 8-20a). There was 'tissue' loss around the outer margins and some radial splits. There was black discolouration around the defect along with tiny window fragments. Bone injury consisted of a channel to the left side of the nasal bridge and medial to the left orbit (Figure 8-21a).

Exit wound

There was a 12 mm slit like wound with some radial splitting and eversion of the margins (Figure 8-22c). The underlying bones were comminuted with radiating fractures (Figure 8-21d).

Fracture pattern

Of note the fracture appeared to have crossed the post-mortem cut line in an area where the adhesive had held (Figure 8-21c), similar to that seen in model 14 (Figure 8-8). In other areas the cut impeded fracture propagation. Extensive fractures were visible in the skull base (Figure 8-22a).

Brain injury

There was some evidence of bullet yaw within the PermagemTM brain and there was a fragment of the bullet jacket close to the exit wound on the surface of the brain (Figure 8-21b, green arrow). Bone fragments were visible along the wound within the brain (Figure 8-21b, white arrow).

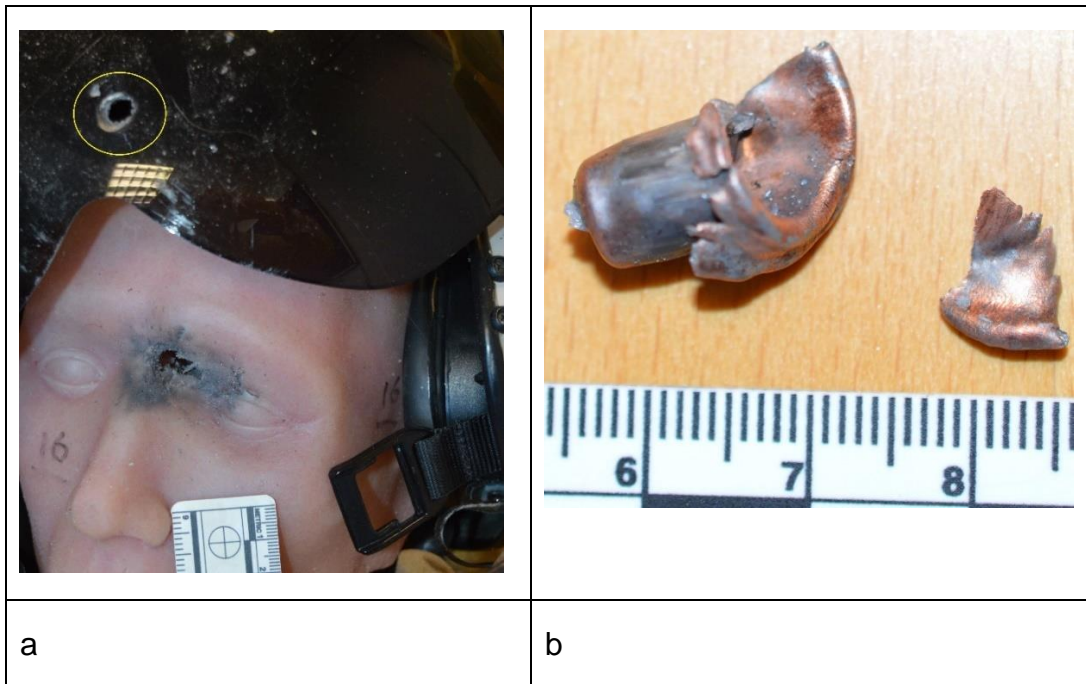


Figure 8-20 Pathologist examination helicopter window impact model 16 (1)

(a) entry wound in face; bullet hole in helmet visor circled (b) fragments of bullet jacket. Large piece recovered between helmet foam and head model; smaller piece (same as that indicated by green arrow in Figure 8-21b) recovered from surface of brain.

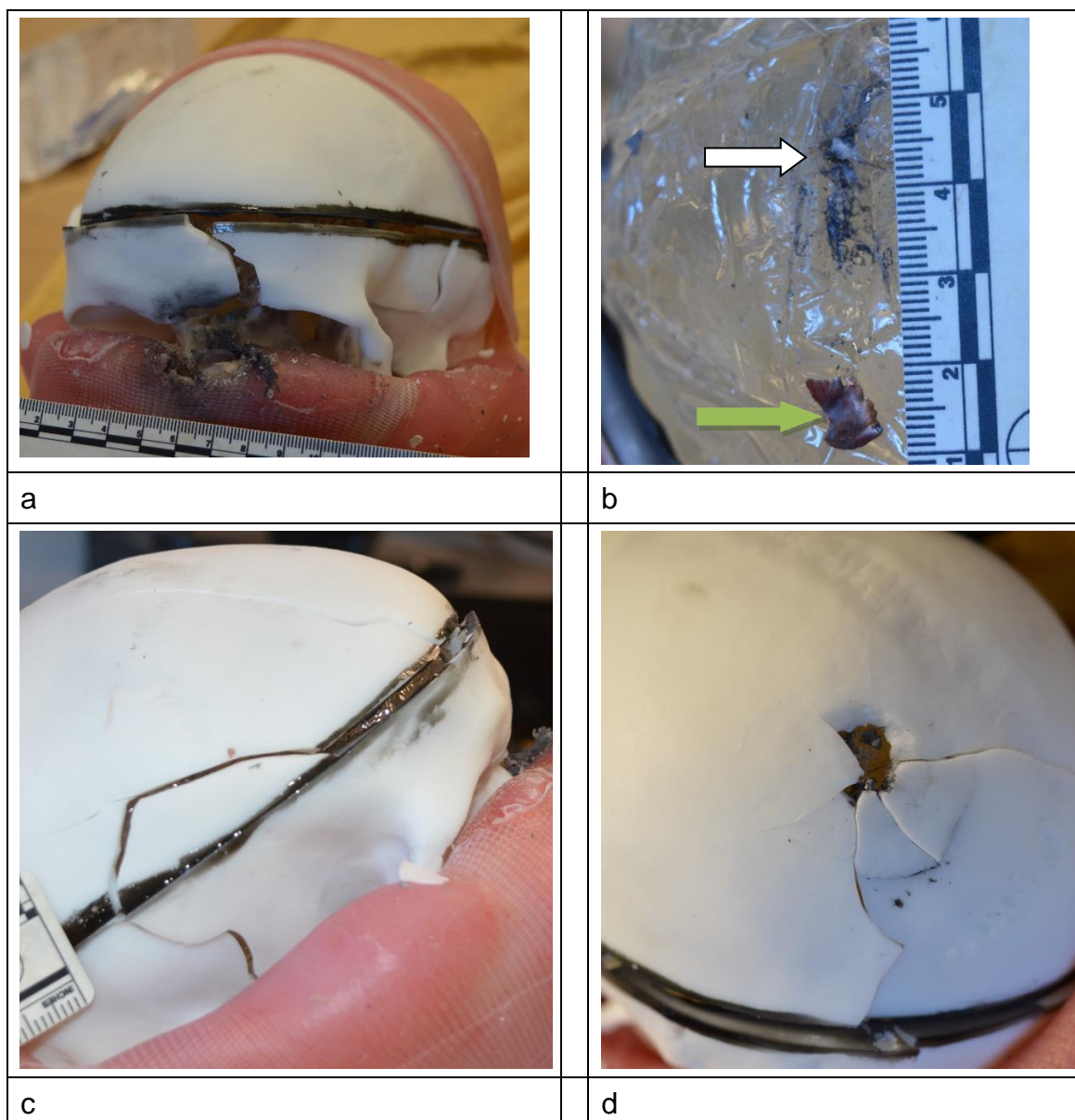


Figure 8-21 Pathologist examination helicopter window impact model 16 (2)

(a) fractures at entrance wound (b) brain injury; jacket fragment (green arrow) and bone fragments (white arrow) visible along with black discolouration (c) fractures right lateral aspect of skull; bond has held post-mortem cut in place (d) Bone exit wound with radiating fractures.

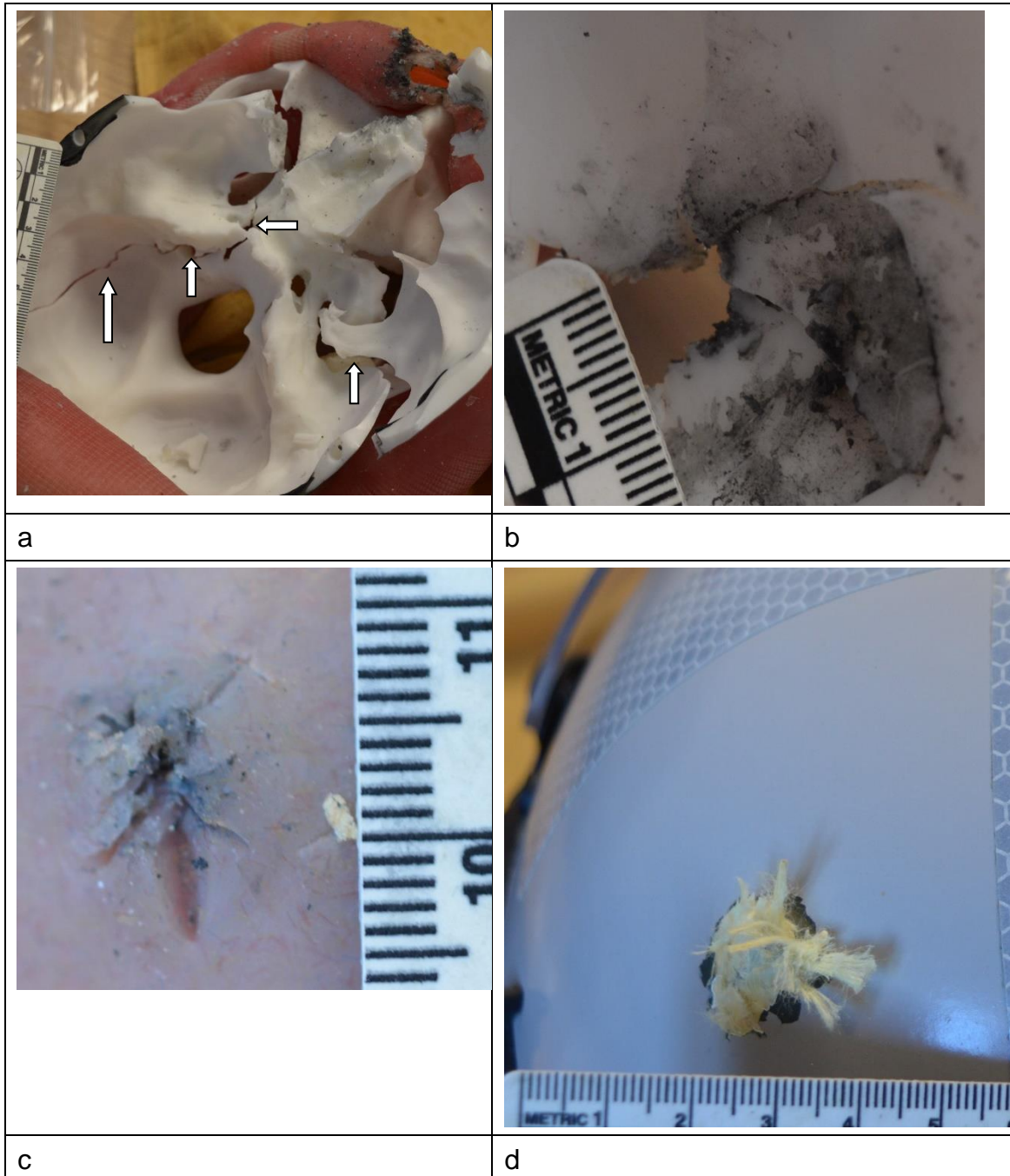


Figure 8-22 Pathologist examination helicopter window impact model 16 (3)

(a) base of skull fractures (arrowed) (b) inner aspect of bone exit wound with black discoloration (c) corresponding skin exit wound (d) helmet exit site.

8.4.2.2.3 Radiologist assessment

Helmet

There was a discreet round hole through the visor with no shattering. There was no delamination of the helmet shell in contrast to the ballistic helmets described in chapter 7. Metallic residue was visible wiped on the internal helmet foam liner from penetrating bullet fragments. A deformed bullet jacket was retained between the helmet foam and the head model (Figure 8-25b, same as left hand fragment in Figure 8-20b).

Face

Metallic fragments and window fragments were visible producing 'peppering' across the face.

Entry wound

The entry wound was a very different appearance to previous models being an irregular large hole with some fragments visible at the margins (Figure 8-23b).

There was minimal propagation of the underlying entry fractures with limited left calvarial disruption.

Exit wound

The appearance of the exit wound was more typical but with heavy contamination visible. The exit fracturing was more consistent with real injury having a large defect and fracture propagation to the foramen magnum (Figure 8-25c).

Brain injury

There was a 'snow storm' effect visible within the bullet path in the brain (Figures 8-24b & 8-26c) with one large piece of metallic debris visible and some smaller fragments visible away from the main track (one located distant within the right hemisphere).

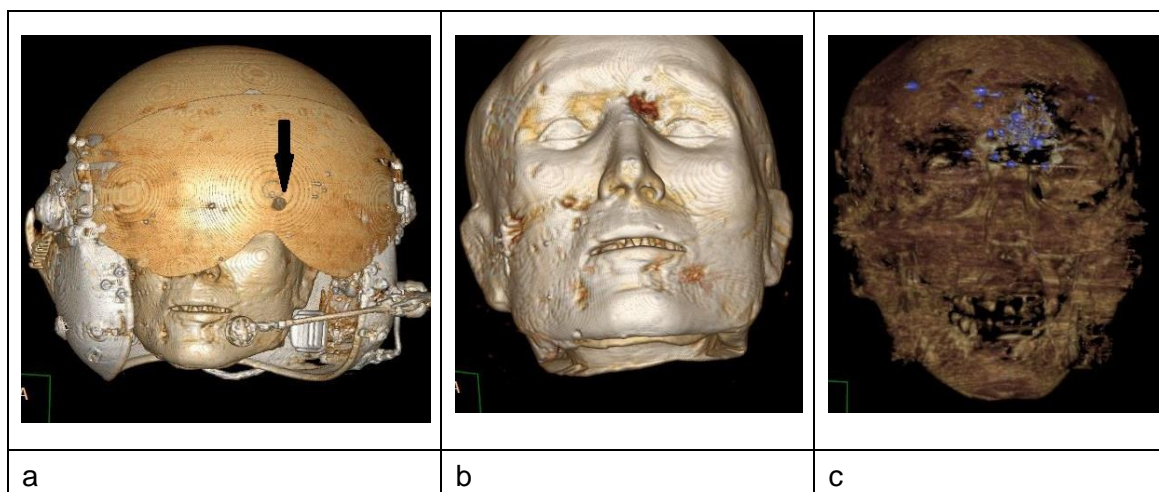


Figure 8-23 Model 16 CT 3D reconstruction front views

(a) helmet in situ, entry site in visor arrowed. Note how head has been moved by the impact in a similar way to that seen in Figure 7-4 (b) underlying skin and soft tissue with impacts visible (c) view optimised for dense fragments showing cluster behind entry wound.

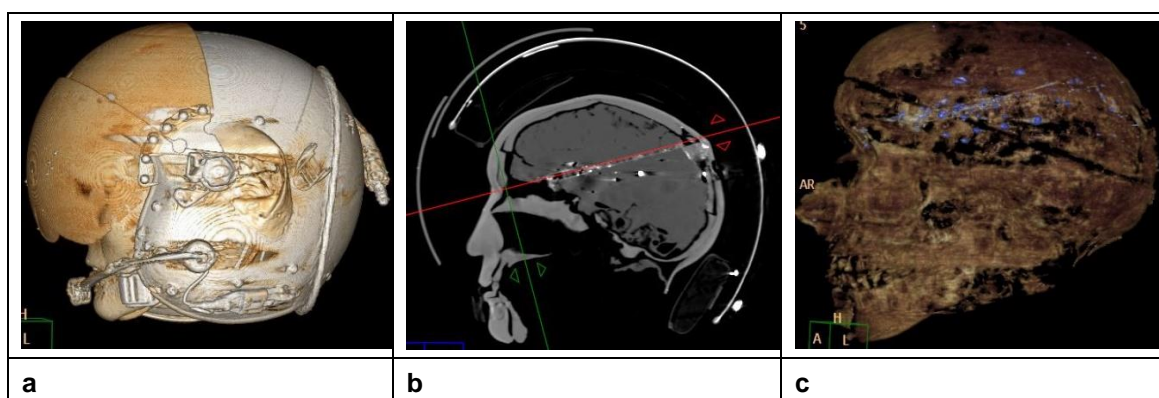


Figure 8-24 Model 16 CT 3D reconstruction side views

(a) helmet in situ (b) image optimised for 'bone'; bullet path marked in red (c) optimised for dense fragments plus tissue removal; metallic fragments appear blue.

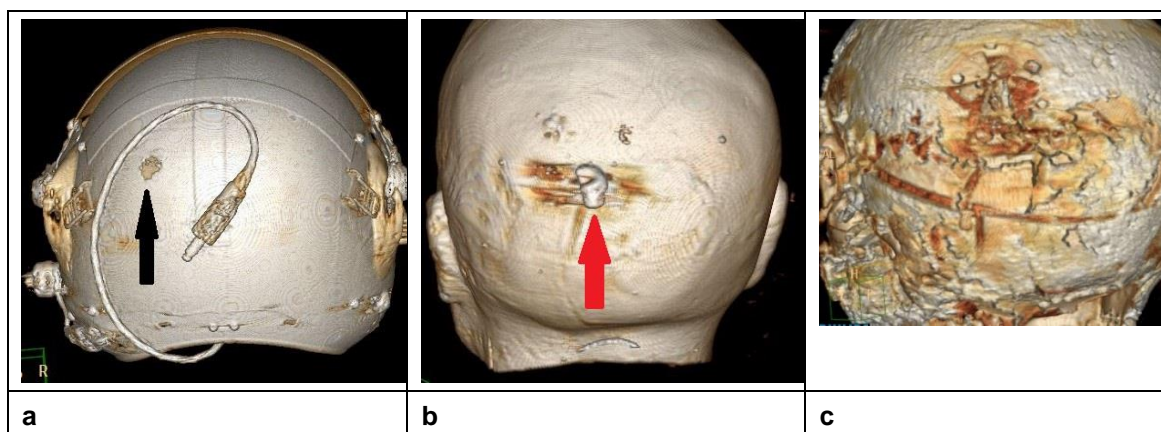


Figure 8-25 Model 16 CT 3D reconstruction rear views

(a) helmet in situ, exit site arrowed (b) underlying soft tissue; bullet jacket arrowed (see figure 8-20b) (c) underlying fractures.

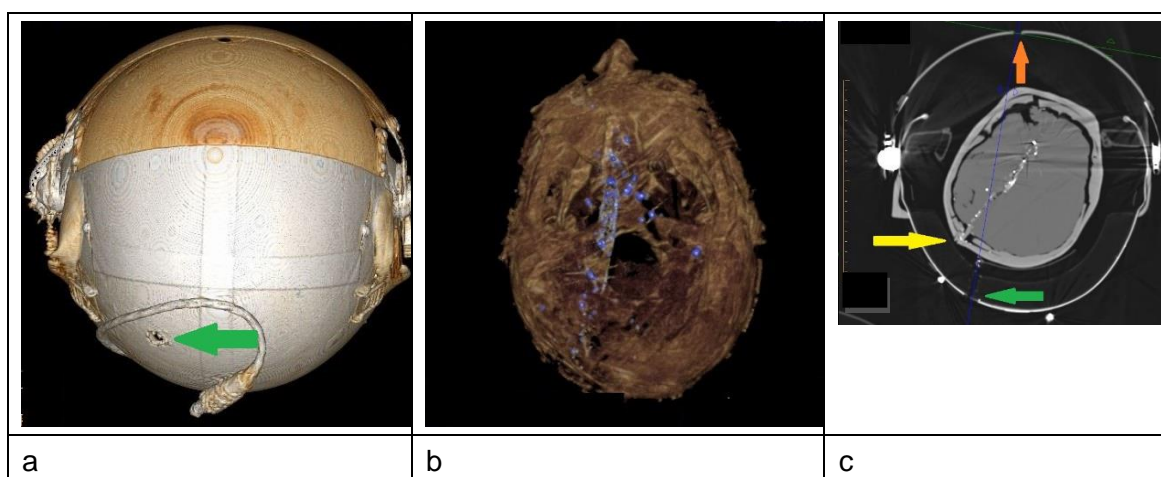


Figure 8-26 Model 16 CT 3D reconstruction viewed from above

(a) helmet in situ, bullet exit site arrowed (b) helmet digitally removed, image optimised for fragments, metal appears blue (c) axial cut orientated to match panels (a) and (b); normally in medicine CT scans are viewed as if from the patient's feet looking upwards; visor entry (orange arrow), head exit (yellow arrow) helmet exit (green arrow).

8.5 Discussion

The purpose of this experiment was to assess the head injury model developed in chapters 5, 6, and 7 against a number of different experimental conditions.

The first condition, a contact wound with 5.56 x 45 mm ammunition was assessed against an actual incident by a forensic pathologist and military radiologist.

The entry site on the model was noted on the CT imaging to be more into the orbit than on the actual case. The bullets in both models 13 and 14 impacting the thin orbital bones might explain the lack of bullet fragmentation which occurred in the actual incident. A MSC bullet fractured after impacting one of the models in an earlier experiment having hit the right petrous ridge (see chapter 6, section 6.4.2.5). The mechanisms underlying ballistic head impacts and producing the resulting injury are complex and multifactorial.

Kneubuehl and Thali [7] simulated two unrelated cases of gunshot head injury (a suicide and an attempted suicide) from an assault rifle bullet using a polyurethane sphere as a surrogate. The fatal gunshot was a contact wound [1] and gas pressure at the muzzle of the weapon on the surrogate caused it to burst open, mirroring the injuries in their casualty. The survivor had moved his head a few centimetres from the muzzle before firing, avoided the majority of the gases, and suffered a wound with a long neck length [see chapter 3]. The authors noted that at longer ranges the formation of a temporary cavity by bullet impact (as demonstrated in chapter 3, Figures 3-7 and 3-8) will also cause a bursting injury but stated at distances beyond 100 m, depending on the bullet type and calibre, bullets may pass cleanly through the skull.

The lack of yaw in the Permagem™ brains in the contact wound experiment compared with earlier work [17] demonstrates that the bullets are in different stages of flight in the two experiments.

The calvarial fracture patterns in this experiment appeared more realistic on imaging than at examination, although model 14 was noted to have more realistic fracture patterns by the pathologist.

This multidisciplinary approach to assessing the models has proved valuable throughout the experiments, mirroring the approach taken in assessing UK operational casualties [14] and supporting the view of Karger [15] on the benefits of a combined approach (see also discussion at chapter 6, section 6.5).

The stellate discolouration around the entry site was realistic although the entry wounds were smaller than the actual ones due to the extendable nature of the synthetic skin. While the 'new' synthetic skin/soft tissue used on model 14 is less extendable further work is needed to match it to real skin/soft tissue behaviour at ballistic strain rates.

In the second experiment the MSC 7.62 x 39 mm bullet was destabilised by both the windscreen and the helicopter window as previous authors had indicated [11,12] and larger entry wounds produced as described by Di Maio [1]. The bullet perforating the helmet visor appears to strike at close to 90° on the HSV and produce a neat circular hole in the visor (Figure 8-17a) but had turned horizontally before impacting the skin/soft tissues, demonstrating how rapidly destabilisation can occur. Within Catanese et al. [6, p334] there is an image and brief description of a bullet causing an irregular entry wound having perforated the lens of spectacles.

The combined effect of the helicopter window and the helmet did significant damage to the bullet, stripping off the jacket and exposing the core. This is more damage than seen with the helmets in chapter 7 and could be the subject of further investigation. Imaging was effective in visualising the fragments within the models in line with the views of Oehmichen et al. [16].

The Permugel™ fill was a satisfactory substitute for 10% gelatine in this experiment but black discolouration was seen along the bullet path in all models, not just those involved in the contact wound simulation. This was as expected [see Appendix H]. On a positive note parts of the adhesive bond

between the two halves of the model survived the ballistic impact in models 14 and 16 and required further assessment.

8.6 Conclusions

A surrogate head model was assessed against two further experimental conditions, a contact gunshot wound with 5.56 x 45 mm ammunition and 7.62 x 39 mm MSC ammunition through intermediate targets. The wounds, fractures and images were assessed by experienced clinicians. Elements of the injuries produced were clinically accurate but further work is needed on developing the synthetic skin/soft tissue material.

8.7 Caveats

This experiment involved a very limited number of replicates. Different results may be observed with additional experiments

8.8 Acknowledgements

1.Cranfield University, Defence Academy of the United Kingdom, Shrivenham, SN6 8LA.

David Miller

Alan Peare

2. Ammunition Hall, Defence Academy of the United Kingdom, Shrivenham, SN6 8LA.

Lt Col Liz Nelson

WO2 Ian Morton

3.Centre for Defence Imaging, Queen Elizabeth Hospital Birmingham, Mindelsohn Way, Birmingham B15 2TH.

Catherine Bean

Lauren Potts

Military CT Specialist Radiographers.

4. Nottingham Trent University, Flexural Composites Research Laboratory, 107 Bonington Building, Dryden Street, Nottingham, NG1 4GG, UK.

Richard Arm, Research Fellow.

5. Boeing UK for providing the helicopter window used in the second case study.

8.9 References

1. Introduction to the classification of gunshot wounds. In: Di Maio VJM (2016) Gunshot Wounds: Practical Aspects of Firearms, Ballistics and Forensic Techniques. (3rd Edn). CRC Press, Boca Raton, FL. pp 57-108
2. Taylor SC, Kranioti EF (2018) Cranial trauma in handgun executions: Experimental data using polyurethane proxies. Forensic Science International 282: 157-167
3. Rothschild MA (2011) Conventional forensic medicine. In: Kneubuehl BP (Ed) Wound Ballistics: Basics and Applications. Springer, Berlin Heidelberg. pp253-285
4. Vellema J, Scholtz H (2017) Forensic aspects of ballistic injury. In: Breeze J, Penn-Barwell JG, Keene D, O'Reilly D, Jeyanathan J, Mahoney PF (Eds). Ballistic Trauma: a Practical Guide (4th Edn). Springer Nature, Cham, Switzerland. pp 409-435
5. Dodd MJ (2006) Terminal ballistics: a text and atlas of gunshot wounds. CRC Press, Boca Raton, FL
6. Catanese CA, Gilson T, Andrew T (2010) Gunshot wounds. In: Catanese (Ed) Color atlas of forensic medicine and pathology. CRC Press, Boca Raton, FL. pp283-352
7. Kneubuehl BP, Thali MJ (2011) Experimental reconstruction. In: Kneubuehl BP (Ed) Wound Ballistics: Basics and Applications. Springer, Berlin Heidelberg. pp291-303

8. Kieser DC, Carr DC, Leclair SCJ, Horsfall I, Theis J-C, Swain MV, Kieser JA (2013) Clothing increases the risk of indirect ballistic fractures. *J Orthop Surg Res* 8: 42 DOI: 10.1186/1749-799X-8-42
9. Farrugia A, Raul JS, Geraut A, Tortel MC, Ludes B (2009) Destabilisation and intracranial fragmentation of a full metal jacket bullet. *Journal of Forensic and Legal Medicine* 16: 400-402
10. Mahoney PF, Carr D, Miller D, Teagle M (2017) The effect of helmet materials and simulated bone and tissue layers on bullet behaviour in a gelatine model of overmatch penetrating head injury. *Int J Legal Med* 131:1765-1776
11. Harper WW (1939) Behaviour of bullets fired through glass. *Am. Inst. Crim. L. & Criminology* 29:718-723
12. Lambert HC (1994) The effects of commercial tempered glass on rifle bullet deflection. MSc dissertation Californian State University (accessed 28/02/2018)
13. Bullet hole and wound characteristics. In: Hueske EE (2016) *Practical Analysis and Reconstruction of Shooting Incidents* (2nd edn). CRC press, Taylor & Francis Group, Boca Raton. pp223-257
14. Russell R, Hunt N, Delaney R (2014) The mortality peer review panel: a report on the deaths on operations of UK service personnel 2002-2013. *J R Army Med Corps* 160:150-4
15. Karger B, Puskas Z, Ruwald B, Teige K, Schuirer G (1998) Morphological findings in the brain after experimental gunshots using radiology, pathology and histology. *Int J Legal Med* 111: 314-319

16. Oehmichen M, Gehl H-B, Meissner C, Petersen D, Höche W, Geeling I, König HG (2003) Forensic pathological aspects of post-mortem imaging of gunshot injury to the head: documentation and biometric data. *Acta Neuropathol* 105: 570-580
17. Mahoney PF, Carr DJ, Delaney R, Hunt N, Harrison S, Breeze J, Gibb I (2017) Does preliminary optimisation of an anatomically correct skull-brain model produce clinically realistic ballistic injury fracture patterns? *Int J Legal Med* 131: 1043-1053

9 DISCUSSION

9.1 Introduction

The work presented in chapters 3 through 8 [1-4] has described a series of experiments to create a surrogate for ballistic head injury and test it against the findings from real incidents and simulated military shooting scenarios. The assessments by experienced military and civilian clinical personnel have, on the whole, been positive. The first part of this discussion will briefly summarise the work to demonstrate the underpinning academic processes and new learning produced. The rest of the discussion will consider the experimental methods chosen and their validity.

9.2 The requirement

Operational experience (described in the thesis introduction) and research [5] in conjunction with summaries of other operational experience [6] and research literature [7, 8] indicated that work was needed to unravel ballistic head injury mechanisms. While a number of recent projects have considered BABT/BHBT [9-12] there has not been the equivalent for overmatch penetrating impacts on heads wearing helmets. Penetrating ballistic head injury has been modelled physically by a number of authors e.g. [7,13] which provided the foundation for the experiments set out in this thesis.

The concern expressed by the Committee on Review of Test Protocols [14] echoing that of Aare and Kleiven [8] regarding the lack of correlation between helmet standards and clinical injury is significant.

Researchers investigating BHBT, have described grading the damage to skulls [10] cadaveric heads [10,12] and a hybrid model [11] and the likely resulting brain injury after helmet impact. The BHBT work and the work in this thesis link in turn with Breeze et al. [15] mapping helmet coverage of external anatomical

markers with the underlying brain structures that need protecting. Linking anatomical coverage, anatomical injury, ballistic wounding and the effect of helmet materials on bullet behaviour is essential to fully understand military penetrating head injury. Potential utility and further development of this work will be considered in the 'further work' section (chapter 10).

9.3 Review of the academic processes and summary of new knowledge

This section will briefly review the thesis chapters in turn, summarise the key points and set out the new knowledge within each chapter.

Chapter 3 described a project assessing the sequential effect of bone, synthetic bone, synthetic skin and actual helmet materials on 7.62 x 39 mm MSC bullet behaviour in 10 % gelatine. Animal scapulae have been used by other researchers as a surrogate for human crania [16,17].

The thickness of the horse scapulae (mean thickness 6.5 mm; SD 1 mm) impacted in these experiments is close to that of human frontal bone (6.15 mm SD 1.91 mm) described in [18]. The combination of the horse bone with residual tissue had similar effects on bullet behaviour (assessed by temporary cavity formation) to one of the synthetic bone polymers, MU51, with a layer of synthetic skin, indicating that this deserved further assessment [1]. Measuring temporary cavity formation within the gelatine blocks using High Speed Video has been confirmed as a superior method to that of assessing cracks within the gelatine [19].

Chapter 4 considers Synbone® spheres. A number of studies have used Synbone® spheres for ballistic experiments with good effect [7, 20-22] but in the study described in chapter 4, forensic pathologists familiar with modern combat injury felt that the impacted spheres did not produce realistic injury patterns when impacted with 7.62 x 39 mm MSC ammunition at the simulated

engagement distances used. The observations of Fenton et al. [23] are that the skull architecture influences fracture propagation. This observation, (and the requirement for a model that could wear a helmet), lead to investigation of impacts on anatomically correct synthetic skulls (chapter 5 and [2]), building on the work of Carr et al. [24].

The experiments described in chapter 5 assessed the effect of 3 different polymers on fracture patterns in skull models impacted by 7.62 x 39 mm MSC ammunition and found no significant difference in the assessor scores. Further work assessing the effect of a Permangel™ fill, and of different gelatine fills (5%, 7% and 10 % at a range of temperatures) on fracture patterns in the shot synthetic skulls also found no significant difference in the assessor scores. Jussila [25] states that *'the question on concentration is irrelevant as long as gelatine has been validated to produce results that can be extrapolated to living tissue'*. (see Figure_A2).

Of the 39 skulls shot, 23 were given scores of 3 ('quite like a real incident') by at least one assessor and 7 a score of 4 ('exactly like a real incident') by at least one assessor (see Appendix G for comments on skulls where more than one assessor gave a score of at least 3).

Of note the assessors were all operationally experienced but came from different clinical backgrounds and between them gave a range of different scores reflecting their past experience.

Two other points stand out:

- The post-mortem cut line (a feature of the manufacturing process of this model) influenced fracture propagation (as expected from previous authors observations [26]) and thus assessor scores.
- The exit wounds were generally regarded as more realistic than the entry wounds which contrasts to findings with Synbone® [21, 22].

The next stage was the addition of a layer of synthetic skin/soft tissue to the skulls (chapter 6 and [3]) using material that had similar hardness to reported values for real skin but lower tear strength (see Appendix D). The material had been developed as part of a project to create a surgical training model [27] and feel 'realistic' to clinicians using the model. The skin/soft tissue was the same composition as that shot in combination with the blocks of gelatine and MU51 polymer in chapter 3 and [1].

Key learning points were:

- At ballistic strain rates the synthetic skin/soft tissue was found to be too extendable in comparison with real skin which affected the appearance of the resulting wounds. Biological tissues also show strain rate dependent behaviour [28, 29].
- This project introduced CT imaging assessment of the model in line with the approach described by Thali [30] and the combined assessment techniques described by Karger [31].
- The synthetic bone and the synthetic skin/soft tissue appeared very similar at imaging despite having different mechanical properties which made removing layers in the 3-D image reconstructions more difficult.
- Although the exit injuries scored lower than the entry wounds they were described by assessors in their comments as being the more realistic (in line with the shot skulls described above), and the fracture patterns over all scored well.

The model was then used to reconstruct two military shooting incidents of casualties wearing a helmet which required synthesis of operational military data by DSTL to extract the required information around engagement distances and ammunition types (chapter 7 and [4]).

Key learning points were:

- The mean nL in the models from 'Incident 1' ($n=3$) was similar to that in the gelatine blocks using the same materials as intermediate targets [1] although the variability was greater in the blocks ($n=6$). Of note, van Hoof et al. [32] undertook FE modelling of ballistic panels and helmets under impact by 1.1g .22" Fragment Simulating Projectiles (FSPs). The helmets were found to undergo higher deformation than the flat panels. Further work to understand to what extent flat panels can be used to model helmet impacts, both with FE simulations and actual materials is required.
- The helmets altered the appearance of both the entry and exit wounds which, according to one of the pathologists, can occur with real incidents.
- Flash x-ray as used by Watkins [13] and Freitas [11] captured the bullet yaw in three of the models.

The wounds produced in 'Incident 2' were unlike those of the event under consideration due to variability in the bullet pathway but did reproduce realistic examples of tangential bullet strikes [33, 34] This emphasised that post hoc matching of clinical events to recreations is useful to establish clinical congruence in a model [2, 7, 21, 24, 33] but runs the risk of misinterpreting evidence if accepted uncritically.

In the final experiment the model was tested against further conditions of a contact wound produced by 5.56 x 45 mm ammunition and the wounding effects of 7.62 x 39 mm MSC ammunition fired through intermediate targets (laminated glass and a transparent thermoplastic). There were two replicates for the contact wound (each assessing different synthetic skin/soft tissue responses) and one each for the laminated glass and thermoplastic, so the work may be seen more as proof of concept rather than a detailed study.

Key learning points were

- The two skin/soft tissue surrogates assessed using the contact wound did respond differently to ballistic impact but further work is needed to achieve responses closer to that of real tissue.
- The glass and thermoplastic intermediate targets destabilised the 7.62 x 39 mm MSC ammunition as expected resulting in more realistic entry wounds than the work described in chapters 6 and 7 in line with appearances described in [34].

9.4 Quality of the experiments

9.4.1 Choice of materials and eliminating confounders

The series of experiments described in chapters 3 through to 7 [1-4] were designed to build and test the model in logical stages, with clinical assessments of both the spheres and the anatomical surrogates. A number of factors were kept constant in an attempt to minimise variability both within and among experiments, in accordance with Chalmers [35]. There was variation in the experimental conditions described in chapter 8, but as noted above this work was proof of concept to explore further avenues for the model's use.

9.4.1.1 Ammunition

The Ukrainian 7.62 x 38 MSC ammunition was all from the same manufacturer's batch and was quarantined within a secure ammunition bunker. Composition and batch consistency was assessed as shown in Appendix B. In chapter 5 Czech ammunition is used for a number of the skull shots but as shown in Table_A 2 is of very similar hardness to the Ukrainian bullets. The Russian ammunition used in chapter 8 did not undergo SEM and microhardness testing but samples were cut open to ensure they had a MSC rather than a lead core (Figure 8-2b).

9.4.1.2 Gelatine

The gelatine used for the blocks (chapter 3) and head models (spheres, skulls, skulls with faces, skulls with faces wearing helmets, chapters 4 to 7) was all from one batch of Gelita® ballistic gelatine and prepared according to an agreed internal Impact and Armour protocol. The stages in manufacture are illustrated in Appendix A. The validation of the blocks (similar to that described in [25]) is demonstrated by the graph of depth of penetration (DoP) in mm of the 5.5 mm ball bearings shot into each block before the experiments, against ball bearing impact velocity in m/s (Figure_A 3). Figure_A 4 demonstrates performance of the blocks for these experiments and comparison with earlier work [36].

9.4.1.3 Synthetic Bone versus real bone

A number of researchers have used real bone for ballistic impact studies [9-13, 20]. Disadvantages with real bone are that the ages of the specimens can vary [12, 20] as can the sex [20] and dried samples may need to be 'refreshed' [11].

Testing the mechanical properties of cranial bone has demonstrated variation among individuals and at different sampling points within the same individual [37].

Issues with age are demonstrated by Rafaels et al. [12] who undertook a further study of BABT/BHBT, building on the work of Sarron et al. [10, 38] using seven post-mortem human subjects (PMHS) wearing protective helmets. The head/helmet combinations were impacted with 9 mm bullets at a series of nominal test velocities between 400 and 460 m/s. The velocities were chosen based on previous work on skull fracture tolerances by Bass et al. [39] as likely to provide low, moderate and high risk of skull fracture. Injury to the specimens was assessed by both dissection and radiological evaluation. Limitations declared in the study included (a) tissue decomposition of the specimens and (b) the mean age of the specimens being 69.1 years [range 47 to 93] compared

with the mean age of the military trauma patient of 26 years. The authors state that older bone is more brittle than younger bone so they undertook 'scaling [25] to predict injuries in the 20 to 29-year-old age group. Of note, this study only found linear fractures associated with depressed fractures near the point of impact compared to the range of injury described by Freitas et al. [11] using 'refreshed' skulls in their HHS model.

Smith et al. [21] stated that an advantage of using synthetic bone substitutes is that the materials should be identical. The consistency of the models is demonstrated in Appendices E and F, Tables_A 4, A 5, A 6, A 8 and A 9 where mean, SD and CV % values are given for mass of the spheres and skulls both empty and filled with gelatine or Permugel™.

A potential disadvantage of the model may be its relatively small size compared to published values for the human head in the literature. Yoganathan et al. [40] summarise and review a series of reports and data sets of cadaveric anthropometric data. Mean values for adult head mass are in the order of 3.5 to 4.5 kg depending on data set but minimum values as low as 2.45 kg were reported. As the model has accommodated full size ballistic helmets, an aviation helmet, and produced realistic injury on impact this limitation is acknowledged but not seen as an issue to invalidate its use.

The synthetic bone sheets used in chapter 3 were sourced respectively from single manufacturers and handled carefully to ensure there was no extraneous damage prior to the ballistic impacts. The horse scapulae were shipped refrigerated soon after the post mortem and maintained at 4°C until the experiments to minimise degradation and avoiding the decomposition issues experienced by Rafaels [12]. As discussed in chapter 3, and summarised above the use of cattle and pig scapulae to simulate human crania in experiments has been accepted [16, 21]. The micro CT images [Appendix C] of the horse scapula (Figure_A 13) after bullet impact show the complexity of bone structure when compared to those of Synbone® (Figure_A 14) and MU51 (Figure_A 15).

The similar high-speed video results obtained with the MU51 synthetic bone/synthetic skin combination when compared with the horse scapulae /residual soft tissue targets noted previously suggests that the former has merit as a bone/skin surrogate and gives weight to the choice of the same combination for the ballistic experiments described in chapters 5 to 7 [1-4].

This is not the case with all synthetic bones. While Thali and Kneubuehl [41] found that their long bone model (gelatine/polyurethane/latex) was '*absolutely equal*' when compared with swine bone under ballistic impact (7.62 x 39 mm and 7.62 x 51 mm ammunition), Quenneville et al. [42] had different findings with another model.

Quenneville et al. [42] compared Sawbones® synthetic tibias with human cadaveric data under axial impact loads (not ballistic impacts). The impact energy was relatively low (20-80 J) compared to that from the 7.62 x 39 mm impacts described in this thesis (in the order of 1500-1700 J) but they found that the synthetic bones failed at lower energies and by different mechanisms compared to the cadaveric bones. The different failure mechanism (a delamination of material layers) meant that the lower energy failure could not be 'scaled' to that of real bone.

This agrees with Jussila's view, already noted in chapter 3 and above [25], that tissue simulants do not need to be biomechanically the same as living tissue as long as '*the results can be measured and appropriately extrapolated or scaled*'.

9.4.2 Use of the Likert-type scale and fracture characteristics

One of the aims of the project was to build a surrogate for ballistic head injury that would have clinical fidelity. A challenge was deciding how this 'clinical fidelity' could be assessed and scored.

There are a number of ways to describe and classify gunshot characteristics in bone. One example is Boylston in *The Guidelines to the Standards for Recording Human Remains* [43]. Characteristics include the size and shape of the hole in the bone, the type of bevelling present and the presence and extent of radiating fractures. While this is a good framework for describing injury, it does not meet the requirement for assessing 'realism' in the model.

Previous projects from the Royal Centre of Defence Medicine, UK, have used Delphi methodology [44, 45] and Likert-type scales to successfully unravel complex clinical issues around combat casualty care. This gave the background to construct a simple four-point Likert-type scale [46] that could be completed quickly by the assessing clinicians but still capture their opinion on how the models compared with actual combat injury. A four-point scale was also used by Sarron et al. [10] in their BHBT model and Freitas [11] as described in the introduction to this thesis and chapter 7 [4]. Where Freitas and colleagues were assessing BHBT and mapping fractures across to the likely severity of underlying injury, all the simulated injuries in this thesis were overmatching the model, would have been fatal, and the key question was how they compared to actual battlefield injury, hence the different scoring system.

The Likert-type scale allowed collection of qualitative data as a score and use of the scores for quantitative assessments allowed appropriate analysis [2].

The Likert-type scores had particular utility with regard to the synthetic skin. As described in chapter 6 [3], and above the surrogate skin/soft tissue had been assessed by members of surgical teams as part of a larger project to build realistic surgical training manikins [27] While the 'tissue' appeared realistic for surgical training scenarios and produced suitable wounds when cut with scalpels, its extendable nature under ballistic impact meant that the skin entry wounds were unrealistic [3]. A combination of the Likert-type scores, comments and HSV images allowed this to be assessed and analysed- and developments formulated and trialled as shown in chapter 8.

9.5 Does the model need to be this complex?

Appendix I illustrates a number of alternative models for ballistic injury.

The Clear Ballistic Gel head illustrated in Figure_A 23 is marketed as a viable model for ballistic injury. While it does allow good imaging of the temporary and permanent cavities it does not allow assessment of skin wounds and fracture patterns.

The impact sequences shown in Figures_A 24 & A 25 are of an MU51 polymer skull with a Permagel™ fill and face. While the fracture propagation could be seen well on HSV the entry and exit 'tissue' appearances were unrealistic hence the assessment of PDMS alternatives.

Polystyrene heads have been used successfully to capture fragments from police equipment attached to body armour and impacted with 9 x 19 mm FMJ ammunition, demonstrating areas of potential vulnerability [47]. Figure_A 26 shows the effect of a contact shot (5.56 x 45 mm) into a polystyrene head, demonstrating the material burning and structure disintegrating, and illustrating why it would be unsuitable for this type of work.

All of the models described above have utility but need to be matched with the type of event under investigation. The HHS developed by Freitas et al. [11] is one example of a model with greater complexity. Freitas compared the intracranial pressure/time histories generated in their model from ballistic impact with those from Liu et al. [48] who impacted live anaesthetised pigs with 9 mm rounds and used flat plates of protective material to represent the helmet. The model of Freitas et al.[11] exhibited similar characteristics to that of Liu et al. but changes in the latter had a greater magnitude. Greater complexity is required when a model is aiming to investigate both physiological changes along with anatomical injury.

As shown in chapters 5 through 8 the model developed in this thesis also has limitations but does demonstrate elements of clinical fidelity which is needed when assessing the clinical implications of gunshot wounds. Areas for development will be considered in chapter 11.

9.6 Conclusions

This chapter has reviewed the academic process and new learning from the experiments presented in chapters 3 through 8 and, where relevant, made comparisons with previously published literature. Measures taken to ensure the quality of the work have been described, and data to assure the findings is presented in the appendices.

9.7 References

1. Mahoney PF, Carr D, Miller D, Teagle M (2017) The effect of helmet materials and simulated bone and tissue layers on bullet behaviour in a gelatine model of overmatch penetrating head injury. *Int J Legal Med* 131:1765-1776
2. Mahoney PF, Carr DJ, Delaney R, Hunt N, Harrison S, Breeze J, Gibb I (2017) Does preliminary optimisation of an anatomically correct skull-brain model produce clinically realistic ballistic injury fracture patterns? *Int J Legal Med* 131: 1043-1053
3. Mahoney P, Carr D, Arm R, Gibb I, Hunt N, Delaney RJ (2018) Ballistic impacts on an anatomically correct synthetic skull with a surrogate skin/soft tissue layer. *Int J Legal Med* 132: 519-530
4. Mahoney PF, Carr DJ, Harrison K, McGuire R, Hepper A, Flynn D, Delaney R, Gibb I (2018) Forensic reconstruction of two military combat related shooting incidents using an anatomically correct synthetic skull with a surrogate skin/soft tissue layer. *Int J Legal Med* <https://doi.org/10.1007/s00414-018-1802-z>
5. Keene DD, Penn-Barwell JG, Wood PR, Hunt N, Delaney R, Clasper J, Russell RJ, Mahoney PF (2016) Died of Wounds: a mortality review. *J R Army Med Corps* 162: 355-360
6. Carr DJ, Lewis E, Horsfall I (2017) A systematic review of military head injuries. *J R Army Med Corps* 163:13-19
7. Thali MJ, Kneubuehl BP, Zollinger U, Dirnhofer R (2002) The 'skin-skull-brain model': a new instrument for the study of gunshot effects. *Forensic Science International* 125 (2-3): 178-189

8. Aare M, Kleiven S (2007) Evaluation of head response to ballistic helmet impacts using the finite element method. *International Journal of Impact Engineering* 34: 596-608
9. Bass C, Bolduc M, Wacawik S (2002) Development of a non-penetrating, 9 mm, ballistic helmet, trauma test method. *Personal Armour Systems Symposium*, November 18-22, The Hague, The Netherlands. pp61-68
10. Sarron JC, Dannawi M, Faure A, Caillou J-P, Da Cunha J, Robert R (2004) Dynamic effects of a 9 mm missile on cadaveric skull protected by aramid, polyethylene or aluminium plate: an experimental study. *J Trauma* 57: 236-247
11. Freitas CJ, Mathis JT, Scott N, Bigger RP, MacKiewicz J (2014) Dynamic response to a behind helmet blunt trauma measured with a human head surrogate. *Int J Med Sci* 11: 409-425 DOI: 10.7150/ijms.8079 (Accessed 23/03/2016)
12. Rafaels KA, Cutcliffe HC, Salzar RS, Davis, M, Boggess B, Bush B, Harris R, Rountree MS, Sanderson E, Campman S, Koch S, Bass CR (2015) Injuries of the head from backface deformation of ballistic protective helmets under ballistic impact. *J Forensic Sci* 60: 219-225
13. Watkins FP, Pearce BP, Stainer MC (1988) Physical effects of the penetration of head simulants by steel spheres. *The Journal of Trauma* 28: S40-54
14. Combat helmet testing. In: *Review of Department of Defense Test Protocols for Combat Helmets* (2014). Committee on review of test protocols used by DoD to test combat helmets, Board on Army Science and Technology; Division on Engineering and Physical Sciences; National Research Council, National Academies of Science. ISBN 978-0-309-29866-7. pp25-31

15. Breeze J, Baxter D, Carr D, Midwinter M (2015) Defining combat helmet coverage for protection against explosively propelled fragments. *J R Army Med Corps* 161: 9-13
16. Patten Report Recommendations 69 and 70 Relating to Public Order Equipment (2002). The Northern Ireland Office in consultation with the Association of Chief Police Officers. Third Report, December. Page 92
17. Smith MJ, Brickley MB, Leach SL (2007) Experimental evidence for lithic projectile injuries: improving identification of an under-recognised phenomenon. *Journal of Archaeological Science* 34: 540-553
18. De Boer HH, Van der Merwe AE, Soerdjbailie-Maikoe V (2016). Human cranial vault thickness in a contemporary sample of 1097 autopsy cases: relation to body weight, stature, age, sex and ancestry. *Int J Legal Med* 130:1371–1377.
19. Ragsdale BD, Josselson A (1988) Predicting temporary cavity size from radial fissure measurements on ordnance gelatine. *The Journal of Trauma* 28: S5-9
20. Raymond DE, Bir CA (2015) A biomechanical evaluation of skull-brain surrogates to blunt high-rate impacts to post mortem human subjects. *J Forensic Sci* 60: 370-3
21. Smith MJ, James S, Pover T, Ball N, Barnetson V, Foster B, Guy C, Rickman J, Walton V (2015) Fantastic plastic? Experimental evaluation of polyurethane bone substitutes as proxies for human bone in trauma simulations. *Legal Medicine* 17: 427-435
22. Taylor SC, Kranioti EF (2018) Cranial trauma in handgun executions: Experimental data using polyurethane proxies. *Forensic Science International* 282: 157-167

23. Fenton TW, Stefan VH, Wood LA, Sauer NJ (2005) Symmetrical fracturing of the skull from midline contact gunshot wounds: reconstruction of individual death histories from skeletonized human remains. *J Forensic Sci* 50: 1-12
24. Carr D, Lindstrom A-C, Jareborg A, Champion S, Waddell N, Miller D, Teagle M, Horsfall I, Kieser J (2015) Development of a skull/brain model for military wound ballistics studies. *Int J Legal Med* 129: 505-10
25. Jussila J (2004). Preparing ballistic gelatine; review and proposal for a standard method. *Forensic Science International* 141: 91-98
26. Viel G, Gehl A, Sperhake JP (2009) Intersecting fractures of the skull and gunshot wounds. Case report and literature review. *Forensic Science, Medicine, and Pathology* 5: 22-7
27. Arm, R (2015) Development of a Thoracic Trauma Trainer for the advancement of military operational surgical training. DMS RSG 20140911 [Internal Report]
28. Mota A, Klug WS, Ortiz M, Pandolfi A (2003) Finite-element simulation of firearm injury to the human cranium. *Computational mechanics* 31:115-121
29. Zhu F, Saif T, Presley BR, Yang KH (2017) The mechanical behaviour of biological tissue at high strain rates. In: Franklyn M, Lee PVS (Eds) *Military Injury Biomechanics: the Cause and Prevention of Impact Injuries*. CRC Press, Boca Raton. pp103-118
30. Thali MJ, Kneubuehl BP, Vock P, Allmen G, Dirnhofer R (2002) High speed documented experimental gunshot to a skull-brain model and radiological virtual autopsy. *Am J Forensic Med Pathol* 23: 223-228

31. Karger B, Puskas Z, Ruwald B, Teige K, Schuirer G (1998) Morphological findings in the brain after experimental gunshots using radiology, pathology and histology. *Int J Legal Med* 111: 314-319
32. van Hoof J, Cronin DS, Worswick MJ, Williams KV, Nandlall D (2001) Numerical head and composite helmet models to predict blunt trauma. 19th ISB Switzerland.
33. Thali MJ, Kneubuehl BP, Zollinger U, Dirnhofer R (2003). A high-speed study of the dynamic bullet-body interactions produced by grazing gunshots with full metal jacketed and lead projectiles. *Forensic Science International* 132: 93-98.
34. Introduction to the classification of gunshot wounds. In Di Maio VJM (2016) *Gunshot Wounds; Practical Aspects of Firearms, Ballistics and Forensic Techniques* (3rd edn). CRC press, Taylor & Francis Group, Boca Raton. pp 57-108
35. Chalmers AF (2013) *What is This Thing Called Science?* (4th edn) University of Queensland Press, St Lucia, Australia
36. Mabbott. A (2015). *Wound ballistics: behind police body armour*. PhD, Cranfield University, UK
37. Motherway JA, Verschueren P, Van de Perre G, Sloten JV, Gilchrist D (2009) The mechanical properties of cranial bone: the effect of loading rate and cranial sampling position. *Journal of Biomechanics* 42: 2129-2135
38. Sarron JC, Caillou JP, Da Cunha J, Allain JC, Tramecon A (2000) Consequences of non-penetrating projectile impact on a protected head: study of rear effects of protections. *J Trauma* 49: 923-9

39. Bass CR, Boggess B, Bush B (2000) Ballistic helmet backface deformation testing with a dummy subject. Proceedings of the Fifth Personal Armour Systems Symposium Sept 5-8 Colchester UK. pp 331-52
40. Yoganathan N, Pintar FA, Zhang J, Baisden JL (2009) Physical properties of the human head: mass, center of gravity and moment of inertia. *Journal of Biomechanics* 42:1177-92
41. Kneubuehl BP, Thali MJ (2003) The evaluation of a synthetic long bone structure as a substitute for human tissue in gunshot experiments. *Forensic Science International* 138: 44-49
42. Quenneville CE, Greeley GS, Dunning CE (2010) Evaluation of synthetic composite tibias for fracture testing using impact loads. *Proc IMechE* 224 Part H: J Engineering in Medicine. pp 1195-1199
43. Boylston A (2004) Recording of weapon trauma. In: Brickley M, McKinley JI. *Guidelines to the Standards for Recording Human Remains*. IFA Paper no. 7. BABAO, Southampton and IFA, Reading. pp 40-42
44. Hodgetts TJ, Mahoney PF (2004) Operational Surgical Services Review. Literature and Doctrine Review, Original Delphi study. Report to the Surgeon General
45. Hodgetts T, Mahoney PF, Mozumder A, McLennan J (2005) Care of civilians on military operations. *IJDM* 3: 3-24
46. Clason, DL, Dormody, TJ (1994) Analyzing data measured by individual Likert-type items. *Journal of Agricultural Education* 35: 31- 35

47. Milliner MS, Carr DJ, Mabbott A, Malbon C, Miller D (2016) The effect of ancillary police equipment on behind armour blunt trauma. In: Proceedings of Personal Armour Systems Symposium, 19-23 September, Amsterdam, the Netherlands.

48. Liu H, Kang J, Chen J, Li G, Li X, Wang J et al. (2012) Intracranial pressure response to non-penetrating ballistic impact: an experimental study using a pig physical head model and live pigs. *Int J Med Sci* 9: 655-664

10 CONCLUSIONS

Conclusions for each experiment are presented at the end of the respective chapter. The following are overarching conclusions for the thesis as a whole.

A. This thesis has described the systematic development of a synthetic head model suitable for ballistic testing with military ammunition.

This included: -

1. Analysing the effects bone, synthetic bone, synthetic skin and helmet materials had on bullet behaviour when impacted as intermediate targets in front of a gelatine block (chapter 3) and demonstrating greater variability in bullet behaviour as the model became more complex.

2. Critique of the utility of the current standard head surrogate (a synthetic bone sphere) for modelling military ballistic head injury (chapter 4) and showing that this has limited utility for impacts with 7.62 x 39 mm MSC ammunition at the simulated engagement distances considered.

3. Evaluating the effect of different gelatine fills and structural polymers on the fracture patterns produced in a realistic synthetic skull under ballistic impact (chapter 5) and demonstrating that the fill and polymer had no effect under the experimental conditions described.

B. The model was evaluated against actual military ballistic incidents of casualties wearing ballistic helmets (chapter 7), a recreation of a contact gunshot wound (chapter 8) and proof of concept work with ballistic impacts on intermediate targets (chapter 8). The impacts on the model produced a range of simulated injuries, some of which were assessed as clinically realistic, while others have indicated areas for further development.

C The synthetic skin and soft tissue (chapter 6) proved to be more extendable than real tissue and is an area for future work.

Further development and future work will be considered in the next section.

11 FUTURE WORK AND FURTHER DEVELOPMENT OF THE MODEL

This will be considered in two sections; future work and further development of the model.

11.1 Future work

The development of this model of penetrating injury has potential value in investigating broader aspects of combat injury than those described in the thesis.

11.1.1 Benefits and risks of helmets

Missliwetz and Wieser [1] suggested that helmets can make ballistic head injury worse when compared to not wearing a helmet. The mechanism they described included the bullet becoming unstable or deforming due to the helmet and delivering greater energy to the casualty. Balanced against this argument is the role of the helmet in preventing injury completely. Breeze et al. [2] found that casualties wearing a combat helmet were 2.7 times less likely to sustain a *fragmentation* head injury than those without.

Modelling is needed to fully understand the risks and benefits of ballistic protection and match these with the ballistic threats being faced.

11.1.2 Ballistic mechanisms

Can et al. [3] reviewed 104 patients admitted from Syrian war with gunshot brain injury. None were wearing a helmet. They looked at clinical factors that were associated with good or bad outcome. Unsurprisingly CT features of severe injury including pneumocephalus (air within the head) and midline shift

(brain structures being pushed towards one side due to swelling or bleeding) were associated with a poor outcome. While single lobe head injury was, as expected, associated with a higher survival rate, so was perforating head injury (i.e. the bullet enters and leaves the cranium) correlated with temporal bone fracture. The authors suggested that this was due to less energy being deposited within the cranium by a perforating wound when compared to a penetrating one but acknowledged within the study limitations that the patients were only followed up for 24 hours, and data could have been lost due to the retrospective nature of the review. Nevertheless, this does deserve further investigation and contrasts with the devastating perforating wounds simulated in chapters 5 to 8. Kneubuehl and Thali's simulation [4] of contact gunshot wounds [5] described in chapter 8 (section 8.5) indicates that there is a complexity here and further investigation is needed to match clinical effect with engagement distances and bullet behaviour.

11.1.3 Anatomical Injury

Anatomical injury is a major factor when considering clinical outcome. Ran et al. [6] reviewed the forensic reports of forty-nine Israeli Defence Force casualties who had suffered seventy-six gunshot entry wounds. These were plotted onto anatomical drawings and the actual frequency of impacts on anatomical regions was compared with the expected frequency from the surface area. They found that the occiput and anterior-temporal areas suffered 51% of the hits (while only being 15% of the skull surface area). Addition of the frontal regions gave 39% of the surface area and 71% of hits. The authors stated that they could not find any reports or studies detailing the influence of helmets on bullet injury patterns nor could they explain why the distribution occurred but postulated that helmets could be designed with greater protection for these particular areas, an area that could be assessed through ballistic modelling.

A recent review of gunshot head injury conducted using PRISMA guidelines [7] confirms that wounds crossing the midline of the brain are associated with a

high mortality but military experience with aggressive neurosurgical monitoring and intervention has produced improved outcomes.

11.1.4 Future work-summary

Modelling ballistic impacts may help work through the benefits and limitations of ballistic protection, and, in a validated model, allow comparison of the effect of strikes with and without a helmet in situ. This needs to be done across a range of engagement distances and with a greater selection of ammunition types to fully understand target effects and clinical implications.

11.2 Further development of the model

Several elements of the model have been criticised in the post impact assessments. These are (1) the synthetic PDMS skin/soft tissue (2) the brain simulant and (3) the post-mortem cut line in the skull. These will be considered in turn.

11.2.1 The synthetic PDMS skin/soft tissue

Positive aspects of the PDMS skin/soft tissue include (a) realistic entry wounds in the experiments with intermediate targets (chapter 8) (b) exit wounds that change appearance in models wearing a helmet (reflecting reality) (chapter 7).

Negative aspects are the material being too extendable under impact and the entry wounds not involving intermediate targets being described as too small (chapter 6). Changing the skin/soft tissue formulation for 3 of the replicates in chapter 8 did alter wound appearances but not to the extent of being clinically accurate.

An article by Fenton et al. [8] has reviewed published studies describing the properties of human skin, animal skin and synthetic surrogates. The authors describe how comparison among these studies is difficult due to use of different test methods to investigate the materials and reported data types varying between studies. The authors note that *'physical and quasi-static mechanical properties appear to be reasonably well documented in the literature. High strain rate properties are much less well understood so that whilst it is possible to be able to match quasi-static properties to a synthetic material, matching at higher strain-rates might be challenging'* [8]. This is in line with the views of Zhu et al. [9].

Additional work is therefore needed to develop skin surrogates that mimic human skin behaviour under ballistic impact at high strain rates.

11.2.2 Brain simulant

Brain simulants were reviewed in section 3.2.1 of this thesis. 10% Gelatine is not a completely biofidelic brain simulant [10] and does not produce the range of injuries seen in real brain [11,12].

On the positive side both the 10% gelatine and Permugel™ fills have induced bullet yaw within the models and produced realistic fracture patterns in the skulls (chapter 5).

If, however, a model needs to produce realistic brain injury then alternative materials are needed such as those described by Falland [13].

11.2.3 The post-mortem cut line in the skull

The post-mortem cut line is a feature of the manufacturing process of the MU51 skull which is made in two parts to allow detailed internal architecture to be

created (see chapters 5 to 7). Discussion with the UK based part of the company, ARRK, confirmed that this could not be altered if the same level of detail was required in the model. The fracture patterns produced in the model described in this thesis (chapters 5 to 8) do support Fenton's view [14] of anatomical structure influencing fracture development so for this model anatomical accuracy is essential.

Two areas of work are proposed:

(a) Further assessment of agents to bond the two parts of the skull (see Appendix F, Table_A 5).

(b) Re-visit of 3-D printed skulls. Previous assessment of 3-D printed skulls by the Impact and Armour Group found they shattered along the layers created by the printing process producing results that were unrealistic (unpublished data – not part of this thesis). If a 3-D printed model could be produced that broke up in a realistic manner under impact then this would merit further assessment.

11.2.4 Further development summary

Further development of the model should concentrate on refining the materials for the surrogate head components and exploring other options for skull manufacture.

11.3 References

1. Misliwetz J, Wieser I (1989) Bullet head wounds in members of the military wearing protective helmets-general observations and experiments on the biomechanics involved and the wound morphology. *Z Rechtsmedizin* 102:41-54
2. Breeze J, Allanson-Bailey LS, Hepper AE, Midwinter MJ (2015) Demonstrating the effectiveness of body armour: a pilot prospective computerised surface wound mapping trial performed at the Role 3 hospital in Afghanistan. *J R Army Med Corps* 161:36-41
3. Can C, Bolatkale M, Sarihan A, Savran Y, Acara AC, Bulut M (2017) The effect of brain tomography findings on mortality in sniper shot head injuries. *JR Army Med Corps* 163:211-214
4. Kneubuehl BP, Thali MJ (2011) Experimental reconstruction. In: Kneubuehl BP (Ed) *Wound Ballistics: Basics and Applications*. Springer, Berlin Heidelberg. pp291-303
5. Introduction to the classification of gunshot wounds. In Di Maio VJM (2016) *Gunshot Wounds; Practical Aspects of Firearms, Ballistics and Forensic Techniques* (3rd edn). CRC press, Taylor & Francis Group, Boca Raton. pp 57-108
6. Ran Y, Yagudaev M, Kosashvili Y, Yegorov Y, Ganor O, Ash N, Hirschhord G (2010) Anatomic distribution of bullet head injuries in combat fatalities. *J Trauma* 69:541-543
7. Turco L, Cornell DL, Phillips B (2017) Penetrating bihemispheric traumatic brain injury: a collective review of gunshot wounds to the head. *World Neurosurgery* 104:653-659




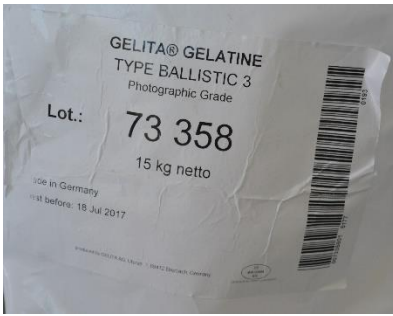




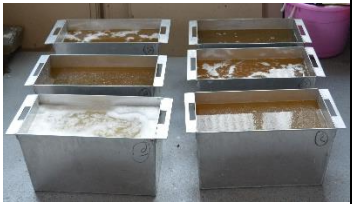
8. Fenton L, Horsfall I, Carr DJ (2018) Skin and skin simulants. Accepted for publication Australian Journal of Forensic Science
9. Zhu F, Saif T, Presley BR, Yang KH (2017) The mechanical behaviour of biological tissue at high strain rates. In: Franklyn M, Lee PVS (Eds) Military injury biomechanics: the cause and prevention of impact injuries. CRC Press, Boca Raton. pp103-118
10. Lazarjan MS, Geoghegan PH, Jermy MC, Taylor M (2014). Experimental investigation of the mechanical properties of brain simulants used for cranial gunshot simulation. Forensic Science International 239: 73-8
11. Karger B, Puskas Z, Ruwald B, Teige K, Schuirer G (1998) Morphological findings in the brain after experimental gunshots using radiology, pathology and histology. Int J Legal Med 111: 314-319
12. Oehmichen M, Meissner C, Konig HG, Gehl H-B (2004) Gunshot injuries to the head and brain caused by low-velocity handguns and rifles. A review. Forensic Science International 146: 111-120
13. Falland L (2017) Development of an anatomical head model using simulant materials to measure traumatic brain injury. PhD thesis, University of Otago, New Zealand
14. Fenton TW, Stefan VH, Wood LA, Sauer NJ (2005) Symmetrical fracturing of the skull from midline contact gunshot wounds: reconstruction of individual death histories from skeletonized human remains. J Forensic Sci 50: 1-12

APPENDICES

Appendix A Gelatine block preparation

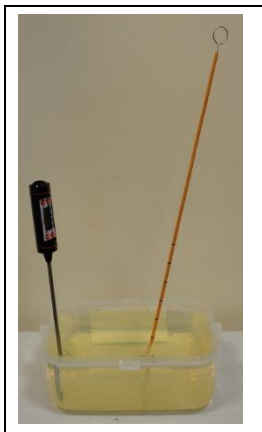
A.1 Method

Gelatine block preparation is described in chapter 3. The purpose of this appendix is to give additional detail.

		
a	b	c
		
d	e	f
		
g	h	i

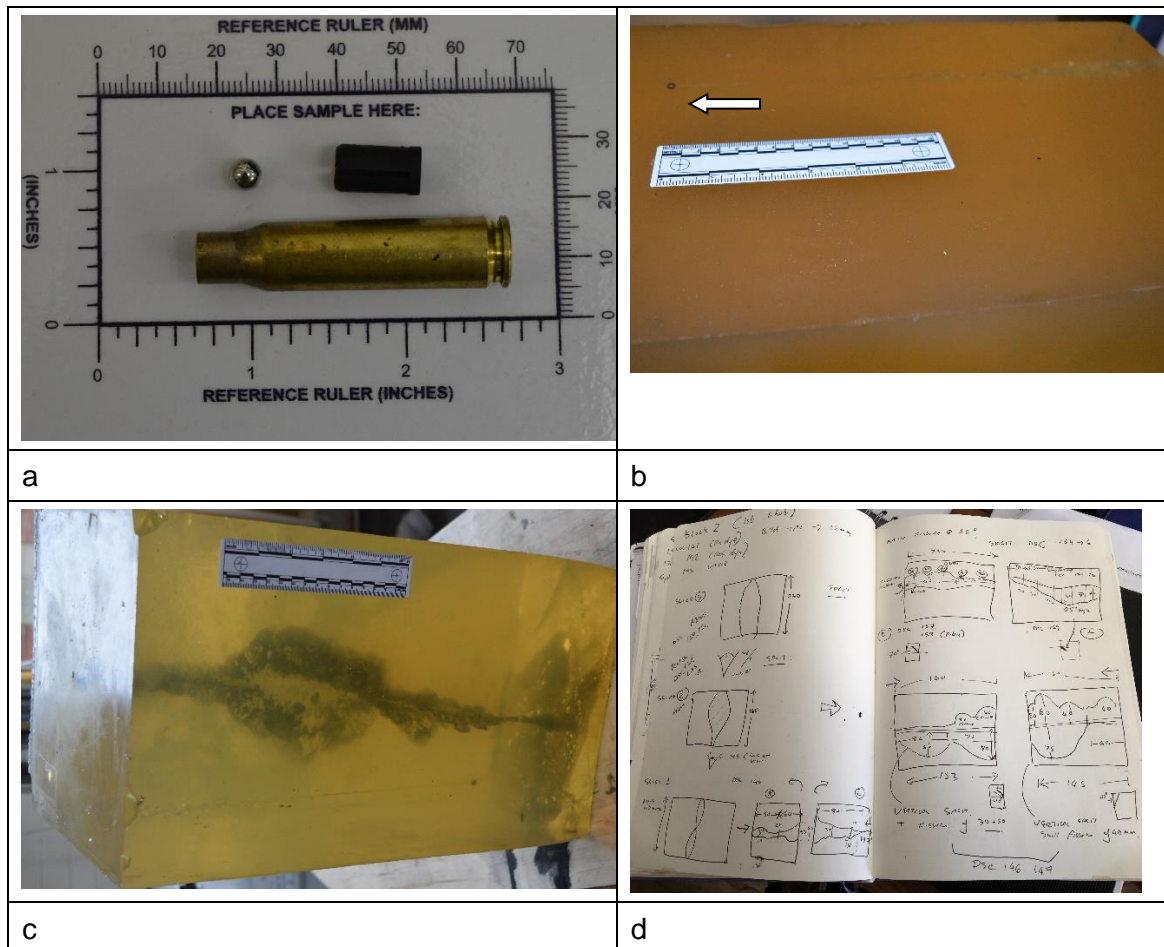
Figure_A 1 Gelatine block preparation

- (a) 250mm (w) x 250mm (h) x 500mm moulds are checked for cleanliness and damage
- (b) the inner surfaces of each mould is sprayed with a silicone based lubricant to ensure the set blocks can be removed from the moulds without tearing (<https://www.rocol.com/products/silicone-mould-release-spray>; accessed 27/02/2018)
- (c) moulds are allowed to dry
- (d) gelatine from one batch is used to make the blocks
- (e) the correct amount of gelatine to make a 10% by mass block is weighed and placed in a mixing bucket; water is added in stages to the correct mass (see Table A_1); half the required volume is added at around 15 to 20°C: the remaining mass is added at around 55 to 65°C to facilitate mixing
- (f) appearance of gelatine mix with about half the required water volume added
- (g) appearance of the gelatine mix with all the water added
- (h) cinnamon oil is added to help remove bubbles from the gelatine as it sets
- (i) gelatine setting within the moulds prior to being conditioned at 4°C.



Figure_A 2 Assessment of different gelatine % by mass for ‘biofidelity’

A neurosurgeon was invited to use a probe to assess different gelatine % and comment on how this related to the feel of brain tissue at surgery.



Figure_A 3 Block validation and dissection

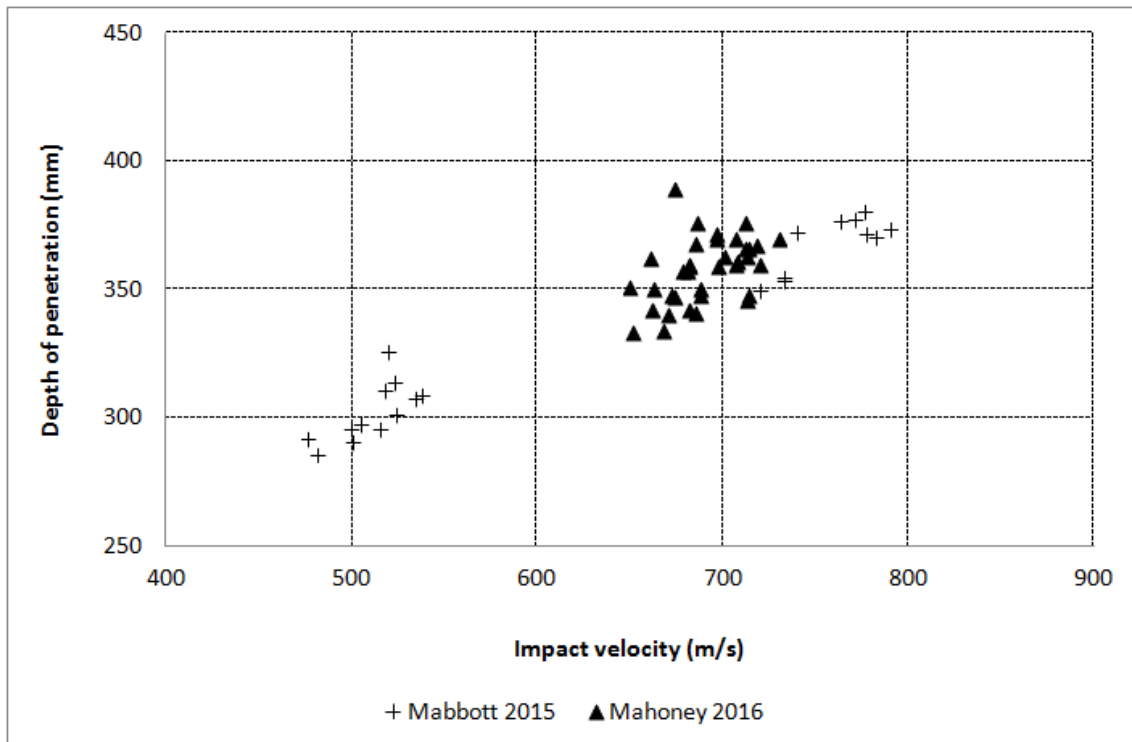
- (a) 5.5 mm ball bearing and cartridge for depth of penetration (DoP) measurements (Similar method to that described in [1])**
- (b) ball bearing visible within gelatine block after firing (arrowed); ball bearing has entered block on the right-hand side of the image; forensic scale visible in the foreground**
- (c) permanent cavity visible within gelatine block after 7.62 x 39 mm bullet impact; cavity highlighted with black food dye**
- (d) example gelatine block dissection notes within laboratory note book.**

A.2 Results

Table_A 1 Gelatine block raw data

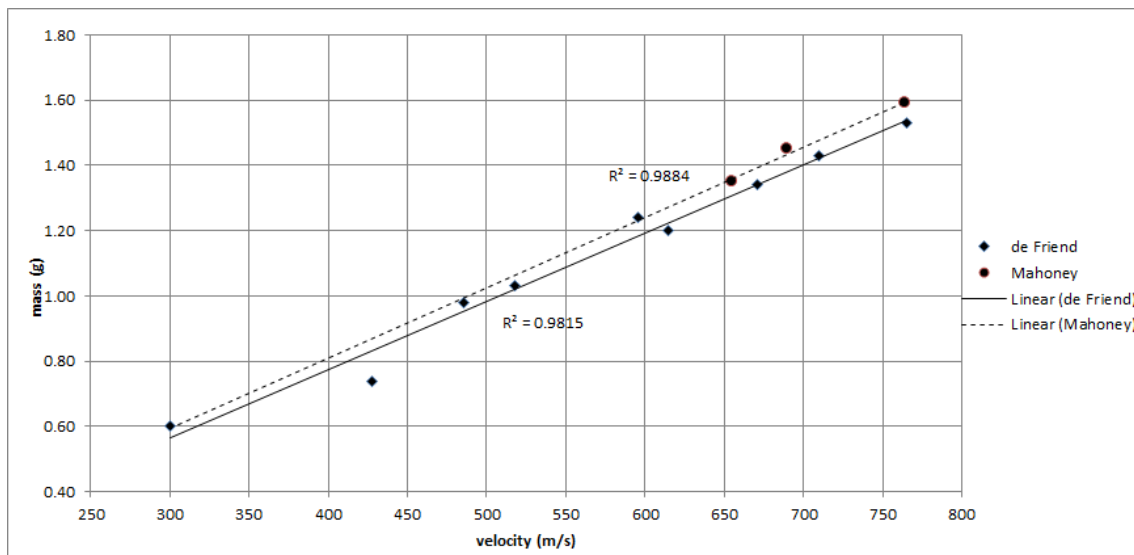
Block number	Mass water g	Mass gelatine g	% gelatine by mass	Temp shot °C	Ball bearing impact velocity m/s	Ball bearing depth of penetration mm	Bullet impact velocity m/s
1	28796	3204	10.01	7.7	697	359	649
2	28000	3200	10.00	6.7	682	360	658
3	28745	3202	10.02	10.4	718	367	661
4	28783	3200	10.00	9.8	730	370	649
5	28766	3209	10.03	5.7	714	348	648
6	29602	3211	9.78	8.6	707	360	658
7	28824	3202	9.99	9.7	712	376	651
8	28793	3203	10.01	8.6	686	376	640
9	28807	3201	10.00	5.9	685	341	649
10	28798	3203	10.01	5.9	688	348	661
11	28813	3200	9.99	10.7	696	370	654
12	28806	3201	10.00	10.6	730	372	671
13	29486	3201	9.79	9.4	674	398	646
14	28793	3201	10.00	10.5	681	357	649
15	28814	3207	10.01	10.6	707	347	654
16	28812	3205	10.01	10.6	678	357	644
17	28805	3203	10.00	8.6	674	347	648
18	28804	3202	10.00	8.3	662	342	649
19	28217	3201	10.19	3.3	668	334	659
20	28797	3200	10.00	4.0	651	333	661
21	28804	3202	10.00	9.5	690	351	650
22	28810	3204	10.00	9.7	670	350	636
23	28803	3199	9.99	9.2	682	359	647
24	28804	3203	10.01	9.8	688	350	647

Block number	Mass water g	Mass gelatine g	% gelatine by mass	Temp shot °C	Ball bearing impact velocity m/s	Ball bearing depth of penetration mm	Bullet impact velocity m/s
25	28798	3202	10.00	9.2	714	366	651
26	28797	3202	10.00	9.4	712	366	655
27	28800	3199	9.99	8.8	708	361	628
28	28800	3200	10.00	8.4	713	363	649
29	28799	3201	10.00	5.9	713	346	659
30	28796	3202	10.00	6.0	720	360	655
31	28799	3202	10.00	6.8	701	363	654
32	28806	3201	10.00	6.3	685	368	656
33	28798	3201	10.00	5.6	672	348	638
34	29575	3200	9.76	5.5	661	362	640
35	28805	3202	10.00	3.1	670	340	639
36	28802	3203	10.01	2.9	682	342	639
Mean	28823.81	3202.19	9.99	7.83	692.25	357.14	650.06
SD	276.71	2.54	0.07	2.33	20.53	13.41	8.59
CV %	0.96	0.08	0.73	29.82	2.96	3.75	1.32



Figure_A 4 Graph of DoP against ball bearing impact velocity

5.5 mm ball bearings; comparison of current project with previous work [2].



Figure_A 5 Graph of propellant mass against bullet impact velocity

7.62 x 39 mm bullets; comparison of current project with previous work [3].

A.3 References

1. Jussila J (2004). Preparing ballistic gelatine; review and proposal for a standard method. *Forensic Science International* 141: 91-98
2. Mabbot A (2015). Wound ballistics: behind police body armour. PhD thesis Cranfield University UK
3. Defriend JP (2015) Overmatching of military soft body armour. MSc Thesis Cranfield University

Appendix B Bullet analysis

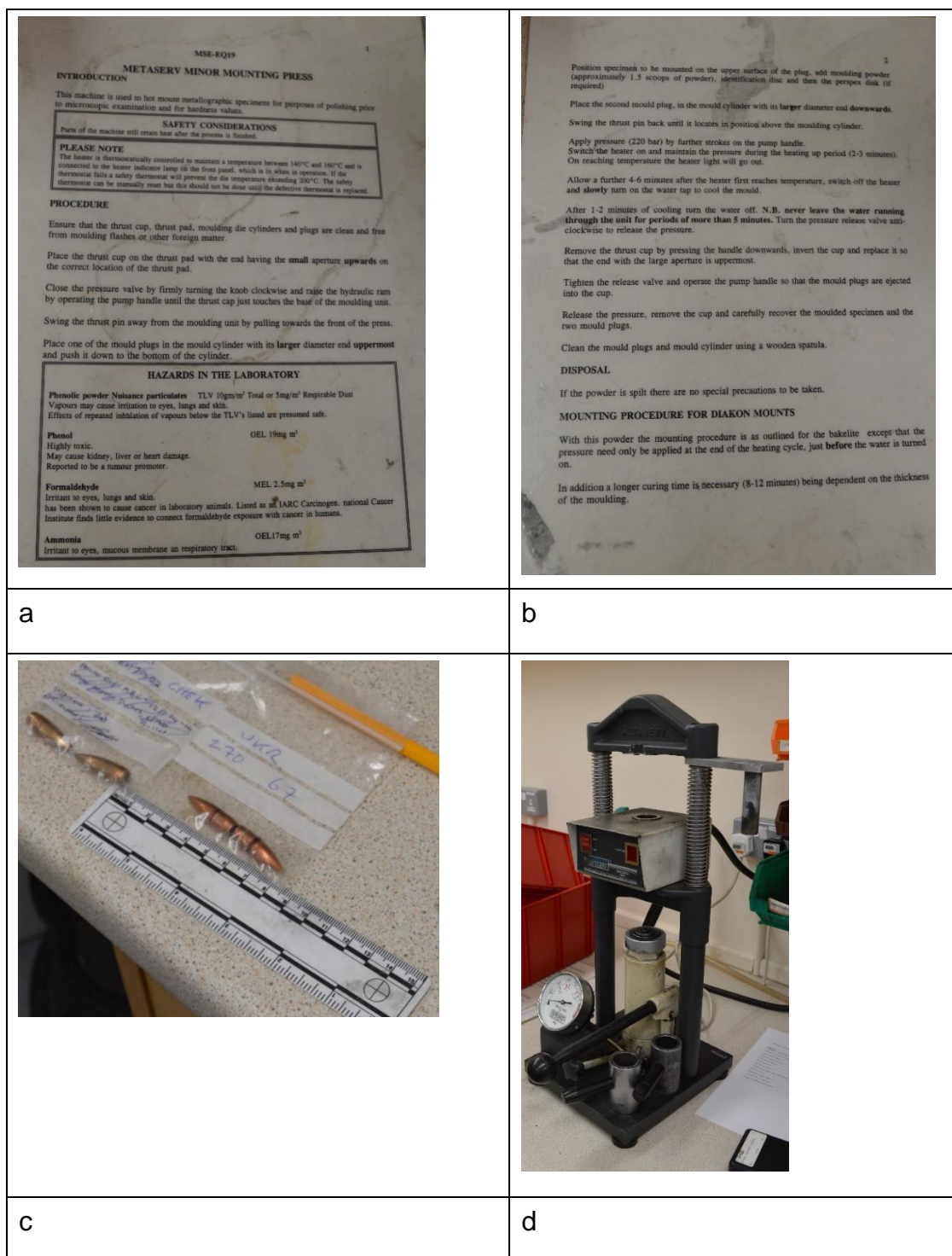
B.1 Methods

This appendix illustrates the stages needed to mount and prepare bullets for analysis. Bullets are 'pulled' from the cartridge case and mounted as a specimen within Bakelite using a combination of heat and pressure. (Figures_A 6 & 7).

The specimen is then polished to reveal a hemi-sectioned bullet demonstrating its layered structure (Figures_A 7c & A 8a).

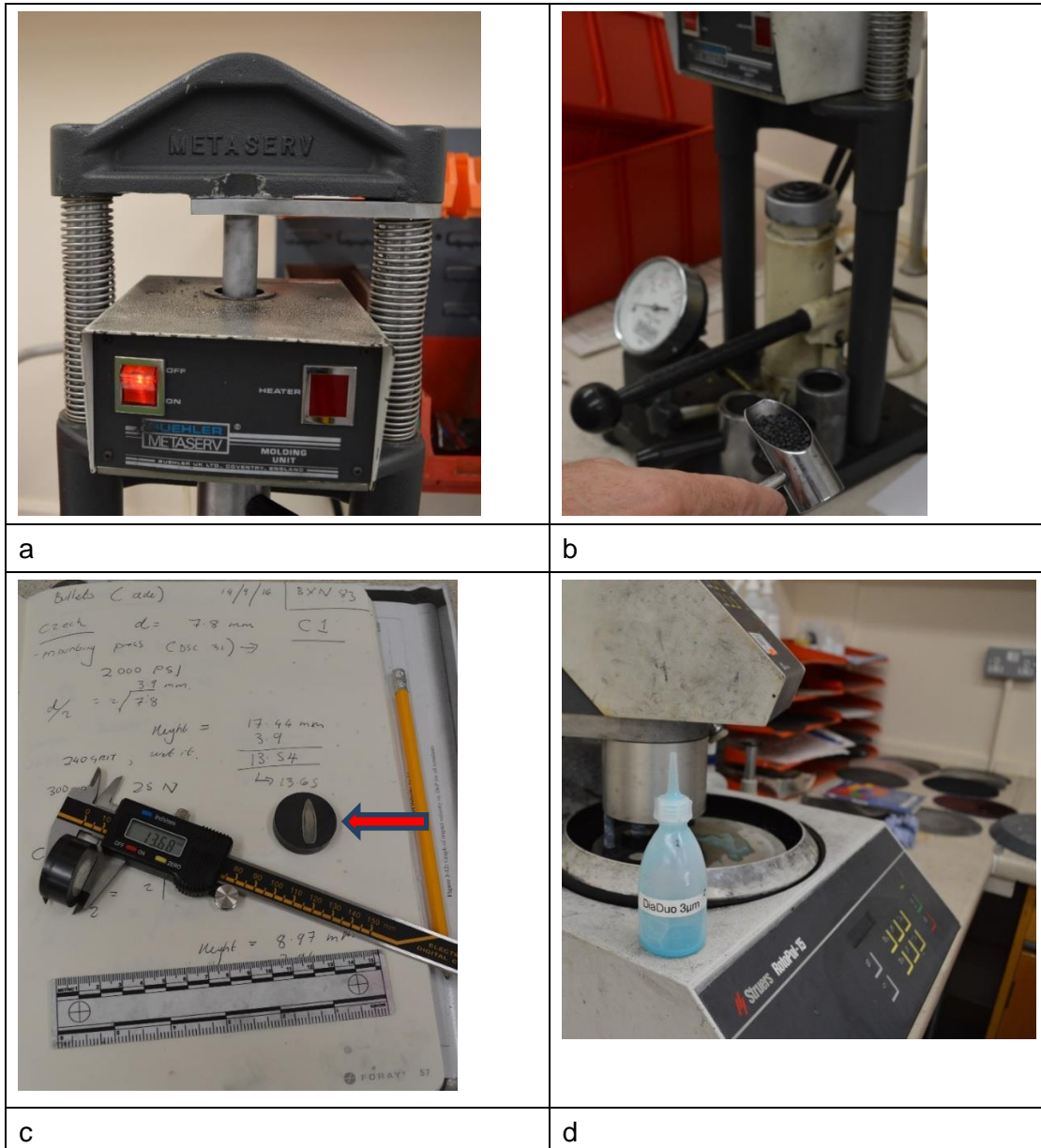
The required amount of polishing is calculated by measuring the bullet diameter and the height of the Bakelite mount (Figure_A 7c). Example of a mounted sectioned bullet is arrowed. (Figure _A 7c).

These specimens are then analysed using a combination of microhardness testing with a diamond tipped indenter (Figure_A 8b) and Scanning Electron Microscope (SEM) elemental analysis (Figures_A 9, A 10, A 11 & Table_A 2).



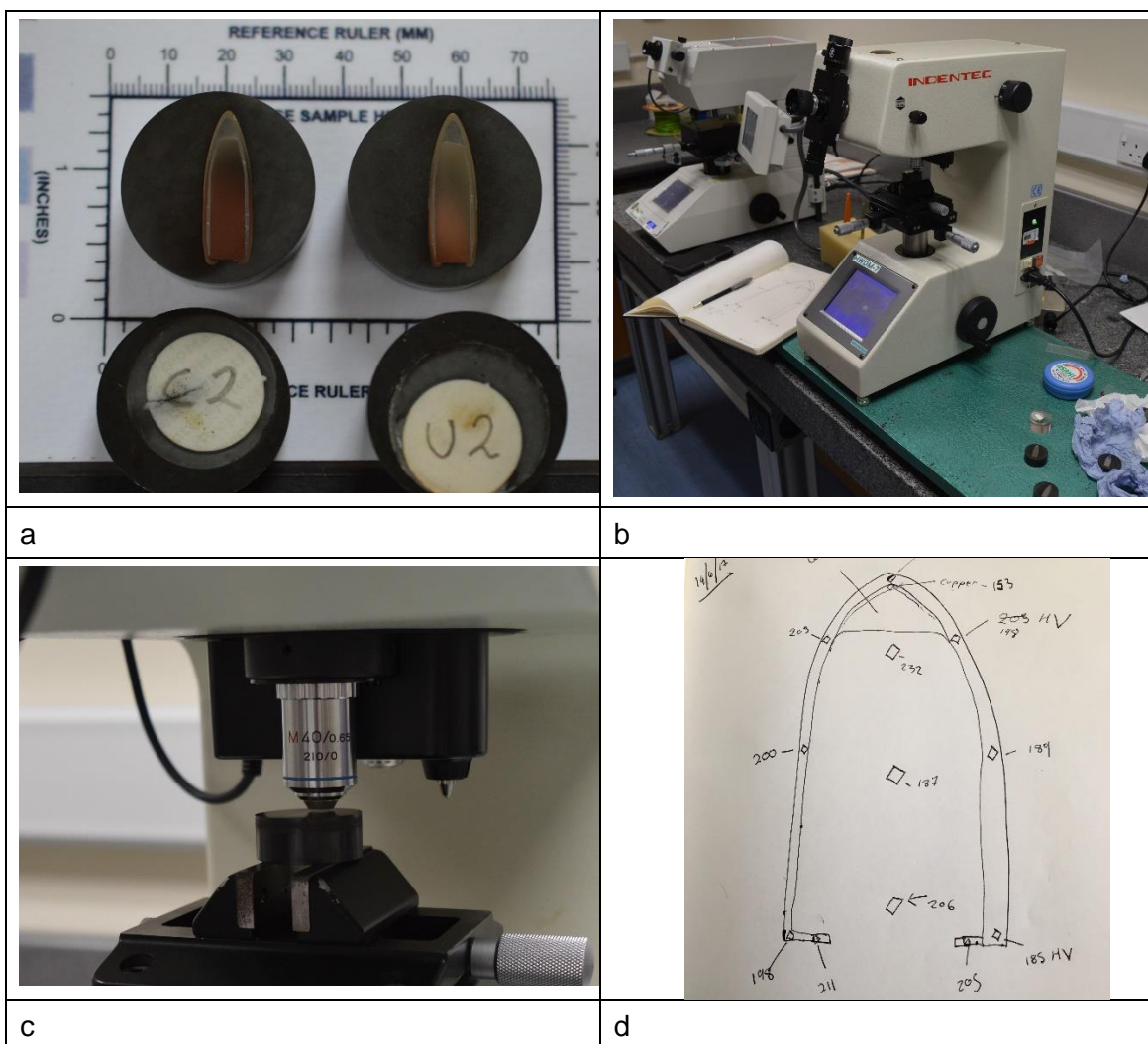
Figure_A 6 Mounting bullets within Bakelite (1)

(a, b) instructions for use of the Metaserv mounting press (c) Bullets (not fired) awaiting processing (d) view of the Metaserv press.



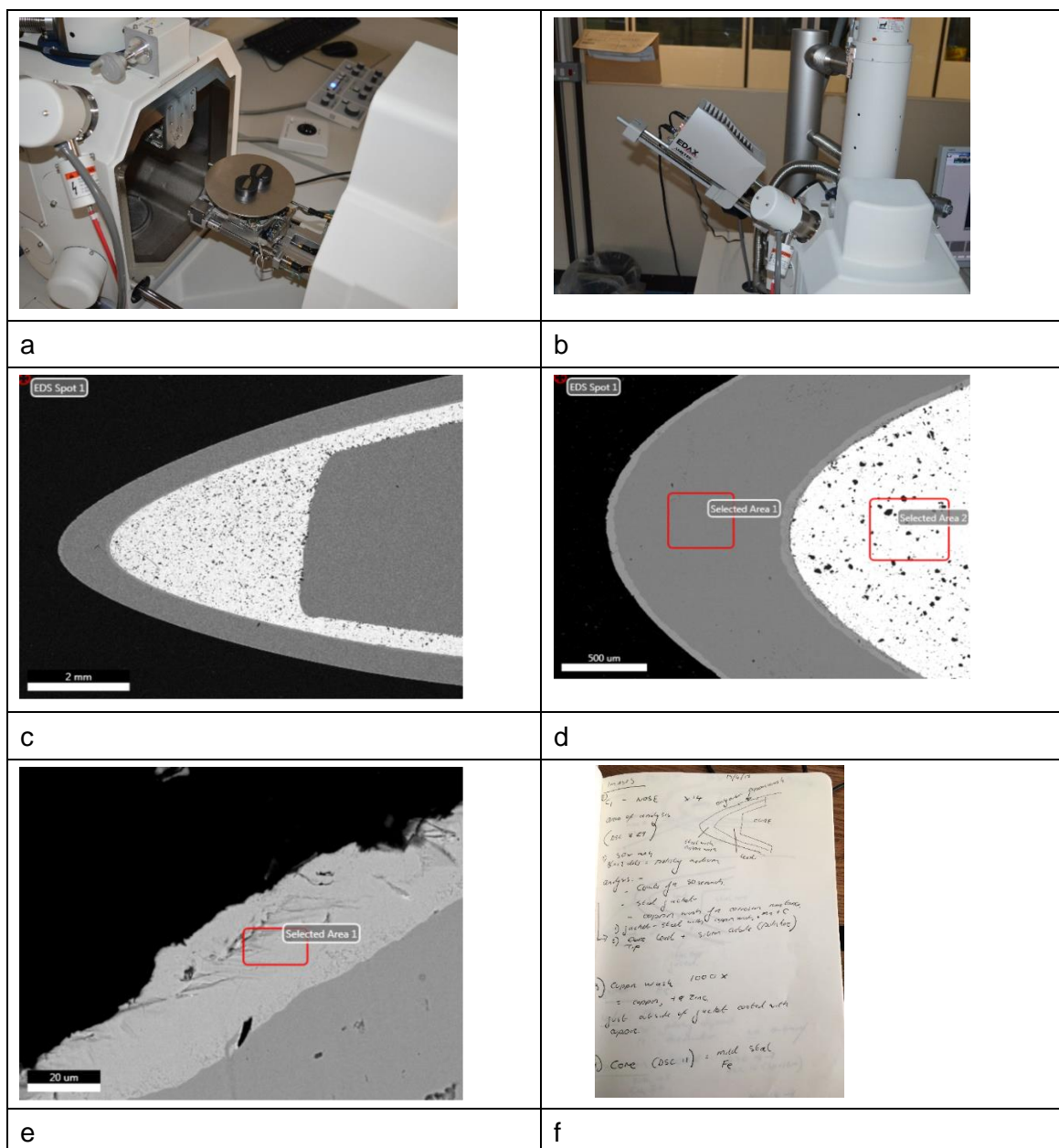
Figure_A 7 Mounting bullets within Bakelite (2) and bullet sectioning

(a) control panel for heating elements Metaserv mounting press (b) pressure gauge, Metaserv mounting press plus Bakelite powder being added to sample cup (c) calculations to assess degree of polishing needed of the mounted bullets to achieve hemi section of bullet; example of a mounted sectioned bullet is arrowed (d) grinding of mounted specimens using silicon carbide abrasive papers.



Figure_A 8 Microhardness testing

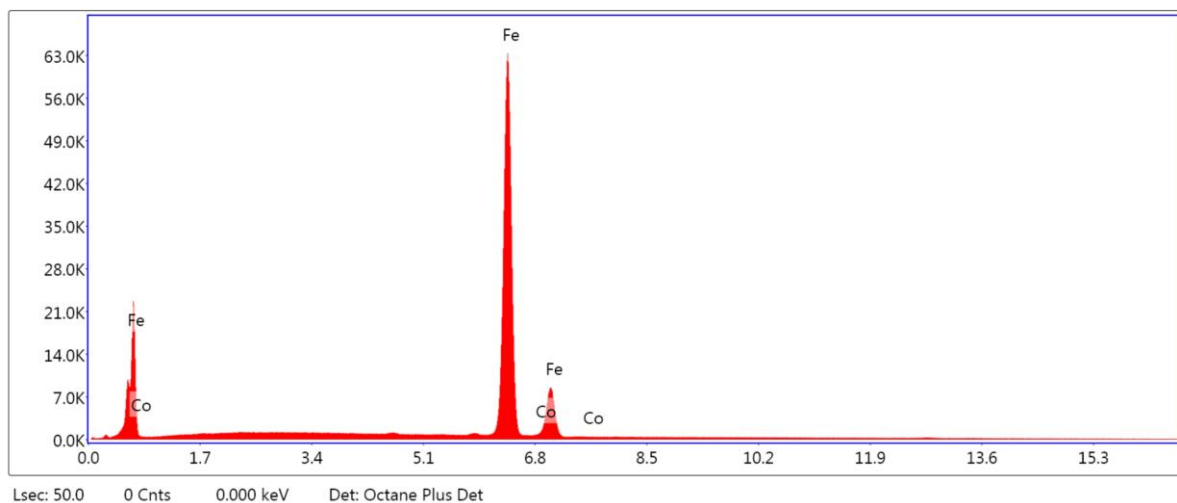
(a) examples of mounted and sectioned Czech {C} and Ukrainian {U} ammunition (b, c) microhardness testing (d) example laboratory note book page of microhardness values (see Table_A 2).



Figure_A 9 SEM imaging and elemental analysis

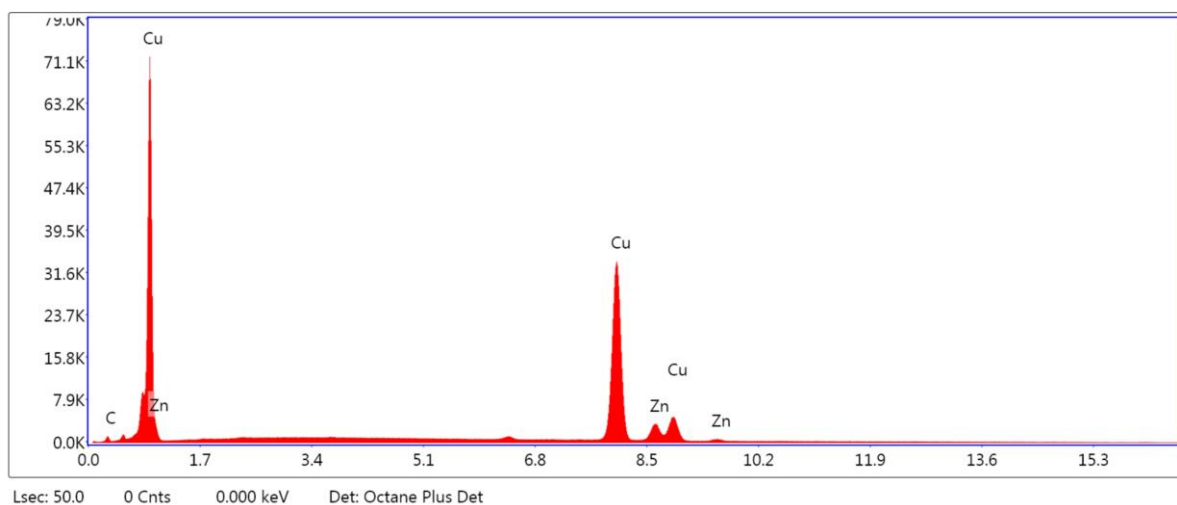
(a) prepared bullet samples being placed within the Hitachi SU3500 SEM with (b)EDAX microanalysis system and Texture & Elemental Analytical Microscopy software version 4.4 (www.edax.com); sample chamber temperature minus 35°C, accelerator voltage 25kV (c) example bullet tip (sample U1) at 14x magnification (bullet layers, left to right: steel jacket, lead fill, mild steel core) (d) example bullet tip (sample U2) at 50x magnification (bullet layers, left to right: copper wash, steel jacket, copper wash, lead fill) (e) example copper wash (sample U2) at 1000 x magnification (layers top to bottom: copper wash, steel jacket); black specks (c-e) are Bakelite (f) example laboratory note book results for elemental analysis.

B.2 Results



Figure_A 10 Elemental analysis, selected area 1 (steel jacket)

(from Figure_A 9d)



Figure_A 11 Elemental analysis, selected area 1, (copper wash)

(from Figure_A 9e)

Table_A 2 Microhardness results

Bullet	Steel Jacket HV	Mild Steel Core HV
Ukrainian 1	200	232
	200	187
	189	206
	198	
	185	
Ukrainian 2	216	225
	206	195
	190	230
	206	
	200	
Ukrainian 3	188	208
	196	193
	203	191
	213	
	199	
Mean	199	207
SD	9	18
CV %	4.5	8.5
Czech 1*§	184	235
	-	200
	-	192
Czech 2 §	221	208
	194	206
	188	200
	181	
	185	

Bullet	Steel Jacket HV	Mild Steel Core HV
Mean	192	207
SD	15	15
CV %	8	7

*Bakelite mould failed so additional core measurements could not be made

§ The only obvious difference between the Ukrainian and Czech bullets was at SEM. The Ukrainian bullets have a layer of copper wash on both the inner and outer aspects of the jacket. In the Czech bullets it is confined to the outer aspect.

B.3 Acknowledgements

Cranfield Forensic Institute

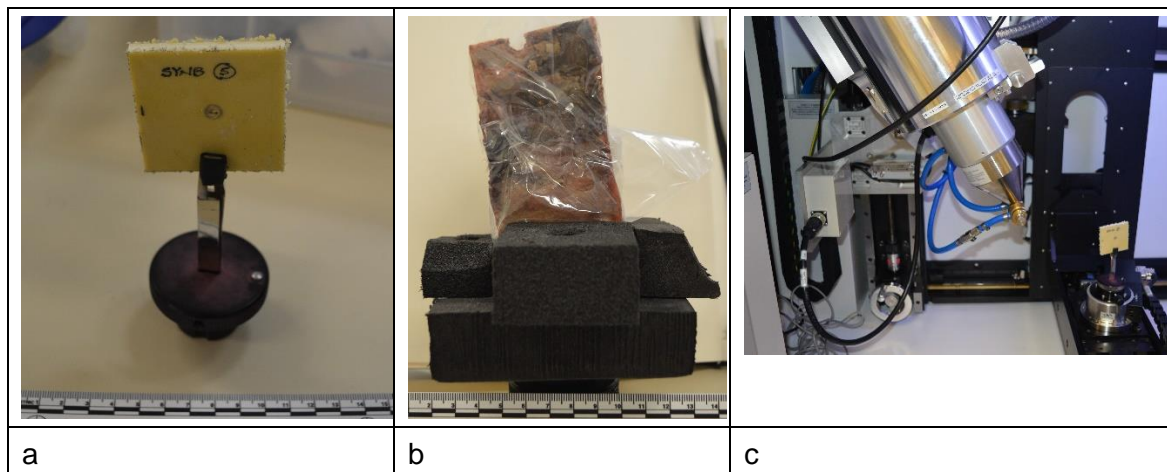
Dr Jon Painter (SEM)

Mr Ade Mustey (Bullet preparation)

Appendix C Micro CT images from intermediate layers

C.1 Method

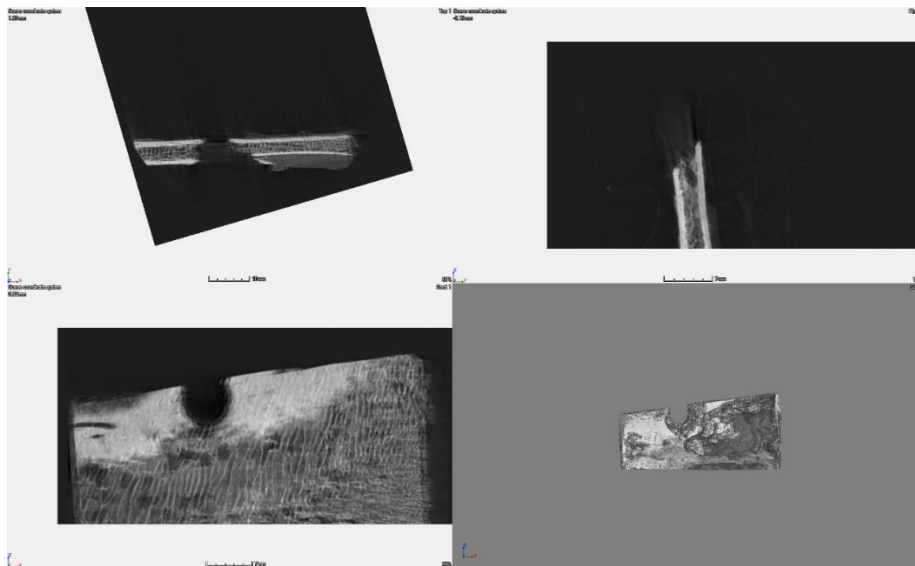
Specimens were cut around the GSW and placed in suitable holders to fit into the sample chamber of the X-TeK XTH 225 scanner (Figure_A 12 a-c). Biological material (horse scapula) was placed within a plastic bag to protect the scanner from contamination. The horse scapula was shot 15/9/16, frozen 16/9/16 and defrosted 12/12/16. The horse scapular gunshot injury was sectioned across the wounded area (Figure_A 12b).



Figure_A 12 Micro CT samples and set up

- (a) Synbone® 50 x 50 mm specimen cut around GSW prepared for the micro CT sample chamber (b) specimen of horse scapula cut across the GSW
(c) Synbone® specimen entering the micro CT sample chamber.

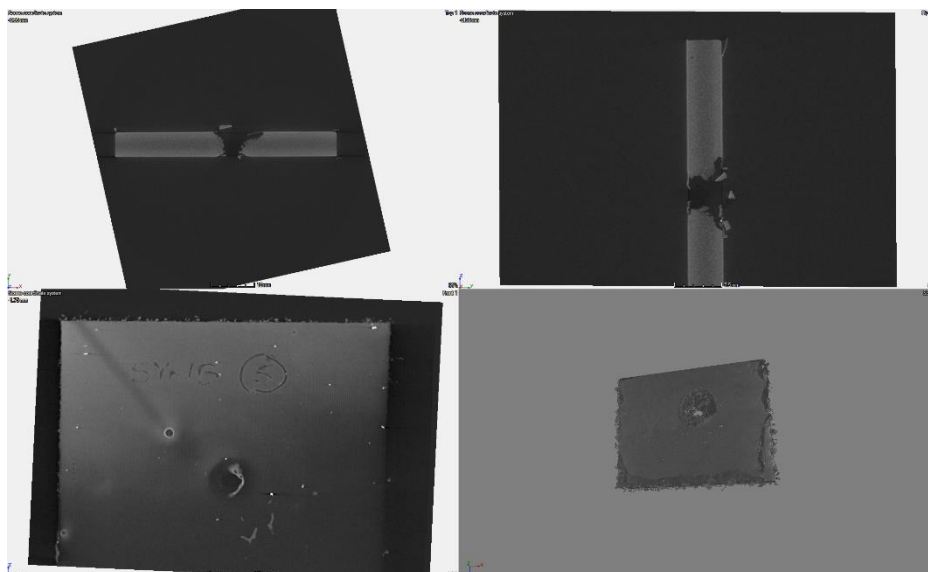
C.2 Results



Figure_A 13 Scapula images

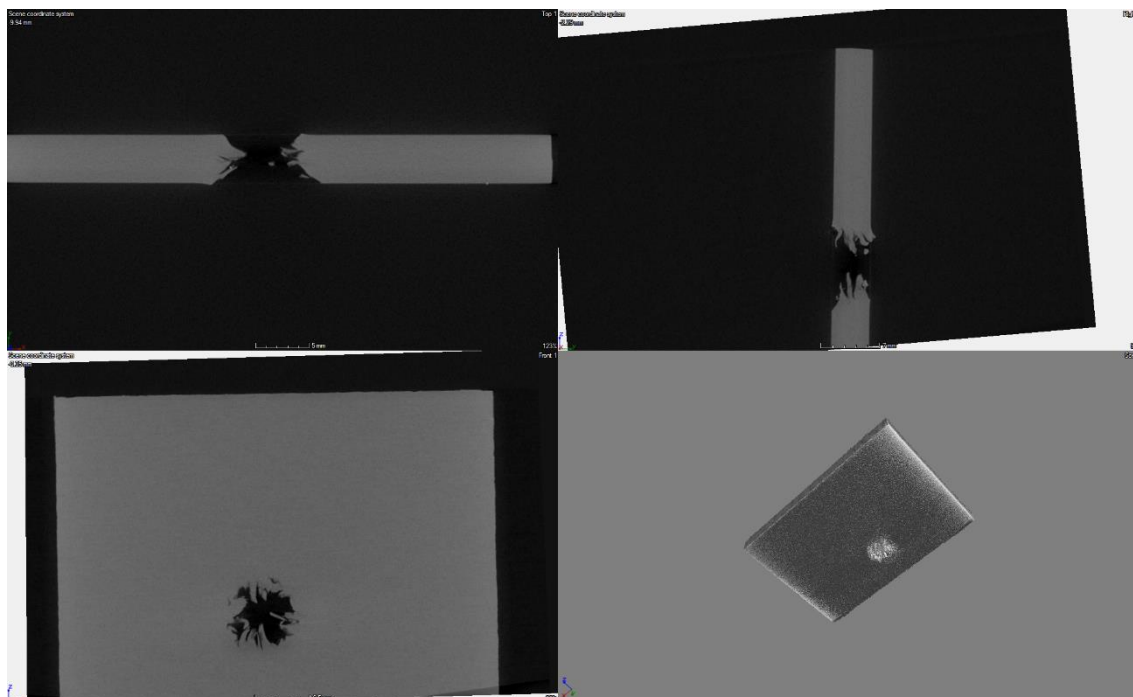
Imaging software Inspect-X. Processing software CT-Pro. CT settings: 500 mS exposure; 100 kV; 40 μ A (bone settings).

Top left: looking from above onto the specimen. Top right: looking at lateral edge of specimen. Bottom left: looking at strike face of specimen. Bottom right 3-D reconstruction of specimen.



Figure_A 14 CT sections through Synbone® specimen

(same settings and views as in Figure_A 13).



Figure_A 15 Section through MU51 impact site
(same settings and views as in Figure_A 13).

C.3 Note

The images in Figure_A 13 show the complexity of bone when compared to the synthetic materials illustrated in Figures_A 14 and A 15. This is in concordance with the views of Smith [1] and is discussed further in chapter 3

C.4 Acknowledgement

Dr Fiona Brock, Cranfield Forensic Institute.

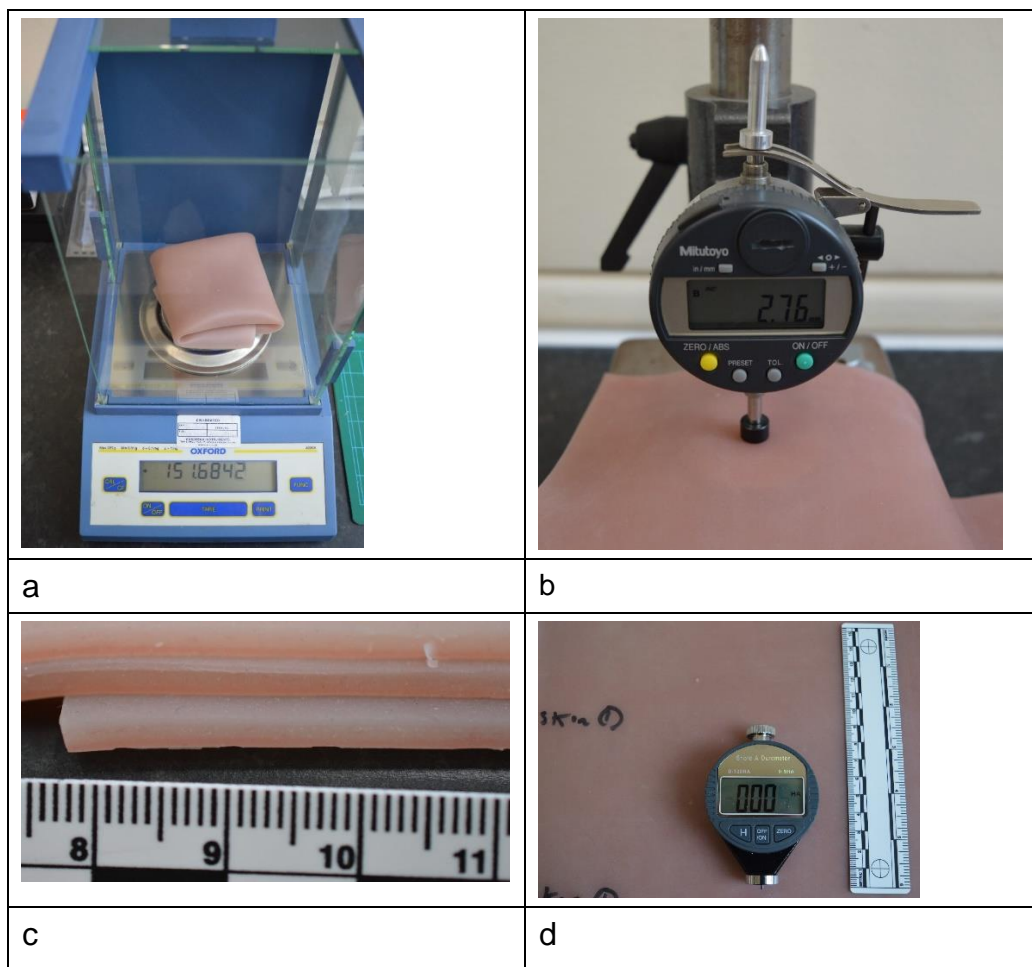
C.5 Reference

1. Smith MJ , James S, Pover T, Ball N, Barnetson V, Foster B, Guy C, Rickman J, Walton V (2015) Fantastic plastic? Experimental evaluation of polyurethane bone substitutes as proxies for human bone in trauma simulations. Int J Leg Med 17: 427-35

Appendix D Synthetic skin analysis

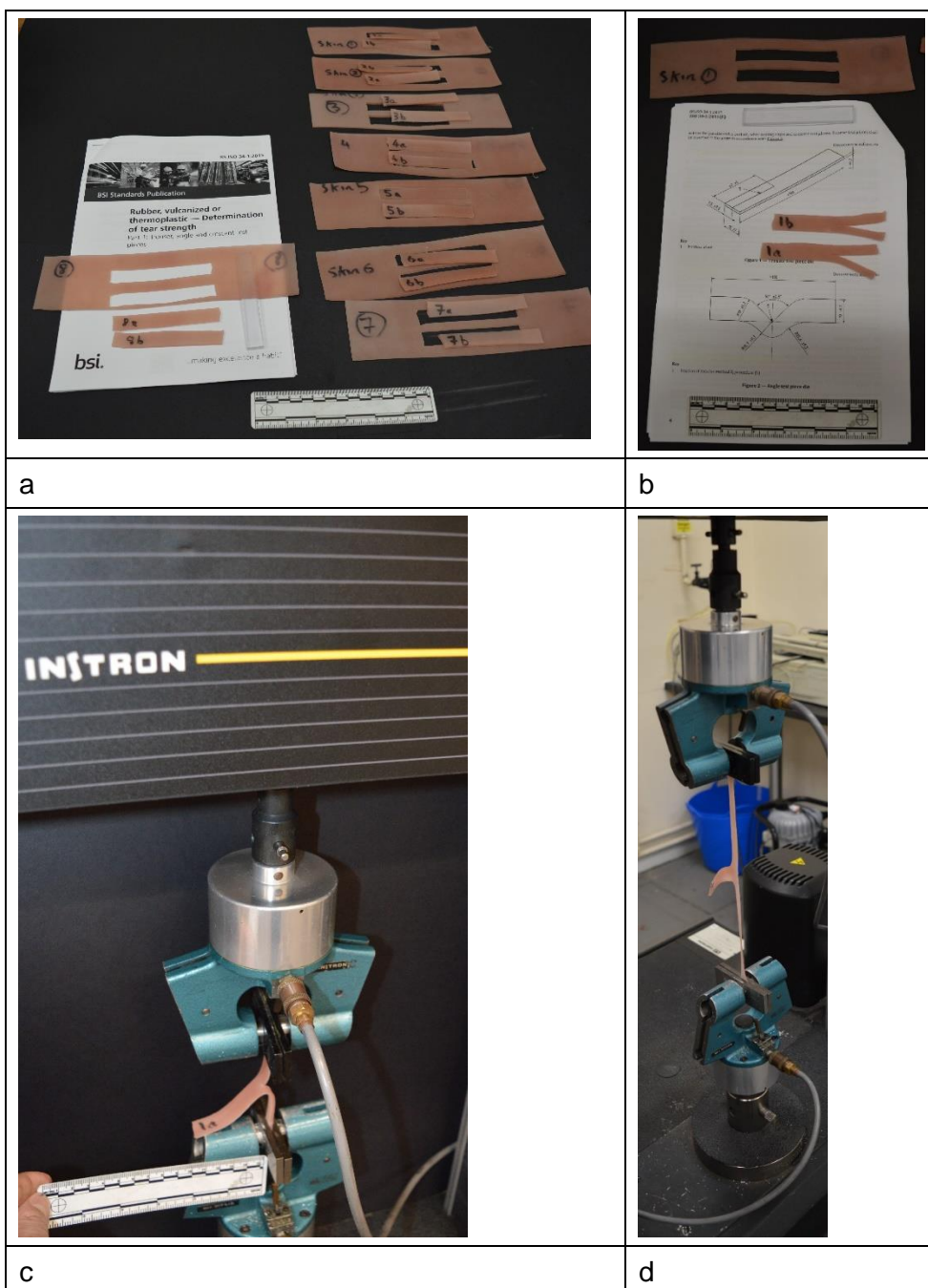
D.1 Methods

The sheets of synthetic skin used in the experiments described in chapter 3 underwent a series of tests. This included measurements of mass, thickness and hardness. Section 3.3.4 describes how the skin samples underwent a trouser tear test [1, 2] on an Instron 5567 Universal Test Machine (30kN frame limit), computer controlled using Bluehill 2.6 software. Figures_A 16 to A 18 illustrate the process.



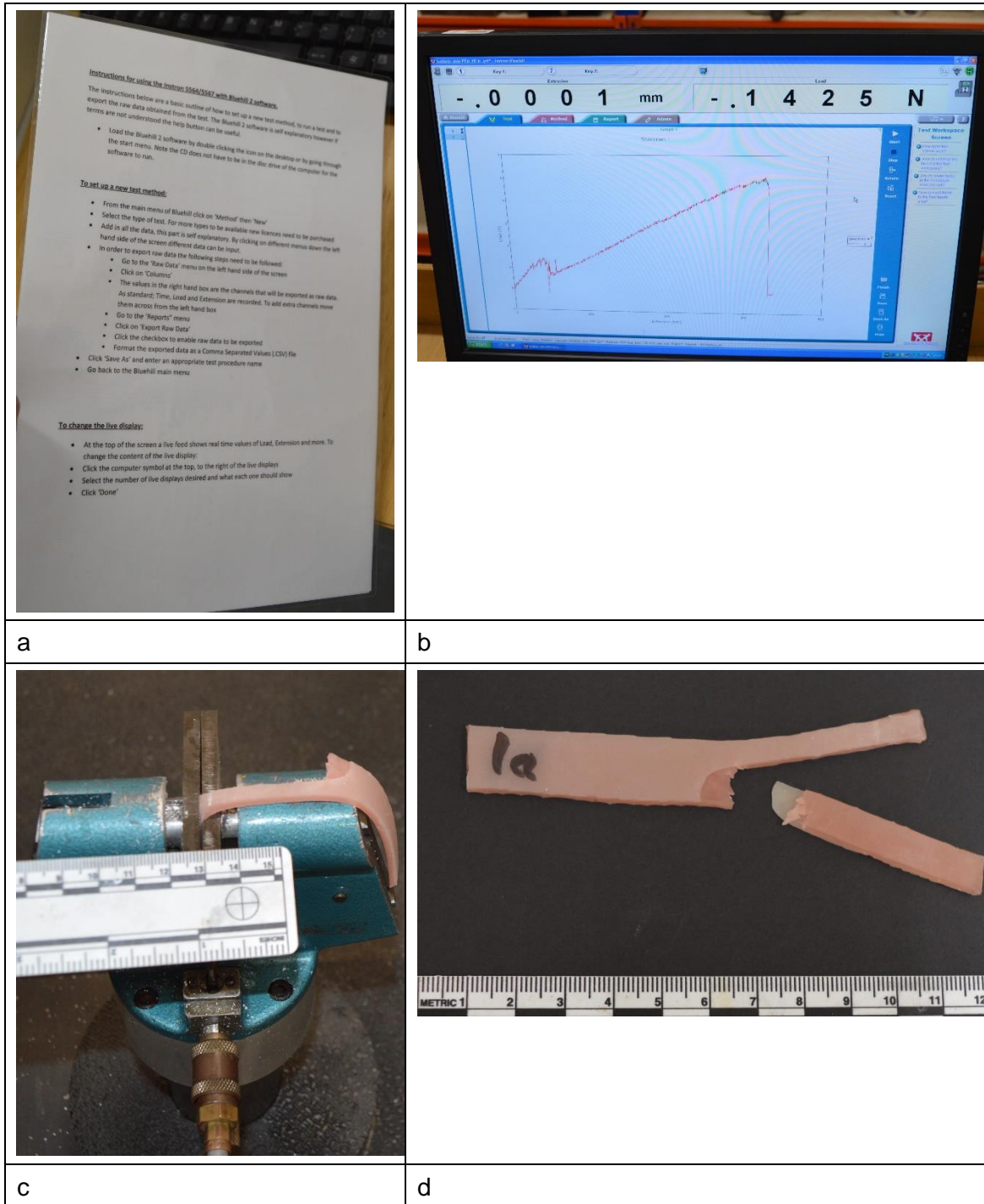
Figure_A 16 Assessment of synthetic skin samples

(a) synthetic skin sample being weighed (b) thickness measurement (c) detail of the two-layered structure (d) hardness measurement with Shore A Durometer.



Figure_A 17 Trouser tear test (1)

(a, b) preparation of samples in accordance with [1] (c) example sample in situ on Instron 5567 Universal Test Machine (d) example sample under test.



Figure_A 18 Trouser tear test (2)

(a) instructions for use of Blue Hill software (b) example computer screen trace demonstrating sample failure (c) example sample in situ after failure (d) example sample post failure.

D.2 Results

Table_A 3 Results of tests on synthetic skin samples

Specimen	Mean Thickness mm (n=3 per specimen)	Mean Hardness Outer surface DU (n=5 per specimen)	Mean Hardness Inner surface DU (n=5 per specimen)	Median force, N	Tear strength kN/m
1a	2.58	26.5	23.8	Test failed	-
1b	2.57	26.5	23.8	5.12	1.99
2a	2.91	21.3	21.4	5.2	1.78
2b	2.88	21.3	21.4	4.47	1.55
3a	3.11	19.8	19.4	5.16	1.66
3b	3.07	19.8	19.4	4.37	1.42
4a	3.10	20.4	20.1	Test failed	-
4b	3.12	20.4	20.1	6.53	2.09
5a	3.04	21.1	20.8	7.44	2.45
5b	3.05	21.1	20.8	3.57	1.17
6a	2.6	19.9	19.1	4.5	1.73
6b	2.81	19.9	19.1	4.27	1.52
7a	2.18	23.5	24.1	4.87	2.23
7b	2.16	23.5	24.1	3.16	1.46
8a	2.27	22.1	22.0	3.5	1.54
8b	2.33	22.1	22.0	4.01	1.72
Mean	2.74	21.8	21.3	4.73	1.74
SD	0.35	2.8	1.8	1.16	0.35
CV %	12.91	9.9	8.5	24.52	20.00

D.3 References

1. Rubber, vulcanised or thermoplastic: Determination of tear strength Part 1: Trouser, angle and crescent test pieces BS ISO 34-1:2015
2. Rubber and plastics: Analysis of multi-peak traces obtained in determinations of tear strength and adhesion strength. BS ISO 6133:2015

Appendix E Synbone® sphere data

Table_A 4 Synbone® sphere data

Sphere number	Mass empty g	Mass full g	Fill % gelatine by mass	Temperature shot °C	Bullet impact velocity m/s
1	545	3390	10	19	649 *
					666#
2	527	3375	10	19	658*
					650#
3	516	3355	10	19	650*
					662#
4	550	3352	7	19	651
5	527	3489	7	19	643
6	510	3313	7	18	656
7	524	3338	5	19	660
8	524	3372	5	19	655
9	519	3367	5	19	646
Mean	527	3372		19	654
SD	13	49		0.3	7
CV %	2.5	1.5		1.8	1

*First shot

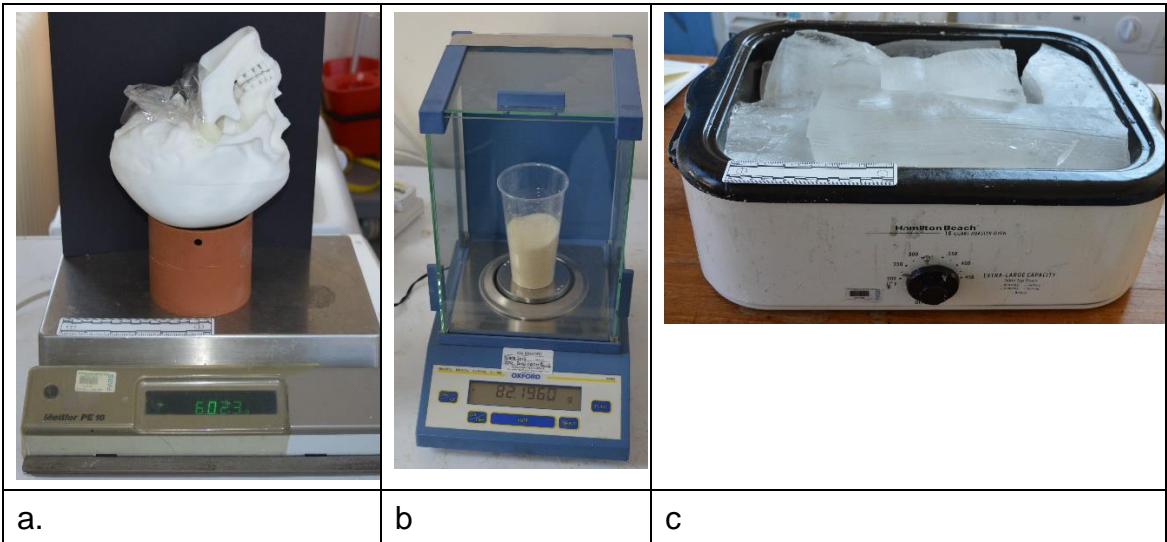
#Second shot

Appendix F Skull data and preparation

F.1 Method

Preparation of skulls, skulls with faces and skulls with faces and helmets is described in chapters 5, 6 and 7 respectively. This appendix gives some additional detail and raw data.

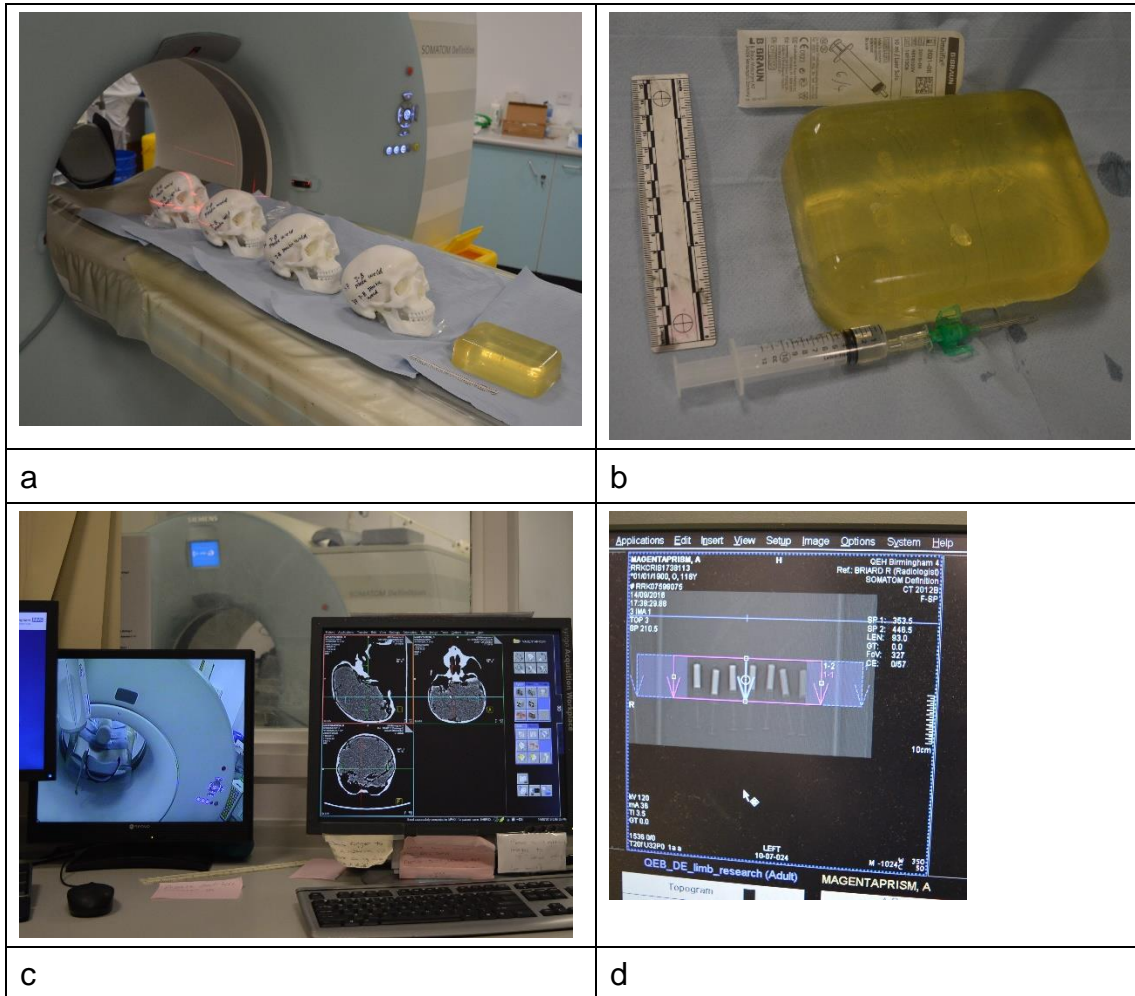
The mass of each skull was measured and recorded. Ballistic gelatine was prepared to give a % by mass depending on the experiment. If a Permangel™ fill was required then blocks of Permangel™ were melted at 120°C and poured into a skull containing a roasting bag rather than a thin polyurethane bag. (Figure _A19).



Figure_A 19 Skull preparation

(a) measuring mass of skull prior to fill (b) measuring mass of gelatine powder prior to preparation (c) melting Permangel™ prior to filling skull.

Prior to the CT imaging described in chapters 6, 7 and 8 preliminary work was undertaken to assess the optimal concentration of contrast agent for use in the models. This is shown in Figure_A 20.



Figure_A 20 Preliminary skull CT imaging

(a) imaging of skulls with different plastic bonds between upper and lower components and with injections of contrast material (b) 10% by mass gelatine block (visible in Figure_A 20a) injected with contrast then imaged (c) example skull images on the computer screens at QEHB CDI (d) syringes containing a series of contrast media concentrations undergoing imaging to assess which would be optimal in the models.

F.2 Results

Table_A 5 Raw data for skulls 1 to 19 and 26 to 46, gelatine fills

Skull number	Fill % gelatine by mass	Mass empty g	Mass full g	Temperature shot °C	Bullet Impact velocity m/s
1	10	-	1712	4.0	696
2	10	-	1722	4.0	690
3	10	-	1720	4.0	698
4	10	-	1720	4.0	689
5	10	-	1725	4.0	699
6	3	-	1721	4.0	701
7	3	-	1723	25.0	697
8	3	-	1742	4.0	699
9	3	-	1710	25.0	699
10	3	-	1743	25.0	696
11	10	-	1714	16.9	706
12	10	-	1723	16.5	704
13	10	-	1711	16.9	704
14	5	-	1705	16.8	697
15	5	-	1718	16.6	696
16	5	-	1717	17.1	695
17	3	-	1707	17.1	704
18	3	-	1717	17.7	689
19	3	-	1716	17.7	700
26	7	531	1693	17.0	651
27	7	537	1685	17.2	650
28	7	539	1517	18.0	651
29	7	539	1587	17.5	641
30	7	536	1561	17.8	647
31*	10	547	1498	18.8	648

Skull number	Fill % gelatine by mass	Mass empty g	Mass full g	Temperature shot °C	Bullet Impact velocity m/s
32*	10	546	1600	18.8	652
33*	10	556	1517	19.0	651
34#	10	548	1665	22.3	637
35#	10	553	1684	22.3	648
36#	10	549	1401	22.2	659
37#~	10	544	-	frozen	-
38¥	10	540	1725	20.4	654
39¥	10	537	1625	20.9	662
40¥	10	546	1726	21.2	663
41¥	10	540	1720	21.5	653
42§	10	534	1665	15.9	651
43§	10	524	1715	15.8	641
44§	10	542	1704	15.7	655
45§#	10	534	1688	15.8	642
46§#	10	533	1636	16.7	650
Mean		541	1674		673
SD		8	79		25
CV %		1.5	4.7		3.7

*assessing EA3455 Loctite glue on post mortem cut line

assessing (1) J-B Plastic Weld on post mortem cut line and (2) trialling different concentrations of contrast for CT scanner

#~ shot frozen to assess effect on gelatine

¥ assessing PU resin bond with 50% kaolin

§ assessing PU85 bond §# assessing PU55 bond

Note on temperature: skulls shot at 4°C were taken from a fridge; skulls at 25°C were taken from an oven. Skulls shot at 'room temperature' showed the greatest variability in temperature.

Table_A 6 Raw data for skulls 20 to 25, Permagem™ fill

Skull number	Fill	Mass empty g	Mass full g	Temperature shot °C	Bullet Impact velocity m/s
20	Permagem™	531	1508	18.0	655
21	Permagem™	555	1484	19.2	665
22	Permagem™	531	1442	18.1	641
23	Permagem™	535	1415	17.6	641
24	Permagem™	533	1441	18.1	642
25	Permagem™	537	1446	17.8	657
Mean		537	1456	18.1	650
SD		9	34	0.5	10
CV %		1.7	2.3	3.0	1.5

Table_A 7 Raw data for skull 47 mineral oil elastomer fill

Skull number	Fill	Mass empty g	Mass full g	Temperature shot °C	Bullet Impact velocity m/s
47§#	Mineral oil elastomer (no cavity)	-	1461	16.9	640 643 760

§# assessing PU55 bond

Table_A 8 Raw data for skulls 48- 63 with synthetic faces 1-12

Skull /face number (bond PU55)	% gelatine fill by mass	Mass skull plus face g	Mass skull plus face plus gelatine g	Temperature shot °C	Bullet impact velocity m/s
Faces 1-6					
48/1	10	1221	2429	13.5	653
49/2	10	1216	2385	13.4	656
50/3	10	1227	2381	13.2	657
51/4	10	1229	2481	13.0	650
52/5	10	1234	2461	12.9	655
53/6	10	1233	2404	14.6	642
Mean		1227	2423	13.4	652
SD		7	41	0.6	6
CV %		0.6	1.7	4.6	0.9
Faces 7-12					
54/7§	10	1241	2441	15.6	581
55/8§	10	1244	2456	16.8	578
56/9§	10	1237	2417	16.1	585
57/10§	10	1240	2426	15.9	409
58/11§	10	1225	2307	14.9	424
59/12§	10	1240	2451	16.2	422
Mean		1238	2418	16	581 418
SD		7	56	0.6	3.5 8
CV %		0.6	2.3	4	0.6 2

§ Shot with helmet in situ; forensic recreation studies

Table_A 9 Raw data for skulls 60-63, faces 13-16, Permagem™ fill

Skull /face number (bond PU55)	Fill	Mass skull plus face g	Mass skull plus face plus Permagem™ g	Bullet impact velocity m/s
60/13	Permagem™	1203	2106	Contact shot
61/14#	Permagem™	1246	2256	Contact shot
62/15#	Permagem™	1245	2164	670
63/16#	Permagem™	1231	2261	691
Mean		1231	2197	
SD		20	75	
CV %		1.6	3.4	

New skin formulation

Appendix G Skulls with more than one Likert-type score for fracture pattern of 3 or 4

Table_A 10 Reviewer comments for skulls

Comments summarised where available

Skull designation/ Polymer/ Fill. (Number = gelatine %, PG = Permagem™)	Score assessor 1	Score assessor 2	Score assessor 3	Score assessor 4	Score assessor 5
C/UP5690/10	3. No comment.	2. some entry radiating fractures. Exit wound bevelling, local comminution but insufficient fracture.	2. Entry- some radiating fractures. Exit fracture pattern does not look like expected exit wound- i.e. multiple fragments 'blown out' with radial fractures from main part of damage but has been affected by cut/moulding line.	3.No comment	2.Entry- Not as much vault or base comminution in relation to entrance as would expect to see- suspect has been affected by entrance being just below saw cut. Some extension inferiorly into right orbit. Exit- Fragmentation at exit area quite representative but would expect extension inferiorly into base.

Skull designation/ Polymer/ Fill. (Number = gelatine %, PG = Permager™)	Score assessor 1	Score assessor 2	Score assessor 3	Score assessor 4	Score assessor 5
G/PU8098/10	3. No comment	3. Entry wound radiating fracture lines; fracture to maxilla and base of skull. Exit wound- good radiating fractures but less comminution.	1. Entry- right frontal wound; skull seems to have fractured away through right orbit. Superior half of mould has cracked away. Exit- some fragment loss posteriorly.	3. If it hadn't been weakened by the artificial join (cut line) the fracture pattern around the entry and exit holes would be correct.	2. Entry- comminution of anterior fossa below entrance and extension into middle fossa with bone loss quite realistic but no extension across midline and no comminution of anterior vault (saw cut) Exit- Vault comminution around exit but some of the fracture lines too regular. No extension into base posteriorly.

Skull designation/ Polymer/ Fill. (Number = gelatine %, PG = Permager™)	Score assessor 1	Score assessor 2	Score assessor 3	Score assessor 4	Score assessor 5
1/ MU51/10	3. Difficult to reconstruct - perhaps comminution a bit extreme for range	3. Entrance-fracture lines with comminution. Exit- massive comminution- maybe too much.	1. Over 20 fragments. Bottom half of skull unaffected. Entry is to frontal area but then top half of model has cracked into multiple parts. Exit- unable to comment on loss of 'bone' posteriorly.	1. Doesn't feel right that the neurocranium fractured in isolation and so extensively	3. Vault path. Entry- Entrance partly preserved. Exit- point not precisely seen. Saw cut prevents extension to skull base but otherwise realistic.

Skull designation/ Polymer/ Fill. (Number = gelatine %, PG = Permager™)	Score assessor 1	Score assessor 2	Score assessor 3	Score assessor 4	Score assessor 5
3/MU51/10	3. Good radiating lines around entrance; significant comminution of occiput.	3.Entry-multiple radiating fracture lines. Exit- bullet wipe marks* with comminution	2. Anterior entry with associated fracture in frontal bone. Exit- multiple fragments in occipital bone- would expect this to be held together by soft tissues which would clarify the exact fracture pattern.	2. Entry fracture looks correct other than the artificial cut line. Exit fracture pattern too large.	2. Entry-Entrance incomplete superiorly and inferiorly with associated bone loss terminated inferiorly by saw cut. Some radiating fracture lines but pattern of bone loss unusual. Exit-Exit much more realistic - multi fragmentary but does not extend into skull vault due to saw cut. Would also expect some extension into middle fossa.

Skull designation/ Polymer/ Fill. (Number = gelatine %, PG = Permager™)	Score assessor 1	Score assessor 2	Score assessor 3	Score assessor 4	Score assessor 5
8/MU51/3	3.Reconstructi -on could move this up to a 4	4.Entry- fracturing out into orbit Exit- extensive comminution and distant fracture lines.	2.Left frontal entry wound. Fracture involves left orbit. Large fracture through left temporal bone- too many fragments. Exit- whole of posterior skull looks fragmented.	2.Too broken	2.Entrance at 11 o'clock - similar to others. No vault involvement and defect connected by fracture at posterior part ant fossa but no obvious radiating fractures. Exit more realistic. Heavily fragmented; base and vault, precise point not identified.

Skull designation/ Polymer/ Fill. (Number = gelatine %, PG = Permager™)	Score assessor 1	Score assessor 2	Score assessor 3	Score assessor 4	Score assessor 5
11/MU51/10	3.Would look more convincing following reconstruction	4. Entry-emanating fracture lines; undisplaced frontal fractures. Exit-massive comminution with widespread fractures into base of skull/occiput.	2.Right frontal entry just on cut/mould line. Superior half of model generally intact. Significant injury but too many fragments. Exit-significant disruption-over 20 fragments. Complete destruction of posterior fossa.	2.Too destroyed	2. Entrance bordering on cutline anteriorly. No extension into vault. Ipsilateral involvement anterior fossa but no extension across midline. Exit-Multifragment ary exit more realistic.

Skull designation/ Polymer/ Fill. (Number = gelatine %, PG = Permager™)	Score assessor 1	Score assessor 2	Score assessor 3	Score assessor 4	Score assessor 5
12/MU51/10	3.No comment	1. Entry- not seen a single fracture line from entry wound. Exit- too well marginated and minimal fracturing.	3. Right frontal entry- right orbital injury as expected producing orbital fracture. Exit- fragments blown out with associated fracture running parallel and then crossing sagittal suture. Fractures bounded by casting lines.	4. Fracture pattern correct; only the entry hole looks too well circumscribed.	2. Entry- Radiating fractures into base and vault- not quite as extensive Exit-Radiating fractures into base and vault- not quite as extensive

Skull designation/ Polymer/ Fill. (Number = gelatine %, PG = Permager™)	Score assessor 1	Score assessor 2	Score assessor 3	Score assessor 4	Score assessor 5
21/MU51/PG	3. No comment.	3. Entry-minimal fracture. Exit- external bevelling. Radiating fracture to foramen magnum and calvarium comminution.	3. Permager™ in place. Entry has small wound right frontal area. Exit-multiple fragments posteriorly equally above and below the casting/cut line. Fracture line on skull continuing from where fragments have fallen out.	2. Entry fracture pattern looks too small; rear exit fractures look right.	2. Entry-External and Internal bevelling. Would expect more comminution Exit-Extensive comminution - and vault/base extensions more realistic but would expect more comminution and extension to foramen magnum: almost a '3' for the exit.

Skull designation/ Polymer/ Fill. (Number = gelatine %, PG = Permagerl™)	Score assessor 1	Score assessor 2	Score assessor 3	Score assessor 4	Score assessor 5
23/MU51/PG	2. Hovering between 1 and 2.	1. Not the expected fracture pattern at entry or exit.	3. Entry- small fragment. Exit- small fragments blown out posteriorly, bounded by casting line.	3. Size of entry point realistic but can see demarcation of cut line. Size of exit realistic.	1. Entry- Superior defect but no inferior radiation to base. No vault extension. Exit-Pattern of fragmentation not realistic and limited by saw cut. No radiation into distant vault.

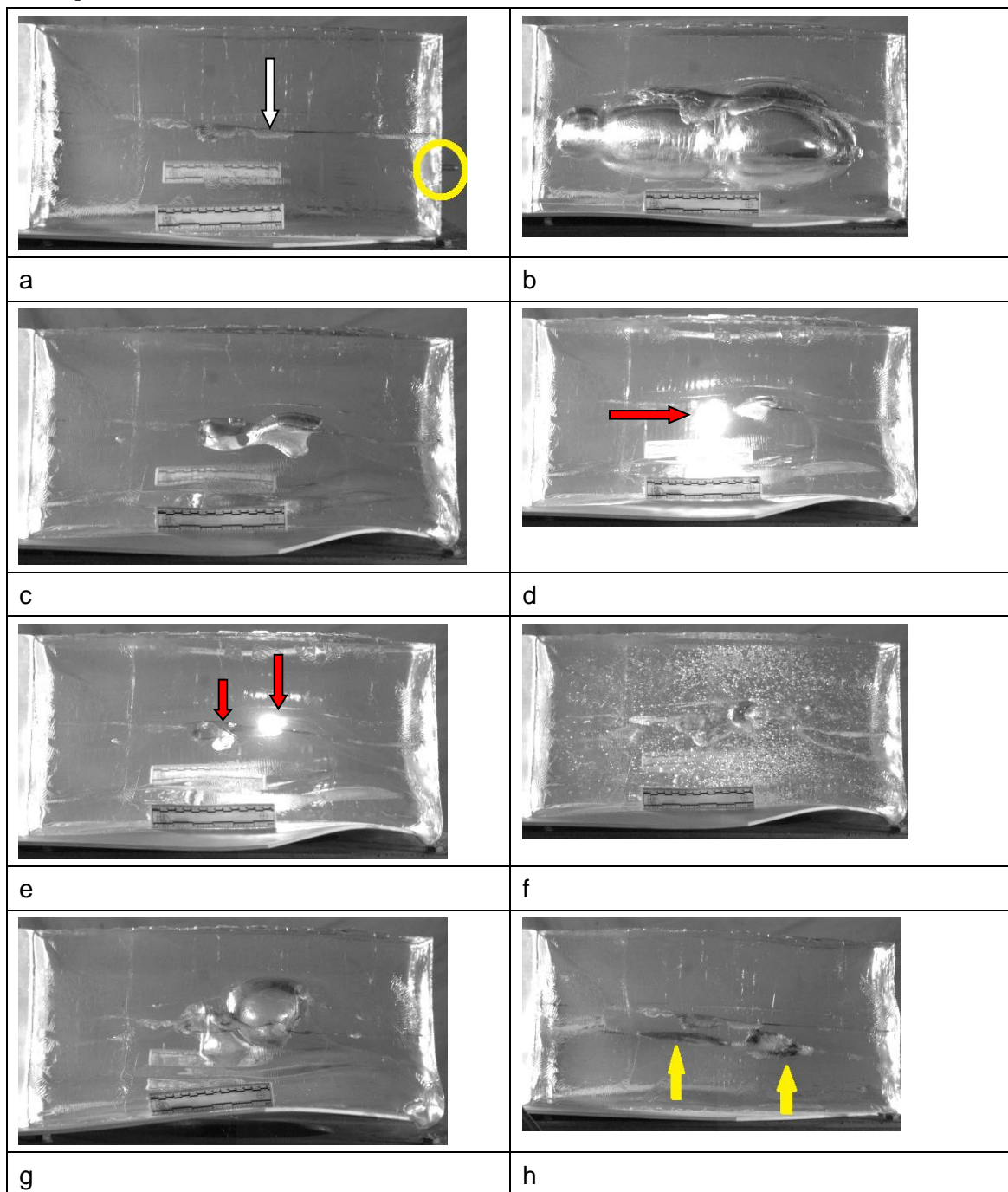
Skull designation/ Polymer/ Fill. (Number = gelatine %, PG = Permager™)	Score assessor 1	Score assessor 2	Score assessor 3	Score assessor 4	Score assessor 5
25/MU51/PG	2. Lack of radiation from entrance.	3. Entry: internal bevelling, minimal fracture patterns. Exit- external bevelling; some radiating fractures and comminution. Needs more exit fractures!	3 Fractures have been altered by moulding/cut line. Entry- right frontal. Exit- small fragments posteriorly from small exit wound with stellate fracturing surrounding.	2. Sizes look correct but there is no fracture propagation and false demarcation around cut line.	1. Entry- Defect at 11 o clock but shows no other radiating fractures. Exit- near limb of lambdoid-fracture does extend towards sagittal suture- ? minimal diastasis. Not as much fragmentation as would expect- limited by saw cut.

Skull designation/ Polymer/ Fill. (Number = gelatine %, PG = Permagan™)	Score assessor 1	Score assessor 2	Score assessor 3	Score assessor 4	Score assessor 5
26/MU51/7	3. Radiation from entrance stopped by cut line.	3. Entry- some emanating fracture and distant (right orbit/maxilla) fracture but no comminution. Exit- comminution and obliquity of fracture margins in keeping.	3. Some fracture lines across temporal bones. Entry- anterior entry point with associated radial fractures into frontal bone and orbit. Exit- widespread posterior injury with multiple fragments 'blown out'	4. Commenting primarily on the entry point this is the closest I've seen in terms of entry hole size and fracture pattern.	2. Entry- Bevelling quite prominent. Cleaved obliquely but not crossing midline, stopped by saw cut so no vault involvement. Defect at post ant fossa away from entrance but comminuted by fracture. Similar in appearance to other cases seen here but not a typical appearance in real life. Exit-More realistic. Multi-fragmenting.

Skull designation/ Polymer/ Fill. (Number = gelatine %, PG = Permager™)	Score assessor 1	Score assessor 2	Score assessor 3	Score assessor 4	Score assessor 5
27/MU51/7	2. Perhaps with reconstruction closer to a 3.	3. Entry- local comminution, reverse bevelling, some fractures into face. Exit- external bevelling with comminution.	1. Appears to be too many fragments to be realistic- shattered appearance. Entry- small right frontal entry wound with loss of right frontal bone. Exit- multiple smaller fragments involving posterior fossa.	3. No frontal sinus (in the model) so no fracture.	3. Entry- Entrance at saw cut but does produce base and vault involvement. Similar post anterior fossa defect as with others. Exit- Heavily fragmented exit with: vault and base. Precise point not seen.

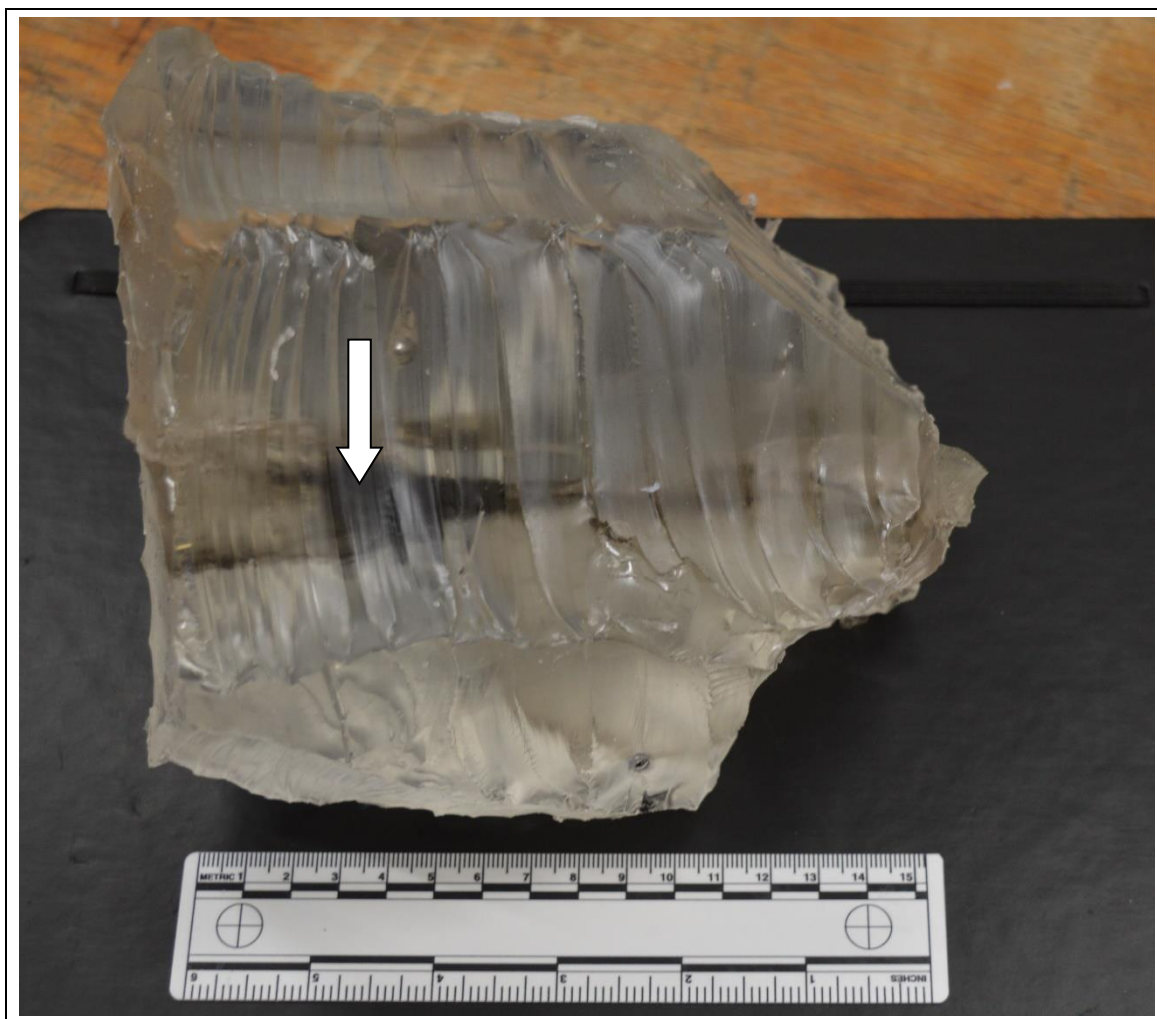
Skull designation/ Polymer/ Fill. (Number = gelatine %, PG = Permager™)	Score assessor 1	Score assessor 2	Score assessor 3	Score assessor 4	Score assessor 5
28/MU51/7	3. No comment.	3. Entry- some comminution, limited radial fractures. Exit- bevelling present, comminution with extending fracture lines.	3. Entry- frontal wound in area of frontal air sinuses. Some bone fracturing. Exit- posteriorly widespread loss of bone. Possible stellate pattern of fracture. Fracture extends down to foramen magnum.	2. Entry and exit points incorrect due to cut line.	2. Entry-Some fragmentation superiorly but not passing through saw cut. No radiation into skull base. Exit-area more realistic. Multifragmenting. Base involvement including radiation to foramen magnum. Precise point not identified.

Appendix H Clear Ballistics synthetic gelatine impact sequence and burn



Figure_A 21 Impact sequence Clear Ballistics 10% Synthetic Gelatine

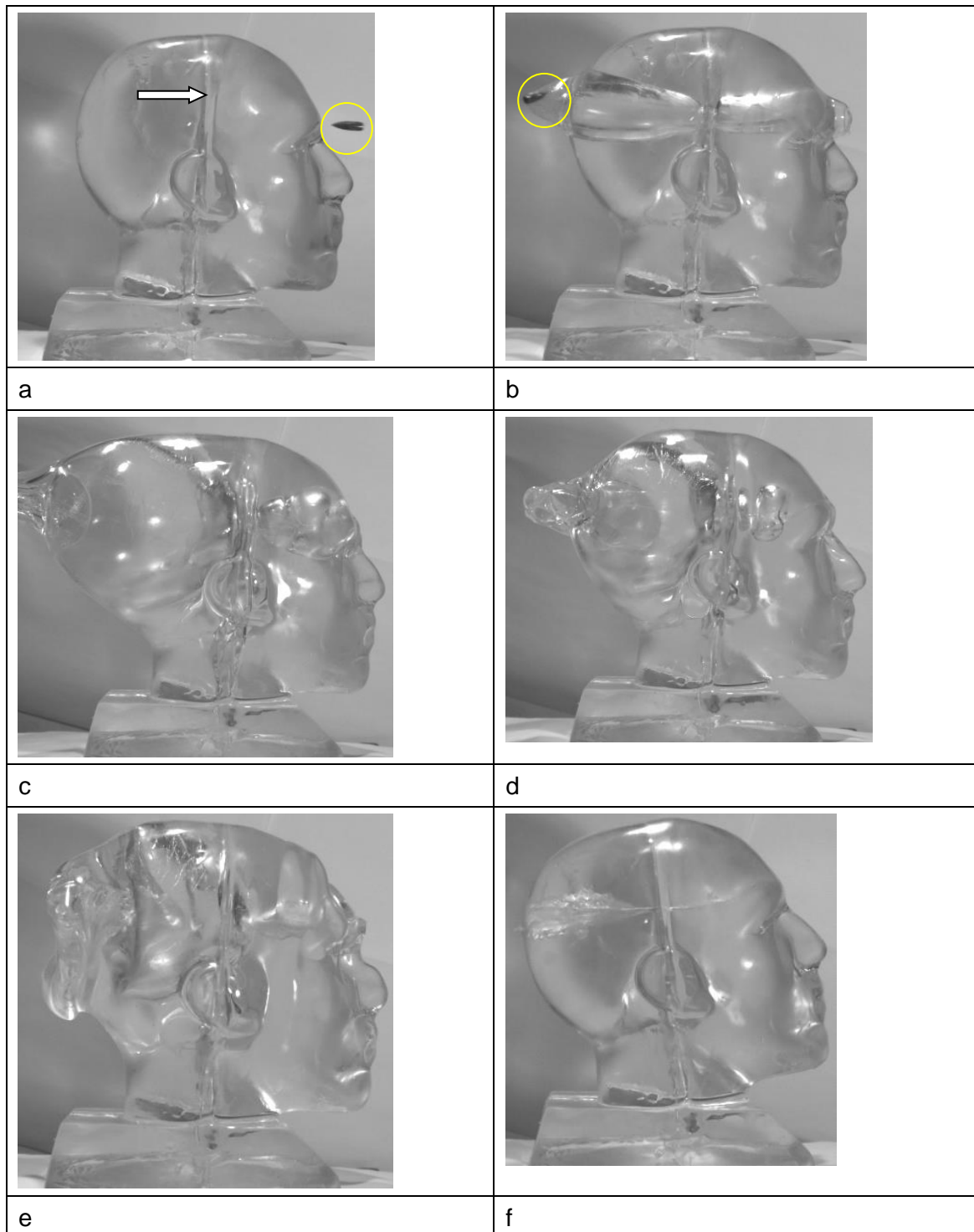
(a) pre-impact, bullet circled; track from 5.5 mm ball bearing validation shot visible (arrowed) (b) cavity development, bullet has traversed right to left, light is reflected from range lamps (c) cavity collapses (d) area of burn within the collapsed area (arrowed) (e) second area of burn (arrowed) (f) shock wave within block (g) cavity oscillations (h) burnt areas visible within the block (arrowed).



Figure_A 22 Permagel™ burn

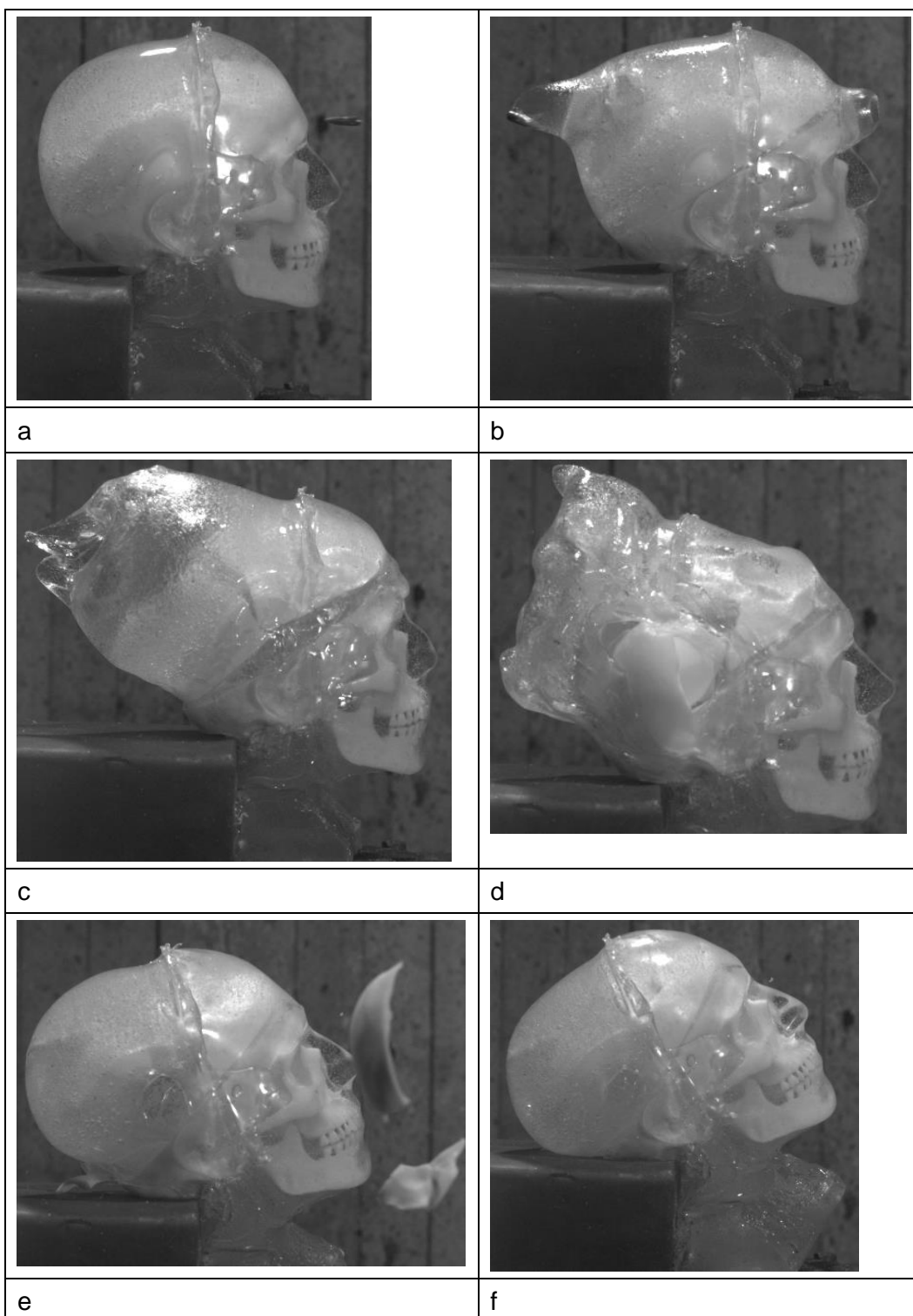
Section of Permagel™ cut out of larger block impacted with 7.62 x 39 mm bullet to demonstrate burnt area (arrowed).

Appendix I Other head models



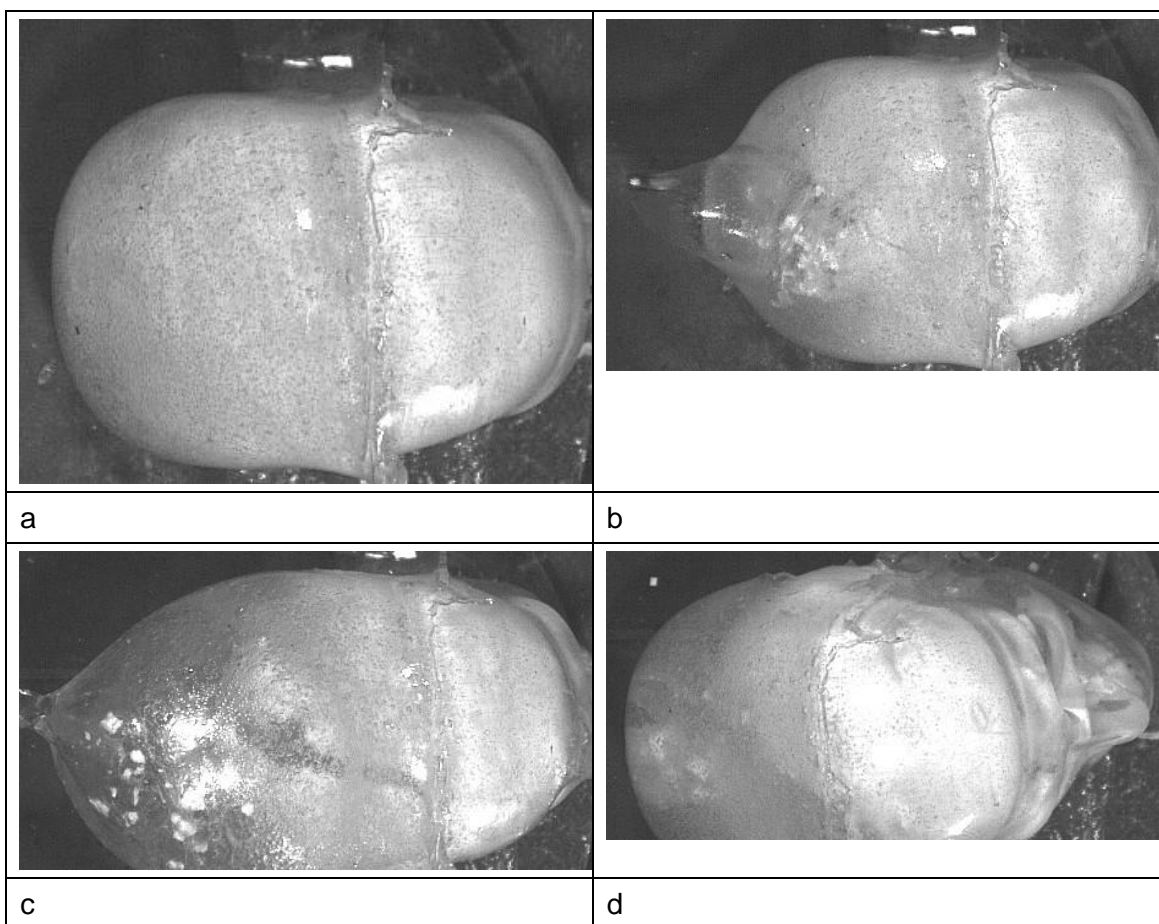
Figure_A 23 Clear Ballistic Gel impact sequence, Clear Ballistic Gel head

Images in order, (a-f), 7.62 x 39 mm bullet, impact velocity 651 m/s. Bullet circled in panels (a & b). White arrow in panel (a) points to the line made by casting the two halves of the model. Temporary cavity visible in panels (b-e); permanent cavity in panel (f).



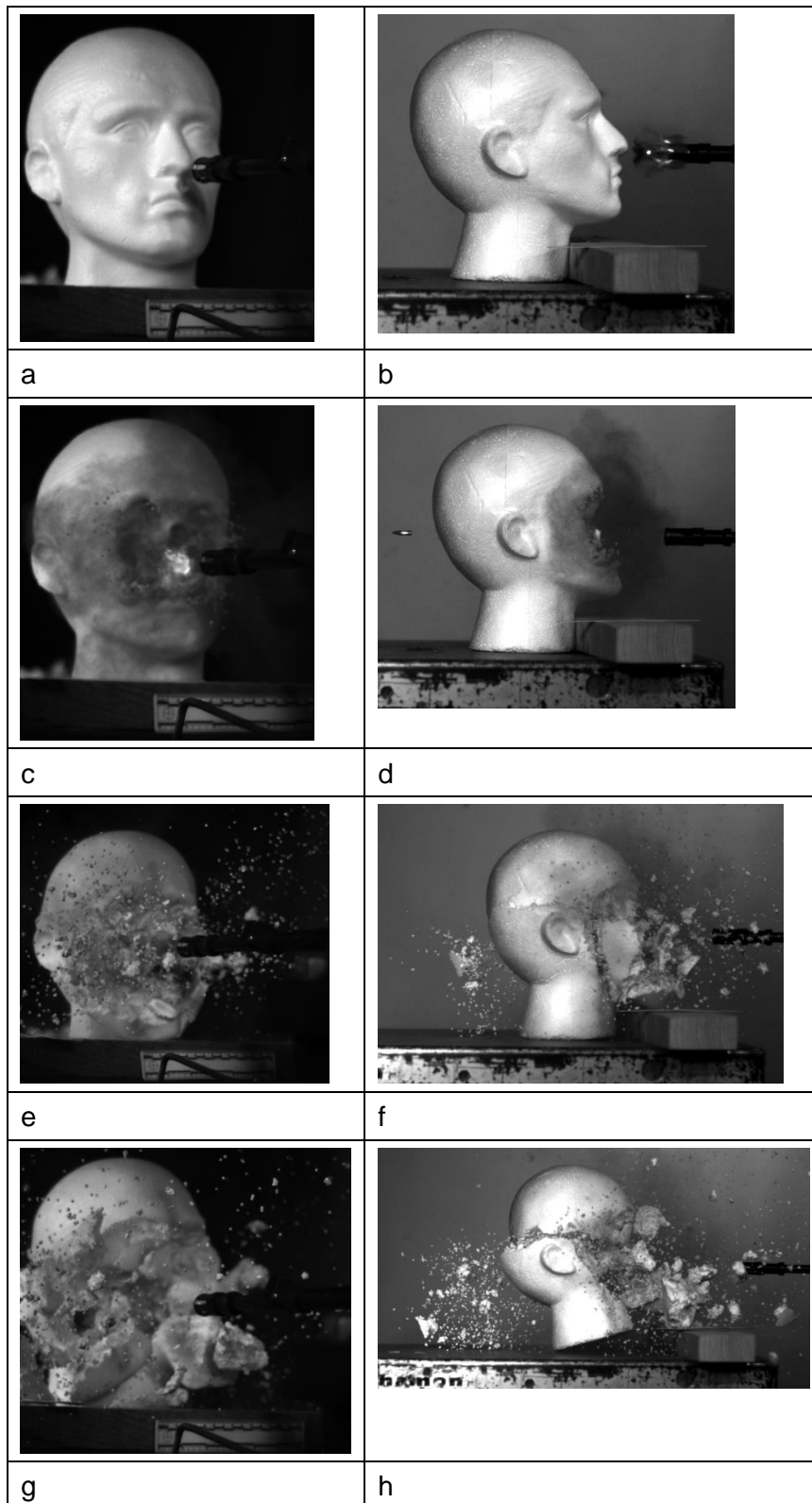
Figure_A 24 MU51 skull with Permagem™ face (side view)

7.62 x 39 mm bullet impact velocity 655 m/s



Figure_A 25 Impact sequence MU51 Polymer skull with Permagem™ face

View from above; same impact as Figure_A24.



Figure_A 26 Impact sequence polystyrene head, 5.56 x 45 mm round.

Contact discharge; front view a, c, e, g; sideview b, d, f, h